



---

# **Small Size Telescope SST-2M GCT Technical Design Report**

---

<b>This Version:</b>				
Ver.	Created	Comment	Distribution	Corresponding...
4.1	2016-06-10	Final version	Open	Editor: D. Berge (full list App. F) Checker: _____ Approver: _____

<b>Keywords:</b>
Technical Design Report; TDR; GCT; SST-2M; Small Size Telescope; GATE; CHEC

<b>Version History:</b>				
Ver.	Date	Comment	Distribution	Corresponding...
1.0	2014-06-09	Initial version	PO	Editor: Author list App. F Checker: R. White D. Dumas Approver: T. Greenshaw H. Sol
2.0	2014-10-31	Second version	PO	Editor: Author list App. F Checker: R. White D. Dumas Approver: T. Greenshaw H. Sol
3.0	2015-01-05	Third version	PO	Editor: Author list App. F Checker: R. White D. Dumas Approver: T. Greenshaw H. Sol
4.0	2015-03-02	Fourth version	PO	Editor: Author list App. F Checker: R. White D. Dumas Approver: T. Greenshaw H. Sol

# Table of Contents

<b>Table of Contents</b> . . . . .	<b>3</b>
<b>1 Summary and Introduction</b> . . . . .	<b>5</b>
1.1 Overall Concept . . . . .	5
1.2 Summary of Design . . . . .	5
1.3 Summary of Plans . . . . .	7
1.4 Summary of Organisation . . . . .	7
1.5 Work Remaining, Major Unknowns and Risks . . . . .	8
<b>2 Design &amp; Prototyping</b> . . . . .	<b>11</b>
2.1 Design . . . . .	11
2.2 Interfaces . . . . .	45
2.3 Prototypes and Tests . . . . .	52
<b>3 Design Validation and Product Acceptance</b> . . . . .	<b>75</b>
3.1 Safety . . . . .	75
3.2 Performance . . . . .	80
3.3 Reliability . . . . .	97
<b>4 Plans</b> . . . . .	<b>101</b>
4.1 Construction Plans . . . . .	101
4.2 Management Structures . . . . .	119
4.3 Milestones . . . . .	129
4.4 Construction Costs . . . . .	132
4.5 Maintenance & Operation Plans . . . . .	137
4.6 Assumptions, Dependencies and Caveats . . . . .	138
4.7 Risks . . . . .	141
<b>5 Lessons Incorporated</b> . . . . .	<b>143</b>
5.1 Mechanical Assembly Lessons Learnt . . . . .	143
5.2 Optical Assembly Lessons Learnt . . . . .	144
5.3 Camera Lessons Learnt . . . . .	144
<b>A Full Product Breakdown Structure</b> . . . . .	<b>149</b>
<b>B Full Work Breakdown Structure</b> . . . . .	<b>155</b>
<b>C Cost Estimates</b> . . . . .	<b>157</b>
<b>D Risk Register</b> . . . . .	<b>159</b>

---

<b>E Finite Element Analysis</b> . . . . .	<b>163</b>
<b>F Author List</b> . . . . .	<b>173</b>
<b>References</b> . . . . .	<b>175</b>
<b>Glossary</b> . . . . .	<b>179</b>

# 1 Summary and Introduction

## 1.1 Overall Concept

The Gamma-ray Cherenkov Telescope (GCT), a sub-consortium of the Cherenkov Telescope Array (CTA), proposes to construct 35 Small Size Telescopes (SSTs) for CTA, providing these as an in-kind contribution to the CTA Observatory (CTAO). The GCTs are designed to cover the energy range from about 1 to 300 TeV.

## 1.2 Summary of Design

The GCT telescope, illustrated in Figure 1.1, is a dual mirror Schwarzschild-Couder (SC) design with a primary mirror of diameter  $D_1 = 4$  m, a secondary mirror of diameter  $D_2 = 2$  m, a focal length of  $F = 2.3$  m and a focal ratio  $f = F/D = 0.57$ .

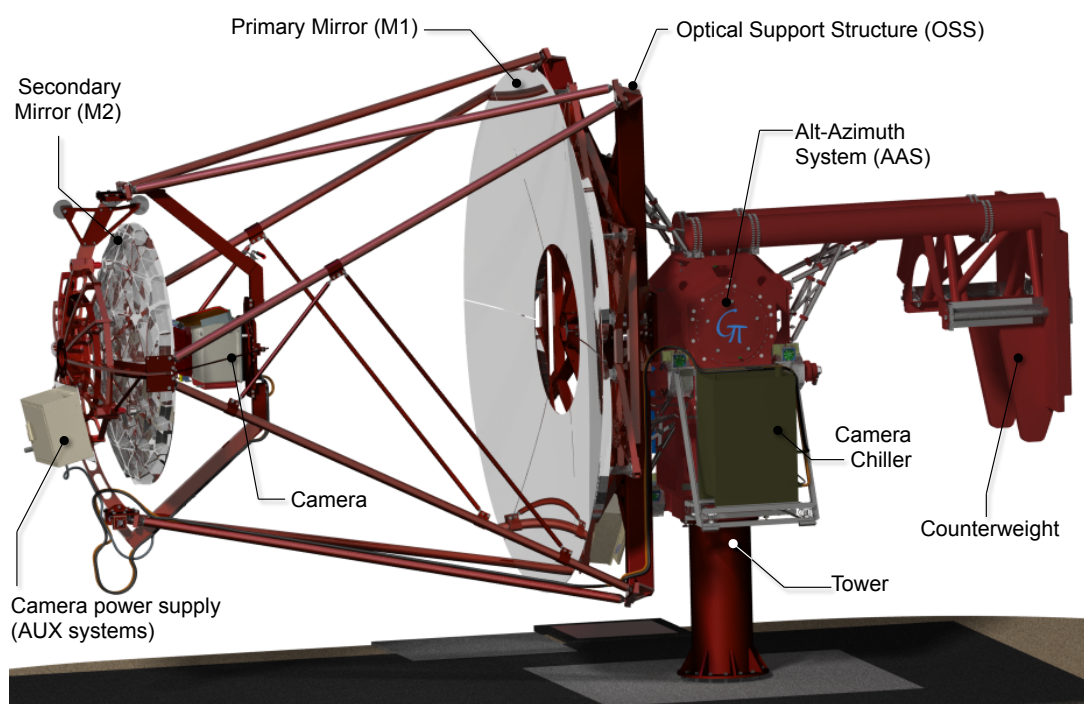


**Figure 1.1** – The GCT telescope with camera attached. Note, circular petals will not be used for the primary mirror segments in the final (Pre-Production and Production) design.

The small focal length of the telescope implies that the approximately  $0.2^\circ$  angular pixel size required by CTA for the SSTs is achievable with pixels of physical dimensions of 6 to 7 mm, while the dual mirror optics ensure that the point spread function (PSF) of the telescope is below 6 mm up to field angles of  $4.5^\circ$ . The field of view (FoV) of  $8^\circ$  required by CTA for the SSTs can therefore be covered with a

camera of diameter about 0.4 m, composed of 2048 pixels. This allows the use of commercially available photo-sensor arrays, significantly reducing the complexity and cost of the camera. Suitable packages consisting of multi-anode photo-multipliers (MAPMs) or silicon photo-multipliers (SiPMs) are under investigation for the GCT.

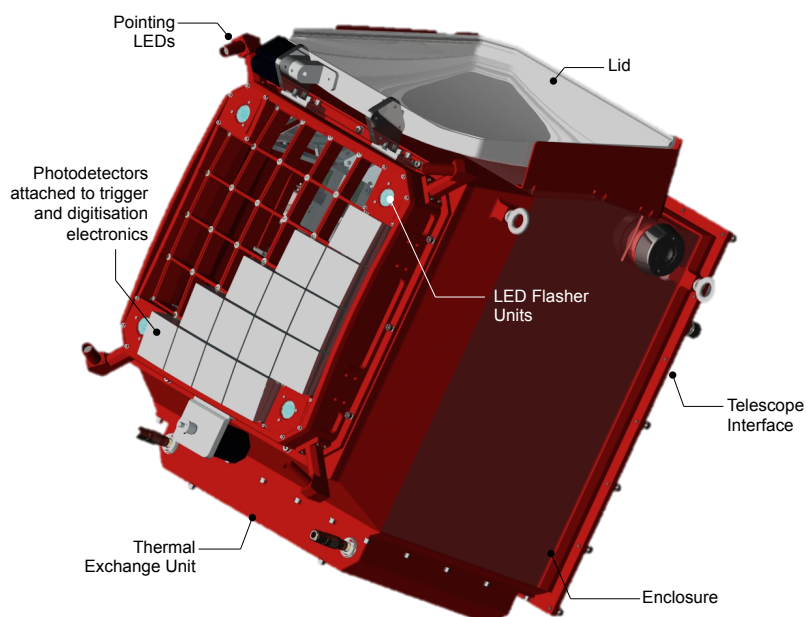


**Figure 1.2** – The GCT camera with primary components indicated. The CAD model shown is for the prototype camera equipped with MAPMs. In the final design it is likely that SiPMs will be used. In addition a protective window may be used to protect the photodetectors.

The GCT telescope structure consists of a foundation onto which a tower is mounted which supports the altitude-azimuth (alt-az) structure. Drive motors in the alt-az structure allow motion in the azimuth and altitude directions and are attached to the optical assembly and counterweight support structure. This holds the optical assembly, which consists of the primary dish support structure and the masts that hold the secondary dish and camera support structure, and the counterweights. The optical assembly and the primary dish support structures are separated to ensure that the stresses in the former do not directly influence the shape of the primary mirror. The camera is held by the secondary and camera support on a swivelling mount that provides easy access to the camera for installation and maintenance while minimising the risk to the mirrors during these operations.

The mirrors are constructed using either polished and coated aluminium or glass. The primary is formed of 6 petals, each of which can be mounted from ground level thanks to the design of the mirror support structure, which can be rotated about the telescope's axis during the installation procedure. Subsequent locking of the support ensures the necessary stability. The secondary mirror is constructed of 6 petals, but these are assembled mounted on the telescope as a monolithic unit. The possibility of construction of a truly monolithic mirror is under investigation. All primary segments and the secondary mirror are mounted via actuator systems which allow alignment of the mirrors and focussing of the telescope.

The GCT structure is designed to support the mirrors with the precision and stability required to ensure that the image quality required for CTA is achieved. Finite Element Analysis (FEA) has demonstrated that this is achieved for the full range of operating conditions required by CTA. FEA has also shown that the telescope can survive both the highest wind speeds to which it will be subjected on the southern site, either Aar in Namibia or Paranal in Chile, and the expected worst case seismic activity. The mechanical structure has been validated by an external reviewer.

The GCT camera is shown in Figure 1.2. This uses either MAPMs or SiPMs. A pre-amplifier amplifies and shapes the signals from the sensors before passing them to the readout chain, which is based around the 'TARGET' ASIC. The TARGET chip samples and digitises the incoming waveforms at a rate

of 1 Gs/s. The amplification and shaping provided by the pre-amplifiers for the MAPMs and SiPMs is chosen to ensure that both sensors provide suitable signals to the TARGET ASIC. Each TARGET chip has 16 parallel input channels and is placed on a board which provides the power necessary for the chip and the associated sensors. It also steers the readout and some control functions via a Field Programmable Gate Array (FPGA). Four such boards are grouped together to form a TARGET module, which provides readout for an  $8 \times 8$  array of pixels, attached via the pre-amplifiers to its front end. The attachment system allows the compensation of the 1 m radius of curvature of the focal plane on which the sensors lie, so that the TARGET modules can be placed in a rectilinear crate structure inside the camera body. The rear end of each of the TARGET modules is attached to the Backplane. This multi-layer printed circuit board takes the trigger signals from the TARGET modules and combines them in a large FPGA to form the camera trigger. Following a trigger, formed by requiring signals above threshold in a number of neighbouring trigger pixels (each of which is a  $2 \times 2$  block of camera pixels), readout is initiated and steered by two data acquisition (DACQ) boards which pass the waveform information provided by the TARGET ASICs to the remote CTA camera server in the central data acquisition and control room.

### 1.3 Summary of Plans

The GCT consortium is constructing two camera prototypes and one telescope prototype and will have completed these and tested them by the end of 2015. The two camera prototypes allow comparison of two types of photo-sensors, MAPMs and SiPMs. The first camera prototype is based on MAPMs and laboratory testing at the University of Leicester is planned to finish by the second quarter of 2015. The second SiPM camera prototype will be assembled and tested by late summer 2015. The prototype telescope structure will be assembled and tested in Meudon, Paris, throughout spring and summer of 2015. When this is finished, the MAPM-based camera will be mounted on the telescope and complete system tests will be performed. In late 2015, the SiPM camera prototype will replace the MAPM version and a further round of tests performed.

Using the experience and test results of the prototyping phase and industrial input on mass production processes, the GCT consortium will produce the final telescope and camera designs by early 2016. With these, 3 pre-production systems (telescope plus camera) will be implemented and assembled on the southern CTA site in early 2017. These 3 systems will be used to test and potentially refine the manufacturing and assembly techniques needed to produce and commission GCTs.

Funding for the pre-production systems is partially secured. Further funding applications for these telescopes will be made in 2015. The GCT consortium will then seek funding for the production of a further 32 GCTs, making any design changes necessary as a result of the pre-production phase. Together with the pre-production systems, which will be upgraded as needed to the final design, these will be the 35 GCTs on the southern CTA site, completed by mid-2020 and forming part of the CTAO.

### 1.4 Summary of Organisation

The GCT consortium is formed from two separate CTA prototyping efforts, the SST-GATE telescope team in France and the international CHEC camera team, and currently consists of the following partners: Adelaide University (Australia); Aix-Marseille Université/CPPM (France); Centre National de la Recherche Scientifique (France); Durham University (UK); Max-Planck Institut für Kernphysik, Heidelberg (Germany); Nagoya University (Japan); Observatoire de Paris (France); Universität Erlangen-Nürnberg (Germany) and the Universities of Amsterdam (Netherlands), Leicester (UK), Liverpool (UK) and Oxford (UK) The GCT teams have agreed a Declaration of Intent to formalise their cooperation to construct 35 GCTs for the southern site of CTA. Note that the terms SST-GATE and CHEC will occasionally be used in the TDR for aspects of the project which have received funding under these names.

The design of the telescope foundations, structure, mirrors and camera are the responsibility of the GCT sub-consortium. This group will construct and assemble the telescopes with their mirrors and cameras for CTA, but the foundations will be provided on the southern site by CTA. The interface to the

telescope structure is the point on the foundation at which power and access to the CTA control and data networks is provided. The GCT management structure, which is steering the design, testing, pre- and final production of the telescope systems, is shown in the organigram in Figure 1.3. This group is also responsible for managing the interfaces to the CTA infrastructure.

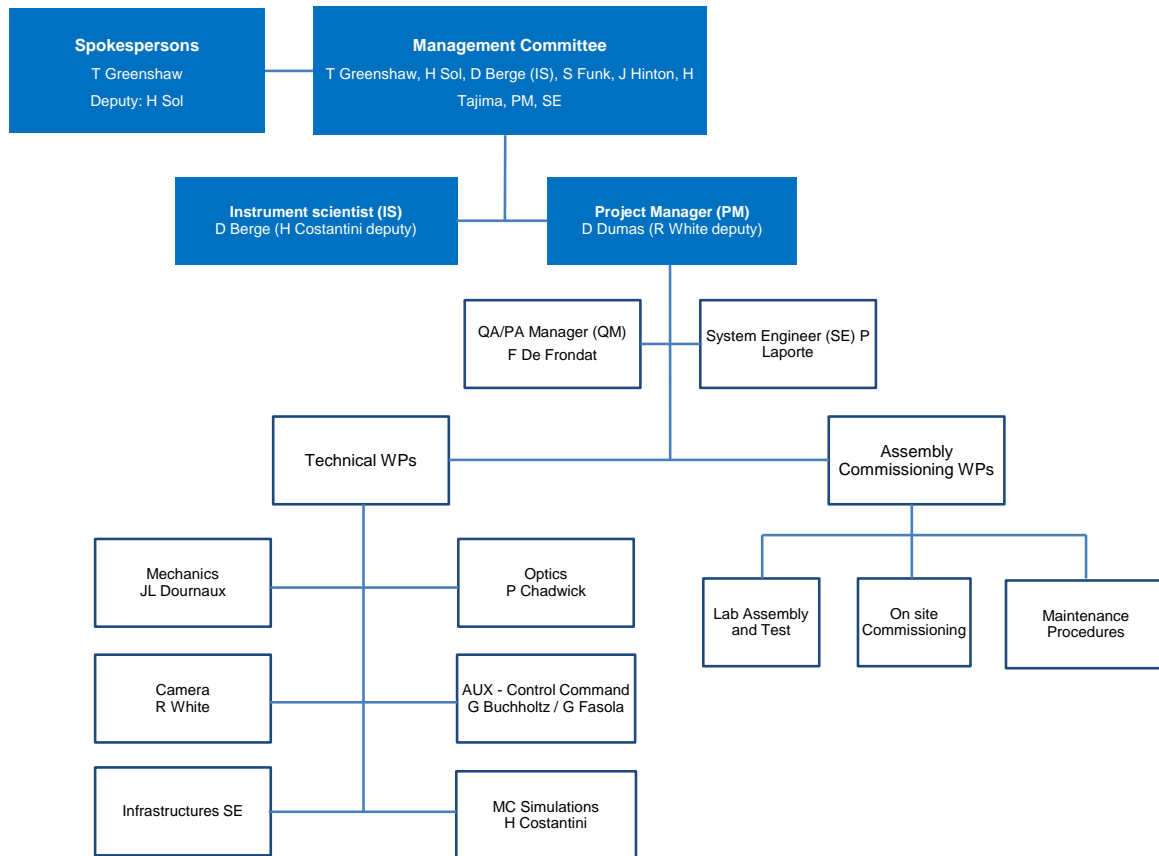


**Figure 1.3** – Top-level organization chart of the GCT consortium, including names of people assigned to different organizational roles.

## 1.5 Work Remaining, Major Unknowns and Risks

The design of the structure, mirrors and cameras for the prototype telescope is now complete. The structure and mirrors will be assembled on the Meudon site in 2015. Subsequent tests will cover all mechanical, optical and control elements of the telescope. A complete MAPM camera is currently being studied in Leicester, with all aspects of camera performance from sensor efficiency to camera cooling under test. When this round of studies is complete, the MAPM camera will be operated on the telescope. The SiPM camera will also be tested first in the Lab and then on the telescope. These studies, together with ongoing measurements of new sensors, will inform the design of the pre-production structure, mirror and camera. Several changes may be made during 2015, including to the motors for the Alt-Az system, the location and configuration of the cabinets containing the camera chiller and the telescope control electronics and the manufacturing process used for the mirrors. A major decision that must be taken is the sensor choice for the camera. Rapid development has been made in recent years and months, in particular in the performance of SiPMs. The GCT groups therefore wish to choose the sensors for the pre-production cameras at the latest possible time, to ensure the best possible devices are used. The GCT is working with other CTA groups to develop a SiPM specification suitable for several CTA applications. The goal of this work is to obtain the best possible sensor at a price that benefits as much as is possible from savings due to mass production.



Pre-production telescope structures and mirrors will be constructed in industry. Tenders for this stage of the project must be written, companies chosen for structure and mirror production, safety and quality assurance processes put in place and mechanisms for documenting all production and testing processes developed. Elements of the cameras will be constructed in industry, for example printed circuit boards and mechanical enclosures, but assembly, integration and performance verification will be carried out by GCT institutes. The pre-production phase will be used to ensure that sufficient institutes develop camera integration and testing expertise to allow the production run that follows to be completed in a timely manner: current plans foresee three assembly centres. The existence of these will also provide some mitigation against risks such as the failure of test apparatus or the loss of key personnel.

Some funding has already been obtained for the pre-production telescope series, other funding bids are in preparation and will be submitted in 2015. The GCT institutes are spreading the load for the funding of the pre-production telescopes beyond current boundaries. For example, in addition to French institutes, UK institutes are applying for funding for mirrors. This ensures a more equitable spread across the countries involved in the GCT pre-production phase. Any funding shortfall would of course represent a serious risk to the timely completion of the pre-production and following production phases of the project.

The pre-production telescopes will be shipped to the CTA southern site. The first will be delivered in the third quarter of 2016, and it is assumed that site negotiations and infrastructure preparations will be completed by then so that the telescope can be installed. The second and third telescopes will follow after three months. This period allows assembly and testing of the first telescope, but will also be used to train local technical staff in the assembly procedures and to refine the documentation provided for those staff. The effectiveness of this will be determined, and further improvements made, during the assembly and testing of the second and third telescopes.

There are many unknowns at this stage of the project. For example, without knowledge of the site, it is difficult to determine travel and subsistence costs for GCT staff working on site, and to estimate the costs of and request funding for local technical support.

Once assembled and individually tested, the pre-production GCTs will be operated as elements of the array of telescopes that will be on site at that time, allowing first experience to be obtained with CTA data acquisition and operation. Maintenance and operation procedures will be intensively tested and any lessons for the production telescope design drawn. Further design changes at this stage could result from the availability of improved, or lower cost, sensors. Again, with others in CTA, the GCT groups will continue to study any relevant new sensors that come on the market. Here, specifications such as sensor array size and output signal characteristics will ensure any camera redesign is kept to an absolute minimum.

The final phase of the GCT project involves increasing the pre-production construction, shipping, assembly and testing efforts by a factor of over 10, as the number of telescopes to be produced goes up from 3 to 32 and the time available for production of each telescope decreases. The experience of the pre-production phase will be invaluable in achieving this, but there will be new challenges. For example, as regards personnel: quality control, production monitoring and documentation will require additional full-time staff who in many cases must be appointed; a team of on-site technicians must be trained, hopefully involving personnel from the pre-production phase; and technical support at an adequate level for the construction period must be ensured at the institutes constructing and testing cameras and responsible for other elements of the telescope.

To summarise, the GCT group has designed a prototype telescope that satisfies the requirements for the SSTs of CTA. A programme has been developed that foresees the testing of that prototype, any necessary redesigns and then the construction of three pre-production telescopes on the CTA southern site. This pre-production series will help to develop the procedures for the subsequent production phase, in which a further 32 telescopes will be built, and establish operation of the telescopes as an array. In common with the entire CTA project, this is an ambitious programme, but adequately funded it will result in an instrument that will allow significant steps to be taken in our understanding of aspects of astroparticle and fundamental physics.



## 2 Design & Prototyping

This section describes the design of the GCT telescope and camera. The internal and external interfaces are outlined and a description of prototypes, testing and possible design changes given.

### 2.1 Design

The design of the Gamma-ray Cherenkov Telescope structure, mirrors and camera is described in this section, which includes a summary PBS and the key specifications for the GCT. The design presented here is that currently envisaged for the final GCT. Results from the development and test of the prototype presented in Section 2.3 are continually being taken into account. As prototype testing is not yet complete, modifications to the GCT design may still be made. Where clear design options exist, they are presented here.

#### 2.1.1 Introduction

The GCT follows a Schwarzschild-Couder (SC) optical design utilising primary and secondary mirrors, denoted M1 and M2 respectively, to focus Cherenkov light onto a camera located at the curved focal surface, as shown in Figure 1.1.

The use of a SC telescope for gamma-ray astronomy was first proposed in [1]. The authors showed that the dual aspherical mirror SC design [2, 3] provided excellent off-axis imaging performance and allowed for a reduction in the plate-scale of an  $8^\circ$  field-of-view telescope by a factor of  $\sim 3$ . This reduces the area that must be equipped with sensors, allowing the use of modern photosensors, such as multi-anode photomultipliers (MAPMs) and silicon photomultipliers (SiPMs). These offer reduced cost and/or improved performance with respect to the individual photomultipliers (PMs) used in the cameras of conventional IACTs. This was the motivation for using SC optics for the GCT. The approximate parameters of the telescope then follow from the CTA requirements for the SSTs and the dimensions of suitable commercially available sensors. Achieving an energy threshold of around 1 TeV requires a primary mirror of diameter  $D \sim 4$  m. Matching the available  $\sim 6$  mm pixel size of low-cost photosensors to the required angular scale of  $\sim 0.2^\circ$  (somewhat less than the full width half maximum of 1 TeV  $\gamma$ -ray images), requires a focal length of  $f \sim 2$  m and hence that  $f/D \approx 0.5$ . For such a system, obtaining a  $9^\circ$  FoV requires a  $\sim 30$  cm diameter camera with  $\sim 2000$  pixels.

Optimisation across a range of field angles resulted in a GCT design with a 2 m diameter M2, placed 3.56 m in front of a 4 m diameter M1. This creates a compact layout with a detector surface of radius of curvature 1.0 m, placed 0.51 m in front of M2. The effective focal length of the system is 2.283 m. Figure 2.1 illustrates the optical design under illumination at different field angles whilst the primary characteristics of the GCT design are listed in Table 2.1.

The GCT telescope itself is an altitude-azimuth design with a range in azimuth of  $[-90^\circ, 360^\circ]$  and of up to  $91^\circ$  in elevation, with a parking position of  $0^\circ$  in azimuth and elevation. The primary mirror M1 is 4 m in diameter and consists of six trapezoidal petals. The secondary mirror M2 is 2 m in diameter and consists of a monolithic surface. The focal plane is instrumented with a camera consisting of 32 photosensors and digitisation modules. Each module contains 64 pixels, with a nominal size of  $6 \text{ mm} \times 6 \text{ mm}$ . The GCT camera is compatible with both the GCT telescope structure and the ASTRI telescope structure

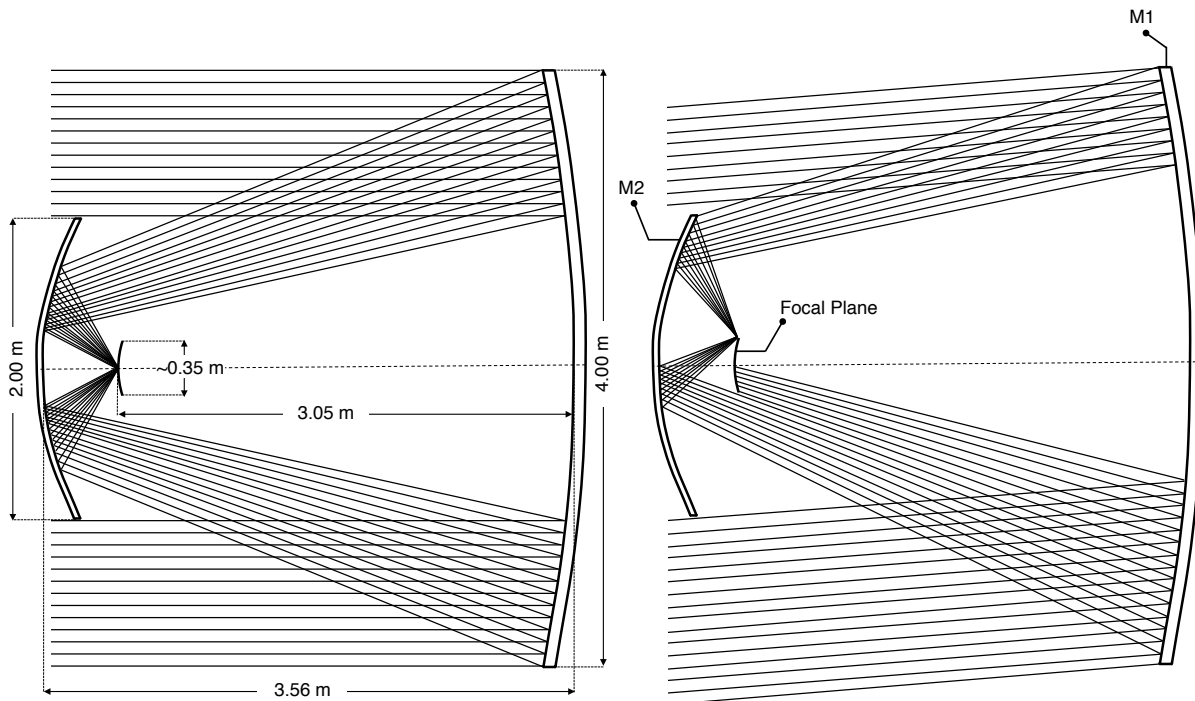


**Figure 2.1** – Optical layout of the GCT for the on-axis case (left) and at a field angle of 4.5° (right). At field angles larger than 2.3°, the detector leaves the shadow of M2 and creates additional obscuration.

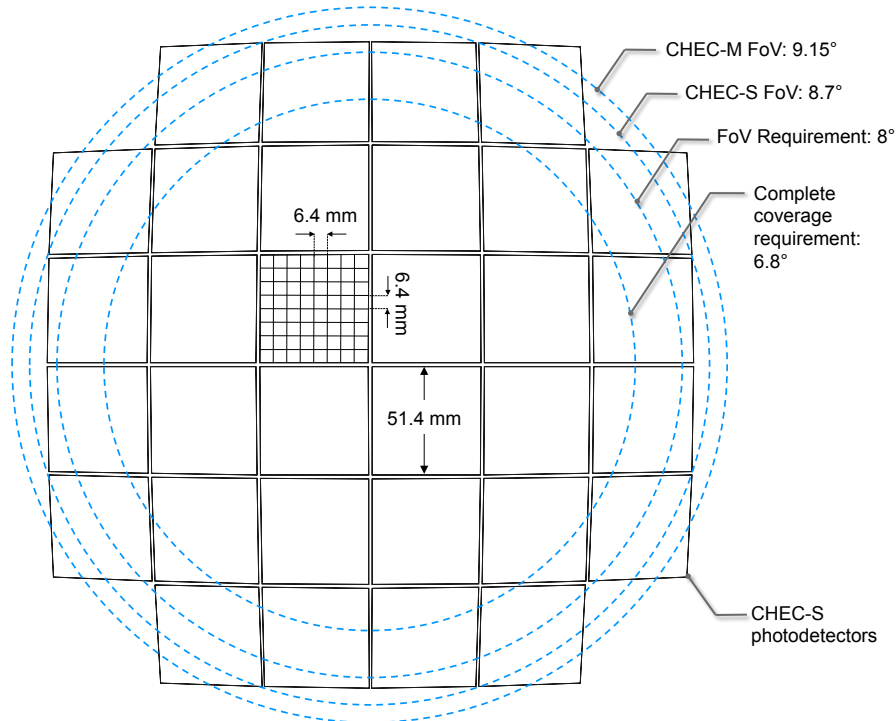


**Figure 2.2** – Illustration of the GCT focal plane instrumented with the CHEC-S photodetectors. Circles indicate the CTA requirements for the field of view and the area that must be fully instrumented (85% of the required field of view), and these are compared to the field of view of CHEC-M and CHEC-S. In this example the focal plane is populated with SiPM tiles, where a gap between modules of roughly 2.2 mm is required to position the detectors on the curved focal plane.

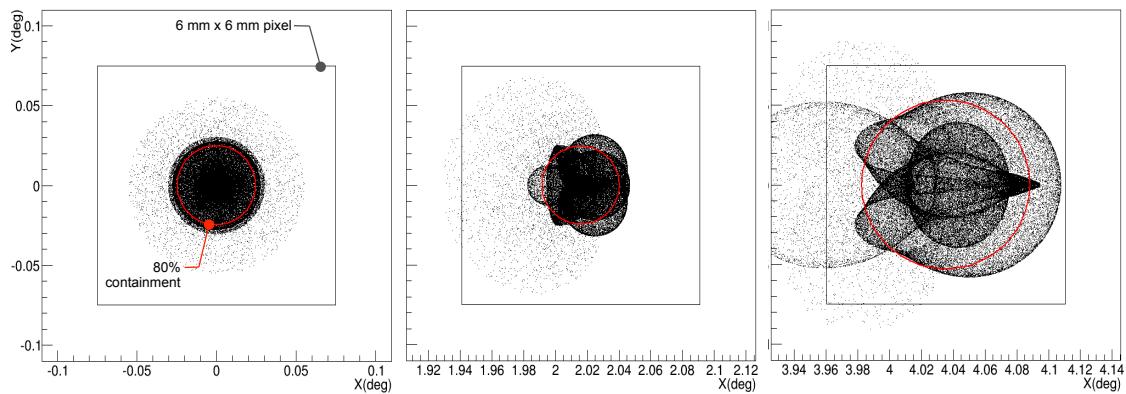


**Figure 2.3** – The Point Spread Function (PSF) as simulated using *sim-telarray* for field angles of 0°, 2° and 4°. In each case, the 6 mm×6 mm pixel outline is shown by the square, and the radius enclosing 80% of the total energy by the red circle.

(described in [4]). As indicated in Figure 2.2, the camera instruments a field of view of 8.5° to 9.2°; the exact value depends on the final choice of photosensor (see also Table 2.1).

Figure 2.3 shows the PSF of the GCT optical design at several field angles compared to the nominal camera pixel size. At all field angles the PSF is well contained within a single pixel, leaving adequate margin for manufacture and alignment tolerances. Including mis-alignment, the diameter of the circle enclosing 80% of the PSF for all field angles does not exceed 4.8 mm (corresponding to 7.3 arc minutes in the sky). Further details of the optical performance can be found in Section 3.2.2.

A high-level PBS chart is shown in Figure 2.4 and serves as a guideline for the detailed design descriptions throughout this section (see Section 4.2.1 for a more detailed PBS breakdown). The primary elements are explained below:

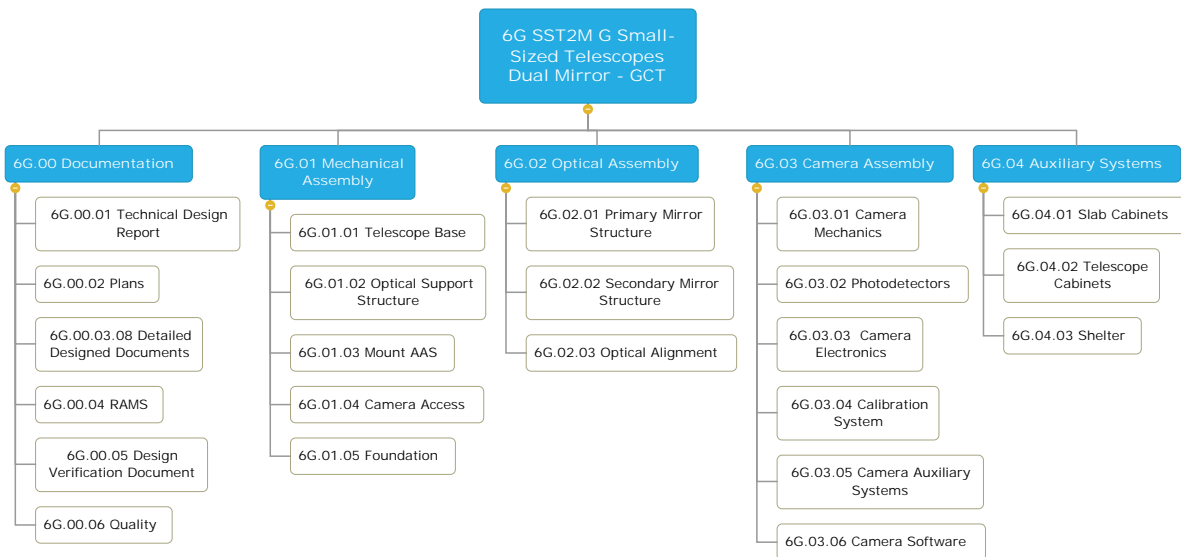


**Figure 2.4** – The high-level PBS chart for the GCT project.

- **PBS 6G.01 Mechanical Assembly:** comprising the telescope base (tower), OSS (Optical Support Structure), AAS (Alt-Azimuthal Structure), camera access mechanics, and the telescope foundation.
- **PBS 6G.02 Optical Assembly:** consisting of the primary and secondary mirrors and the optical

alignment system.

- **PBS 6G.03 Camera Assembly:** the Cherenkov camera including mechanics, photosensors, digitisation and readout electronics and the associated auxiliary systems such as the power supply and chiller.
- **PBS 6G.04 Auxiliary Systems:** consisting of the cabinets needed to house electronics and cabling across the telescope, both on the foundation, and on the telescope itself as well as the proposed protective shelter for the entire telescope.

**Table 2.1** – The main parameters of the GCT telescope and camera.

Optical Parameters		Mechanical Parameters		Camera Parameters	
FoV <sup>(a)</sup>	8.5° - 9.2° <sup>(b)</sup>	M1 diameter	4 m	Number of pixels	2048
Focal length	2283 mm	M2 diameter	2 m	Physical pixel size	6 x 6 mm <sup>2</sup> - 7 x 7 mm <sup>2</sup> <sup>(f)</sup>
F-number	0,58	Telescope size (width x height)	5.4 m x 8 m	Angular pixel size	0.15° - 0.2° <sup>(f)</sup>
Effective Plate Scale <sup>(c)</sup>	38.9 mm/°	Telescope and mirror mass	7.8 tons	Camera size	~ 0.35 m x 0.35 m x 0.5 m <sup>(g)</sup>
Throughput <sup>(d)</sup>	> 60%	Distance M1 to M2	3.56 m	Camera Mass	45 kg
PSF size on axis	0.05° @ 80% <sup>(e)</sup>	Distance M2 to camera	0.51 m	Camera power consumption	~ 450 W <sup>(h)</sup>
Focal plane radius	1.0 m			Pixels per electronics module	64
				Number of electronics modules	32
				Sampling rate	1 GSa/s <sup>(i)</sup>
				Readout window size	96 ns <sup>(j)</sup>
				Transmitted data	12-bits per sample, all samples
				Data rate (at 600-Hz)	~3 Gbps <sup>(k)</sup>

<sup>(a)</sup> The FoV is defined according to the CTA requirements as the average angular distance from the edge of pixels at the outside of the camera to the camera centre.

<sup>(b)</sup> The FoV will depend on the final sensor choice and associated mechanical tolerances. The range shown encompasses that achieved with CHEC-M and CHEC-S and includes some safety margin for potentially improved SiPM tile geometries.

<sup>(c)</sup> The plate scale becomes distorted off axis in an approximately linear way. The effective plate scale includes this distortion.

<sup>(d)</sup> The optical throughput of the telescope including vignetting (excluding photon detection efficiency in the camera).

<sup>(e)</sup> The size of the PSF is defined as the diameter of a circle containing 80% of the total PSF energy.

<sup>(f)</sup> The physical and angular pixel size depend on the final choice of photosensor.

<sup>(g)</sup> The final physical camera size will depend on results from the prototyping phase. 0.35 m refers to the size at the front of the focal plane.

<sup>(h)</sup> The final peak/observational power consumption will depend on electrical measurements made with the prototype cameras.

<sup>(i)</sup> The sampling rate is tunable, and whilst will nominally be operated at 1 GSa/s, can be altered down as low as 500 MSa/s.

<sup>(j)</sup> The readout window size is tunable in 32 sample blocks. Nominally 3 blocks per pixel will be read out. At a sample rate of 1 GSa/s this corresponds to 96 ns.

<sup>(k)</sup> The exact data rate depends on the number of samples read out, here a ~100 sample window is assumed.

## 2.1.2 Mechanical Design

The essential parameters driving the design of the telescope structure are given in Table 2.1.

The mechanical structure of the GCT telescope is described below according to the high-level PBS chart shown in Figure 2.4.

### PBS 6G.01.01: Telescope base

The telescope base consists of the tower, the foundation and the interface to the altitude-azimuth system (AAS). The tower is fixed on the foundation by 16 M20 stud anchors. Three of these bolts allow the vertical alignment of the tower. The AAS is attached to the tower using M16 bolts.

#### The tower (PBS item 6G.01.01.01)

The tower is the only stationary part of the telescope. It provides the interface between the foundation and the AAS via the azimuth drive. Finite Element Analysis (FEA) was used to compare various tower and fork combinations and demonstrated that the chosen long tower and short fork solution provides the best mechanical performance for a given cost, providing the most accurate telescope tracking/pointing, improved ease of assembly, lower mass and better maintainability (details can be found in the trade-off document and in section 2.3). The tower is a steel (E36) tube, 1210 mm long, with two flanges. The lower flange provides the interface to the foundation, while the upper facilitates the attachment of the AAS. The outer tower diameter is 470 mm, which is constrained by the diameter of the azimuth bearing. The tower has a thickness of 35 mm. This value was determined analytically by considering the compression due to the mass of the elevation subsystem, the bending related to wind loads and the buckling limits. Figure 2.5 shows the technical drawing of the tower and a picture of the tower on the foundation in Meudon, Paris.

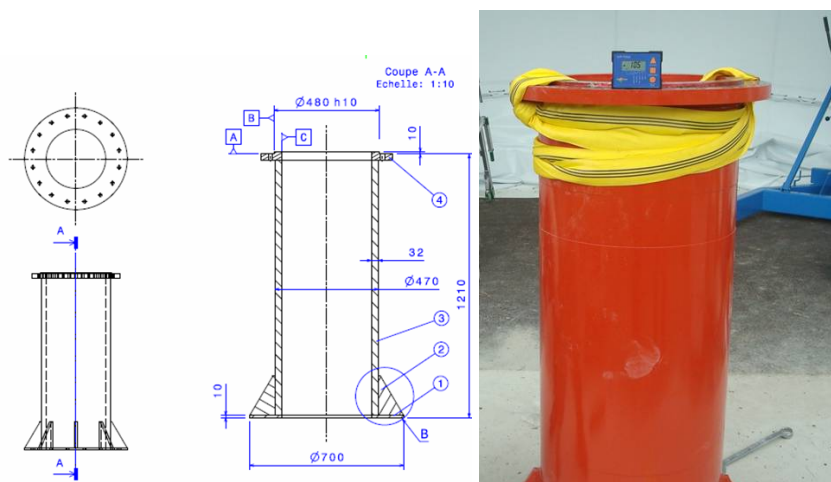


**Figure 2.5** – Drawing of the GCT telescope tower (left) and a picture of the tower installed and aligned on the foundation in Meudon.

### PBS 6G.01.02: Optical Support Structure

The Optical Support Structure (OSS) is the mechanical system that holds the mirrors, the camera and the counterweight. The latter balances the weight of the mirrors, their supports and the camera. The OSS is mounted on the AAS and is composed of three main parts:

- PBS 6G.01.02.01: the Mast and Truss Structure (MTS);
- PBS 6G.01.02.02: the M1 dish holding the primary mirror;

- PBS 6G.01.02.03: the Counterweight (CW).

### The MTS (PBS item 6G.01.02.01)

The two mirrors and the camera which together form the Schwarzschild-Couder optical design are supported by the MTS. A large number of FEA simulations were performed on this structure to ensure that it provides the required stiffness with the lowest possible mass and shadowing; the mass of the optical structure (M1, M2, camera, M1 dish and MTS) is only 2381 kg. The main torque caused by the structure is due to M2 at a distance of 4.78 m from the telescope's centre of gravity. FEA shows that the best MTS layout is the chosen Serrurier-like configuration. The principle of the Serrurier configuration is to minimise tilt and defocus due to gravity. Its advantage is that only slight decentering (within the performance budget allocation) is introduced when the elevation of the telescope changes. Thus, the optical performance remains unchanged whatever the elevation. In our case, an asymmetric configuration is chosen to counteract downward gravitational forces on the MTS. The structure was reinforced to reduce the decentering due to its weight.

The two functions of supporting the masts, camera and M2 and of holding the M1 mirror, which were initially all supported from the same dish, have been separated to increase the overall stiffness. This separation also decreases the loads on the primary dish and hence the deformations of M1 are also reduced. The telescope therefore has an MTS bottom dish which supports the both the M1 dish (which holds the primary mirror petals) and the MTS.

The MTS (figure 2.6) consists of:

- The MTS bottom dish (PBS 6G.01.02.01.01) is the interface between the M1 dish and the AAS. The MTS bottom dish is made of two flanges (one interfacing to the AAS and the other to the M1 dish) and two welded structures with two reinforced beams (the architecture of this structure has been optimized by FEA). All parts are made in steel (E36).
- The MTS top dish (PBS 6G.01.02.01.03) which is a monolithic welded structure in aluminium grade 6. The architecture of this structure has been optimized by FEA. The material has been chosen in order to reduce its mass. The MTS top dish holds M2 via three actuators and the camera support structure.
- The MTS arms (PBS 6G.01.02.01.02): these are tubes, assembled in a Serrurier configuration, which connect the MTS dishes. The arms consist of steel (E36) cylindrical section tubes with an external diameter of 71 mm. Mounting of the arms is done with spherical bearings with a self-lubricating steel-to-steel contact. The spherical bearings permit the compensation of the 17° angle between the axis of the MTS arms and their supports on the MTS bottom dish. Spacers are used at the connections to the MTS top dish in order to adjust the distance from the MTS bottom dish to the MTS top dish. Four reinforced cylindrical steel (E36) braces with an external diameter of 33.7 mm are added to reinforce the structure in the vertical direction.

The interface with the AAS system is via a flange connecting the bottom MTS dish and the bosshead. This flange has a large contact surface to decrease stresses and improve the dynamic behaviour of the mast.

Two reinforcing beams (PBS 6G.01.02.01.01.03) have been added to strengthen the telescope structure; one connects the MTS bottom dish to the upper face of the bosshead while the other attaches to the lower face of the bosshead.

Two electronic cabinets are fixed on the MTS, one at the back of the MTS bottom dish (PBS 6G.04.02.03) and one at the back of the MTS top dish (PBS 6G.04.02.04). Their weight has been taken into account in the FEA. Details on these cabinets are given in the auxiliary design section.

### The M1 dish (PBS item 6G.01.02.02)

The M1 dish (figure 2.8) holds the primary mirror. The structure is composed of nineteen parts which are bolted together. All these parts are constructed using steel (E36). They are:

- the central core with a hexagonal outer shape;



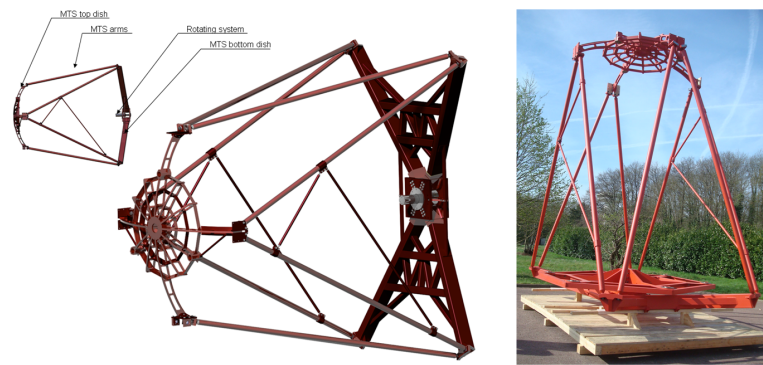


**Figure 2.6** – MTS system: CAD view (left) and picture of the MTS mounted on the Meudon site (right).

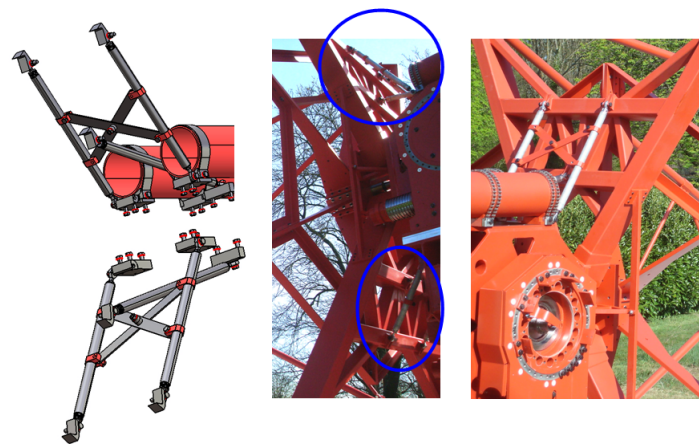


**Figure 2.7** – Reinforced beam structures: the CAD view of both reinforced structures is on the left, these structures are circled on the telescope picture in the middle, the left picture is a zoom on the upper reinforced structure.

- six arms bolted on to the outer faces of the central core;
- six reinforcing structures, made by welding L-shaped beams, which will fit between the arms;
- six interface flanges for the M1 panels.

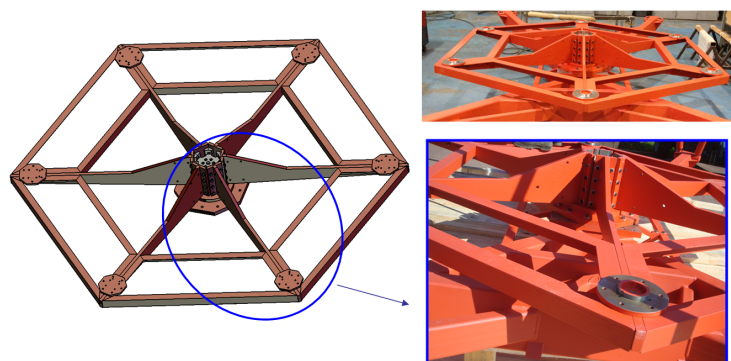


**Figure 2.8** – Left: CAD view of the M1 dish. Right: pictures of the M1 dish on the Meudon site

The M1 dish is separated from the MTS support structure for the reasons described above. The interface between the MTS bottom dish and the M1 dish is formed by a flange which has been designed to allow rotation of the M1 dish in order to ease the mounting and maintenance of the M1 petals and their

actuators. The petals forming M1 can therefore be mounted in turn from ground level and the dish clamped to ensure the alignment and rigidity of the structure.

The rotating system is composed of a steel axis with two cylindrical self-lubricating bushings. A steel pin defines the reference position of the M1 dish after each rotation of the system. The system is shown in Figure 2.9.

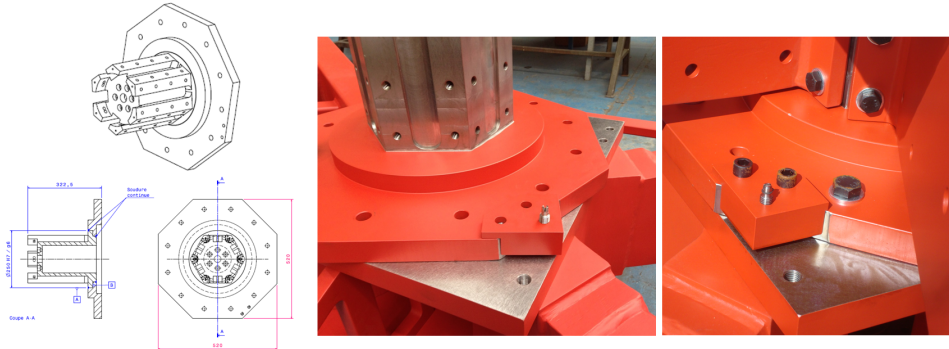


**Figure 2.9** – Left: CAD view of the rotating system. The picture in the middle shows the rotating system mounted on the dish and the right-hand picture the pin and reference point for clamping the dish

### The counterweight (PBS item 6G.01.02.03)

The counterweight is designed to balance the weight of the optical structure. It is manufactured using steel (E36) tubes (PBS 6G.01.02.03.01) with fixed and moveable masses (PBS 6G.01.02.03.02 and 6G.01.02.03.03) and is attached to one face of the bosshead via a structure (PBS 6G.01.02.03.04) composed of tubes (Figure 2.10).

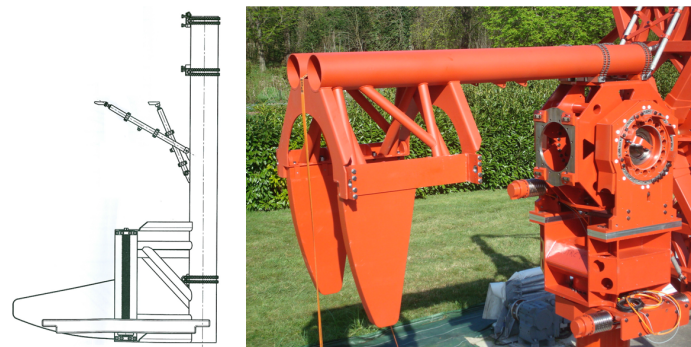


**Figure 2.10** – CAD view of the counterweight and picture of the counterweight mounted on the telescope structure in Meudon (without moveable mass).

Two kinds of weight are foreseen (Figure 2.11); two fixed weights with a total mass of 590 kg and two moveable weights with a total mass of 871.4 kg. All weights are machined from steel. Removal and/or movement of some weights is foreseen to allow the balancing of the telescope during assembly and maintenance. The movement system is composed of a worm gear and bush bearing.

### PBS 6G.01.03: Alt-Azimuth System Mount

The Alt-Azimuth System (AAS) Mount drives movement of the telescope in the azimuth and elevation directions. Figure 2.12 shows a CAD view of the system and the assembled AAS.

This system is composed of:

- PBS 6G.01.03.01: The structure including the two main mechanical parts of the AAS system - the fork and the bosshead - allowing rotation of the structure.

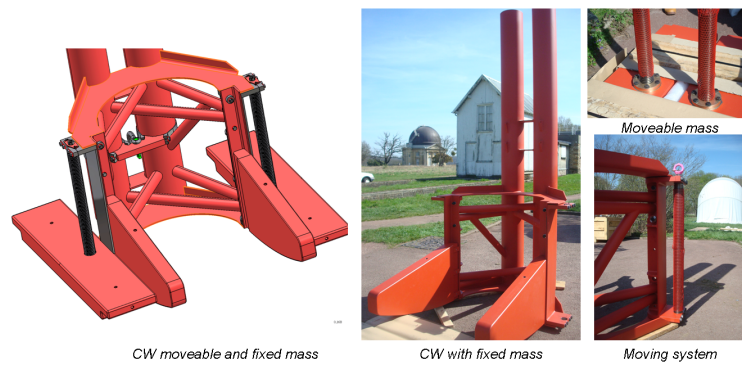


**Figure 2.11** – Fixed and moveable counterweight masses. CAD view and pictures of the weights on the Meudon site.

- PBS 6G.01.03.02: The azimuth and elevation drives which are the motors which power the movements of the telescope.

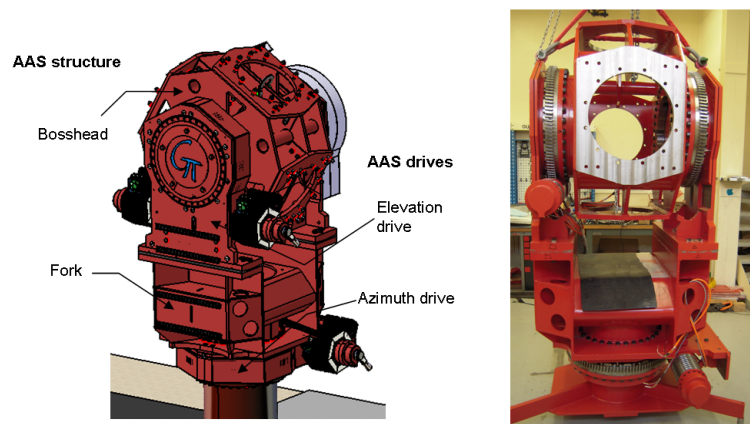


**Figure 2.12** – CAD view of the AAS composed of the structure and drives (left). Picture of the AAS mounted in the integration hall in Meudon (right).

Azimuth movement is provided by the rotation of the fork on the azimuth bearing. Rotation of the bosshead, held between the elevation bearings, allows elevation changes.

### The AAS Structure (PBS item 6G.01.03.01)

The AAS Structure consists of the two main mechanical parts of the AAS.

- PBS 6G.01.03.01.01: Fork  
The fork is U-shaped and connects the azimuth bearing to the two elevation bearings. FEA has shown that it achieves the required rigidity. The optimization of the fork is detailed in the mechanical prototype and test section of this report. Figure 2.13 shows drawings of the fork and a picture of the manufactured system.
- PBS 6G.01.03.01.02 Bosshead:  
The bosshead (Figure 2.14) is approximately octagonal in shape and has a four-fold symmetry with respect to the elevation axis. It connects the two elevation bearings, the optical structure and the counterweight. The bosshead consists of an assembly of lateral octagonal plates with a central hole connected by beams and plates. The octagonal structure has been designed to minimise the risk of manufacturing errors but also to reduce the number of spares needed. The bosshead rotation range is  $[0, 90^\circ]$ , so only a quarter of the crown bearing is used. If the bearing displays wear, rotating the assembly by  $90^\circ$  brings the unused section into play, doubling the lifetime of the bosshead.

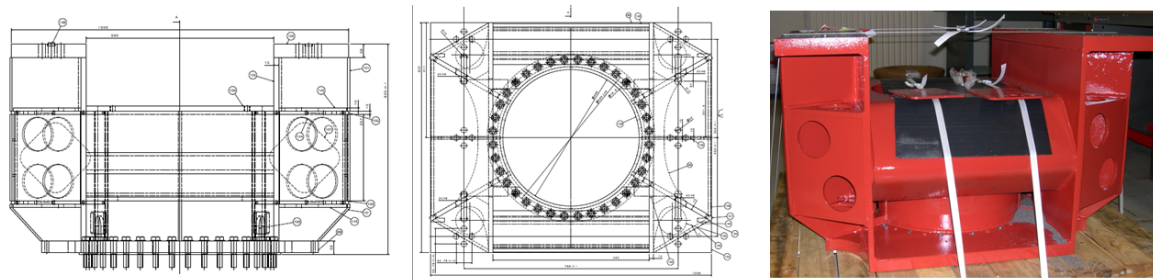


**Figure 2.13** – Drawing of the fork (left). Picture of the fork in the Meudon integration hall (right).

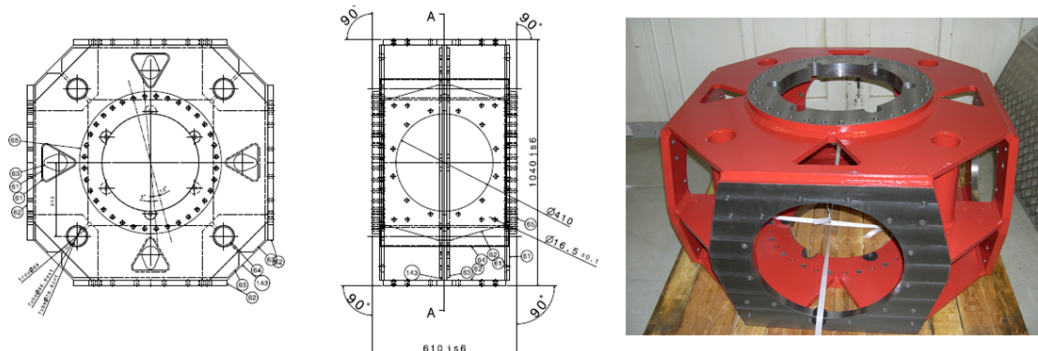


**Figure 2.14** – The bosshead (left picture), its location linking the elevation subsystem, the optical structure and the counter-weight (centre) and the manufactured part in the Meudon assembly hall (right).

### The AAS drive (PBS item 6G.01.03.02)

The designs of the AAS drives for the elevation and azimuth axes are similar. They consist of two parts.

- The drive system, composed of:
  - A ROLLIX slew bearing with nominal diameter 685 mm and 114 external teeth. The inclination of the teeth ensures an irreversible movement when used with the ROLLIX worm gear.
  - Absolute angle encoders with an integral bearing (HEIDENHAIN) which give the rotation of the slew bearing with an accuracy of  $\pm 2$  arc-seconds (via a bidirectional EnDat 2.2 29 bit numeric interface which allows 536 870 912 positions per revolution).
  - Safety systems such as limit switches and a brake to fix the bearing during installation and maintenance.
- The motor shaft, composed of:
  - A worm gear: a custom worm gear has been designed. A motor can be mounted at each end of the worm gear. Two motors are used due to size and performance requirements. The prototype motors provide some margin in terms of torque; the power required for the final telescope will be investigated using the prototype.
  - The motors: two motors are used on each axis. ETAL torque motors are used as they can ensure high and low speeds and provide no torque when no power is available. These allow the CTA requirements to be met. The maximum torque that the telescope drives must provide under various conditions (wind speed and elevation) is estimated to be 3 000 Nm with a 15% margin (at a wind speed of 50 km/h). Having a peak torque equal to 191 Nm and a continuous torque of 42 Nm, two motors are capable of moving the telescope whatever the conditions (the coefficient of friction = 0.28 and the mechanical reduction of the bearing is 114).
  - Rotary encoders from HEIDENHAIN which give the effective rotation of the motor (rotor versus stator). These have an accuracy of  $\pm 20$  arc-seconds (and a bidirectional EnDat 2.2 25 bit numeric interface which allows 33 554 432 positions per revolution).

The encoders must satisfy two constraints: they must fit into the volume available and provide the accuracy needed. During CTA operation, an accuracy of 1 arc-minute should be enough for tracking. For the prototype, the telescope will be equipped with an enhanced encoder with 3 to 5 arc seconds precision which will aid investigations of the mechanical performance of the structure during the test phase.

The drive system for one axis consists of one slew bearing with an encoder and a motor shaft formed of one worm gear with two motors and encoders (Figure 2.15).

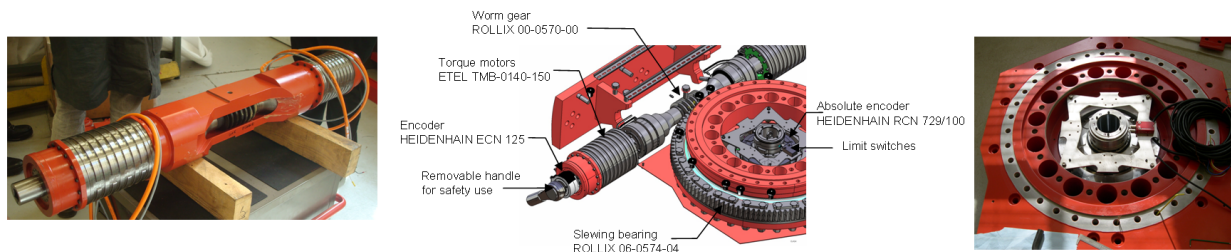


**Figure 2.15** – Centre: CAD view of the assembled drive system. Left: assembled motor shaft with motors, gear, encoders and cables. Right: bearing system with encoder and limit switches.

The azimuth and elevation drive systems are similar. The azimuth system consists of one drive with its motors, while the elevation system is has motors and a bearing on one side and only a bearing on the other. The use of similar systems for azimuth and elevation reduces manufacturing costs, simplifies maintenance and aids spares management.

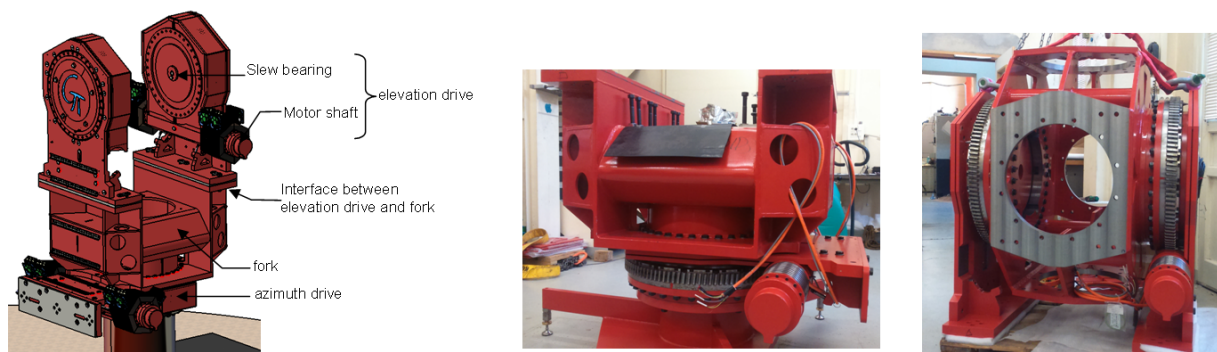


**Figure 2.16** – Left: CAD view of the azimuth and elevation drives. Centre: picture of the azimuth drive system with the fork mounted on it. Right: picture of the elevation drive system, with and without motors, fixed to the bosshead.

The azimuth system, which is attached to the tower, is horizontal, whereas the elevation drives are vertical (Figure 2.16). Covers that take account of these orientations are added to protect against water and dust, as are systems to manage greasing (Figure 2.17).

## PBS 6G.01.04: Camera Access

The camera support structure is composed of three sub-systems:

- PBS 6G.01.04.01: the Mechanical Support Structure which attaches the camera to the OSS.
- PBS 6G.01.04.02: the Camera Alignment and Fastening system, which allows adjustment of the position of the camera (tip, tilt and translation).
- PBS 6G.01.04.03: the Removal Mechanism which eases the mounting and maintenance of the camera.



**Figure 2.17** – Pictures of the lids covering the bearing. The rightmost picture shows the AAS mounted on the tower on the Meudon site.

The camera support is compatible with both the ASTRI and GCT cameras.

#### **The Mechanical Support Structure (PBS 6G.01.04.01)**

The camera is mounted between the primary and secondary mirrors at a distance of about 50 cm from the secondary reflective surface. It is attached to the Support Structure via a flange at the back of the camera (Figure 2.18 left). This structure is made of steel (E24, S235) plates. When the camera is in observing position, it is supported by two main arms, which are connected to the MTS dish, and by two lateral reinforcing tubes which provide additional stiffness to prevent movement under wind loads.

#### **The Camera Alignment and Fastening system (PBS 6G.01.04.02)**

The camera is attached using a system of bolts, spring washers and pins which allow adjustment of the position of the focal surface (Figure 2.18 centre). The system allows the setting of tip/tilt in a range of  $1^\circ$  and adjustment of the lateral position over a range of 6 mm.

#### **The Removal Mechanism System (PBS 6G.01.04.03)**

The camera support system has been designed to allow rotation about a pivot where the lower support arm attaches to the M2 dish. This makes it possible to access the camera from ground level to aid installation and maintenance (Figure 2.18 right). In its lowered position, the focal surface is horizontal and at a height of about 1 m above ground level.

To remove the camera, it is necessary to unlock the upper arm, then use the winch at the back of the M2 dish to lower the camera support structure. A cable and pulley system allows controlled movement. Once rotation is complete, the camera is supported by the lower arm and by the cable in tension. Stands are then inserted to support the lower arm/camera (not shown). The cable is then released and the camera can be removed.

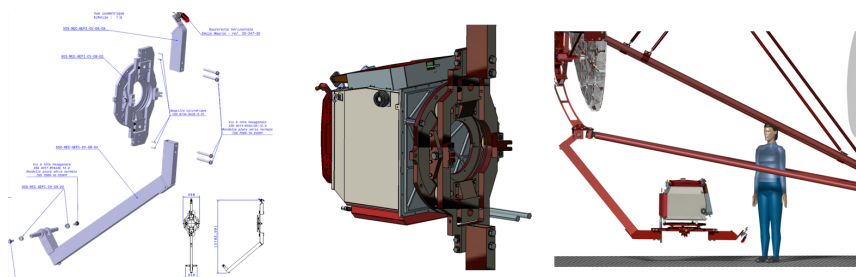


**Figure 2.18** – Left: CAD drawing of the camera support structure; Centre: view of the flange with the system to adjust the position of the camera focal plane; Right: camera in lowered position.

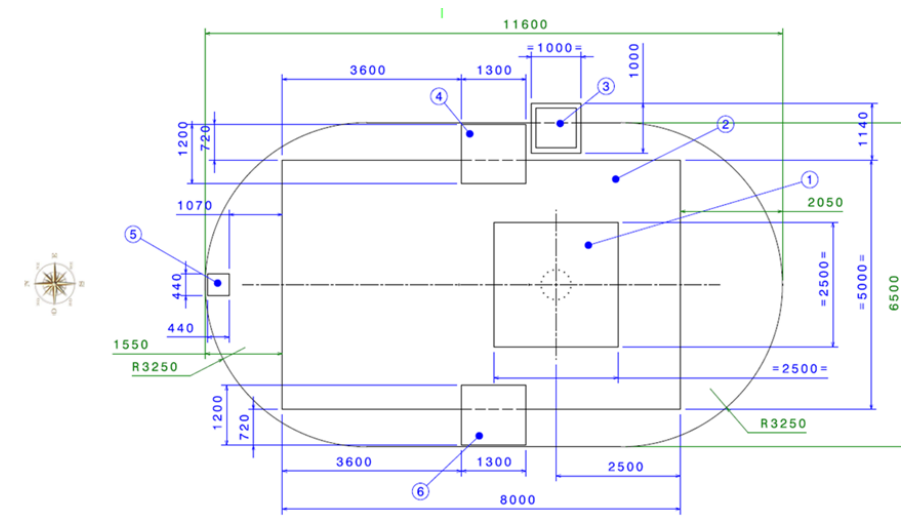


Figure 2.19 – The foundation on which the Meudon prototype stands.

### PBS 6G.01.05: Foundation

The foundation for the GCT is based on the foundation constructed for the prototype. The design may be updated depending on the conditions at the chosen site (e.g. soil type) and following prototype tests. Figure 2.19 shows the foundation in Meudon with the shelter area and the reinforced concrete slab required for the telescope (number 1 in the Figure). This is surrounded by a further concreted area (number 2) to aid work on the telescope. The GCT requires a reinforced square slab of dimensions  $2.5 \times 2.5 \text{ m}^2$  which can resist a torque of 105 kN/m (value with margin). Three points must be provided for the fixing of the shelter, two rectangles of size  $1.3 \text{ m} \times 1.2 \text{ m} \times 0.8 \text{ m}$  (numbers 4 and 6) and one square of size  $0.44 \text{ m} \times 0.44 \text{ m} \times 0.8 \text{ m}$  (number 5). The manhole for access to power and network cables (number 3) is close to one of the shelter slabs (number 4).

The GCT telescope can be installed on a foundation of this type for both southern sites foreseen for the SST array. The Paranal site in Chile is more susceptible to seismic activity than the Aar site in Namibia, but reinforcements have been added to the GCT structure which ensure that it can cope with the expected level of activity in both locations. (This conclusion has been validated by Josef Eder, who has carried out FEA for all CTA telescope prototypes.)

The mechanical structure installed on the slab is presented in figure 2.20.



**Figure 2.20** – The mechanical structure mounted at the Observatoire de Paris in Meudon.



### 2.1.3 Optical Assembly

The optical assembly consists of the primary mirror, secondary mirror and the optical alignment system.

The mirror surfaces are defined by a polynomial equation of degree 16. Their profiles are aspherical with substantial deviations from the closest spherical shape, as shown in Figure 2.21. The approximate radius of curvature of M1 is 9.7 m and that of M2 is 2.1 m. The deviations between the actual mirror shapes and the closest sphere have a maximum value of 2.8 mm (Figure 2.21 left) for M1 and 3.5 mm for M2 (Figure 2.21 right).

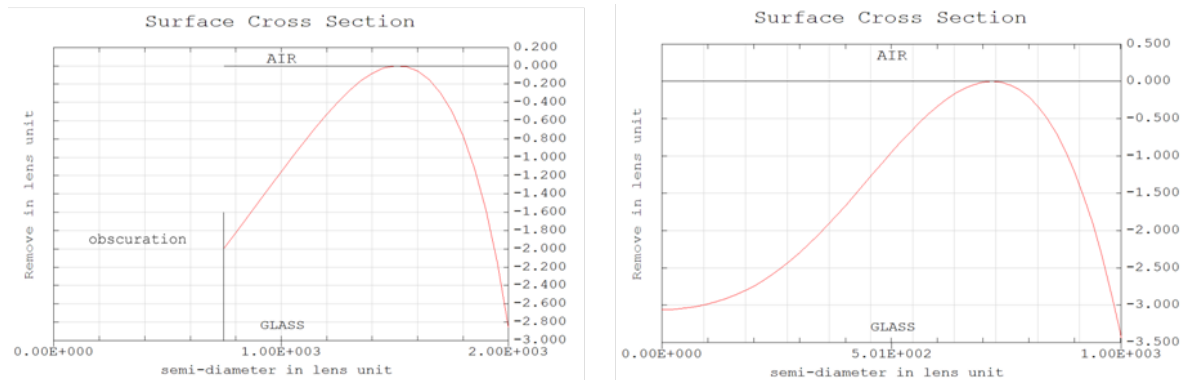


Figure 2.21 – Deviation of the curvature of M1 (left) and M2 (right) from spherical.

#### Primary Mirror (PBS item G6.02.01)

The primary mirror diameter of 4 m makes segmentation essential. M1 is therefore constructed of six petals which are aligned with respect to each other. The petals for the prototype and pre-production telescopes are shown in Figure 2.22. The prototype petals are smaller than those that will be used on the final telescope to reduce prototyping costs. Both petal sizes and shapes are described in the following.

- The prototype petal will fit inside a 1380 mm diameter circle (Figure 2.22 left).
- The final petal is trapezoidal. Its length in the radial direction is 1350 mm while the transverse dimension is 1991 mm (Figure 2.22 right).

Both sets of petals have been simulated using a Zemax model of the telescope (see Figure 2.23). The PSF size is very similar in both cases, as is the behaviour with tip-tilt and defocus. Thus the same alignment process can be used and the same accuracy is expected for the alignment. The only difference is the occurrence of dark wings in the outer regions of the PSF of the prototype due to the missing mirror surface. The mirror area corrected for obscuration with the final petals is 8.8 m<sup>2</sup>, while with the prototype petals it is 6.8 m<sup>2</sup>.

#### Secondary Mirror (PBS item G6.02.02)

M2 is also formed from six petals for the prototype telescope. Techniques for the manufacture of monolithic M2 mirrors are being investigated for the final telescope (see Section 4.1). Even though the prototype M2 is tessellated, the high-precision segments are bolted together and behave like a monolithic mirror. The dimensions of one petal are shown in Figure 2.24 and the secondary mirror after assembly is presented in Figure 2.25. The assembly is aligned using a set of precision dowels (2 per petal) and fixed with M16 bolts. The assembly will take place in a thermally controlled environment in order to decrease material stress and to optimise the mechanical precision. In the centre of M2 is a hole with a diameter of 100 mm to aid mirror alignment on telescope and to allow installation of pointing and calibration hardware. The reflecting surface of M2 has an area of 3.324 m<sup>2</sup> and the area of each petal is 0.554 m<sup>2</sup>.

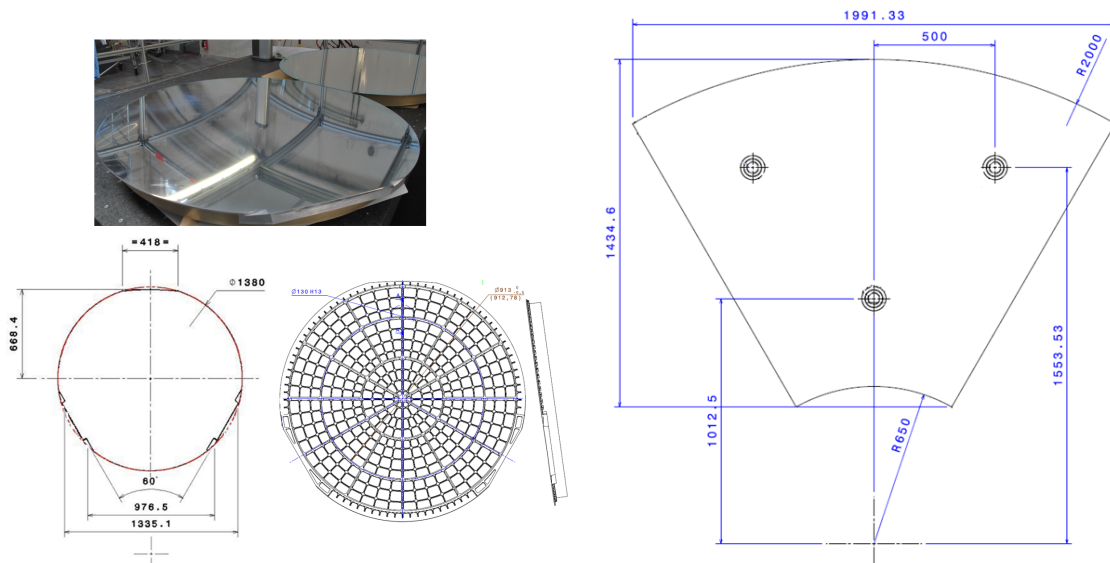


**Figure 2.22** – CAD drawing and pictures of the prototype M1 petals (left) and of the petals to be installed on the telescopes on the CTA site (right).

## Design of the Rear Surfaces of the Mirrors

The primary and secondary mirrors are manufactured in a three-step process developed and tested during the prototyping phase. These three steps are: the machining of aluminium bulk samples to the required shape; polishing to achieve low surface roughness and coating to improve the reflectivity. The process is described in Section 4.1 and tests to validate the process are detailed in Section 2.3.2.

In order to reduce the weight of the mirrors while maintaining the required rigidity, the rear surface of the petals is formed from cells delimited by stiffeners. The mirror deformation must stay under the waviness requirement of 50  $\mu\text{m}$  RMS for M1 and 20  $\mu\text{m}$  RMS for M2.

The mass goal for the final mirror is 28  $\text{kg/m}^2 \pm 10\%$ . The final M1 will have a mass of about 250 kg, and each petal a mass of about 40 kg. M1 is self-supporting. Its rigidity has been studied in the elevation range between 0° to 91°. M1 will have two kinds of stiffeners, primary stiffeners, forming large cells, to keep the mirror rigid during operation, and secondary stiffeners, forming small cells, to prevent deformation of the mirror during polishing. Several configurations have been analysed using FEA (Figure 2.26). The primary stiffeners are 5 mm thick and of depth 65 mm to 85 mm, depending on their position. The area of the primary cells is between 260  $\text{cm}^2$  and 490  $\text{cm}^2$ . The secondary stiffeners are 2 mm thick, and the area of the secondary cells is between 10  $\text{cm}^2$  and 30  $\text{cm}^2$ . FEA shows that the mirror deformation is less than 10  $\mu\text{m}$ . This is less than the waviness requirement of 50  $\mu\text{m}$ , including thermal effects. The stiffeners also act as radiators and help to dissipate heat from the mirror.

A similar structure has been designed for the rear of the secondary mirror. M2 will be manufactured in 6 petals and then assembled to form a monolithic, circular, self-supporting mirror. The size and shape of the cells have been designed using FEA and optimised to minimize the weight of the structure while maintaining its stiffness. Three gravitational load cases were considered in the first step of the optimisation process, in order to take into account the range of orientations of the mirrors. The resulting conceptual design consists of triangular shaped cells. In a second step, the position of the actuators was optimized by comparing the normal oscillation modes and gravity-induced deformations of the mirror for various locations of the actuators. Gravity-induced deformations of such a mirror are improved by a factor of 3 compared to those of a mirror with trapezoidal cells; the displacements perpendicular to the surface decrease from 200  $\mu\text{m}$  to about 60  $\mu\text{m}$  (Figure 2.27). The size of the stiffeners forming the boundaries of the cells depends on their position. The smallest ones have a height of 45 mm and a thickness of 3 mm, and the largest a height of 58 mm and a thickness of 5 mm. To reduce the time and cost of machining, the rear surface of M2 within a cell is flat. The thickness of the mirror, excluding the stiffeners, therefore varies, and has a minimum value of 5 mm. The area of the surface within the cell

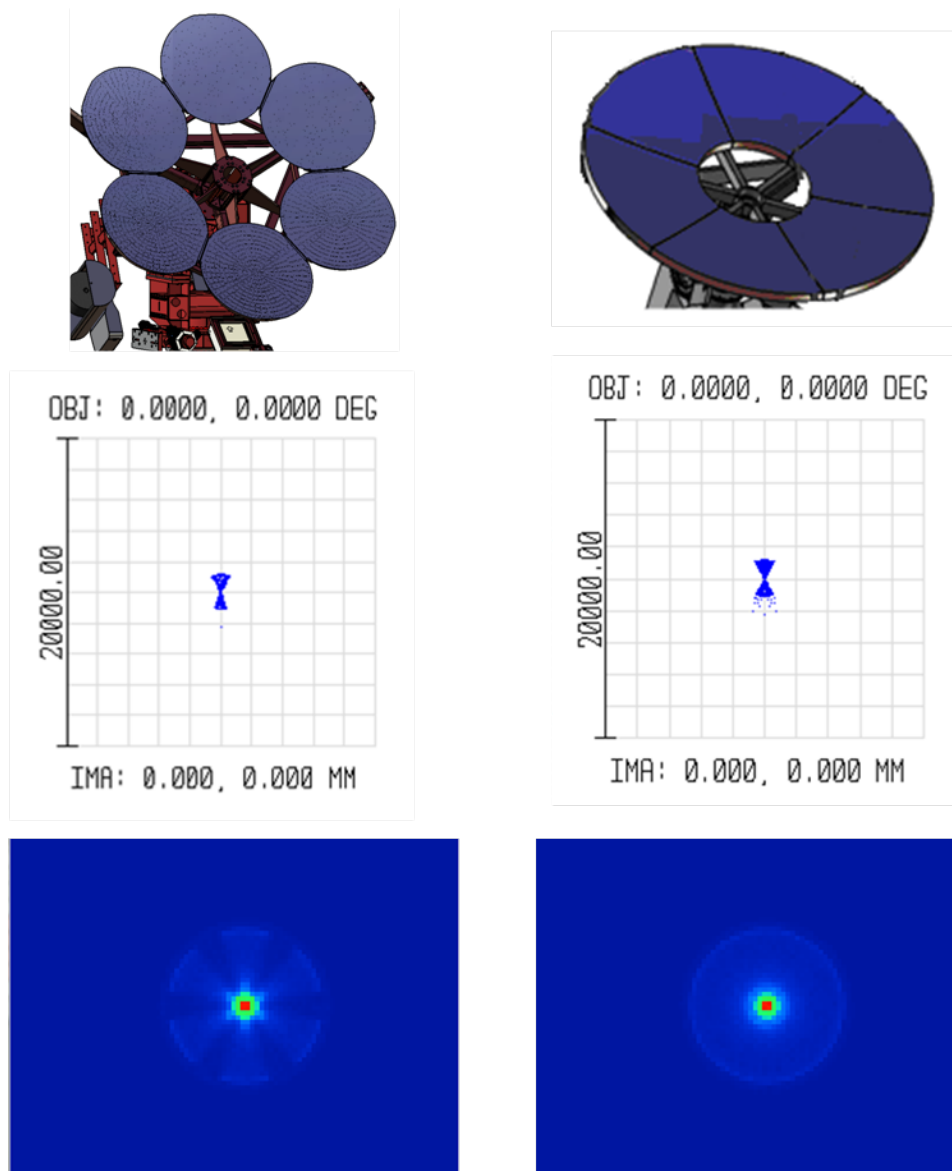


**Figure 2.23** – Simulated PSF of the M1 petals foreseen for the prototype and for the final telescope. The left column shows results for the prototype petal and the right for the final petal. The top row shows the M1 mirror with different petal sizes; the middle row shows the spot diagrams for one petal; the bottom row shows the PSF for the complete primary mirror.

varies from 150 cm<sup>2</sup> to 320 cm<sup>2</sup> (see Figure 2.24).

Each secondary mirror segment is machined from a parallelepiped with dimensions 1000 × 1000 × 150 mm<sup>3</sup>. The mass of the M2 segments is 25 kg.

### Optical Alignment (PBS item 6G.02.03)

The optical requirements for atmospheric Cherenkov telescopes in general and the GCTs in particular are less stringent than those of traditional optical telescopes (see mirror tolerances in Table 2.2). This allows the use of less demanding machining, polishing and coating processes.

Due to the dual mirror design, the GCT is more difficult to align than a Davies-Cotton telescope. Table 2.2 lists the tolerances in the alignment of each petal of M1. The alignment process is described in more detail in section 2.3. Briefly, once the optical and mechanical telescope axes have been brought into coincidence, the first step is the relative alignment of the M1 petals. The second step is the alignment of M2 with respect to M1 and then with respect to the camera. Using a laser beam to define the axis

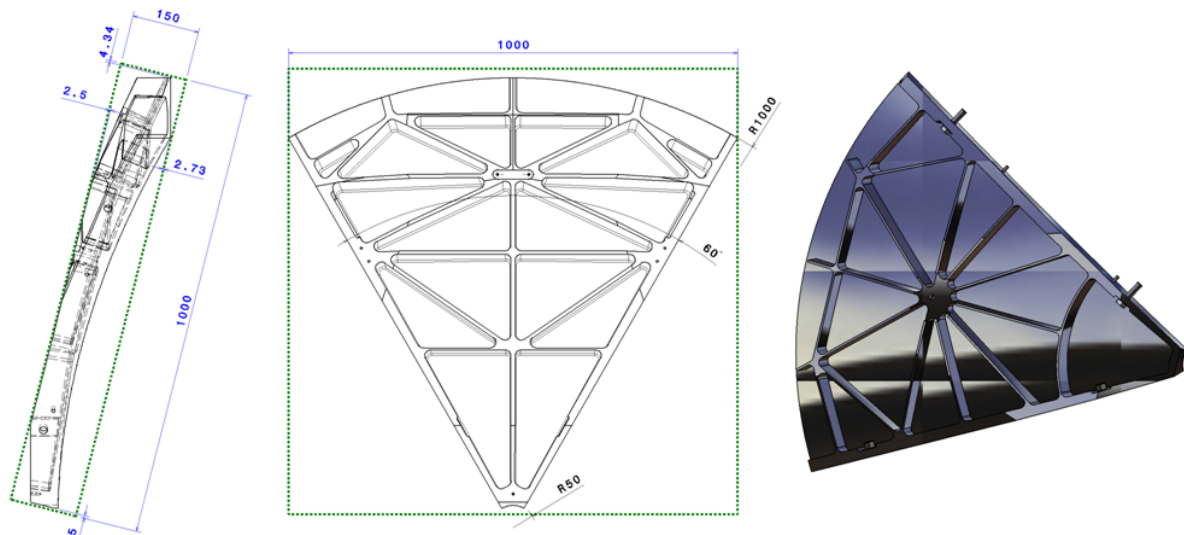


Figure 2.24 – A secondary mirror petal.

**Table 2.2** – The table presents the tolerances in the optical design: mirror tolerances for manufacture are specified for the whole mirror (M1 and M2) and the tolerances for tessellated mirrors are used for the alignment. Tolerances were modeled using the Zemax parameter TEZ1 and are based on the Zernike surface model. Deviations for Zernike coefficients between 2 and 21 describe the “surface waviness” and the higher Zernike terms, between 22 and 231, describe the “surface irregularity”.

Mirror tolerance		Tolerance for tessellated mirrors	
Designation	Value	Designation	Value
Surface waviness M1	50 $\mu\text{m}$ RMS	Element decentering M1	+/- 2 mm
Surface waviness M2	20 $\mu\text{m}$ RMS	Element decentering M2	+/- 2 mm
Surface irregularity M1	1 $\mu\text{m}$ RMS	Element tilt M1	+/- 1'
Surface irregularity M2	1 $\mu\text{m}$ RMS	Element tilt M2	+/- 3'
Radius deviation M1	+/- 10 mm	Element tilt detector	+/- 5'
Radius deviation M2	+/- 3 mm		
Radius deviation detector	+/- 3 mm		

of the telescope, a source is placed at 30 m in front of M1 on this axis to illuminate the M1 petals. The alignment of the petals is then carried out using the PSF visible on a screen located at the focal plane of M1 (i.e. about 5 m from M1). When compared with calculations, the PSF of a petal reveals the presence of tilts or tips, as has been demonstrated by alignment tests performed on a 1/10 scale optical model of the telescope. This requires that some optical elements such as the laser, targets, screen and tip-tilt mounts must be attached to the structure. These optical elements are fixed to the M1 and M2 dishes.

In order to align the petals, three actuators are used per M1 petal, and three for the complete M2. The specifications of the actuators (see Table 2.3) must be compliant with the alignment tolerances. These actuators are also used to fix the mirror on its support (see Section 2.2). The M2 actuators connect M2 to the MTS top dish, while the M1 actuators connect the M1 panels to their triangular supports.

A study has been made in collaboration with two companies to choose suitable actuators. The conclusions reached with both companies were similar: in order to decrease the cost, the same actuators will be used for both mirrors. In this way, the number of spares needed is reduced and the production process and maintenance are simplified. During the prototyping phase, studies will be performed to see if further unification of actuator types can be carried out with other CTA telescopes.

The actuator chosen consists of a ball screw attached to the back of the mirror with springs to maintain

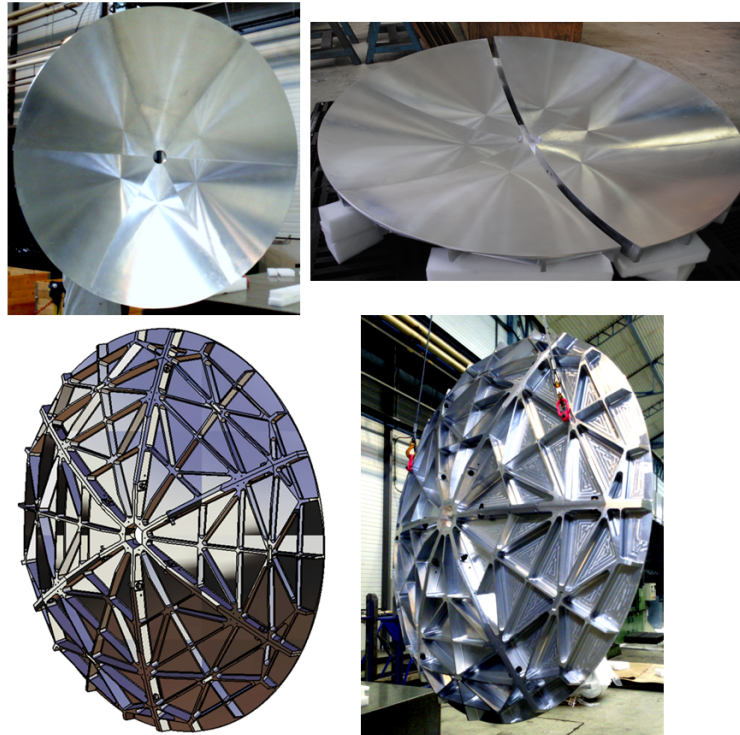


**Figure 2.25** – The secondary mirror. Top row: pictures of the reflective surface with M2 fully assembled (left) and partially assembled (right). Bottom row: CAD diagram (left) and picture (right) of the rear surface.

**Table 2.3** – Specifications for the actuators, described in detail in the internal document 503-OPT-GEPI-SP-0003-Actionneurs.

Specifications	Value for M1	Value for M2
Stroke	+/- 25 mm	+/- 15 mm
Precision	25 $\mu$ m	125 $\mu$ m
Maximum speed	1 mm/s	1 mm/s

the contact and absorb stresses, a stepper motor to create the displacement and encoders to measure precisely the actuator position.

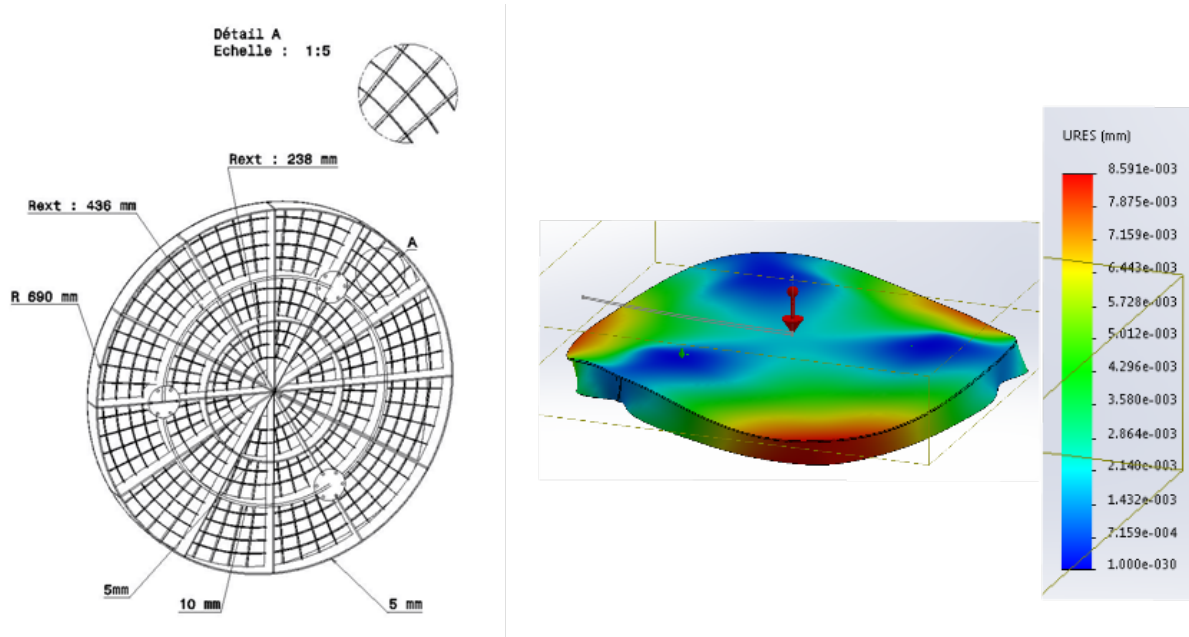


**Figure 2.26** – Design of the M1 petal rear surface. View of primary and secondary stiffeners on the M1 rear structure (left); FEA simulation of one primary mirror petal – deformation scale is in meters (right).

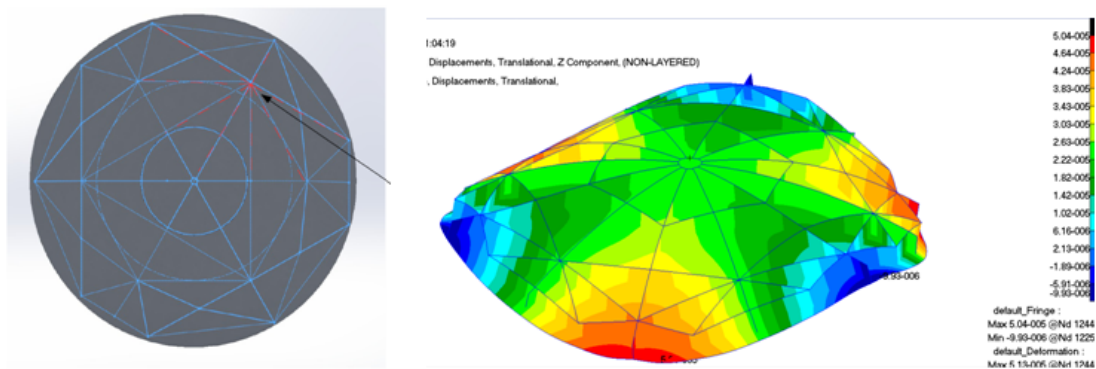


**Figure 2.27** – Design of the rear surface of M2. View of triangular cells of the M2 rear surface (left); FEA of M2 deformation – scale is in meters (right).

## 2.1.4 Camera Design

The GCT camera is a low-cost, high-reliability, high-data-quality solution for the SST-2M. It provides full waveform information for every camera pixel in every event. The camera is fully sealed, excluding the possibility of dust and moisture ingress. To achieve this at low cost, some ease of maintenance is sacrificed by a particularly compact mechanical design trading accessibility of electronics components against compactness.

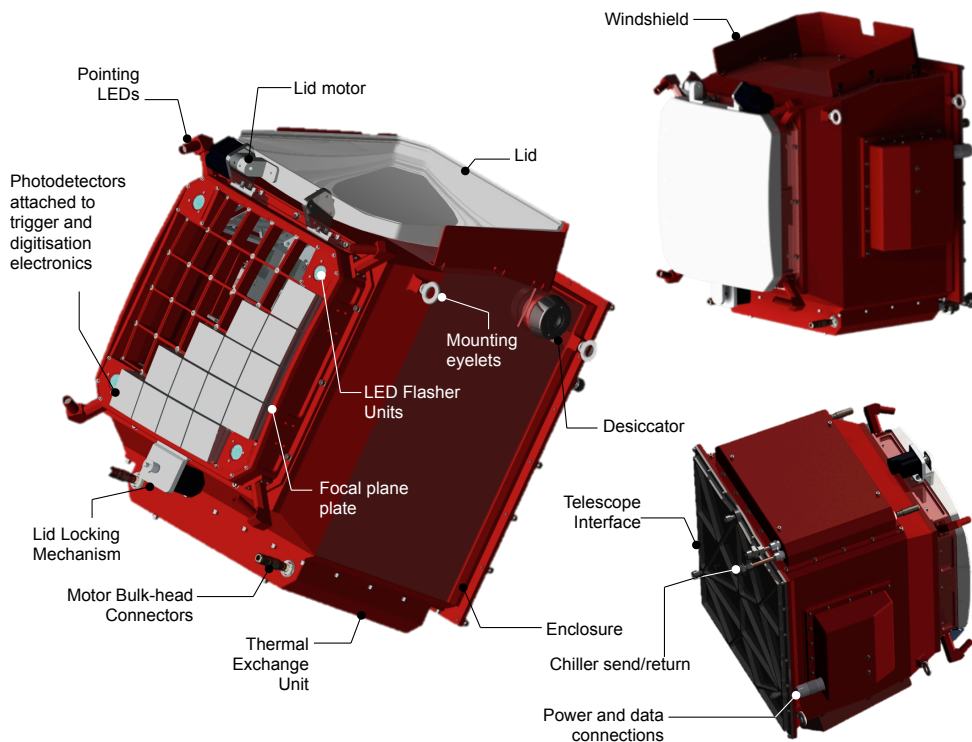


**Figure 2.28** – A detailed overview of the GCT camera. The CAD model shown is for the prototype camera equipped with MAPMs. In the final design it is likely that SiPMs will be used. In addition a protective window may be used to protect the photodetectors.

The GCT camera is designed to record flashes of Cherenkov light lasting from a few to a hundred nanoseconds, with typical RMS image width and length of  $\sim 0.2^\circ \times 1.0^\circ$ , and has a  $8.5\text{--}9.2^\circ$  field of view. The physical camera geometry is dictated by the telescope optics: a curved focal surface with radius of curvature 1 m and diameter  $\sim 35$  cm. The required performance and operational conditions for the camera are defined in the CTA SST requirements document [5]. The essential camera parameters are listed in Table 2.1.

A CAD image of the GCT camera is shown in Figure 2.28, the camera architecture is shown in Figure 2.29. The principal components of the camera are the PBS items G6.3.1 to G6.3.6 in Figure 2.4 (and a more detailed PBS chart is given in Figure 4.9 further down):

- **PBS 6G.3.1 Camera Mechanics:** The camera mechanics consist of an internal rack to support the electronics, a sealed enclosure, a thermal exchange unit and a lid assembly.
- **PBS 6G.3.2 Photodetectors:** The photodetectors will be either MAPMs or SiPMs, to be fixed after the prototype (Pre-Construction) phase. In both cases, 64-pixel tiles would be utilised. This PBS item also includes the circuitry required to bias the photodetector.
- **PBS 6G.3.3 Electronics:** A range of different components are summarised under this item, namely front-end buffers (pre-amplification units to be directly attached to the photodetectors, for

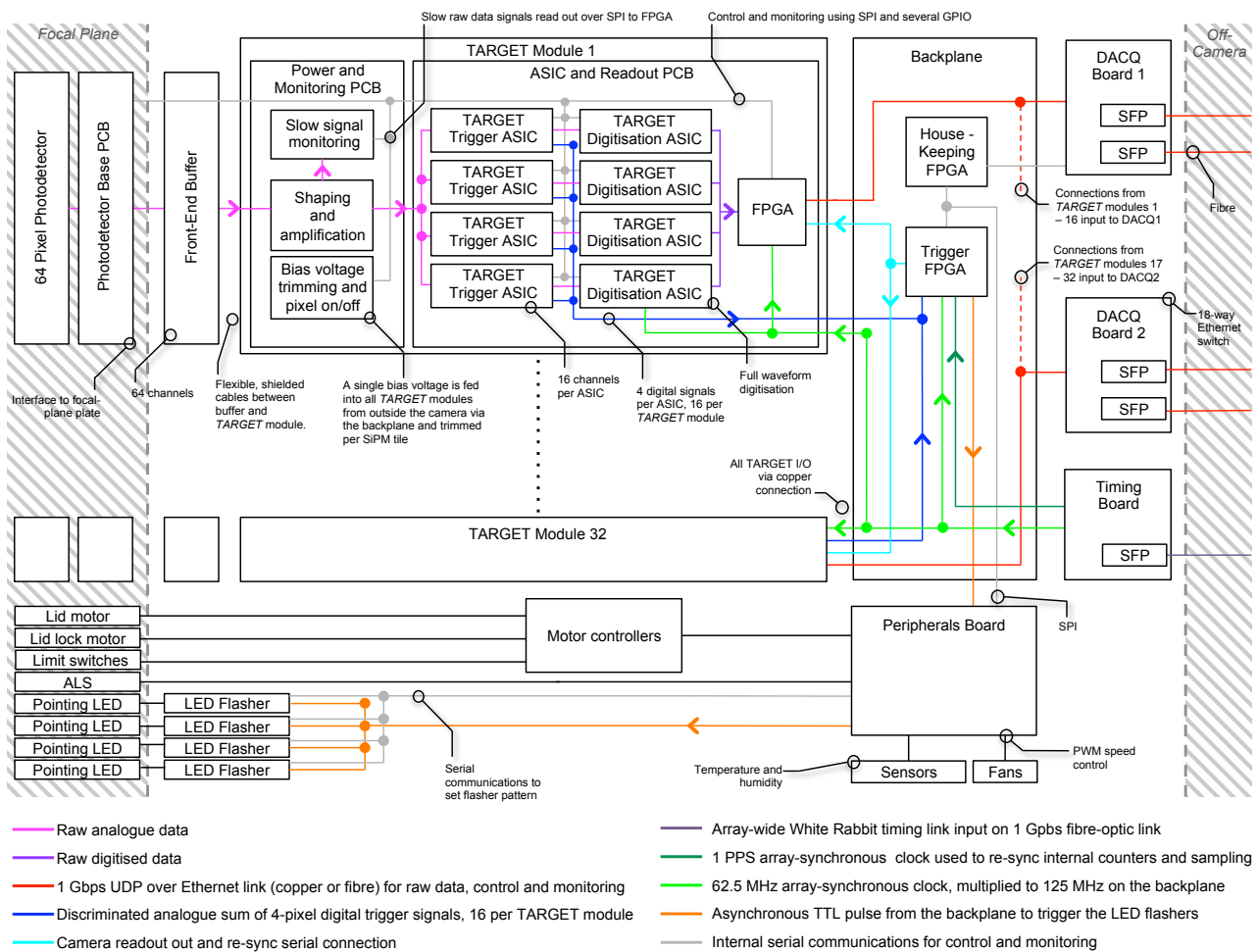


**Figure 2.29** – A schematic showing the logical elements of the GCT camera, the communication between those elements, the raw data flow through the camera, the trigger architecture and the clock distribution scheme. Power distribution is excluded for simplicity.

signal-integrity reasons), readout and digitisation units (*TARGET* modules [6]), the backplane for triggering and signal routing, data and control interface cards (DACQ boards), the peripherals board and finally the internal cabling.

- **PBS 6G.3.4 Calibration System:** LED flasher units to flat-field the camera and monitor linearity, plus continuous positioning LEDs to aid with the absolute pointing calibration of the GCT.
- **PBS 6G.3.5 Auxiliary Systems:** The camera power supply and the chiller system to provide cooling.
- **PBS 6G.3.6 Software:** The camera readout and control software. All activities here will be coordinated with the common CTA ACTL software group and are not outlined further in this section.

### PBS 6G.3.1: Camera Mechanics

The mechanics for the GCT camera consist of: an internal rack, an external enclosure, a thermal exchange unit and a lid assembly. In turn, the enclosure consists of a protective entrance window, a focal-plane plate for holding the photodetectors, a 'backplate' for mounting to the telescope and the external case walls. Figure 2.30 provides an overview of these elements and the interface to the camera electronics.



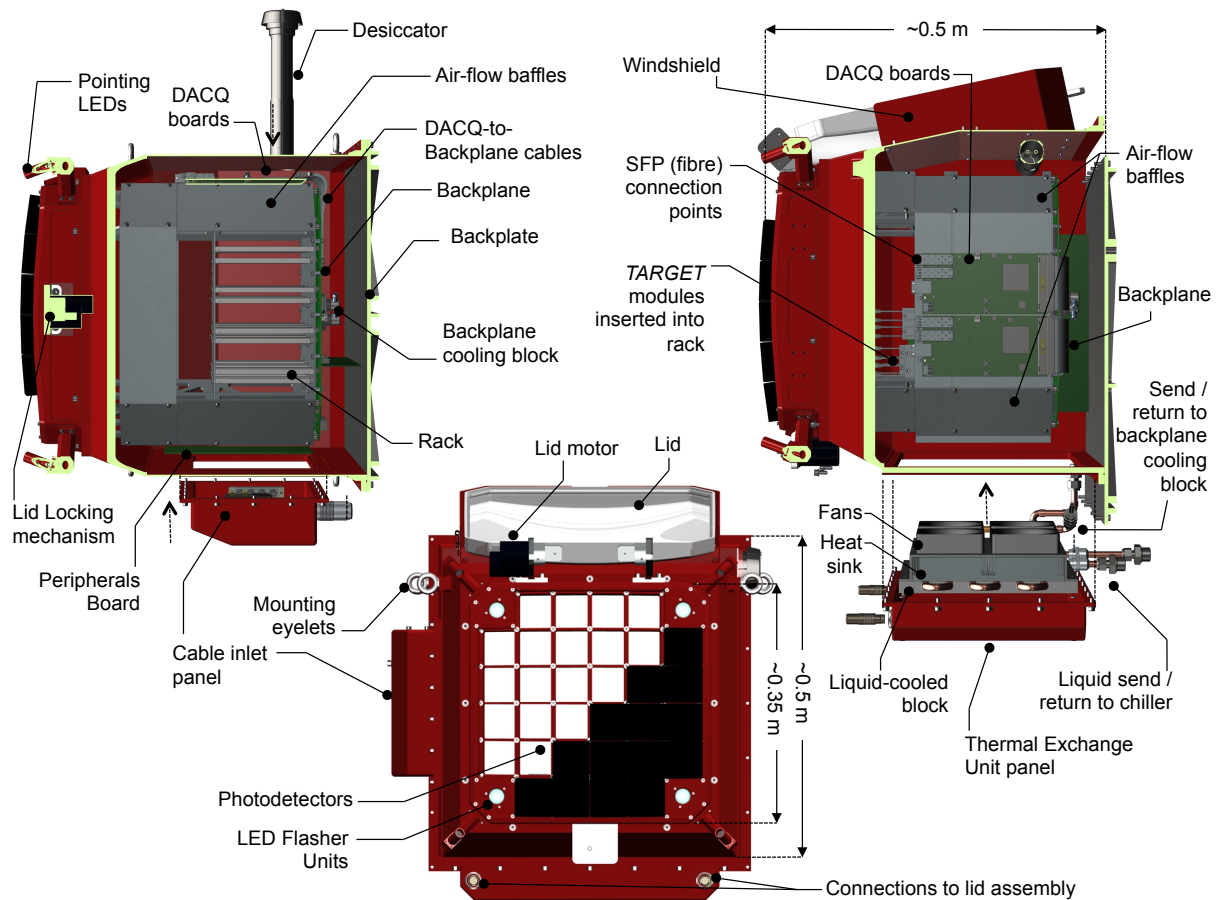


**Figure 2.30** – A detailed overview of the elements of the GCT camera shown using cross-sections through the CHEC-M CAD model.

### PBS 6G.3.1.1: Internal Mechanics and PBS 6G.3.1.2: Enclosure

The focal-plane positioning plate located at the front of the camera is responsible for the accurate positioning of the photodetectors. The *TARGET* modules with front-end buffers attached are slotted through this plate and into the rack. On the rear of the rack is an aluminium plate with through-holes and screws for securing the *TARGET* Modules and through-holes for the *TARGET* Module connectors. The screw on the rear of the rack mates with a custom standoff with threaded insertion hole on the rear *TARGET* module as shown in Figure 2.31. Access to the screw head is provided via a through-hole in the backplane, sized appropriately to allow access via a tool, but to retain the screw between the rack and the backplane.

The front-most front-end buffer module PCB does not go through the focal-plane positioning plate, but rather sits in a recess flush to the surface where it is secured using screws. The photodetector units are then attached. The retention of the photodetectors is provided by 4 multi-pin latching connectors reinforced with removable glue.

A protective entrance window will be used in front of the photodetectors to seal against the elements. The design of the protective window and choice of material will be finalised following prototype tests (see Section 2.3.4). The current baseline design consists of a 2 mm thick 'Polycasa-XT UVT' Polymethyl Methacrylate sheet from POLYCASA with a UV throughput of typically 92% falling to 80% at 300 nm and 50% at 275 nm. The window is thermally formed by precision blowing/moulding into the required 1 m radius of curvature, machine finished, and held 2 mm in front of the detectors. Expected significant dimensional variances due to temperature cycling, which is a function of all PMM materials are compensated for by flexible seals to the focal plane borders. Coatings/materials are under investigation

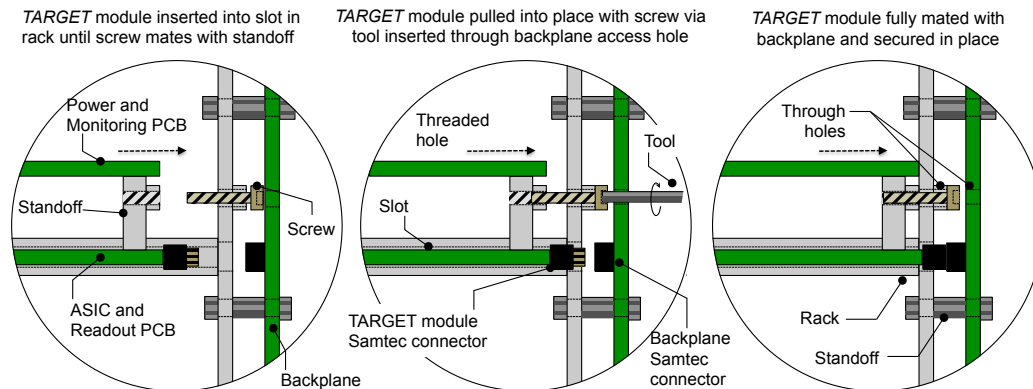


**Figure 2.31** – The connection of the *TARGET* modules to the backplane. A *TARGET* module is inserted into slot in the rack until a screw on the rear of the rack mates with a standoff on the module. The module is pulled into place and secured with screw via a tool inserted through backplane access hole.

to reduce transmission in the red. The formed material will receive an AR coating for UV wavelengths, possibly an IR absorption coating and a protective hydrophobic coating.

The GCT camera enclosure is manufactured entirely from aluminium. The focal plane plate and interface to the enclosure case are machined from solid. The rear telescope interface, or backplate, is machined from plate with pocketing to reduce mass and provide rigidity. Interconnecting walls are 2 mm sheet. All interfaces are welded except the focal plane plate to case interface (which is secured by 16 M5 screws into helicoils and sealed with an O-ring) and the backplate to case rear flange (which is secured by 24 M5 screws into helicoils).

The interface backplate at the rear of the camera provides a stable mounting point for attachment to the GCT telescope structure via 3 M12 screws inserted into helicoils on the backplate side. Overall rigidity is expected to hold the focal plane in position to  $\pm 0.2$  mm in X, Y and Z axes (where Z is the optical axis). A total accuracy plus stability during operation of  $\pm 1$  mm is required at the focal plane along the direction of the optical axis (corresponding to a 10% change in PSF size on-axis). Accurate camera positioning will be achieved via a combination of the mechanical tolerances within the camera (Section 2.3.3), a manually adjustable camera removal mechanism on the telescope structure (see Section 2.1.2 and Figure 2.18), and the throw of the M2 actuators (see Section 2.1.3 and Table 2.3).

There are two access panels in the enclosure sides, into which machined removable aluminium panels are fastened. One access panel contains the feed-through for power and fibre-optical signals via bulk-head connectors, whilst the other houses the thermal-control assembly. A windshield on one side of the enclosure provides protection for the lid whilst open. The prototype CHEC-M camera is painted with corrosion-resistant automotive paint (see Section 2.3.3), whilst CHEC-S will be fully anodised (see Section 2.3.4). The finish for the Pre-Production and Production phase GCT cameras will depend on further trials with these prototypes.

### **PBS 6G.3.1.3: Thermal Exchange Unit**

The total power dissipation in the GCT camera during normal operation is  $\sim 450$  W. The thermal control system is designed to keep the camera temperature stable over a wide range of ambient temperatures up to the maximum required ( $25^\circ$  C) during operations.

The resulting thermal control system consists of fans coupled to a liquid-cooled heat sink. The fans, together with a system of baffles, provide a recirculating airflow within the sealed camera enclosure. A commercially available chilling unit provides a flowing liquid (water glycol mixture) of controllable temperature and delivers a cooling power of at least 1 kW (see Section 2.1.4 for further details on the chiller).

The anticipated operational mode is a  $8^\circ$  C liquid supply at the camera (at maximum ambient temper-

ature, warmer under typical circumstances) and air temperatures of 12-20° C within the camera. A breather desiccator removes humidity from the camera interior, but we note that in the worst possible case of simultaneous maximum ambient temperature and humidity (90%) operation of the camera at higher temperatures for short periods will be required to avoid condensation on the focal plane.

For camera survival, chiller operation is anticipated when external temperatures exceed 30° C, keeping the non-operational electronics below this temperature. The chiller is also capable of heating liquid if required.

The thermal exchange unit itself (PBS 6G.3.1.5) comprises the liquid-cooled heat sink, whilst the fans are specified under 6G.3.3.5.2.2. The chiller and associated pipework are contained under PBS item 6G.3.5.2 (see Section 2.1.4 below).

#### PBS 6G.3.1.4: Lid Assembly

The camera lid will be constructed from carbon fibre and consists of a single hinged unit driven by a motor. A second motor with an accompanying latch secures the lid in place. The camera lid follows the same 1 m radius of curvature as the camera focal plane. When closed, the camera lid is used as a screen onto which star images can be projected. Together with the pointing LEDs (see the *Calibration System* details below), this system is used to monitor the telescope pointing. The lid forms a water-tight seal with the camera and is closable against a maximum wind load of 50 km/hour. When open the lid recesses into a protective wind shield on the enclosure (see Figure 2.28)). An ambient light sensor connected to the peripherals board is used to prevent the opening of the lid in bright conditions.

### PBS 6G.3.2: Photodetectors

There are two choices of photodetector for the GCT camera, MAPMs, or SiPMs. Examples are shown in Figure 2.32. In both cases, 32 modules, each of 64 pixels, are arranged to approximate the 1.0 m radius of curvature of the focal surface as illustrated in Figure 2.2. In the case of MAPMs a standard pixel size of  $\sim 6\text{ mm} \times \sim 6\text{ mm}$  is available. In the case of SiPMs, pixel sizes will be in the range 6 to 7 mm. Each photodetector module will be between  $\sim 50\text{ mm}$  and  $\sim 57\text{ mm}$  across. Tiling modules across the focal plane results in a maximum deviation from the ideal pixel position of 0.5 mm at the corner of each module.

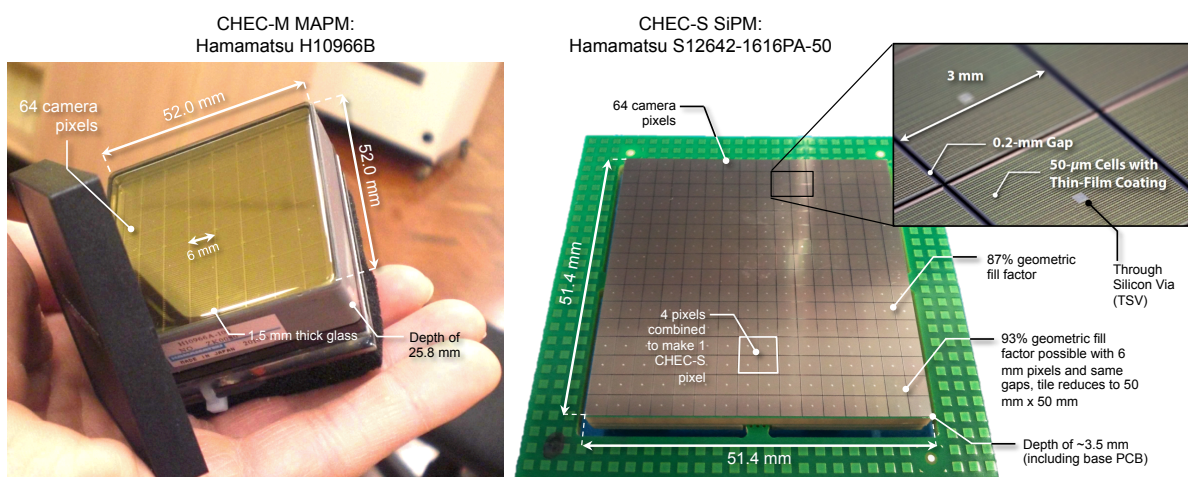


**Figure 2.32** – Examples of photodetector options for the GCT camera: the Hamamatsu H10966B MAPM chosen for CHEC-M and the Hamamatsu S12642-1616PA-50 SiPM chosen CHEC-S. Note the green area surrounding the CHEC-S SiPM is removable and only included for ease of handling.

The Hamamatsu H10966B as used in CHEC-M (see Section 2.3.3) is the baseline choice of MAPM. Each H10966B measures  $52.0 \pm 0.3\text{ mm}$  across. The distance from the front of the glass to the rear PCB of the MAPM is  $25.8 \pm 0.3\text{ mm}$ . The glass is  $1.50 \pm 0.01\text{ mm}$  thick and the photocathode is located directly on the rear of the glass.

The Hamamatsu H10966B MAPM has a super-bialkali photocathode and 64 pixels of size  $\approx 6 \times 6 \text{ mm}^2$ . This corresponds to an average angular size of  $0.15^\circ$  when installed on the GCT telescope structure. The value of  $D_{80}$  (the diameter which contains 80% of the light resulting from a point source) for the SST-2M design is smaller than 6 mm over the full camera FoV. A gap of  $\sim 2 \text{ mm}$  between MAPMs is required to accommodate their depth of  $\sim 26 \text{ mm}$ . When combined with the dead space at the edges of each MAPM, a total maximum dead space of  $\sim 5 \text{ mm}$  (corresponding to the diagonal gaps) is achieved.

A single HV source of  $\sim 800\text{--}1100 \text{ V}$  is generated on the *TARGET* Modules and routed to the corresponding MAPM by an insulated cable (see Figure 2.33). A range of gain from  $\sim 4 \times 10^4$  to  $\sim 6 \times 10^5$  is possible, nominal operation will be at  $8 \times 10^4$ . The MAPMs produce pulses with a FWHM of  $\sim 1 \text{ ns}$  and a rise time of  $\sim 0.4 \text{ ns}$ . The response of the MAPMs extends from a single p.e. to 1000s of p.e. At 1000 p.e. and a gain of  $\sim 2 \times 10^5$  the response is linear to within 20%.

In the case of SiPMs, several options still exist for the photodetector module. The primary vendors are Hamamatsu, Excelitas and SensL. The gain is typically around  $10^6$ . A range of bias voltages is required by different manufacturers, from  $\sim 30 \text{ V}$  (SensL), to  $\sim 70 \text{ V}$  (Hamamatsu) and  $\sim 100 \text{ V}$  (Excelitas). In all cases  $6 \text{ mm} \times 6 \text{ mm}$  pixels are becoming available arranged as 64 pixel tiles. The dead space in a module varies, with Hamamatsu currently achieving the lowest with a  $\sim 92\%$  geometric fill factor achieved by using Through Silicon Via (TSV) technology. The different devices produce different pulse shapes, from approximately  $\sim 50 \text{ ns}$  FWHM in the case of Hamamatsu, down to  $\sim 10 \text{ ns}$  in the case of SensL.

The response of SiPMs extends from a single p.e. to many 1000s of p.e. with resolvable multiple p.e. peaks in the pulse-height spectra up to 10s of p.e. SiPMs are formed from a collection of micro-cells. For an instantaneous light pulse a given cell fires, or does not. The electrical signal from the pixel is proportional to the number of cells that fire. Cells that have fired are insensitive for a short recovery time. The signal from a pixel saturates as the number photons incident on it within the recovery time approaches the number of cells in the pixel. For a cell size of  $50 \mu\text{m}$ , a  $6 \text{ mm} \times 6 \text{ mm}$  pixel will contain up to 14,000 cells. This becomes 3,600 cells in the case of a  $100 \mu\text{m}$  cell size. Further details of the performance and relative merits of the different SiPMs can be found in Section 3.2.5.

The Hamamatsu S12642-1616PA-50 SiPM used for CHEC-S has 256 pixels of size  $3 \times 3 \text{ mm}^2$  (see Figure 2.32). These are summed to provide 64 camera pixels with  $6 \text{ mm} \times 6 \text{ mm}$  active area each. Each SiPM module measures  $51.4 \pm 0.1 \text{ mm}$  across, with a depth of  $\sim 3.5 \text{ mm}$  once soldered on the PCB base. A gap between SiPM modules varying from  $1.9 \text{ mm}$  at the focal-plane edge to  $2.5 \text{ mm}$  at the focal-plane centre is then required to for installation/removal. This gap is filled with a removable sealant.

The SiPM tiles (PBS item 6G.3.2.1) are mounted to PCBs that provide a bias circuit for each pixel (PBS 6G.3.2.2). The SiPM tile is surface mounted onto the base. On the rear of the base PCB, 4 connectors mount the photodetector unit to the front-end buffers (see Section 2.1.4 below).

### PBS 6G.3.3: Camera Electronics

A full camera consisting of 2048 pixels is sub-divided into 32 front-end modules serving 64 pixels each. One front-end module as developed for CHEC-M is shown in Figure 2.33. It consists of front-end buffers (PBS 6G.3.3.1), and *TARGET* signal capture modules (PBS 6G.3.3.2) for data digitisation, read out, pixel-level triggering and slow control. All 32 *TARGET* Modules plug directly into a single large backplane PCB (PBS 6.3.3.3) that provides: camera-level triggering, clock distribution, communication with the *TARGET* Modules and routing to the DACQ interface boards (PBS 6G.3.3.4). High-speed serial data from the *TARGET* modules are routed to either one of the two DACQ boards via the backplane. These DACQ boards provide data acquisition from the *TARGET* modules, the interface to the outside world for the data stream, and slow control of the camera. A separate common timing card, called UCTS board, will be provided by the ACTL group and will act as clock master and trigger time-stamping unit.

#### PBS 6G.3.3.1: The Front-End Buffers

The front-end buffers connect directly to the photodetector base PCBs (PBS item 6G.3.2.2). They provide a first-stage of amplification for the analogue signals before transmission over cables to the pre-amplification/shaping stage. Due to the differences in gain and pulse shape mentioned in Section 2.1.4,

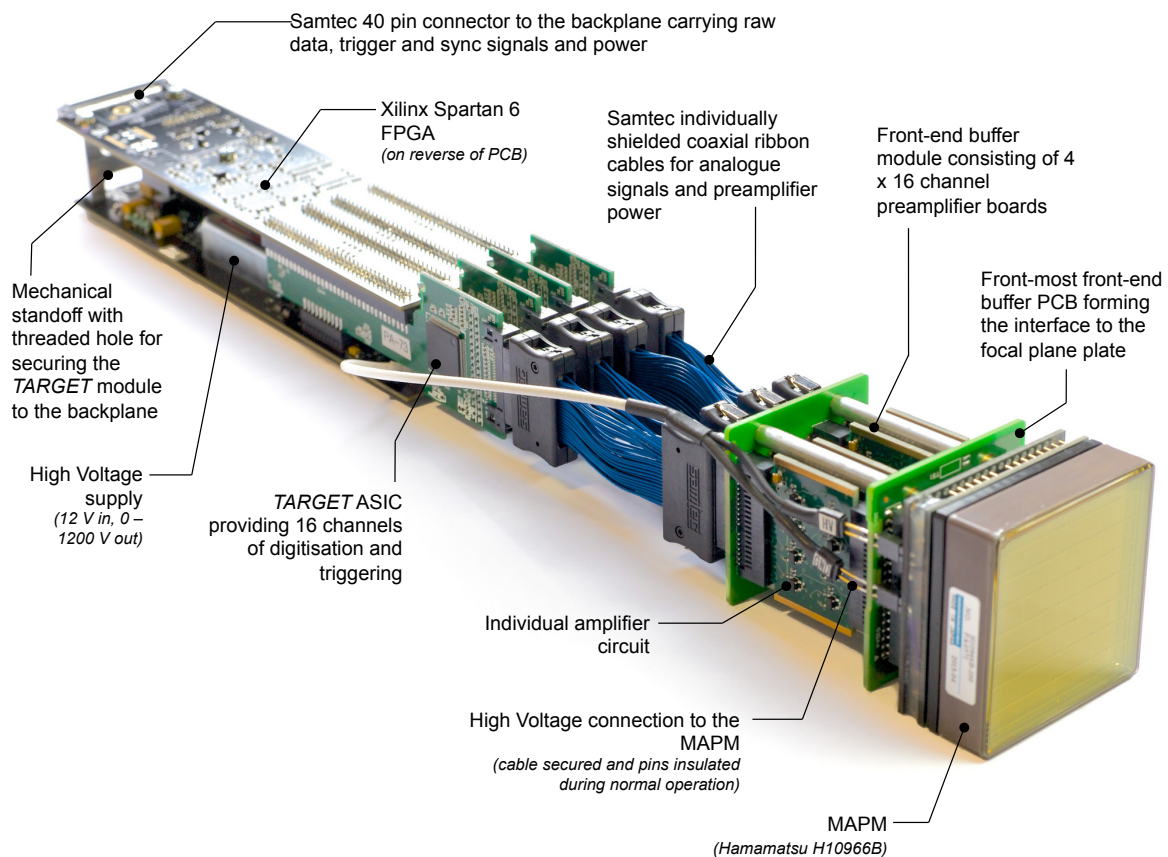


**Figure 2.33** – Photograph of a *TARGET*-based front-end electronics module. This version of the module was designed for CHEC-M. Another version for CHEC-S is currently being produced. One final design iteration will likely follow based on the prototype test results.

the implementation of the front-end buffers depends on the photodetectors chosen. Front-end buffer designs are in place for both CHEC-M and CHEC-S.

Cables connect the front-end buffer board to the *TARGET* modules. The exact cabling solution is yet to be fixed, CHEC-M utilised 4 individually stranded Samtec ribbon cables per camera module, whilst for CHEC-S the use of 64 individual micro-coax cables is under investigation.

There is also the possibility that in the final camera, the front-end buffers are implemented as a multi-channel ASIC, which could in principle provide shaping functionality as well as amplification.

### **PBS 6G.3.3.2: The *TARGET* modules**

The *TARGET* modules developed for CHEC-M, and shown in Figure 2.33 consist of 4 PCBs with 1 *TARGET* ASIC per PCB mounted between 2 further PCBs, one for data readout (via an FPGA) and one for the generation of high voltage. The final *TARGET* modules, will consist of two functional elements, a Power and Monitoring PCB (PBS 6G.3.3.2.3) and a *TARGET* ASIC and Readout PCB (6G.3.3.2.4).

The Power and Monitoring PCB receives the analogue signals via cables from the front-end buffers. It contain 64 channels of fast amplification to shape input signals to match the optimal shape for triggering. This optimal shape is determined from Monte Carlo simulations to be: 5.5-10.5 ns FWHM, 3.5-6.0 ns rise time. These simulations also show that noise levels must be kept below about 0.5 mV (see section Section 3.2.5).

The Power and Monitoring PCB also contains 64 channels of slow-signal monitoring amplifiers with outputs multiplexed to a single ADC, read out to the FPGA on board the *TARGET* ASIC and Readout

PCB via a serial interface. The slow signal measurements integrate photon signals incident on the photodetectors over 100 ms and are going to be used for the precision pointing calibration.

The Power and Monitoring PCB accepts a single  $\sim 30 - 100$  V supply (to be specified depending on the final photodetector choice) and generates a controllable bias voltage for the SiPM tile. In the case of MAPMs, the required 800-1100 V is generated directly on the *TARGET* module from the 12 V input supply. All 64 pixels are supplied with a single bias voltage. A gain spread of no more than 10% across the tile is expected. Simulations show that a deviation of 25% RMS in the gain across all 64 channels is acceptable. Each of the 64 pixels may be individually disabled.

The *TARGET* ASIC and Readout PCB forms the second component of a *TARGET* module. It performs digitisation of the amplified and shaped analogue signals and the first level of triggering. The *TARGET* ASIC and Readout PCB provides these digitised signals together with trigger information to the backplane (see below).

Each *TARGET* ASIC and Readout PCB contains four *TARGET* digitisation ASICs and four *TARGET* trigger ASICs. Digitised signals are read out to an on-board Xilinx Spartan 6 FPGA. The FPGA serialises event data for output to the backplane via UDP connections at a bandwidth of 1 Gbps. Serialisation and readout of 64 channels in this way minimises the connections to modules, but incurs an additional  $\sim 10-20$   $\mu$ s dead time (well inside the specifications). Both event data and control commands will be sent via the UDP link.

The *TARGET* ASICs digitise input signals over a range of  $\sim 0-2$  V with 12 bit resolution, and an RMS noise of  $\sim 0.5$  mV. Assuming a nominal photodetector gain of  $2 \times 10^6$ , a single p.e. at the *TARGET* input has an amplitude of  $\approx 2.5$  mV, corresponding to  $\sim 5$  digital counts, and the signal saturates at  $\sim 800$  p.e. The signal is digitised at 1 GSa/s over a programmable read out window set to  $\sim 96$  ns.

The dead time incurred by the *TARGET* ASIC for conversion and readout over the  $\sim 96$  samples is  $\sim 20$   $\mu$ s. The goal camera trigger rate is 600 Hz.

The *TARGET* trigger ASICs provide the first level of triggering for the camera. The trigger consists of the analogue sum of 4 neighbouring pixels, which is then discriminated. Each *TARGET* trigger ASIC outputs 4 digital trigger signals, which are routed through the *TARGET* module to the backplane, resulting in 16 differential LVDS trigger signals per module.

The *TARGET* modules are each powered by a single +12 V supply. All signals and the power supply are connected to the backplane in parallel via a single 40-pin Samtec connector on the ASIC PCB.

### PBS 6G.3.3.3 The backplane

The backplane connects to all 32 *TARGET* front-end modules. It routes serial data to the DACQ interface boards and provides camera-level triggering. The backplane triggering scheme is implemented in a single Xilinx Virtex 6 FPGA (XC6VLX550T-2FFG1760C). The FPGA forms a camera trigger by requiring that any 2 neighbouring trigger patches be present within a programmable coincidence time. Following a successful camera trigger, a serial message containing an absolute timestamp is generated on the backplane and routed back to the *TARGET* modules to initiate a full camera readout. On the *TARGET* modules the absolute timestamp is compared to a local counter to determine a look-back time in the *TARGET* ASIC buffers. The event timestamp is added to the raw data event on each *TARGET* module. Clocks between the backplane and the *TARGET* modules are kept in-sync via a low-skew fanout network and periodic signals between the backplane and the *TARGET* modules to re-synchronise local counters. A second, smaller ACTEL house-keeping FPGA provides access to status and monitoring registers on the trigger FPGA, provides the current and voltage draw of every *TARGET* module and is capable of cycling the power to every *TARGET* module.

External timing signals are provided to the camera via a White Rabbit timing network. The common UCTS interface board connects to the GCT camera and provides a 62.5 MHz reference clock to the backplane. The backplane utilizes a programmable quad clock generator to generate a 125 MHz clock from the 62.5 MHz reference signal for distribution to the DACQ boards, the trigger FPGA and the *TARGET* modules. Each of the 4 outputs is phase programmable in 20 ps increments and will be routed to a 1:16 fanout buffer, specified to introduce no more than 25 ps delay between the outputs.

The backplane also forms an interface to the peripherals board via a single connector providing a fast trigger output for the LED calibration units and an SPI bus. The backplane accepts a single 12 V input and generates all required voltages on a daughter board mounted perpendicular to the main PCB.

The camera may be externally triggered via slow-control to the house-keeping FPGA, or asynchronously via pulsed input to a header on-board the backplane (the later being only used for lab tests).

### **PBS 6G.3.5 The DACQ boards**

The DACQ boards receive serial data from the *TARGET* modules via the backplane. These boards are commercially available from Seven Solutions, a Spanish company, and they are based around a Xilinx Virtex-6 XC6VLX240T FPGA. Each board provides 18 GTX serial transceivers on two Samtec connectors to accommodate the high-speed serial data inputs. The data are routed off the camera on optical fibres via SFP connectors, which also carry all control and monitoring data to and from the camera.

Each DACQ board is 216 mm by 108 mm in size. There are two such boards per camera, both are located on top of the rack containing the *TARGET* modules as shown in Figure 2.30. The boards connect to the backplane via Samtec connectors and custom flat cables. A single 12 V supply line powers the boards.

Due to the modest event rate per GCT telescope (the required readout rate is 600 Hz), no inter-telescope hardware array trigger is required. When a telescope triggers, all data is read out and transferred from the camera to be processed by the software array trigger system. Trigger decisions are based on the camera event time-stamps. This scheme is integrated into CTA via the ACTL working group, see for example [7].

### **PBS 6G.3.3.5 The peripherals board**

The peripherals board sits on the side of the *TARGET* module rack, opposite to the DACQ boards. It is a common interface to the various peripheral/slow control systems. The peripherals board accepts 12 V directly from the main camera power input, and generates all voltages needed for peripheral control onboard. The SPI from the backplane is bridged by a Programmable System on Chip (PSoC) that in turn controls the following peripherals with their appropriate serial standard:

1. **Power On Reset:** At startup the peripherals board sends a 0.5 s pulse that sets the thermal cut-off power relay for the DACQ. It also has a switch to enable human intervention should power be cut by an overtemperature condition.
2. **Environmental Sensors:** The internal temperature and humidity are monitored by a variety of digital and analogue probes.
3. **Fans:** The internal cooling fans are individually powered with 12 V from the peripherals board and their speeds are pulse width modulated by PSoC to prolong their operational lifetime.
4. **LED Calibration Units:** The 4 LED Calibration Units require a +5 V power supply, a serial interface to set the pattern of LEDs to be flashed, and a fast TTL trigger signal to initiate the flash. Each unit is connected to the PSoC via a serial interface. The fast trigger output signal from the Backplane is converted to the appropriate voltage and routed to each of the LED Calibration Units with a suitable delay to allow ~synchronised flashes.
5. **Lid:** The lid is operated by a commercial stepper motor and controller and locked in place using a screw mechanism operated by a 12 V DC motor controlled by a commercially available Red Drive controller board, with both controllers mounted next to the peripherals board. The motor and latch controller boards are supplied from the peripherals board with 12 V power and +5 V signal lines, including for the end limit switches that determine the motor direction and power off conditions.
6. **Auxiliary Inputs:** The Peripherals Board includes provision for several additional signals, including a digital ambient light sensor that is checked before the lid is opened and can issue emergency close commands in bright light conditions.

### PBS 6G.3.3.6 Internal cabling

The cabling associated with, and connecting, individual camera items is contained within those PBS codes. In addition there exists an internal set of power and fibre-optic cabling.

The internal power distribution (PBS 6G.3.3.6.1) consists of a power cable routed from a bulk-head connector at the entry point of the enclosure to an internal power-distribution busbar. The power is then distributed to the peripherals boards and separately, via a thermostat-power-cutout circuit and relays to the backplane and DACQ boards. The peripherals board controls these relays and can therefore cycle the power to the DACQ and backplane boards.

An internal fibre optic cable assembly (PBS 6G.3.3.6.2) connects a single bulk-head connector to the SFP connectors on the DACQ board.

## PBS 6G.3.4 Calibration System

The GCT camera is equipped with 4 flasher units (PBS 6G.3.4.1) containing multiple LEDs placed in the corners of the focal plane (see Figure 2.28) to illuminate the photodetectors via reflection from the secondary mirror as illustrated in Figure 2.34. A Thorlabs ED1-C20 1 inch circle pattern engineered diffuser is mounted in front of the flashing LEDs to ensure the illumination of the focal plane is well understood. These LED flasher units are used to flat-field the camera across the full required dynamic range of illuminations, providing optical pulses of width  $\approx 4.5$  ns (FWHM) at 400 nm from 0.1 p.e., for absolute single-pe calibration measurements, up to 1000 p.e., to characterise the camera up to and at saturation, and allow an independent absolute calibration using photon-statistics.

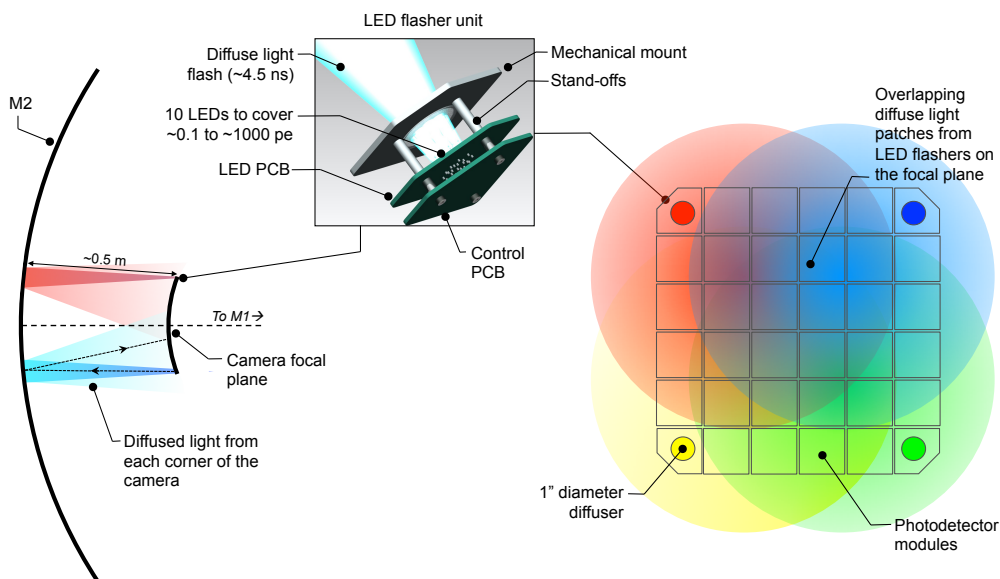


**Figure 2.34** – The calibration flasher geometry for the GCT camera with CAD model of the LED flasher unit inset. For a photograph of the CHEC-M flasher units see Section 2.3.3.

The LED flasher units are based around fast gated TTL drive pulses and 3 mm, low self-capacitance, Bivar UV3TZ-400-15 LEDs. The Bivar LEDs are enabled/disabled by an onboard PSoC and triggered via an external TTL pulse.

Single-photoelectron calibration measurements will be performed at the start/end of observations with the telescope in the park position. Flat-fielding measurements will also be performed by the LED flasher units providing fast flashes of light during normal observations to understand ambient effects (e.g. temperature, NSB), but at a low rate that does not interrupt normal data taking. Each flash is triggered by the camera control system implemented on the DACQ boards that also enforces triggered readout of



the camera and flags the data as a calibration event.

Each unit can also control and power two DC illumination red LEDs for pointing calibration of the camera (PBS 6G.3.4.2), which are also turned on and off by the onboard PSoC. The pointing LEDs are mounted on posts protruding from each corner of the focal plane (see Figure 2.28).

The pointing LEDs will be visible when the camera lid is closed and will be used as geometric markers to indicate the position of the focal plane when taking pointing measurements by imaging stars on the camera lid.

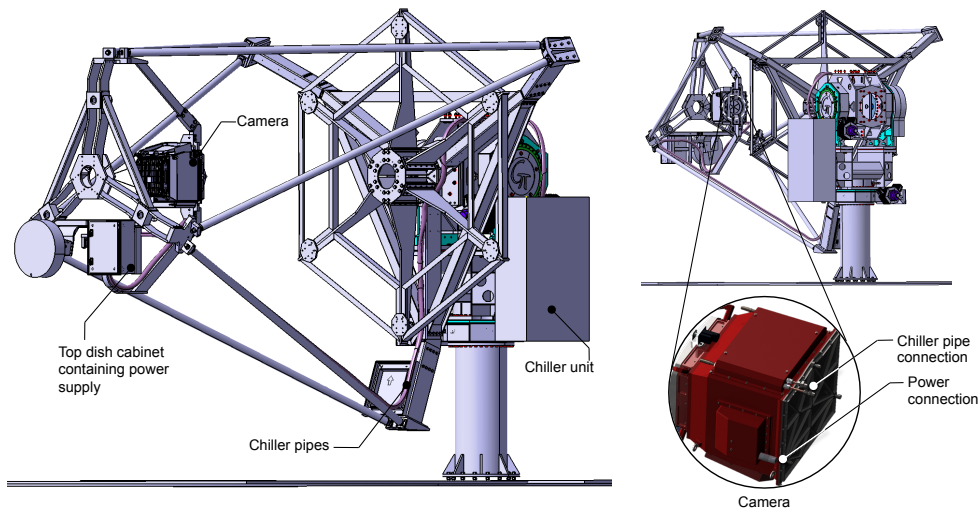


**Figure 2.35** – The location of the camera power supply and chiller as mounted on the telescope structure, with chiller pipes and camera connection points shown.

## PBS 6G.3.5 Auxiliary Systems

### PBS 6G.3.5.1 Camera Power Supply

A single ARTESYN iMP power supply provides the camera with 12 V at up to 60 A for all electronics and 75 V for the operation of SiPMs via internal modules. The power supply weighs  $\sim 1$  kg, measures  $63.5 \text{ mm} \times 127 \text{ mm} \times 254 \text{ mm}$  and is housed at the rear of the secondary mirror in the 'top dish cabinet' (PBS 6G.4.2.3). A 'sense' feed-back input from the camera ensures the desired voltage at the camera. A single Chainflex CF10 12-way cable (CF10.25.12) with outer diameter 19 mm connects the power supply to the camera, and is flexible down to  $-35^\circ \text{ C}$ . Communication to the power supply is via I2C, converted to ethernet in the top dish cabinet.

### PBS 6G.3.5.2 Chiller

Together with the thermal exchange unit (PBS 6G.3.1.5) and fans (PBS 6G.3.3.5.2.2), the chiller forms part of the camera thermal control system. The chiller unit is a KRA20 from TPC (Total Process Cooling) Ltd. with a nominal cooling capacity of 2.2 kW (at  $10^\circ \text{ C}$  liquid and  $32^\circ \text{ C}$  ambient) and remote control and monitoring via ethernet. The chiller provides a flowing liquid (water glycol mixture) at a rate of 5 to 38 L/min, and has a water-tank capacity of 33 litres. In standby mode the chiller consumes 170 W of power.

The unit weighs 97 kg and measures  $485 \text{ mm} \times 965 \text{ mm} \times 650 \text{ mm}$ . It is installed at the azimuth axis of the telescope and connected by pipes to the thermal exchange unit inside the camera as shown in Figure 2.35. From the chiller mount on the telescope a short (1.5 m) piece of hose with a quick-release non-leak coupling will connect to a  $\sim 12$  m piece of hose that runs to the camera. This couples, again via quick-release, to another short (1.0 m) piece of hose that connects to the camera thermal exchange unit. This allows the chiller and the camera to be disconnected quickly from the telescope structure, and with care, should prevent fluid loss / spillage due to the sealed nature of the quick couplings. All hoses are  $3/4$ " diameter, the quick couplings used are PLTX.1313.112 mated to PLTX.1313.113.

## 2.1.5 Auxiliary System Design: the GCT Shelter and Telescope Control System

### GCT Shelter (PBS item G6.04.03)

The GCT telescope is provided with a shelter to protect the structure and mirrors from the weather, dust, animals and other environmental factors and to ensure that there is no risk from reflected sunlight when the telescope is parked. The shelter thus extends the lifetime of the telescope components (electronics, mirrors) reduces the amount of maintenance needed (see section 4.5) and improves safety for both people working on the telescope and the instrument itself.

The shelter already installed at the telescope prototype site (Meudon) is a system that has been used for military applications for many years. It is compliant with the CTA specifications on environmental conditions: it survives wind speeds of up to 200 km/h and protects the telescopes from rain, ice, snow, and light.

The shelter is a structure built of aluminium beams with a PVC fabric cover attached to it. The bottom beam is fixed to the foundation at three points. The structure is light and can easily be mounted in less than a day. Two motors on the foundations drive the opening and closing of the shelter, within less than 30 seconds. The shelter can also be opened and closed manually. The PVC cover is fireproof, tough and opaque to UV light. Sufficient sunlight diffuses through the cover to allow work inside the shelter during the day without artificial lighting.

Figure 2.36 shows the inside of the shelter with its dimensions, and Figure 2.37 shows the shelter in its half-opened and closed positions.

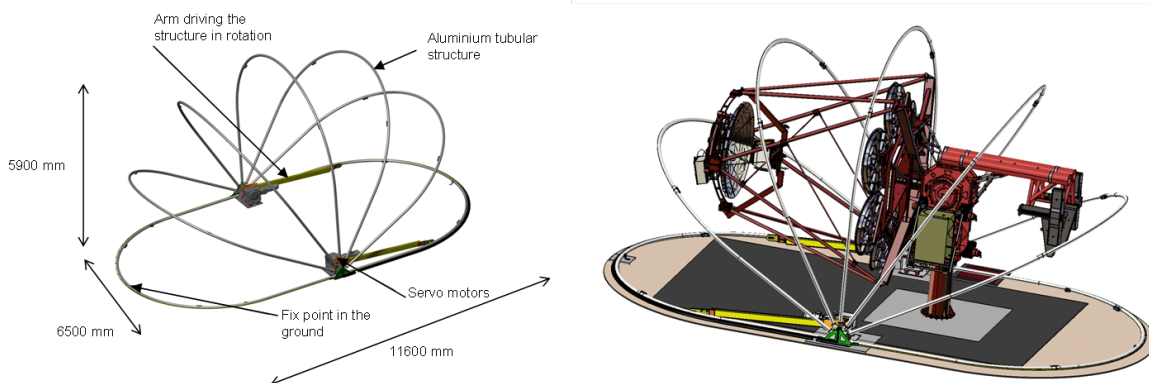


**Figure 2.36** – Schematic diagram of the shelter with its dimensions (left) and illustrating how it encloses the GCT (right).

### Telescope Control System (PBS item G6.04.01 and 6G.04.02)

The primary function of the Telescope Control System (TCS) is to drive the telescope axes for tracking purposes. The drive subsystem includes all the drive-related software modules and hardware devices. It receives high-level commands (from a workstation or the array controller), carries out all computations needed to control the telescope and steers the relevant hardware. Many functions are required to run the telescope in a proper way. These are collected in several subsystems (see Figure 2.38). Each of these is composed of either hardware and the associated software modules or software modules alone.

The TCS is designed to work either as an element of a large array, driven by the array controller, or in a stand-alone mode with remote workstations. Hence it is built to be autonomous with versatile interfacing. As an example, tracking is managed on-board, including astronomical transformations, geometrical transformations (e.g. the telescope bending model) and drive control. The external communications of the TCS are conveyed via an Internet link, while internal communications are transmitted by another flavour of Ethernet: EtherCAT. On the software side, an OPC UA server is the interface for monitoring



Figure 2.37 – External views of the shelter.

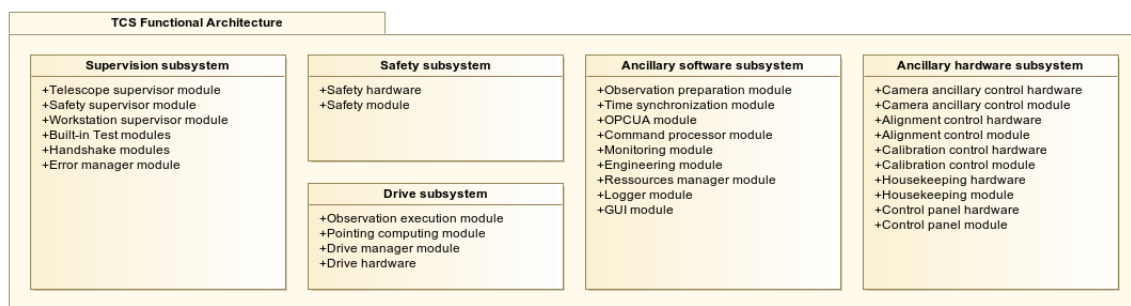


Figure 2.38 – The five subsystems of the TCS with their software modules and associated hardware.

and controlling the telescope. Figure 2.39 shows these elements in the stand-alone configuration.

The OPC UA implementation is Beckhoff's *TwinCAT OPC UA Server* featuring *Data Access (DA)* and *Historical Access (HA)*. The *TwinCAT ADS Communication Library* is used to call methods associated with the server's data or to exchange information with other software.

The hardware layout is shown in Figure 2.40. The core of the TCS is the *Supervisor* while the *Safety PLC* controls safety-related automation and the *Pointing PC* controls the drive hardware – Beckhoff units are used for both of these elements.

Although the drive subsystem is designed to be used remotely, for commissioning and maintenance purposes the telescope can be steered using a local interface – the *Control panel* in Fig. 2.40 – (C-SST-GATE-RAMS-0110-5 and -0335-2), and also manually (C-SST-GATE-RAMS-0210-7). Items related to the safety of the drive system are described in Sections 3.1.2 and 3.1.3.

The modes of operation of the TCS, managed by the Supervisor, are shown in Figure 2.41. The on-line mode allows ACTL's *Observing* and *Transitional* modes; stand-by corresponds to *Safe*; and while in Warm-up, Fault or Maintenance the telescope is *Inoperable*.

The TCS hardware is installed in cabinets to protect it from the environment and for safety reasons. Three of the cabinets are located on the telescope itself (PBS 6G.04.02), the *fork main cabinet*, the *MTS cabinet* and the *top cabinet*. The other cabinets (PBS 6G.04.01) are placed on the foundation. These are the power and network cabinets, the control panel with some TCS modules and the shelter cabinet.

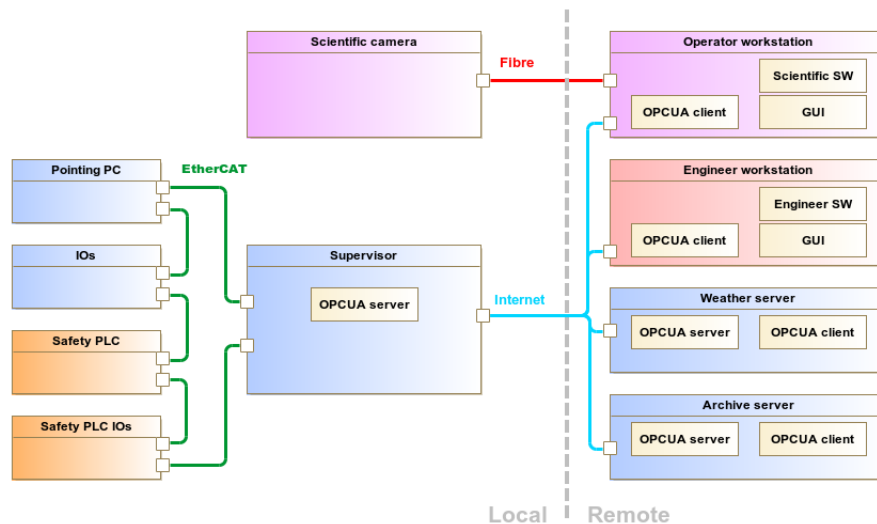


**Figure 2.39** – The communication layout of the TCS. Two flavours of Ethernet are used: Internet for external and EtherCAT for internal communications. Note that the –not essential– ring network for EtherCAT enables the field bus to continue to operate in the case of cable or device failure, thanks to a very short (<math>< 15 \mu\text{s}</math>) self-reconfiguration time. The remote hardware displayed shows the prototype set-up; these elements are replaced by ACTL services in the CTA Observatory. A dedicated fibre bundle is used for camera communications.

The fork main cabinet ( $1000 \times 750 \times 500 \text{ mm}^3$ ) is fixed on the AAS with standard rails. The MTS cabinet ( $500 \times 400 \times 200 \text{ mm}^3$ ) is fixed to the back of the MTS lower dish with two clamps and four bolts. The top cabinet ( $500 \times 400 \times 200 \text{ mm}^3$ ) is fixed to the back of the M2 dish with a frame and three bolts.

To balance the masses of the different electronic cabinets on the GCT telescope structure, the main fork cabinet and the camera chiller have been placed on opposite sides of the AAS fork.

The Figure 2.40 shows the location of the cabinets (white boxes) on the telescope structure and lists the associated modules. The colours used reflect their function:

- the sensors and actuators are shown in green, for instance temperature and strain gauges, or heaters and fans to control temperature and humidity inside the cabinets.
- the safety modules (PLC, sensors, actuators...) are shown in orange.
- the supervisor and monitoring modules are represented in blue.
- the power supply boards, connectors and others general modules are shown in grey.
- the systems related to the camera (power supplies, chiller...) are shown in purple.

To simplify the cabling, the interfaces between the cabinets are limited to:

- the power supply (230 V and 50 Hz);
- the local fieldbus (EtherCAT);
- the network (Internet).

Two cable chains are used for cable routing, one for the azimuth (allowing one and a half turns) and one for the elevation.

For operating the GCT, a 230/400 V and 50 Hz three-phase electricity supply of 10 kW power is required from the grid. The peak power for normal operation is 3 kW, but additional power is needed for the electrical devices used for integration and maintenance.

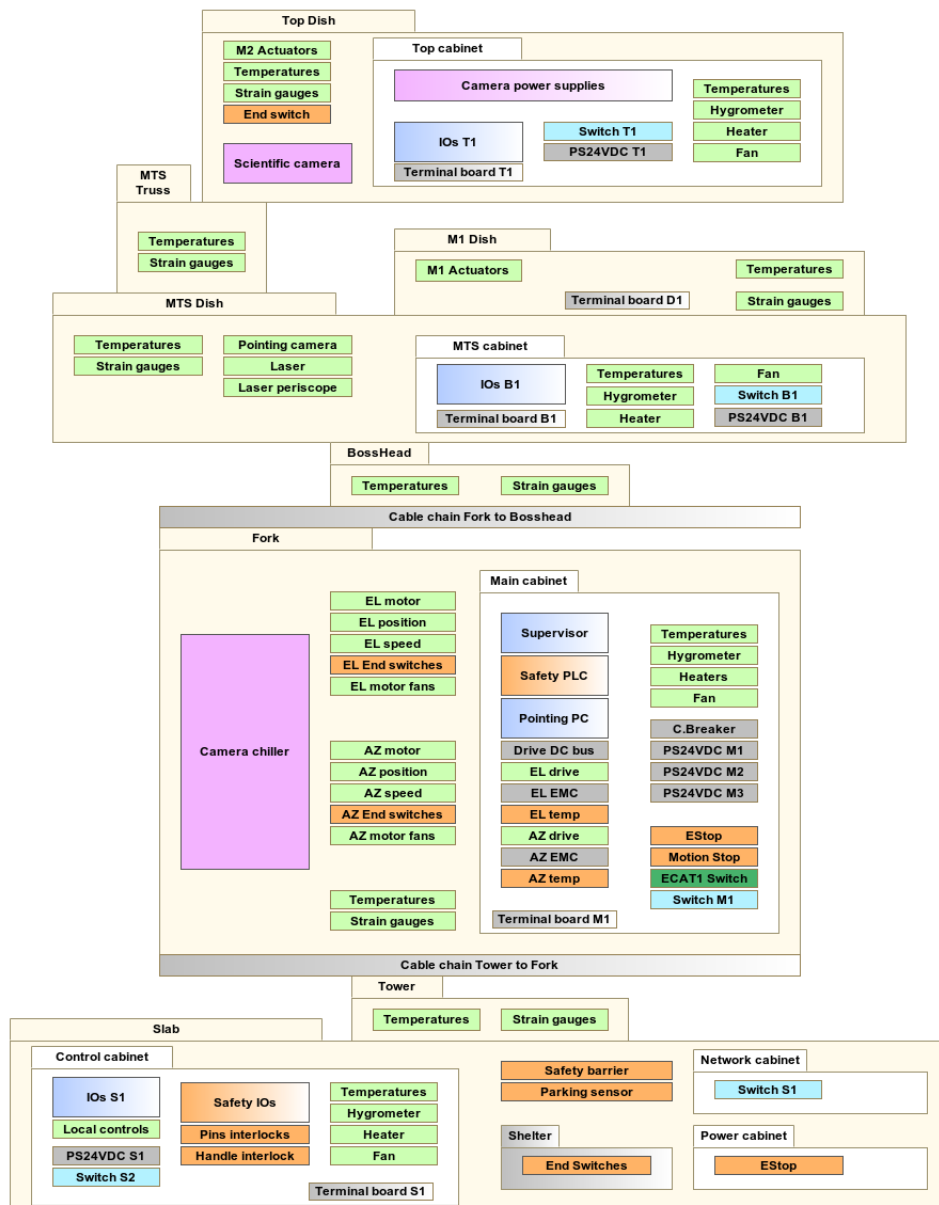


**Figure 2.40** – The hardware layout of the TCS. The camera hardware is shown in magenta, the safety hardware in orange, the actuators and sensors in green and other hardware in blue. The white boxes are the cabinets.

In the case of grid power failure, a backup line at 230/400 V and 50 Hz three-phase supplying 2.5 kW is required.

## 2.2 Interfaces

### 2.2.1 Internal Interfaces

The main telescope structure was designed at the Observatoire de Paris. The interfaces within the structure are managed by the SST-GATE team and described in an Interface Control Document. The camera was designed by the camera group (formerly the CHEC project team) and the interfaces within the camera are managed by this group. The interface between the camera and the telescope was developed by the structure and camera teams in collaboration with the ASTRI SST-2M project to ensure that the GCT cameras are compatible with both the GCT and ASTRI telescopes.

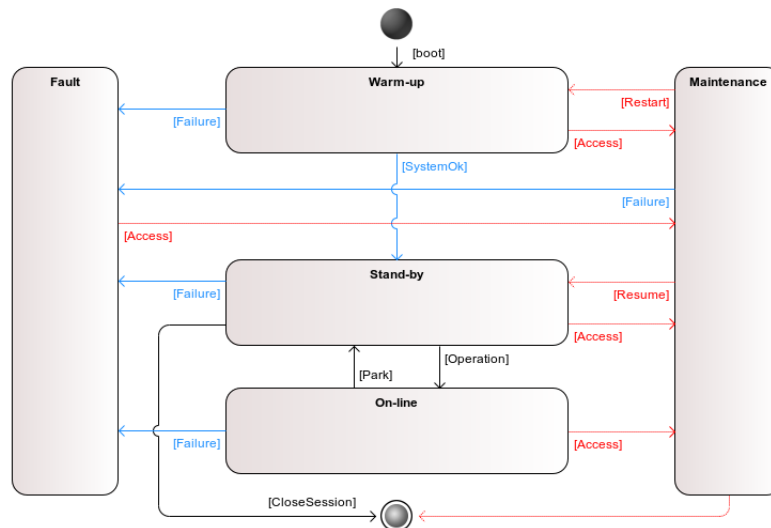


**Figure 2.41** – The modes of the TCS are: **Warm-up**: Start the Supervisor and the safety PLC, start all processes, warm-up electronic devices, etc. **Stand-by**: The telescope is parked. **On-line**: Main mode for the Operator. **Fault**: The transitions to this mode are automatic (as for all blue links). Depending on the situation, possible automated actions are Park telescope, Stop all motion processes, etc. **Maintenance**: Restricted to the Engineer (red links), processes are started/stopped at will, calibration constants may be modified, etc.

This section provides information on the interfaces between the various PBS items. The internal interfaces are:

- from the foundation to the tower;
- from the tower to the AAS;
- from the AAS bosshead to the counterweight;
- from AAS bosshead to the optical support structure via the MTS bottom dish;
- from the MTS bottom dish to the M1 dish;
- from the M1 dish to the primary mirror via the actuator support;
- from the MTS bottom dish to the MTS top dish via the MTS arms;
- from the MTS top dish to M2;
- from the MTS top dish to the camera removal mechanism;
- from the camera removal mechanism to the camera;
- the camera electrical, cooling and mechanical interfaces,
- from the camera chiller to the GCT structure;
- from the electronic cabinets to the GCT structure;
- inside the camera all electronic components have defined interfaces to each other.

Figure 2.42 provides a sketch of all the internal GCT interfaces that are briefly described in the following. The interfaces with the foundation and the camera are also described.

### Foundation to tower

The tower is attached to the concrete foundation by 16 M20 stud anchors arranged on a circle of diameter 600 mm. Three of these stud anchors are used to align the tower with respect to the vertical. This and other possible attachment solutions will be evaluated during the assessment of the prototype telescope.

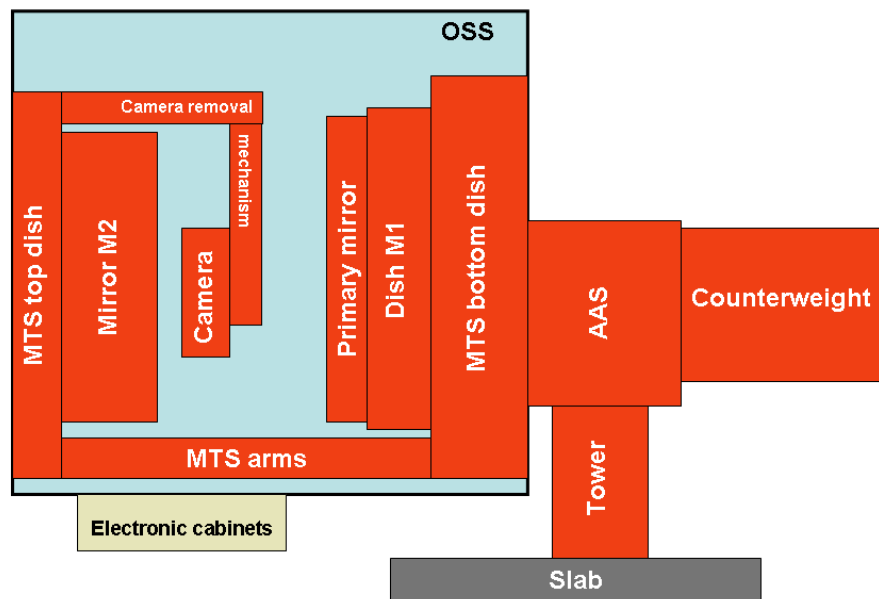


Figure 2.42 – Schematic of all internal GCT interfaces.

### Camera to the camera removal mechanism, mechanical, electrical and data interfaces

The camera shape, size, and mass are fully specified. The rear mounting plate, mounting points, and fixings are defined. The electrical and data interfaces consist of power lines and optical fibres. All of these connections to the camera are fully defined, including pinnings and connector locations. The cable routing through the telescope is defined, as is the power supply location, the power supply input power, and the communications cabling.

### Camera removal mechanism to camera, via the camera support structure

The interface between the camera removal mechanism and the camera is realized via the camera support structure. The support structure has a circular matrix of twelve holes to allow the connection by M8 bolts. The camera support structure has been designed to allow the integration of both the CHEC-M and CHEC-S cameras. The distance between the interface flange at the back of the camera and the focal plane must be at most 500 mm. The camera is fixed using three bolts (M8), with spacers to compensate for the length difference between the two cameras. The camera support structure allows the adjustment of the tip/tilt and the decentering of the camera.

### Camera chiller to GCT structure

Cooling the camera requires an external chiller. This is mounted on the GCT structure. A support has been designed for the chiller which insulates the structure from any vibrations in the chiller using damped springs. It also prevents heat exchange with the telescope. The chiller is oriented to that the hot air it produces is directed away from the mirrors and drive systems. The chiller support is fixed onto the AAS fork via a standard rail.

### Electronic cabinets to camera

The interface with the camera consists of optical fibres, power cables and cooling pipes. The camera is provided with the required power and voltages (12 and 75 VDC) via dedicated power supply modules located in the top cabinet. High power cables are used to ensure the voltage drop between the power supplies and the camera is small.

### Interfaces inside the camera

A range of further internal camera interfaces is defined below. Many of the camera electronics components are produced at separate institutes and are the subject of internal ICDs. For each item, these ICDs include, but are not limited to: the mechanical size; tolerance and fixation points of the item; all connector definitions and pinnings; all signal definitions and the expected power consumption.

**Photodetectors:** These have an interface with the focal plane plate, the photodetector base PCB, and the front-end buffers that are part of the preamplifier circuitry.

**Front-End Buffers and Preamplifiers:** These interface with the photodetectors, the TARGET modules, the focal plane plate and the camera rack mechanics.

**TARGET Module:** The ASIC PCB of the TARGET modules interfaces with the Preamplifier PCB, the Backplane, the DACQ boards, the focal plane plate and the camera rack mechanics.

**Backplane:** The Backplane has an interface with all TARGET modules, the DACQ Boards, the Peripherals board, the internal camera power-supply cable, and the camera rack mechanics. Additionally, the FPGA on the Backplane is actively cooled by a liquid-chilled heat-exchanger block which interfaces to the camera thermal control system.

**Peripherals Board:** The Peripherals board has interfaces with the Backplane, the camera rack mechanics and all peripherals, including the calibration units.

**DACQ:** The DACQ boards interface with the Backplane, the camera rack mechanics and the internal fibre optic cables.

**Lid:** The camera lid has interfaces with the camera enclosure and the Peripherals board.

**Thermal Interface:** The GCT camera requires liquid cooling. The inlet/outlet connector positions on the camera are defined, as are the chiller pipe specifications and the pipe routing. The chiller position is specified. The chiller power and communications cabling and connectors are defined.

## 2.2.2 External Interfaces

The description of the external interfaces of the GCT telescope is divided into three sections. The first concerns the communication of the camera with the data link, the second presents the logical interfaces, and the third is devoted to the structural interfaces (power, Ethernet, the equipment for mounting and maintenance, the foundation, the assembly hall, spares storage, the fence, maintenance equipment, fire protection, parking facilities and the roads on the site). For the sake of clarity, these have been sorted as in the interface database in *Sharepoint* according to the CTA interface management plan.

### 1. Camera to array trigger and timing system

The logical interfaces between the camera and ACTL are with the time synchronisation and array trigger system, the camera control system and the camera server for bulk data transmission.

**2. Telescope to array control** The logical interfaces between ACTL and the telescope are used to control the telescope and monitor its status. They consist of several sets of functions (see Table 2.4) conveyed through the OPC UA protocol. The functions are split into four types, according to their purpose: *mode*, *cmd*, *get* and *set*. Two examples are given below:

- `drive_cmdMotionStop()` to stop the current motion,
- `safety_getSwitchState(switch, state)` to get the state of the specified safety switch (open or closed).



Access to the functions may be restricted, depending on the status of the telescope user (“Operator”, “Commissioning engineer”...).

**Table 2.4** – The logical interfaces between the TCS and ACTL.

Code	Designation
I-ACTL-GCT-XXXX	
0001	Pointing Monitor
0002	Safety system
0003	Drive system
0004	Time synchronization
0005	Weather station
0006	Telescope housekeeping
0007	Active mirror control
0008	Alignment system
0009	Telescope calibration
0010	Technical archive
0011	Scientific camera

### 3. Telescope to infrastructure

This section follows the list of items identified in the Interface Database on SharePoint and the interface with the foundation (see Table 2.5). Most of these interfaces are already described in the design or plan sections. A few are summarized here.

#### **I-INFRA-SOUTH-SST-2M-GCT-0001 – Shipping containers**

The mounting of the GCT telescope does not use any procedures which require expert engineering capability, except for the alignment of the AAS which is carried out in industry by the prime contractor in charge of telescope production (see section 4). The telescopes are therefore shipped as separate modules (see section 4.1.1 for more details) which can be assembled on site. Seven containers are used for the transport of the GCTs to the site. Three containers, containing three telescopes, are shipped to the CTA site while the other three containers are being loaded with a further three telescopes by the prime contractor. The seventh container is used to ship the shelter; this shipment is also managed by the prime contractor.

The containers are:

- Container 1: A 40 foot container to ship 3 completed M1s and 2 M2s.
- Container 2: A 20 foot container to ship 3 AASs, the counterweights, the third M2 and the remaining optical elements.
- Container 3: A 20 foot container to ship the mechanical structure and cabinets.
- Container 4: A shipment of two shelters.

#### **I-INFRA-SOUTH-SST-2M-GCT-0004 – Area around telescope**

The area around the telescope must be flat, with a slight slope to allow rain water to drain away, and free of flammable material. This area must be smooth enough to allow the movement of manual lifting equipment and must resist a pressure of 2000 hPa. The paved/gravelled area must have a size of  $28 \times 31 \text{ m}^2$  in order to allow a crane to manoeuvre around the telescope. This area must resist a pressure of 3000 hPa. Three concrete slabs for the shelter are situated on the flat area. Their dimensions will depend on the nature of the soil.

#### **I-INFRA-SOUTH-SST-2M-GCT-0007 – Delimited area**

In addition to the gravelled area for the telescope foundation, there must be another area of  $42 \times 31 \text{ m}^2$ , adjacent to the gravelled area, to allow lorries to manoeuvre while delivering materials and equipment. As a consequence, the total surface area for one GCT is  $70 \times 31 \text{ m}^2$ . Depending on the overall level of site security, a fence may be needed around this area to prevent access to the telescope while it is in operation. If this fence is required, a gate of 5 m width is needed to provide access to the restricted area. This will have an electro-mechanical alarm to indicate if it is open.

**Table 2.5** – List of the external interfaces.

Code	Designation
I-INFRA-SOUTH-SST-2M-GCT-XXXX	Designation
0001	Shipping containers
0002	Machinery
0003	Storage outdoors
0004	Area around telescope
0005	Telescope structure foundation
0006	Anchorage of the telescope
0007	Delimited area
0008	Power line
0009	Power line backup
0010	Fibre connector
0011	Fire detection
0012	Fire fighting
0013	Lightning protection
0014	Monitoring system
0015	Lighting around telescope
0016	Machinery for maintenance
0017	Buildings
0018	Storage
0019	Roads
0020	Water provision
0021	Cable ducts (data)
0022	Cable ducts (power)
0023	Slab cabinet
0024	--
0025	Backup power

**I-INFRA-SOUTH-SST-2M-GCT-0008 – Power line**

A 230/400 V and 50 Hz three-phase supply of 10 kW power is required from the electricity grid. The normal peak operating power is 3 kW, but additional power is needed for the electrical devices used during integration and maintenance.

**I-INFRA-SOUTH-SST-2M-GCT-0011 – Fire detection**

The fire hazard on a GCT telescope is electrical and associated primarily with the cabinets. The other components that may cause fire, such as the actuators, have no flammable material around them and hence fire cannot propagate from them. As a consequence, fire detection is mandatory in the cabinets on the foundation and the telescope. Several methods exist to detect burning. Three of them fit the GCT requirements: detection of smoke; detection of an unexpected source of heat; and a combination of both techniques. The latter has the advantage that it can detect a fire at its earliest phase, since electrical fires usually produce excess heat before generating smoke. The shelter ensures that there is no risk from another possible cause of fires, the concentration of sunlight by the telescope mirrors during daylight hours.

**I-INFRA-SOUTH-SST-2M-GCT-0012 – Fire fighting**

As the fire will be confined to the electrical cabinets, three options fit the needs of the GCT. All of them require that staff go to the telescope involved, at least to ensure that the fire is out.

- The first solution consists of spraying water into the cabinet. The advantage of this method is that the fire can be rapidly extinguished, before staff arrive on site. It can reduce the amount of damage caused and the cost of repair.
- The second solution is to have a plug which blocks the cabinet's ventilation, hence extinguishing the fire.

- The third solution is to locate a fire extinguisher close to the telescope.

#### **I-INFRA-SOUTH-SST-2M-GCT-0013 – Lightning protection**

See section 3.1.2 for the design of the lightning protection system.

#### **I-INFRA-SOUTH-SST-2M-GCT-0014 – Monitoring system**

All data needed for monitoring will be accessible via the Ethernet interface. Monitoring information will be available in the control room and near the telescope via an Ethernet connection in the cabinet on the foundation.

#### **I-INFRA-SOUTH-SST-2M-GCT-0015 – Lighting around telescope**

The lighting is based on the NBN EN 12464-1 norm. At least 6 lights surround the gravelled area and illuminate it with at least 300 lux. This value is mandatory for an industrial area where manoeuvring and material handling is taking place.

#### **I-INFRA-SOUTH-SST-2M-GCT-0017 – Buildings**

The buildings provided for GCT shall offer an area of 100 m<sup>2</sup> and two adjacent areas of 8 m × 8 m × 9 m (height under the hoist) to allow the mounting of 2 telescopes. A bridge crane capable of lifting at least 10 tons is required for both areas (it could be the same crane). The building has to be at ground level without stairs. A door with 5 metres width and 6 metres height is needed to allow removal of telescope parts.

It may prove possible to relax these requirements. This will be determined following the completion of the prototype on the Meudon site (installation of the mirrors and the camera).

The GCT design and maintenance strategy is to use “plug-and-play” modules. Maintenance and repair of the modules removed from the telescope is performed largely on-site and requires indoor assembly space for major mechanical maintenance and a room (5 m × 5 m × 3 m) for repairs.

Additional facilities required are (1) a well equipped workshop (milling machine, drills...) of at least 30 m<sup>2</sup> with a workbench equipped with standard tools and (2) a dark room (7 m × 4 m) equipped with an optical bench of 3 m × 1.5 m and with standard opto-mechanical hardware.

#### **I-INFRA-SOUTH-SST-2M-GCT-0018 – Storage**

The storage volume includes all the spares needed for 5 years (components with a short life-time) and for 30 years (components with a long life-time). The environmental conditions (temperature, humidity...) are determined by the most stringent requirements of all the stored components. The total volume needed is equivalent to one 40 foot container.

#### **I-INFRA-SOUTH-SST-2M-GCT-0019 – Roads**

The roads must permit 19 ton lorries to drive up to the telescope locations.

#### **I-INFRA-SOUTH-SST-2M-GCT-0021 – Cable ducts (data)**

#### **and I-INFRA-SOUTH-SST-2M-GCT-0022 – Cable ducts (power)**

Metal cable ducts shall be used, with both ends grounded. The cable ducts between the cabinet on the foundation and the telescope shall be buried.

#### **I-INFRA-SOUTH-SST-2M-GCT-0023 – Slab cabinet**

The cabinet on the foundation requires an area of 3 m × 0.5 m at a minimum distance of 6 m from the telescope tower. It shall be fastened to the foundation with stud anchors. This cabinet will hold all the interfaces with the site infrastructure, i.e. power, network, optical fibres and water if required.

#### **I-INFRA-SOUTH-SST-2M-GCT-0025 – Backup power**

The telescope parking and shut down sequence lasts 5 minutes. A power of 2.5 kW is required at its start and the average power consumption is 1.5 kW.

## 2.3 Prototypes and Tests

### 2.3.1 Introduction

This section of the report describes progress with the design, manufacture and testing of prototypes for the GCT. Prototypes of all elements of the telescope have been or are being constructed. The assembly of a prototype structure was completed in April 2015 on the Meudon site of the Paris Observatory. Prototype mirrors for this telescope are now being manufactured, with installation foreseen in the summer of 2015. One camera, CHEC-M, using MAPMs, is currently undergoing commissioning and testing in Leicester. This will be mounted on the prototype telescope in Meudon towards the end of 2015 and its performance on the telescope verified. A further camera, CHEC-S, which is SiPM-based, is being constructed. This will be completed by the end of 2015 and then tested, first in the laboratory and then on the prototype telescope. Beyond the remit of CHEC-S additional development of critical components will be completed prior to the Pre-Production phase camera design.

One goal of this programme is to verify that the performance of the GCT is as expected and required. A second goal is to use the experience gained in the construction of the prototypes to refine the designs of the structure, mirrors and camera, in particular with regard to ease of manufacture and assembly. The latter will involve industrial partners where appropriate. Some design choices will be investigated using the prototypes. For example the final decision on the type of sensor to be used in the camera will be taken following tests of CHEC-S and CHEC-M. (Here, the rapidly improving price and performance of SiPMs makes it very likely that they will be used.) This programme will allow the design of the pre-production GCT to be completed in 2016.

### 2.3.2 Mechanical prototype

Many studies were performed during the design of the prototype GCT structure. These were based on calculations, optical investigations, tests of prototype components and of control systems, and are discussed in the following. The telescope test programme will culminate with a complete system test of the GCT prototype in Meudon.

#### **Trade-offs in the prototype design**

Several trade-offs were made in arriving at the best design solutions for the GCT structure. The main issues studied during the prototype design are described here. Topological optimization was used to help define the best solution with regard to the mass/stiffness ratio for several components, using FE models. These optimizations were made using the SOL 200 package of MD.Nastran (MSC Software). Further details can be found in the GCT FEA report [8]. More information on the FEA of the telescope structure is provided in section 3.2.1.

#### *Tower*

The diameter of the tower is constrained by the azimuth crown's diameter (outer diameter 470 mm). The minimal required thickness is analytically estimated by considering several factors:

- Compression, related to the mass of the OSS;
- Bending, related to wind loads;
- Buckling hazard.

Calculations show that a minimal thickness of 10 mm is required to avoid buckling and to keep bending and compression stresses within admissible values.

#### *Aperture for motors*

FEA has also shown that any aperture in the tower strongly decreases its stiffness. The azimuth motor is therefore mounted outside the tower. This also simplifies cooling of, and access to, the motor.

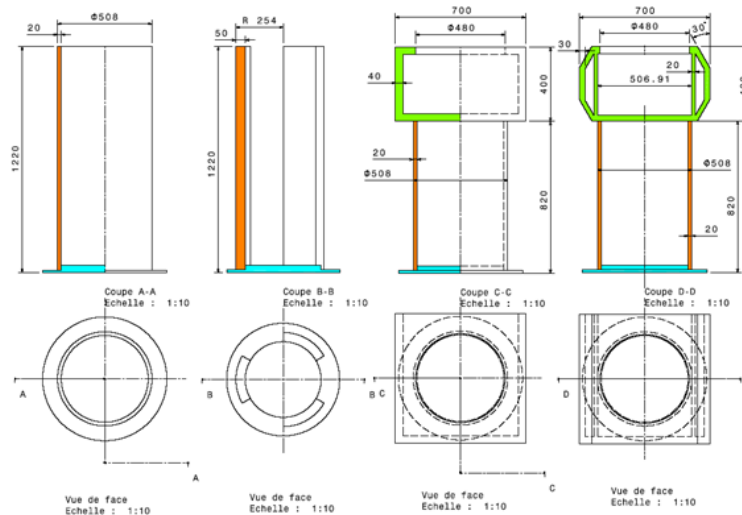


Figure 2.43 – Evolution of the tower structure design.

### Short or long tower

FEA was used to define the dimensions of the tower and the fork mounted on it. The result shows that a relatively long tower and a small fork are preferred for reasons of cost, mechanical performance (see figure 2.44), impact on the global accuracy of the telescope, ease of assembly, mass and maintainability. (Details of the analysis can be found in the internal trade-off document.)

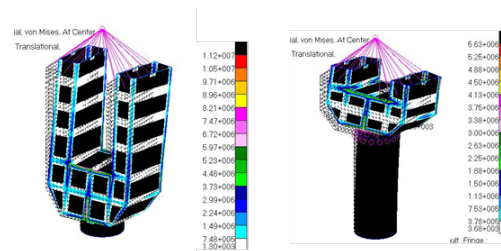


Figure 2.44 – Axial bar stresses calculated using FEA of an AAS with a long (left) and a short (right) fork. The masses of these designs are 1.9 and 1 ton, respectively.

### Alt-Azimuthal System

The design of the alt-azimuthal structure was guided by topology optimizations made using local FE models, as described briefly in the following.

#### Fork

Optimisation of the fork's topology was carried out for two cases, with and without aperture constraint. If the aperture is constrained, the OSS is modelled as one mass, if not, the OSS is modelled as two masses. Gravity and wind loads are taken into account. The resulting structures are shown in figure 2.45. In reality, the fork's aperture is constrained, but with a finite stiffness related to the properties of the bosshead and the elevation drives. The constrained optimized design was thus preferred. The final mechanical design consists of two lateral plates linked by a central rigid base. The validation of its performance is described in section 3.2.1.

#### Bosshead

Similar local finite-element modeling of the bosshead was used to optimise its topology.

#### Mast and Truss Structure (MTS)

Optimization of the MTS focused on the conceptual design of the Truss Structure and of the MTS Bottom Dish.

Using a Serrurier-like design increases the stiffness of the Truss Structure compared to a classical tripod or tetrapod with similar shadowing. The geometry of the tubes (outer diameter and thickness) of the Truss Structure was optimised with respect to the rigidity of the mast, its total mass and the shadowing

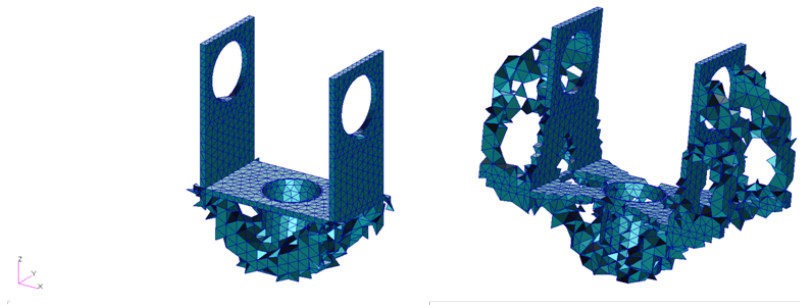


**Figure 2.45** – Topology optimization of the fork with (left) and without (right) constraining its aperture.

caused by the tubes.

The goal of the optimisation of the Bottom Dish was to produce a light and stiff structure which can hold the Top Dish, maintaining tilt and decentering within acceptable limits in observing conditions (e.g. elevation angle between  $20^\circ$  and  $91^\circ$ ). A preliminary topology optimization resulted in a structure with a central flange linked to the bosshead and arms linked to the Truss Tubes. Several parameters were then optimised using a local FE model of the OSS. These parameters are:

**The number of arms.** A four-arm Bottom Dish structure is better than a three-arm structure as it better matches the symmetry of the bosshead and the force and torque per arm are lower.

**The position and orientation of the arms.** Arms parallel to the elevation axis contribute to preventing tilting of the OSS through twisting, rather than bending, providing less stiffness. This orientation is therefore avoided. For the same reason, stiffness is improved if the angle of the arms to the elevation axis is greater than  $90^\circ$ . The final angle between the arms resulted from a trade-off between the rigidity of the Bottom Dish and the rigidity of the Truss Structure.

**The inclination of the arms in the plane perpendicular to the telescope axis.** Slight inclination of the arms of the Bottom and Top Dishes increases their rigidity. These inclinations are limited by the space available due to the geometry of the mirrors.

#### *Conceptual design of M2*

FE studies have been performed to determine the locations of the actuators which hold M2 and the dimensions of the M2 support structure.

The impact of the location of the actuators on the deformation of the mirror was studied using an FE model of a circular mirror supported at 3 points. The gravity-induced displacements were computed for various locations of the actuators and showed that the optimum actuator position is at a radius of 780 mm.

Topology optimisation of the support structure was carried out using the same tools as described for the optimisation of the fork. The actuator support position and the mirror surface were boundary conditions in the optimisation. Several load cases were considered to take into account the orientation of the mirror and the position of the mirror panels. The optimisation led to the introduction of triangular rather than trapezoidal cells for the Mirror Support Structure and a significant increase in the stiffness of the mirror with little change in its mass. The resulting support structure is shown in Figure 2.46.

#### **Further FEA studies**

##### *Camera removal mechanism*

When the GCT is in its parking position, the upper arm of the camera support structure can be unlocked from the Top Dish. This allows the camera support to rotate around its lower attachment to the Top Dish, which is made via two self-lubricating steel bearings. The rotation is controlled by a cable system and pulley on the Top Dish. The cable system is dimensioned to support the load due to the camera and its support structure, a total mass of less than 150 kg. The bearings can withstand a load of 254 kN each<sup>1</sup> and the working load of the steel cable is about 500 kg. FEA of the telescope with the camera

<sup>1</sup> Technical data of the spherical bearings CSS30 are available at <http://shop.hpceurope.com/fr/produit.asp?prid=1030&lie=0&nav=3>

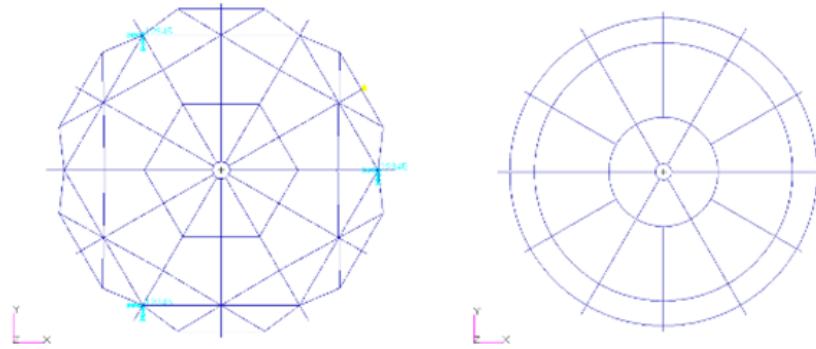


**Figure 2.46** – Triangular optimized cells (left, mass: 117 kg, first normal mode frequency 80 Hz, maximum distortion 60  $\mu\text{m}$  peak-to-valley) vs trapezoidal cells (right, mass: 106 kg, first normal mode frequency 36 Hz, maximum distortion 201  $\mu\text{m}$  peak-to-valley).

in its lowered position has been carried out to determine the stresses in the cables and the structure. The maximum force in the cable is 0.7 kN and is smaller than the working load of the steel cable. The stresses in the structure are largest in the aluminium supporting plates of the camera (about 80 MPa) and in the aluminium Top Dish close to the pulley (about 50 MPa) as shown in Figure 2.47. As these are well below the yield stress of the grade 6 aluminium used (241 MPa), no damage will occur to these components during camera removal.

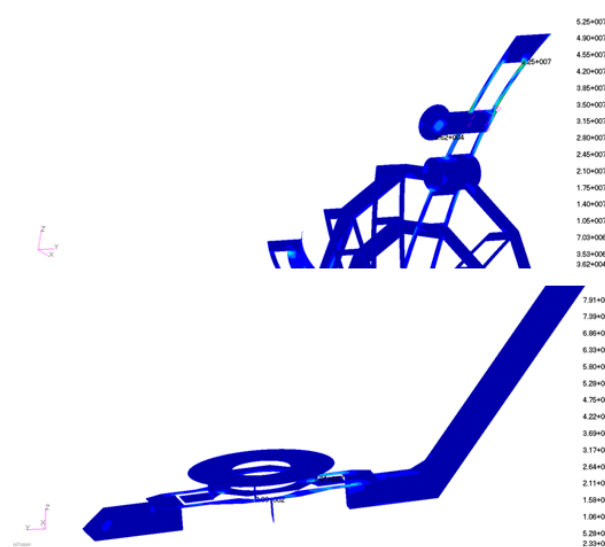


**Figure 2.47** – Plot of the Von Mises stresses in the Top Dish and in the moveable supporting arm of the camera during camera removal.

### *M1 rotation system*

The GCT design provides for the rotation of the M1 Dish about the telescopes axis to facilitate access to the M1 petals during maintenance and installation operations. This rotation is achieved by separating the flange of the M1 Dish from the upper flange of the Bottom Dish. The rotation system must therefore be able to support the gravitational load of the M1 Dish and of the primary mirror. To check this, FEA was performed with the M1 Dish separated from the Bottom Dish and the telescope at 0° elevation; only gravitational loads were considered. Maximum stresses in the stainless steel axis were 170 MPa. These are well below the yield stress of the steel (about 240 MPa).

### *Impact of differential torque on the displacement of the OSS*

Since only one side of the elevation drive is motorized, the two lateral faces of the bosshead are subject to different torques. This might cause shearing of the bosshead and a degradation of the optical

performance. FEA was carried out on a local model of the bosshead in order to evaluate the stresses and deformation induced by the application of the drive torque to only one of its sides. The results show that there is a maximum rotation of the OSS about the optical axis of 37 arcsecs. This has no impact on the telescope performance. All other resulting rotations and translations were negligible. Moreover, maximal resulting Von Mises stresses in the bosshead were about 7.6 MPa, considerably smaller than the allowable stress for this S355 structure (yield stress: 355 MPa).

#### **Mechanical tests:**

The telescope tracking and pointing precision form part of the CTA requirements and are influenced by many mechanical factors such as:

- The verticality of the tower,
- Flexing of the M1 dish,
- Flexing of the overall telescope structure,
- The characteristics of the bearings,
- Play in the gears.

The telescope prototype will be used as a test bench to measure the impact of each of these parameters on the tracking and pointing precision.

Measurements reported here aim to verify that the bearings are within specifications and to investigate the ageing of the mechanical parts involved in the telescope motion, with the attendant effects on maintenance procedures. For this purpose, the following parameters are measured:

- wobble;
- run out;
- the equidistance of the ball bearing teeth;
- tooth shape repeatability;
- the repeatability of drive motion over several turns.

The tolerance on the run out (the distance that separates the rotation axes of the bearing and the worm gear) is 0.25 mm. Exceeding this value generates strains in the worm gear and increases the torque required to move the telescope as well as having consequences for the smoothness of the tracking. A further impact could be premature ageing of the worm gear.

Measurements of the displacement of the rotation axis showed that this is lower than 200  $\mu\text{m}$  for the three bearings tested. There is thus no problem of accelerated ageing (the generated stresses remain below 250 MPa) nor on the smoothness of operation. This was demonstrated using a telescope model including these characteristics. As regards repeatability of the movement, Figure 2.48 shows the variation in the positions of the first 10 teeth of the drive over 9 turns. The variations remain within 20  $\mu\text{m}$  and the telescope model again shows that this has no significant influence on the smoothness of the telescope's movement.

The tooth width was also measured, as variations in their width generate a variation in the speed of the movement of the bearing. The standard deviation of the width was found to be 10  $\mu\text{m}$ , which is 1/1000 of the width of a tooth. This was incorporated in the telescope model and found have no significant impact on the movement. The tracking operation is intrinsically very accurate; deviations are dominated by the bending of the structure caused by wind gusts.

These measurements were also used to select the two bearings for the elevation axis that minimise wobble. Their performance was included in the telescope model.

Finally, these measurements show that all the bearings are well within the manufacturer's specifications.



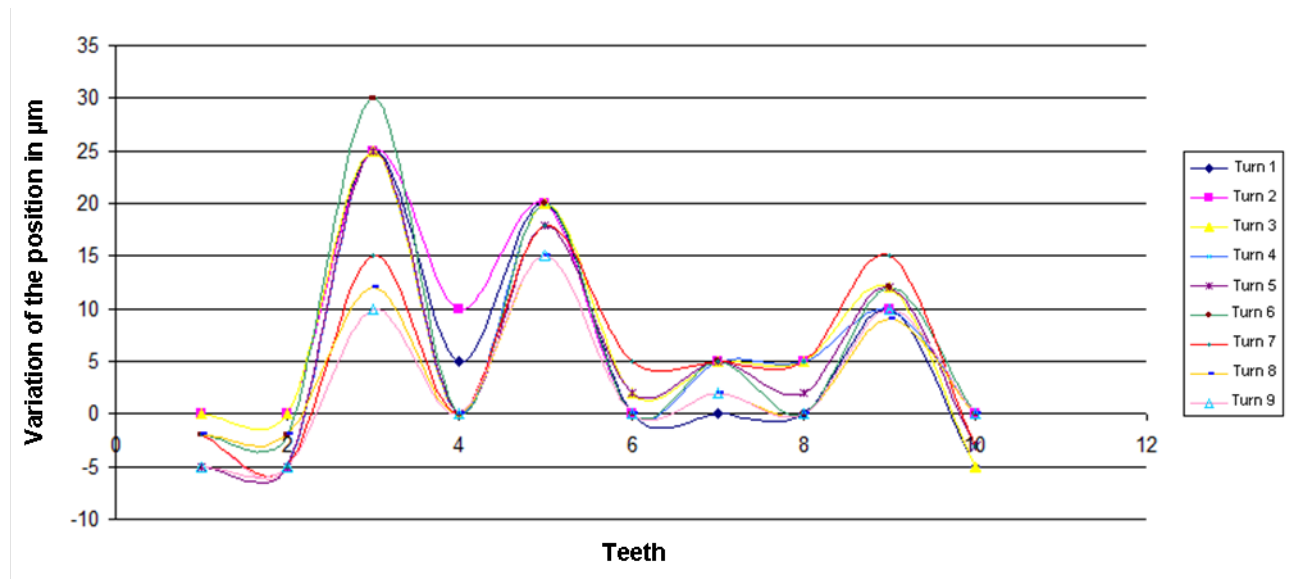


Figure 2.48 – Variation of the position of the first 10 teeth after 9 turns.

### Optical Prototypes and Tests:

The mirrors are amongst the most important parts of the telescope as they directly affect the PSF and the optical throughput. Those for the GCT prototype are being produced by machining bulk aluminium to the required aspherical shape (and machining the rear support structure), polishing and then coating the reflective surface.

Two different M1 petals sizes have been investigated, that for the prototype and that for the final telescope. The impact of the smaller M1 petal surface on the PSF and petal alignment procedure was simulated using a Zemax model of the telescope and confirmed with ROBAST calculations. It was found that the overall size of the PSF remains unchanged, and that tip-tilt and defocus show the same behaviour with the prototype and final petals. Hence the same alignment process can be used in both cases and the accuracy achieved will be similar.

One goal of the prototyping is to test the aluminium mirror production process and compare the resulting mirrors with the glass mirrors being built for other CTA telescopes and with a test mirror being produced for the GCT using hot glass slumping.

### Test of the polishing phase

In order to develop suitable polishing techniques, several tests have been performed on both small and large sample mirrors. In the case of metallic mirrors, the polishing is designed to decrease the roughness of the reflective surface without damaging the aspherical shape obtained in the machining step. For the prototype, manual polishing was performed. This process will evolve towards automatic polishing for the mass production phase, see Section 4.1.1. Several samples have been machined at the Observatoire de Paris to produce M1 petals and an M2 scaled down to 1/10 of their actual size. These mirrors have an initial roughness of  $0.6 \mu\text{m}$ . After polishing, the roughness achieved is of the order of  $0.02 \mu\text{m}$  (see Figure 2.49).

The surfaces of the mirror samples were scanned using three-dimensional metrology equipment before and after the polishing phase, in order to verify that the surface shape has not been changed by the polishing process. The surfaces were divided into 10 by 10 areas and the standard deviation, the maximum and the minimum values of their deviations from the theoretical shape measured, before and after polishing (see Table 2.6).

These measurements confirm that the polishing does not change the mirror shape; the standard deviation is similar, so the shape remains close to that desired. Both the maximum deviation and the peak-to-valley values decrease, which show the improved smoothness due to the polishing process.

These tests have also been done on a larger sample, of size of  $400 \times 420 \text{ mm}^2$ , in order to verify the effect

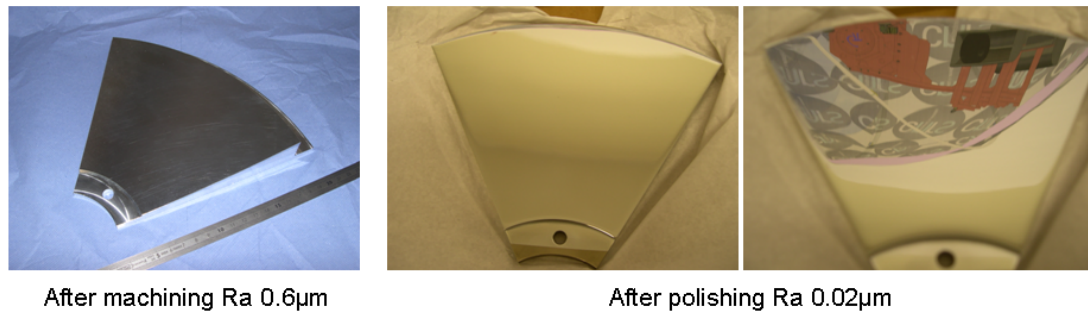


**Figure 2.49** – Pictures of the mock-up mirrors before and after polishing; decreasing the roughness Ra; the right-hand mirror is reflecting a picture of the GCT attached to the wall.

**Table 2.6** – Measurements of mirror samples before and after the polishing step - values are in mm.

Specifications	Before	After
Standard Deviation	0.012	0.013
Max. value	0.024	0.016
Peak to valley	0.062	0.051

**Figure 2.50** – Pictures of the large sample mirror before and after polishing; the polished (right) mirror is reflecting a picture of the GCT attached to the wall.

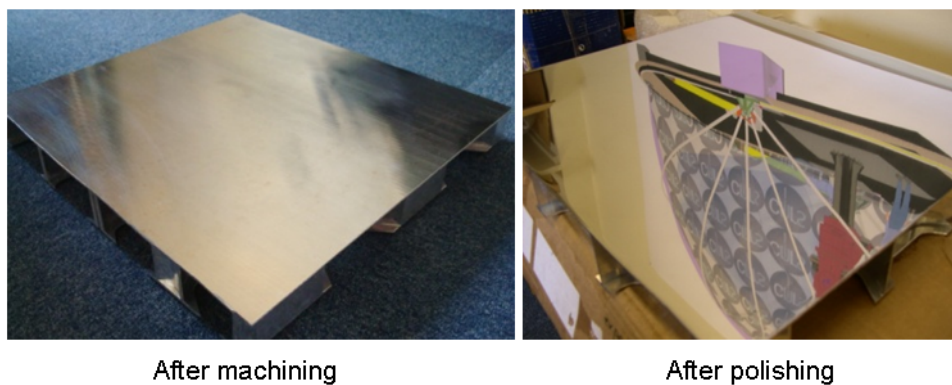


**Table 2.7** – High and low frequencies measured before and after polishing for the large test mirror.

	Before Polishing		After Polishing	
	High frequency	Low frequency	High frequency	Low frequency
<b>Std. Deviation</b>	0.143	0.297	0.097	0.062
<b>Max. value</b>	0.501	0.377	0.333	0.115
<b>Peak to valley</b>	0.068	0.392	0.004	0.028

of the polishing (Figure 2.50) and examine possible larger scale defects. The large mirror was divided into squares of  $100 \times 100 \text{ mm}^2$  so information on low spatial frequencies can be obtained. Four of these squares were subdivided into 4 by 4 smaller squares to study higher spatial frequencies. To facilitate comparisons with the Zemax simulations, the mirror surface was defined using Zernike polynomials. The Zernike coefficients between 2 and 21 are related to the low spatial frequencies of the surface and correspond to the size of the large squares. The waviness value is determined by these coefficients. The Zernike coefficients ranging from 22 to 231 are related to the high spatial frequencies that correspond to the smaller squares. As before, the measurement of the shape was performed before and after polishing. The results of the polishing are visible in Figure 2.50.

Table 2.7 shows that larger samples do not suffer shape changes during polishing. The standard deviation decreases slightly, so the surface is more uniform. The maximum deviation and the peak-to-valley values decrease at both low and high frequencies, showing that the polishing improves the surface quality and that diffraction and scattering will be reduced thanks to this step. The tests performed on both the small and the large mirror samples show that the polishing improved the surface roughness without spoiling the mirror's shape. The improvement in the roughness is most visible on the large sample.

### Test of mirror roughness

The correct mirror shape ensures that the PSF is as required, while the roughness of the mirror determines the fraction of scattered light. In order to achieve the image quality needed for Cherenkov light observations, the surface roughness must be below  $0.02 \mu\text{m}$ . Amra et al. [9], establish a link between surface roughness and scattering, expressed as the Total Integrated Scattering (TIS). They demonstrate that a surface with a roughness of 3 nm has a TIS value of about 112 ppm (0.0112%). Hence, the surface roughness of the GCT mirrors must be better than 20 nm, giving a TIS of  $\approx 0.1\%$  (see [10]), sufficient for our application.

An independent evaluation of the GCT metal mirrors has started to characterise and to validate the full processing chain. Tests of the surface roughness have been performed on small mirror samples by the using the CTA Mirror Test Facility (MTF) at the Joint Laboratory of Optics in Olomouc. Measurements of the reflectivity and the PSF and have been made on two samples. The first (sample mirror number 5) is pure aluminium, while the second (sample mirror number 6) has a nickel coating. The best result is achieved by the latter. The roughness is 25 nm with 88% of the light from a point source being detected within a circle of  $0.25^\circ$ . The amount of scattered light is 2%. This fulfils the CTA requirements.

Optimisation of the manufacturing process is under investigation for mass production and to further improve the surface quality of the mirrors. The aim is to get the PSF down to  $0.15^\circ$  without significantly increasing costs. Improved machining and polishing should make this possible and result in better micro-roughness. The two first segments of the primary mirror have been produced and are currently under study at the IRFU laboratory (CEA, Saclay). The PSF of each petal will be measured and compared with Zemax simulations. For this purpose, an optical test bench is being set up at IRFU. This will also give a complete set of measurements of the reflectivity and the scattered light in order to better estimate the expected GCT performance.

Another major direction for improvements is the coating. A reflective surface made of aluminium or nickel cannot achieve a reflectivity better than 90%. Tests of coatings have been in progress since summer 2014 on test mirrors. The coatings are based on three dielectric and aluminium layers and should increase the reflectivity by 3% to 4% at wavelengths between 300 nm and 650 nm. Test mirrors

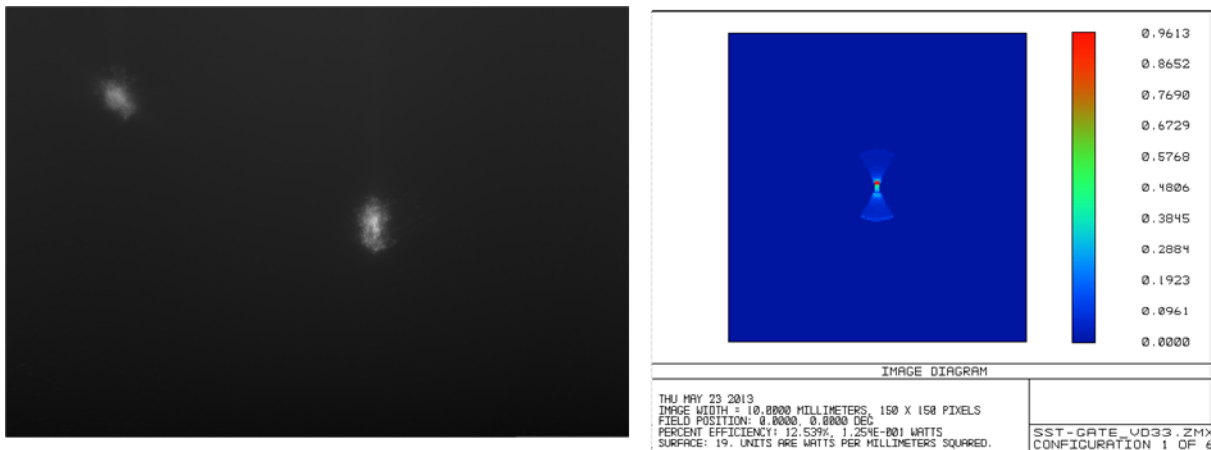


**Figure 2.51** – Left, the PSFs delivered by two petals of the mock-up. The central PSF is for an aligned petal. The scale is not linear. Right, Zemax simulation of the PSF for one perfectly aligned petal in ideal conditions.

with these coatings will be analyzed by the MTF group.

### Test of alignment procedure

The CTA SST-2M telescopes are the first SC telescopes built for gamma-ray astronomy. Care was thus taken to verify all aspects of the optical performance of the GCT. In particular, an alignment procedure has been developed and studied on an optical bench in Meudon. The test bench consists of a 1/10 scale mock-up of the telescope with 6 petals for the M1. Three actuators on each petal permit the focussing of the telescope and the alignment of the petals (Fig. 2.51).

The same CCD camera as is foreseen for studies of the GCT alignment has been used to:

- verify that the PSF has the shape predicted by the Zemax simulations;
- verify the expected behaviour of the PSF when the petals are misaligned and incorrectly focussed, in accordance with the expected tolerances;
- verify that the alignment procedure permits the expected on- and off-axis PSFs to be achieved.

The results of these tests give the GCT team some confidence that the proposed alignment tools and procedures will perform as hoped. This will be verified using the full-scale prototype.

### Telescope Control System Prototypes and Tests

- **Motion control** Simulations of the motion control loop have been carried out which have allowed an estimate of the dynamical behaviour of the telescope to be obtained and determined the power profile required for various telescope operations. Some of the parameters used in these simulations – such as dry friction, viscous friction, rolling resistance – will be refined using measurements on the prototype. This may allow the safety margins applied in the prototype design to be reduced, perhaps leading to lower cost and weight for the motors.
- **Motion profile** The motion profile used for slewing is based on an *S-curve* (see Section 3.2). The  $\alpha$  and  $\beta$  parameters allow the control of quantities such as the maximum speed and the maximum acceleration. The chosen parameters are a trade-off between avoiding excitation of the mechanical structure (oscillations) and power consumption (required current and DC bus voltage).
- **Power consumption** An estimate of the power required by the telescope has been made, with all devices taken into account. Measurements on the prototype will be used to refine this. Lowering the DC bus voltage of the drive system is a good way of reducing the power consumption; measurements on the prototype will help to find the lowest possible voltage value.

- **Brake resistor** The need for a brake resistor depends on the kinetic energy involved in the telescope motion, the energy stored in the drive power supply and the time over which deceleration occurs. The current design does not require a brake resistor (see Section 3.2); if the bus voltage has to be raised, this might be revised.
- **Strain measurements** Tests have been done using standard strain gauges – each requiring one Wheatstone bridge. Glass fibres can also be used. This latter solution allows multiplexed measurements with only one fibre. A second fibre installed alongside the first can give the deformations due to temperature. Only two channels are required for up to 15 measurements. A trade-off has to be carried out to choose between these two possibilities for tests of the prototype.

- **Cabinet layout** The prototype will allow the optimisation of the layout of devices in the cabinets. It may prove possible to merge some of the cabinets, especially on the foundation.

- **Pointing & tracking** One solution for the tracking computation is a static lookup system. This consists of *a*) completely computing the commands *before* the actual motion, *b*) uploading them to the drives' memory and *c*) triggering the drives to read the commands at the required time.

Another solution is a *full real-time* tracking system, i.e. real-time OS computing and sending the commands to the drives on the fly. This removes any preparation time, leading to a more responsive tracking system; moreover, it enables the actual weather conditions to be taken into account.

The latter solution is preferred and has been studied. Along with real-time software, a prototype tracking coprocessor implemented on an FPGA has been developed. This reduces power consumption and optimises the use of hardware. A first module, which calculates inverse trigonometric functions – e.g. arc-cosine – has been designed using an improved CORDIC [11] algorithm. The target used for this development was a CompactRIO (National Instruments) FPGA because the LabVIEW Real-Time module that can be used with this simplifies the programming significantly.

However, the communication between the computer and the ETEL drives cannot be real-time unless ETEL's proprietary protocol is used. This requires a dedicated PCIe card and the CompactRIO does not feature such a backplane. The solution lies either in designing software directly with a real-time OS, without the LabVIEW Real-Time module, on a target with PCIe slots, or the use of a drive/motor compatible with a standard real-time communication protocol, e.g. EtherCAT.

For the prototype, the development of a full real-time tracking system has been put on hold and the static lookup system will be used. This decision will be revisited once the prototype tracking tests have been performed.

- **Safety system** A basic safety system has been set up to experiment with the hardware connections that will be needed for the GCT and to study programming with distributed devices using an EtherCAT field-bus.
- **On-board computers** To ease software development for the prototype, two computers are used, the Supervisor and the Tracking PC. One goal of the prototype studies is to evaluate the possibility of merging these into one computer to both reduce the costs and achieve a simpler system architecture.

### 2.3.3 CHEC-M

The first GCT camera prototype is called CHEC-M and is based on MAPMs. This camera is fully assembled at the University of Leicester as shown in Figure 2.52, and is currently being commissioned.

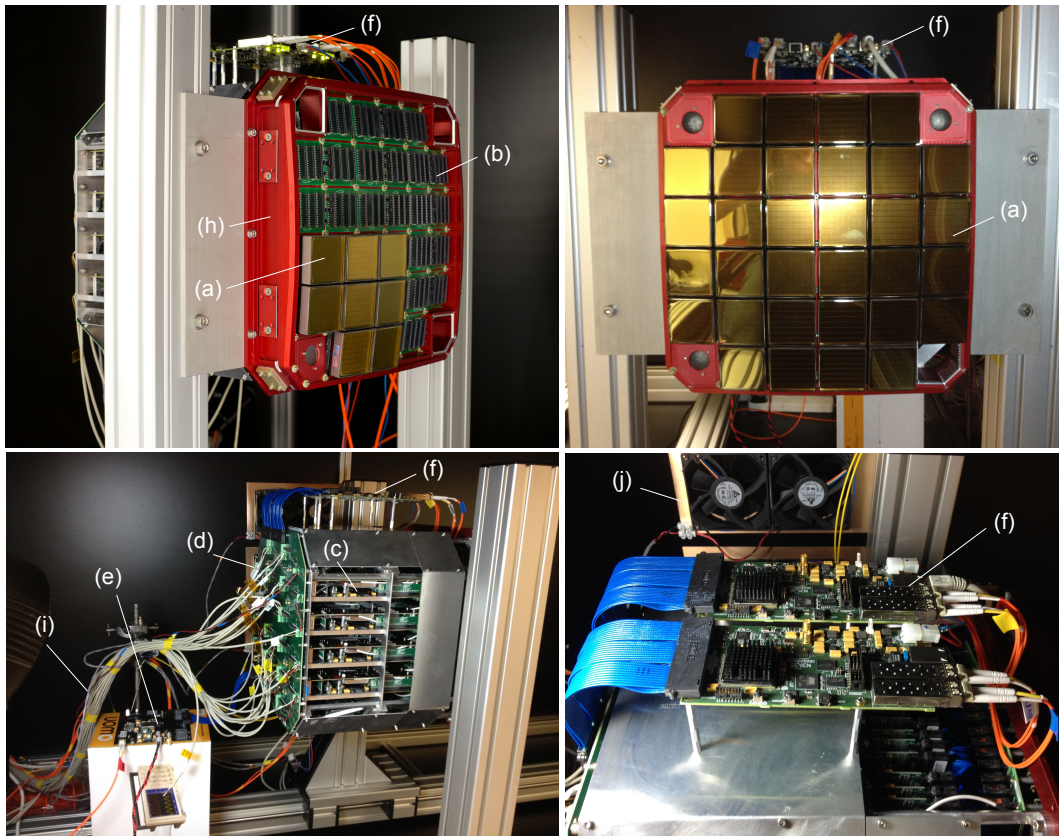


**Figure 2.52** – CHEC-M: (a) MAPM photodetectors, (b) preamplifier modules, (c) *TARGET* modules, (d) proto-Backplane, (e) FPGA test board, (f) DACQ boards, (g) calibration flashers, (h) internal mechanics consisting of focal plane plate and electronics rack, (i) 12 V input cables (j) lab fan-cooling.

terminal

### Mechanics Development

Figure 2.53 shows images of the complete CHEC-M mechanics. To verify the mechanical and thermal concept for CHEC-M, a quarter-scale camera demonstrator was built and qualified. Dummy *TARGET* modules and backplane with a representative heat dissipation were built and integrated into the thermal demonstrator. A scaled thermal control unit with heat-sinks and fans coupled to a building chilled water supply (14°C) was used to dissipate heat. Thermocouples were used to measure temperature as function of time across the demonstrator. One set of thermal results is shown in Figure 2.54. Once both fans and chiller are active, the a steady state across the demonstrator of between roughly 18°C and 20°C.

The mechanical tolerances were measured at the University of Oxford. These measurements were used to calculate the position of the centre of each MAPM relative to the ideal position in the focal-plane. Ray-tracing indicates that a defocus (movement in  $z$  along the optical axis) of 1 mm results in a 10% degradation to the PSF on-axis. The measurements indicate that the MAPM centres are nominally all within 0.35 mm of the ideal position (Figure 2.54(left)). This can be reduced to 0.035 mm with a global adjustment made at the rear of the camera when mounting on the telescope (Figure 2.54(right)). These measurements were made with a single MAPM shifted around the focal plane. The internal tolerances on the MAPM  $z$  dimension are  $\pm 0.26$  mm. Additionally the tiling of the curved focal plane with flat MAPMs

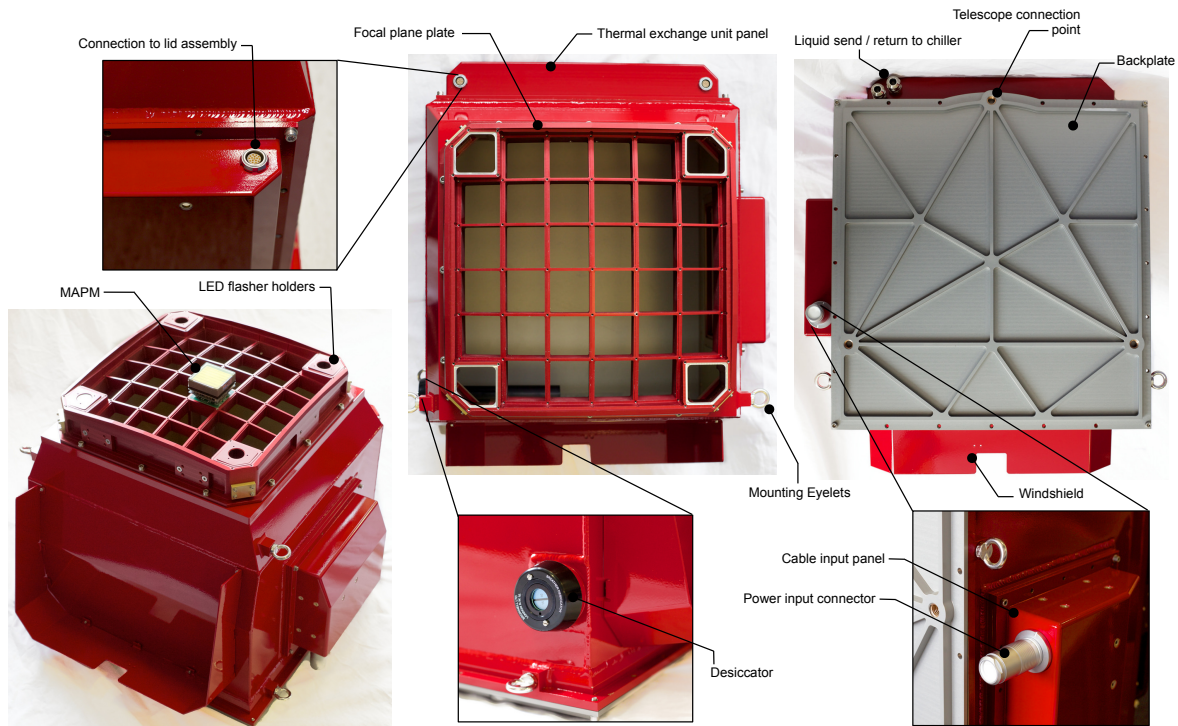


**Figure 2.53** – The CHEC-M mechanical enclosure.

creates a maximum shift of 0.45 mm from the ideal position for the edge pixels. In short: combining the tolerances implies a less than 10% degradation in PSF.

## Photosensor Qualification

The CHEC-M detector plane contains 32 Hamamatsu H10966B MAPMs arranged to approximate the 1.0 m radius of curvature optical focal plane as shown in Figure 2.52(a). The physical details of the MAPMs are given in Figure 2.32 and Section 2.1.4.

A single HV source of  $\sim 800\text{--}1100$  V is generated on the *TARGET* Modules and routed to the corresponding MAPM by an insulated cable (see Figure 2.33). A range of gain from  $\sim 4 \times 10^4$  to  $\sim 6 \times 10^5$  is possible, nominal operation will be at  $8 \times 10^4$

Figure 2.56 (left) shows the measured pulse area spectra for varying illumination levels from 1 pixel of 1 MAPM with a simultaneous fit to determine the pixel gain. The single p.e. peak is clearly visible in some, but not all, MAPM pixels at a high gain. By performing a simultaneous fit a better determination of the pixel gain is obtained.

Figure 2.56 (right) shows the dynamic range measurement for several pixels in a single MAPM. At 1000 p.e. and a gain of  $\sim 2 \times 10^5$  the response is linear to within 20%.

Figure 2.57 shows an example of angular response as measured on a single MAPM pixel. The SST-2M design results in incident light on the focal plane at angles of up to  $70^\circ$ . At this angle, the MAPM response drops by  $\sim 30\%$ . For further details of the MAPM performance see Section 3.2.5.

## Preamplifier Module Development

The CHEC-M preamplifier modules form part of the camera module as shown in Figure 2.52(b). The preamplifier module attaches directly to the MAPM on one side and to the *TARGET* modules on the other as can be seen in Figure 2.33.

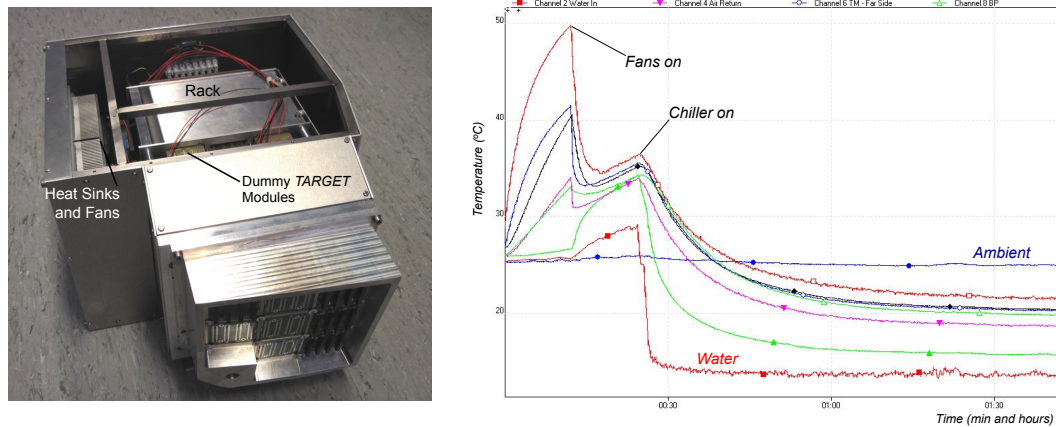


Figure 2.54 – The CHEC-M mechanical and thermal demonstrator (left) and one set of thermal results (right).

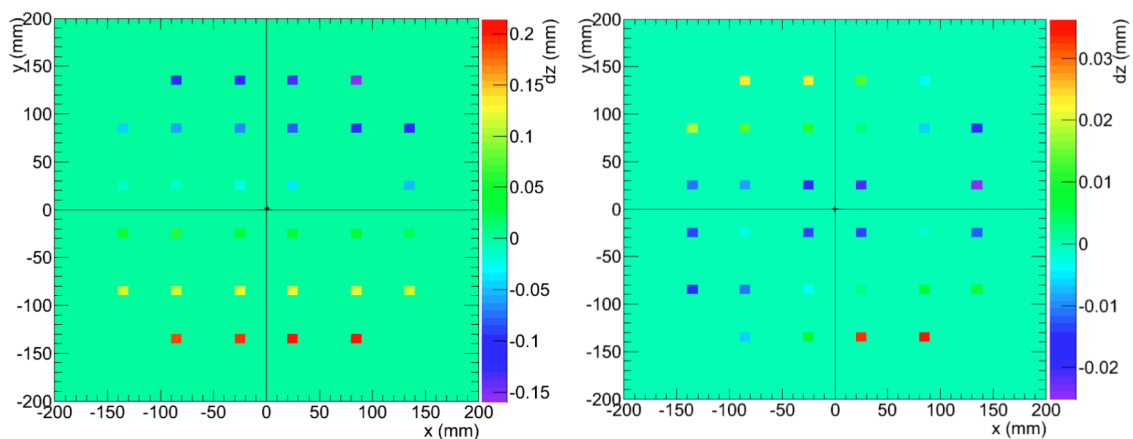


Figure 2.55 – Locations of the MAPM centres relative to the ideal positions before (left) and after (right) a global correction to the camera mounting position.

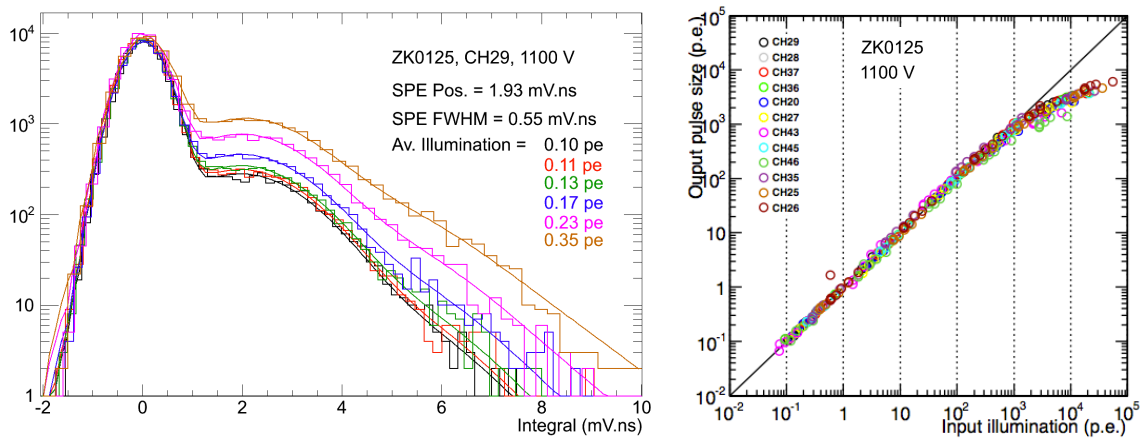
The MAPMs produce narrow pulses that must be shaped to optimise the camera-trigger performance (see Section 3.2.5). They must also be operated at a relatively low gain due to the high background rate associated with exposure to the night sky. Preamplifiers are therefore required to provide a signal matched to the input of the *TARGET* modules. These must be in close proximity to the photosensors to minimise electronic noise (again see Section 3.2.5 for details).

The preamplifier circuit contains an AD8014 operational amplifier operated in trans-impedance mode. The MAPM pulse shape at the output of the preamplifier is shown in Figure 2.58 for a range of MAPM input illumination levels. Saturation occurs above 1.3 V (the maximum input voltage of *TARGET* 5 ASIC. The preamplifier circuit utilises a +5 V supply and consumes  $\sim 1$  mA quiescent current corresponding to a power consumption of between 9 and 20 mW per channel depending on the event rate.

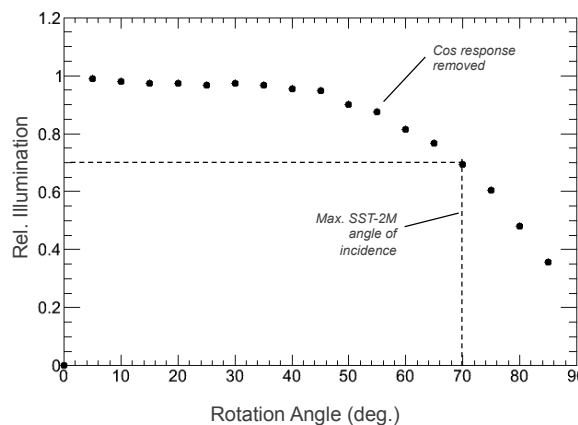
The preamplifier is incorporated into a 64-channel preamplifier module consisting of 4 x 16 channel boards, and is shown in Figure 2.33 attached to the MAPM and *TARGET* module. The preamplifier module consists of the preamplifier boards, connected to PCBs for mechanical attachment of the MAPM, and flexible, Samtec coaxial ribbon-cables. These cables remove the curvature of the focal plane, allowing the *TARGET* modules to be located in a plane-parallel rack. A single 5 V supply on each ribbon cable from the *TARGET* Modules powers the preamplifiers. Each PCB contains a set of 16 preamplifier circuits and an AD590 temperature sensor that can be read out via the *TARGET* module.

Figure 2.59 (left) shows the gain of all 64 channels of one preamplifier module when attached to a *TARGET* and an MAPM relative to that taken with a ‘reference’ preamplifier using the same *TARGET* and MAPM. Whilst Figure 2.59 (right) shows the distribution of relative gains across all pixels of all pream-





**Figure 2.56** – Pulse area spectra for varying illumination levels from 1 pixel of 1 MAPM with a simultaneous fit to determine the pixel gain (left). Dynamic range measurement for several pixels in a single MAPM, showing good linearity up to ~500 p.e., with a deviation of ~20% by 1000 p.e. (right).



**Figure 2.57** – Angular response of a single MAPM pixel, made by illuminating the MAPM with a uniform beam and rotating the MAPM. The geometric reduction in illumination level following a cosine response has been removed. At the maximum angle of incidence expected in the SST-2M the response drops by ~30%.

plifiers. There is a RMS spread in preamplifier gain of 9.5%. The RMS gain variations between MAPM pixels is ~25%. The effect of pixel-to-pixel gain variations on performance is discussed in Section 3.2.5. The gain of the MAPM pixels is expected to decline by < 20% over a decade of operation at nominal HV and NSB levels.

### TARGET Module Development

The *TARGET* module based around four *TARGET-5* ASICs forms the heart of the CHEC-M camera module shown in Figure 2.33 and 2.52(c). Each *TARGET* module supplies a single MAPM with HV, digitises the signals from all 64 channels, and provides these digitised signals together with trigger information to the Backplane. These modules are based on the TARGET ASIC.

A total of 35 *TARGET* modules for CHEC-M (32 required for the camera, 3 spare) were commissioned at SLAC. The test setup for the individual modules is shown in Figure 2.60. Following acceptance tests 16 ASICs (from a set of 173) were identified to have unacceptable performance, defined as having transfer

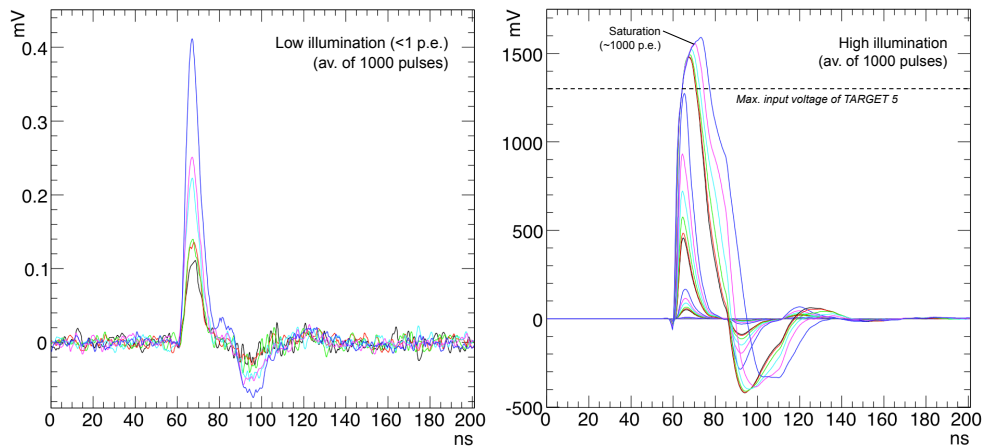


**Figure 2.58** – MAPM pulse shapes at the output of the CHEC-M preamplifier for low (left) and high (right) average illumination levels. The low illumination levels have a maximum of  $\sim 0.2$  p.e. High illumination levels reaches a maximum of  $>2000$  p.e., and begin to saturate at around 50% of that level. Each curve is averaged over 1000 waveforms. The RMS noise is  $\approx 0.4$  mV.

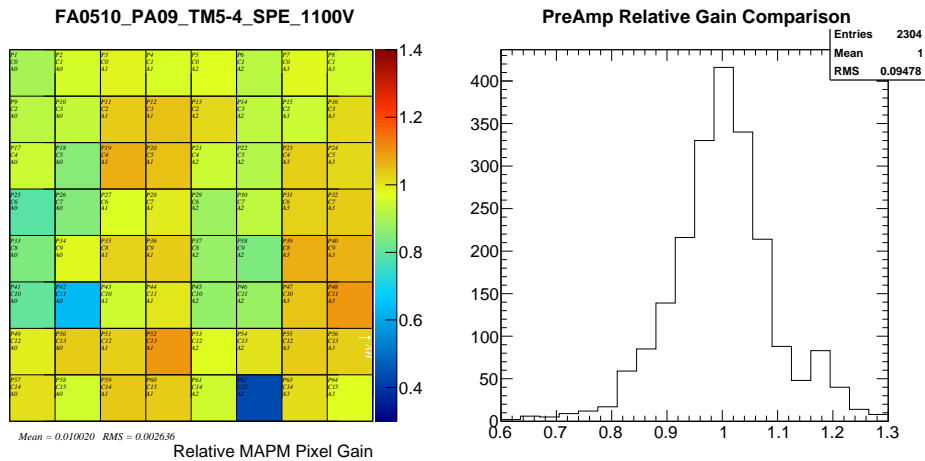


**Figure 2.59** – The gain of every channel of a camera module with preamplifier module 09 relative to that taken with a ‘reference’ preamplifier (left) and the distribution of relative gains across all channels of all preamplifiers (right).

functions outside a normal range (shown in green and red in Figure 2.61).

Upon delivery of the assembled modules to the camera assembly site in Leicester (see Figure 2.60 middle) the *TARGET* modules were catalogued and visually inspected. No major issues were found. Several modules had duplicate IP addresses (see Figure 2.60 bottom right) requiring firmware updates, and 5 modules had missing heat sinks on the FPGAs (see Figure 2.60 top right), which have since been fitted. These small issues have been noted as part of the learning process for the next production run of modules.

### Backplane Development

The CHEC-M backplane is shown in Figure 2.62. The backplane is currently (May 2015) being tested and a first complete firmware version is being produced. Once the firmware is in place (July 2015), integration into CHEC-M for complete system tests will happen. To proceed with the commissioning of CHEC-M a proto-Backplane with reduced functionality was produced in Leicester, electrically tested and integrated in CHEC-M (see Figure 2.52(d)). The proto-Backplane successfully provides power to the *TARGET* modules. The proto-Backplane also distributes clock and trigger signals to all *TARGET*



**Figure 2.60** – Setup for acceptance testing of *TARGET* modules, using a custom made tester board PCB with signal generation and serial command/readout capabilities (left). The *TARGET* modules in Leicester (middle), some of which had duplicate IP addresses (bottom right) and missing heat sinks (top right) - both of which are now fixed.

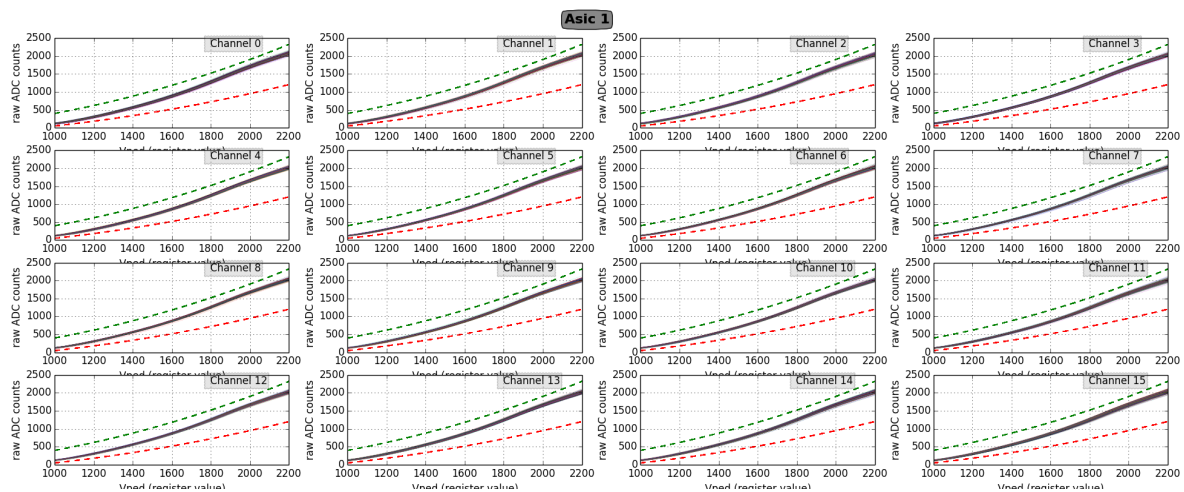


**Figure 2.61** – The transfer functions as measured at SLAC for ASIC 1 of *TARGET* module 30. Green and red show the acceptance window.

modules from a single FPGA board (see Figure 2.52(e)).

## DACQ Board Development

Two DACQ boards were procured and installed in CHEC-M. The DACQ boards are described in the Section 2.1.4. Custom microprocessor code and FPGA firmware adaptations for these boards was required. Design specifications were provided to Seven Solutions who delivered complete boards to the University of Amsterdam 4 months later. Testing of the boards has been performed using a custom bridging board to exchange TX and RX signals and allow the two DACQ boards to exchange information with each other. The DACQ boards were delivered to Leicester in July 2014 for integration and commissioning with the 32 *TARGET* modules and the proto-Backplane as shown in Figure 2.52(f). Following successful commissioning of these boards small changes were made and further copies ordered for use in CHEC-S and at other GCT institutes.

## LED Flasher Development

Four LED flasher units following the design described in Section 2.1.4 were produced. As shown in Figure 2.63 (left) the LED flashers are housed behind a diffuser attached to a mechanical mount that in-turn attaches to the camera focal-plane plate. Figure 2.63 (right) shows the pulse shape from the LED flasher as measured by an MAPM, with a FWHM of  $\approx 4.5$  ns.



**Figure 2.62** – The CHEC-M backplane with Xilinx Virtex 6 trigger FPGA and heat-sink mounted in the centre. Power for the backplane, DACQ and *TARGET* modules is routed from the power input connector to the power board mounted perpendicular to the backplane, where it is regulated and filtered. Connection to the DACQ boards is via the two large Samtec connectors located above the trigger FPGA.

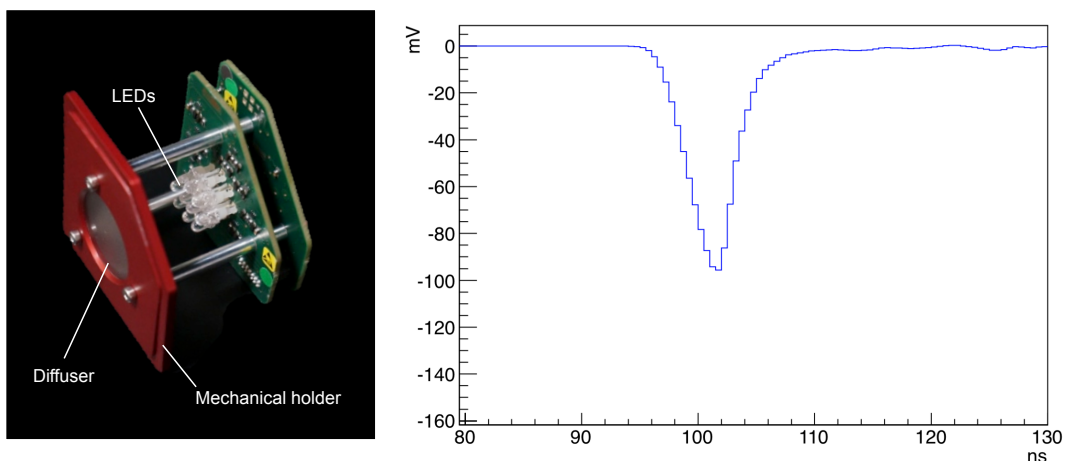


**Figure 2.63** – The LED flasher units for CHEC-M (left) and the pulse shape from a single LED used in the calibration unit as measured by an MAPM with a FWHM of  $\approx 4.5$  ns.

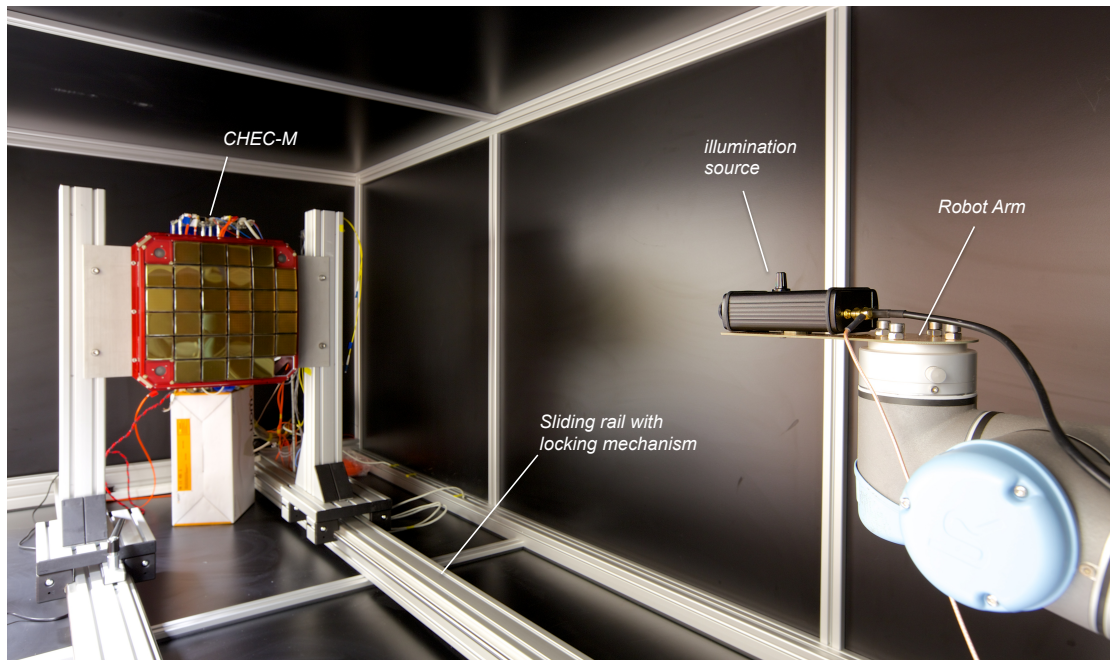


**Figure 2.64** – Light-tight enclosure housing CHEC-M on a sliding rail and an illumination source mounted on a robotic arm.

## Full Camera Tests

CHEC-M is being commissioned in a light-tight enclosure as shown in Figure 2.64. At one end the camera is mounted on a sliding rail whilst at the other end a robot arm is mounted and used to scan the focal plane with a light source.

At the time of writing (May 2015), 31 of the 32 CHEC-M camera modules are successfully being read out. The final module has a problem with the physical connection on the prototype Backplane which requires a hardware fix, and has not been prioritised. Calibration and refining of the data-taking process is in progress. Figure 2.65 shows some initial commissioning results from CHEC-M, showing the pulse area as measured from an approximately uniform light flash (top, middle) and example waveforms from the same data for an individual pixel (top, right, bottom) and averaged of an MAPM (top, right, top). The bottom images are taken with a mask in-front of the camera to approximate a Cherenkov image with a cut on the pulse peak height. In both cases, minimal gain-matching between MAPMs has been applied and pedestals have been subtracted, but no other calibration has been applied.

Once commissioned, testing will include illuminating the full camera with uniform flashes of light at varying brightness (using both a laser and a CHEC LED flasher) in the presence of a realistic background light level (from a diffuse white-light source). The robot arm (see Figure 2.64) will also allow the focal plane to be scanned with a narrow beam from the laser to measure the variation in response as the edge of pixels and gaps between MAPMs are encountered as well as the angular response of the pixels.

On-telescope tests are planned to take place in Paris on the GATE prototype structure. On-telescope testing will include: the alignment of the camera in the focal plane, in-situ calibration, recording Cherenkov images, and procedural aspects of installing, operating and maintaining the camera as part of the telescope system.

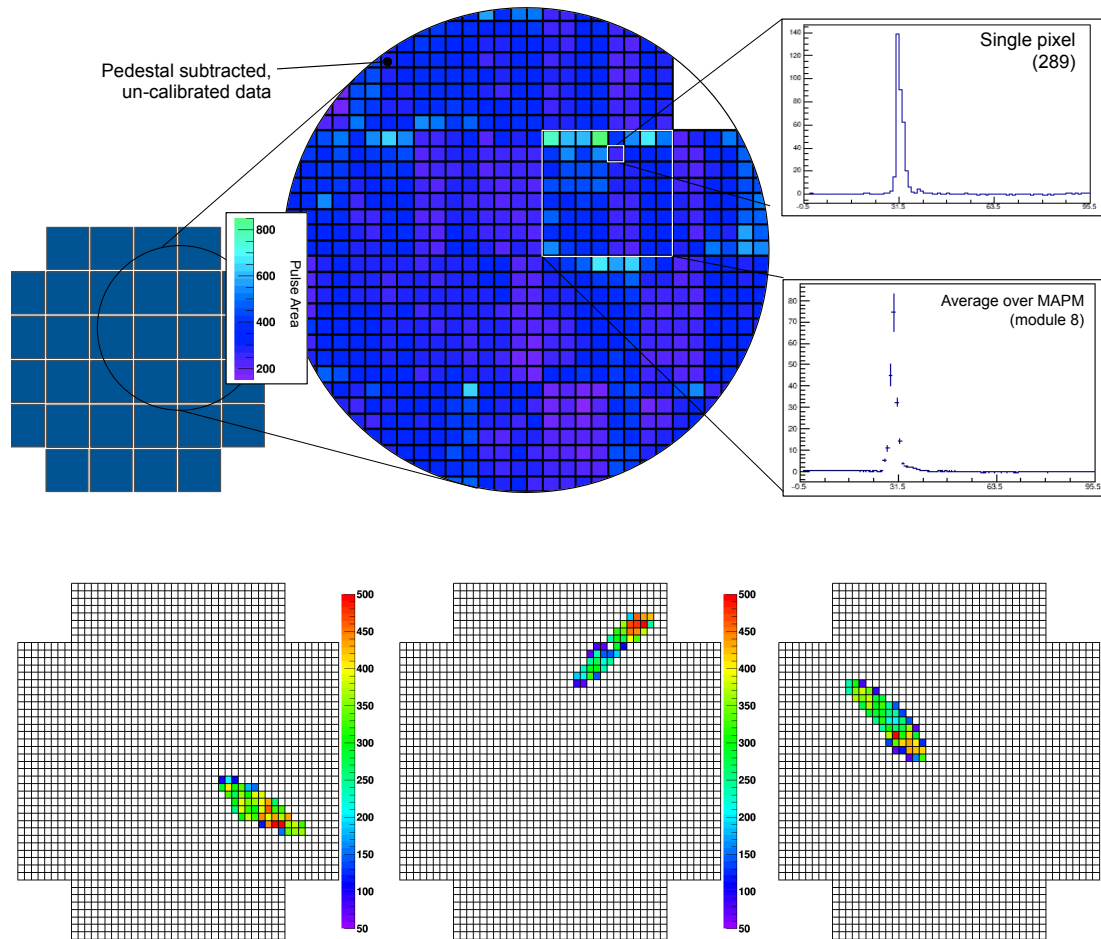


**Figure 2.65** – Initial commissioning results from CHEC-M, showing the pulse area as measured from an approximately uniform light flash (top, middle) and example waveforms from the same data for an individual pixel (top, right, bottom) and averaged of an MAPM (top, right, top). The bottom images are taken with a mask in-front of the camera to approximate a Cherenkov image with a cut on the pulse peak height. In both cases, minimal gain-matching between MAPMs has been applied and pedestals have been subtracted, but no other calibration has been applied.

### 2.3.4 CHEC-S

The second GCT camera prototype is based around SiPMs and is referred to as CHEC-S. Many elements of CHEC-S are similar if not identical to CHEC-M. These include the mechanics, the DACQ boards, LED flashers and Backplane. However, to accommodate the difference in pulse shape and gain between MAPMs and SiPMs a different pre-amplifier design is required. CHEC-S also sees an upgrade in the trigger and data acquisition ASIC from *TARGET-5* to *TARGET-7*.

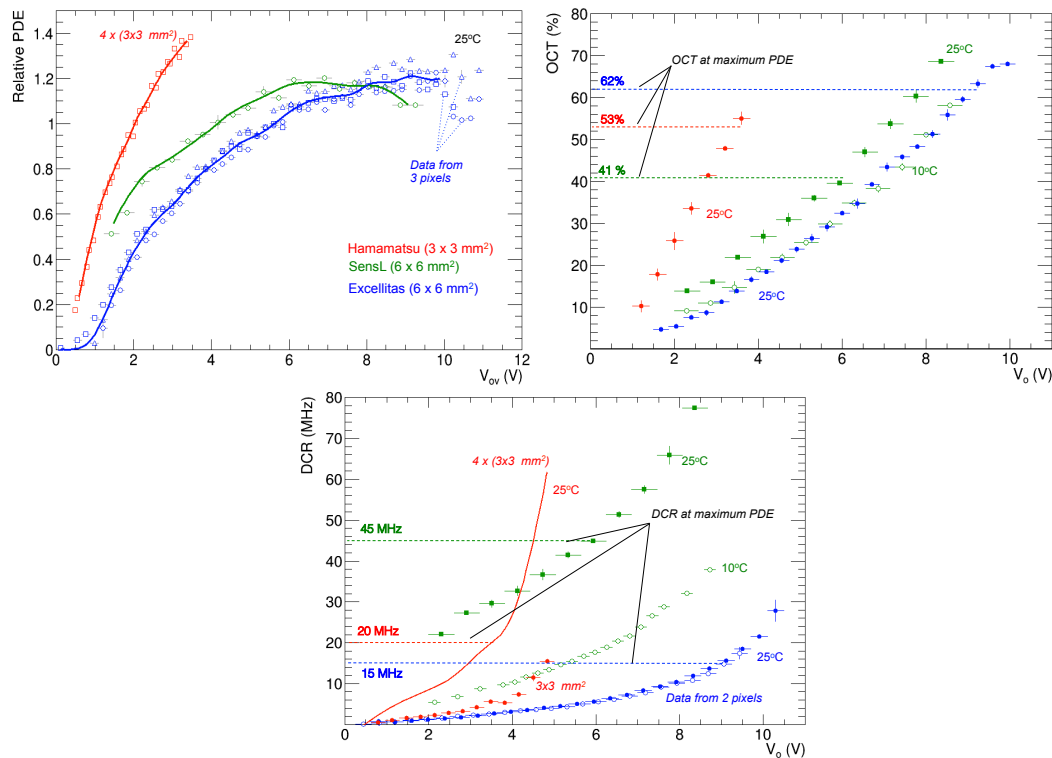
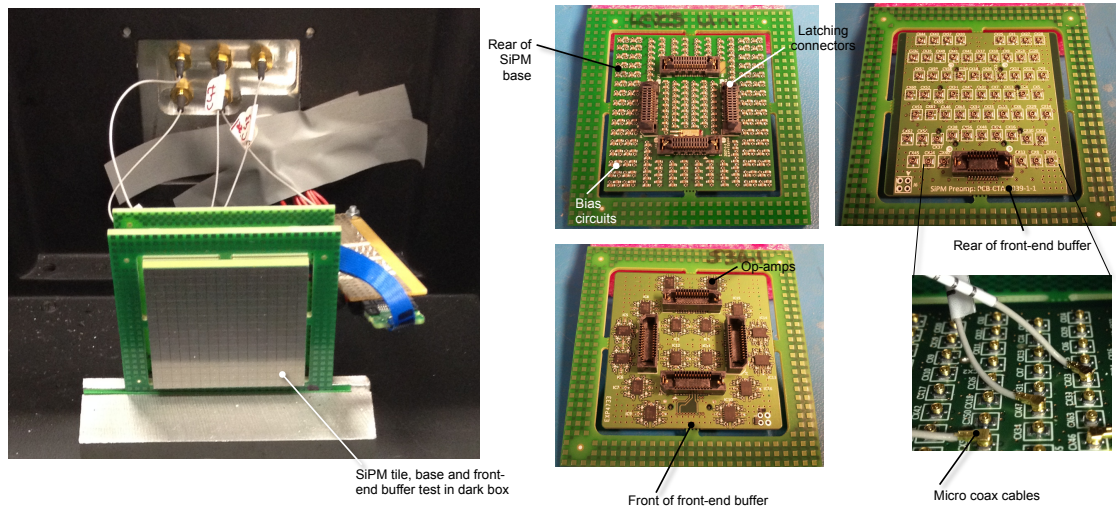


**Figure 2.66** – Results from SiPMs tests for CHEC-S. The Photo Detection Efficiency (PDE) relative to a 3×3 mm<sup>2</sup> Excelitas device as a function of over-voltage is shown to the left. The Optical Cross Talk (OCT) as a function of over-voltage is shown in the middle, and the Dark Count Rate (DCR) on the right. The values achieved when the over-voltage is set to that required to obtain the maximum PDE are indicated with dashed lines. In all cases Hamamatsu is shown in red, SensL in green and Excelitas in blue.

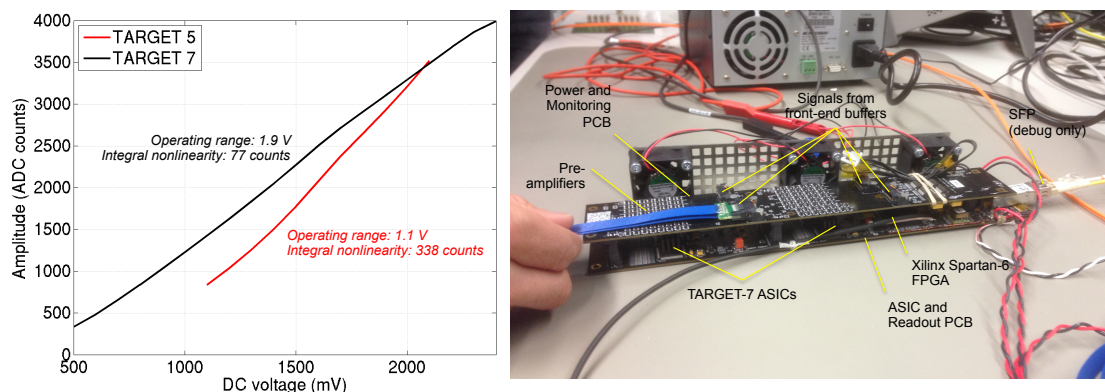
Several candidate SiPMs were tested for use in CHEC-S. Results from the most critical parameters are shown in Figure 2.66 for three such devices commercially available at the time of selection. The Photo Detection Efficiency (PDE) relative to a 3×3 mm<sup>2</sup> Excelitas device as a function of over-voltage is shown to the left. The Optical Cross Talk (OCT) as a function of over-voltage is shown in the middle, and the Dark Count Rate (DCR) on the right. The values achieved when the over-voltage is set to that required to obtain the maximum PDE are indicated with dashed lines. In all cases Hamamatsu is shown in red, SensL in green and Excelitas in blue. Simulations show that a high PDE is desirable at the cost of OCT. Hamamatsu achieved the highest PDE and coupled with the improved geometric fill factor of the camera tile (see Section 2.1.4, and not included in Figure 2.66) proved to be the optimum choice for CHEC-S. The tile chosen for CHEC-S (S12642-1616PA-50 - see Figure 2.32) consisted of 256 3×3 mm<sup>2</sup> pixels, tied together to form 64 pixels on a bias PCB soldered directly to the tile.

Figure 2.67 shows a S12642-1616PA-50 attached to a bias board and front-end buffer (providing the first stage of amplification) under test in Leicester. The SiPMs couple via the front-end buffers to updated *TARGET* modules with the new *TARGET-7* ASICs. The revised module design reduces the PCB count from 6 to 2 as shown in Figure 2.68.

The camera modules sit in the focal plane plate as they did for CHEC-M. Revised mechanics are required (see Figure 2.69 (left)) to house the SiPM tiles, which have a reduced pitch compared with MAPMs.



**Figure 2.67** – The Hamamatsu S12642-1616PA-50 attached to a bias board and front-end buffer (providing the first stage of amplification) under test in Leicester.



**Figure 2.68** – Comparison of transfer functions in *TARGET-5* and *TARGET-7* (left) and the revised *TARGET* module, featuring 4 *TARGET-7* ASICs undergoing lab-tests (right). This version includes an SFP connector for debugging that is replaced during full camera integration by a direct connection to the backplane identical to that featured in CHEC-M.

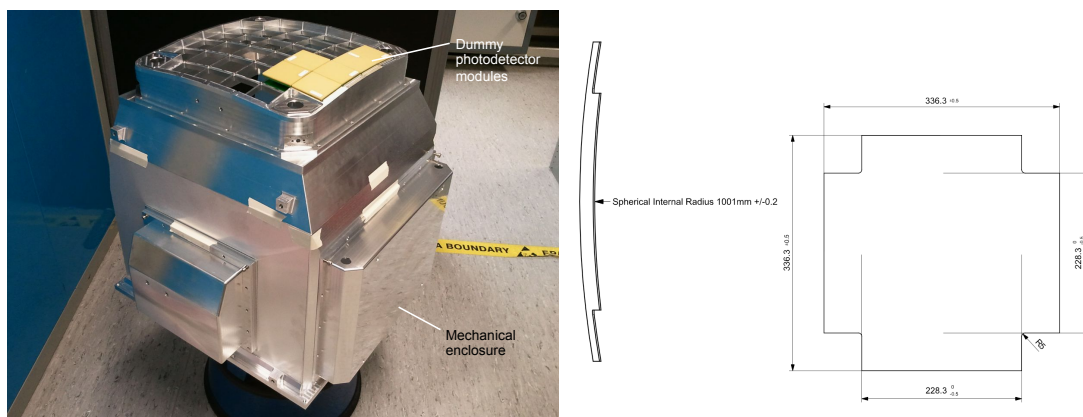


**Figure 2.69** – The CHEC-S mechanics during the build process, with dummy photodetector modules (right), and the design for the prototype CHEC-S protective window (right).



Additionally, CHEC-S will feature the first prototype of a protective window (Figure 2.69 (right)) for the GCT camera: a 2mm thick 'Polycasa-XT UVT' Polymethyl Methacrylate sheet from POLYCASA seated above the SiPMs. This has a UV throughput without coating of typically 92% trailing to 80% at 300nm and 50% at 275nm. The window will be thermally formed by precision blowing/moulding into a 1 m radius, machine finished, and held 2 mm in front of the detectors. Expected significant dimensional variances due to temperature cycling, which is a function of all PMM materials will be compensated for by flexible seals to the focal plane borders. The formed material will receive an AR coating for UV wavelengths, possibly an IR absorption coating and a protective hydrophobic coating.

CHEC-S will be assembled by the end of 2015. Once all test results from the two camera prototypes are available, the final photodetector type (SiPM or MAPM) will be chosen and the Pre-production camera series will be started (see the schedules below). Although CHEC-S will utilise *TARGET-7*, for the Pre-production camera one further ASIC iteration is underway for the GCT camera. In this iteration the trigger and readout paths will be split to optimise the trigger-path noise performance.



## 3 Design Validation and Product Acceptance

### 3.1 Safety

The control system, the optical and mechanical structure of the telescope and the camera have been designed in accordance with the safety regulations applicable in France and the UK respectively. The safety requirements of CTA have also been respected. Human and instrument safety is ensured through the design of the apparatus and documentation of all installation, operation and maintenance procedures. All operation and maintenance plans and manuals will be delivered to the CTAO as part of the GCT, ensuring human and instrument safety during CTA operation.

#### 3.1.1 Safety Management Documents

In accordance with CTA RAMS requirements, several analyses have been carried out and documented in order to ensure that the telescope design respects safety considerations and that risks are managed throughout the duration of the project. These are:

- The risk management plan.
- Risk analysis.
- Failure mode, effects and criticality analysis (FMECA).
- Non conformity document.
- Sparse list and maintenance plan.

The risk management document (reference 503-QLT-GEPI-PL-03) presents the process of risk management in the GCT project.

The risk analysis was generated by the quality manager of the SST-GATE team. Risks are listed, identified and characterized according to their probability of occurrence and the severity of their effects, allowing risks to be prioritized. The severity of the risk includes its impact on:

- CTA specifications: will occurrence result in the telescope failing to meet the requirements?
- CTA deadlines: will corrective actions result in delays to the schedule or loss of telescope availability?
- Costs: will significant resource be needed to implement corrective actions?

The severity is specified using four levels: negligible, major, critical and catastrophic.

The probability that a risk occurs is given as low, medium, high, or very high.

- Low: Probability of occurrence estimated to be <5%, mark 1.
- Medium: Probability of occurrence estimated to be between 5% and 25%, mark 2.

- High: Probability of occurrence between about 25% and 50%, mark 3.
- Very high: Probability of occurrence > 70%, mark 4.

The detectability of events is marked following the CTA scale. There are four levels from absolute uncertainty, where it is impossible to detect the failure before it occurs, to high detectability where monitoring or test measurements can easily detect the failure.

The criticality of the risk is the product of the severity and the probability of occurrence, the risk is then classified by the Risk Priority Number (RPN). This helps to define which risks are of the greatest importance.

After characterization, the criticality of risks is defined as acceptable, to be monitoring or unacceptable by combining their probability of occurrence and their severity. Table 3.1 presents the main safety risks.

In the SST-GATE FMECA file a mitigating action is listed for each risk, which reduces the probability of occurrence of the risk or decreases its impact. The owner of the risk is given; this is the person responsible for the implementation of the mitigating actions. The risk is then re-evaluated. If the mitigating actions are adequate, the risk decreases to an acceptable level. If the risk is still high, further mitigating actions are proposed.

The GCT maintenance strategy foresees a preventative maintenance programme. The maintenance plan reflects this philosophy (specification C-SST-GATE-RAMS-0190-7), which is presented briefly in the following.

### 3.1.2 Instrument Safety

The actions to be taken in case of problems (technical failures, accidents) and the safety policy to be adopted for the drives and the telescope movement have been incorporated into the telescope design and operation plans from the beginning of the project. The following safety considerations have been taken into account during the design of the telescope structure and the control and command software.

System design:

**Parking position** This position has been defined to be 0° in elevation and 0° in azimuth. In order to improve safety, two M16 bolts are provided at the back of the M2 mirror allowing the locking of the telescope to the ground.

**Solar radiation risk** During the daytime, people working on or near the telescope and the instrument itself are protected from concentrated solar radiation generated by reflections from M1 and/or M2 by the shelter, which ensures the sun cannot strike the mirrors. (It also protects the telescope from other environmental effects such as rain, snow, ice, high winds) and decreases the maintenance costs of the mirrors.

**Protection of bearings and drives** Covers have been designed to ensure that bearings and drives are protected from rain, snow, wind-blown sand and animals.

**Protection of camera** The camera enclosure is sealed to IP65 with the lid closed and to IP52 with it open. All external cables enter the camera via bulk-head connectors rated to at least IP65, and the external cables and connectors are also rated to at least IP65. This provides adequate protection against the ingress of rain, snow, wind-blown sand and animals

The mechanical design of the telescope facilitates the mounting and maintenance of sub-assemblies, assemblies, and modules. It minimises the effort needed to undertake these activities. The philosophy has been to keep the amount of additional equipment needed for telescope assembly and maintenance (e.g. scaffolding) to a minimum. The main safety solutions implemented in the design are:

**Mounting of the petals of M1** The risk of damaging M1 during mounting has been decreased by separating the dish holding the mirror and the bottom dish (which supports the MTS). The M1 dish can be rotated and locked in a succession of positions so that the M1 petals can be mounted from ground level. Once all the petals have been installed, the flange is locked and kept fixed in order to perform the alignment and then carry out observations.

**Mounting of the GCT camera** Given the small distance between M2 and the camera, there is a significant risk that the mirror is damaged during camera installation or removal. The camera mounting system was therefore designed to mitigate against this risk. The camera enclosure also has crane points to further ease installation and maintenance.

The Telescope Control System incorporates several features which ensure the safety of the instrument.

**Motion stop process** The purpose of this process is to stop the motion in a quick and safe way (C-SST-GATE-RAMS-0345-1). The drives have a function – called *stage protection* – that manages an emergency stop of the motors: a *speed braking* is performed before the power of the motors is switched off and they enter the *torque off state*.

**Interlocks for safe operation** Interlocks are used to prevent any telescope motion while:

- the shelter is not fully open;
- the stowing pin is engaged to lock the telescope in its parking position (C-SST-GATE-RAMS-0160-5);
- a locking pin is engaged to lock one of the telescope's axes (C-SST-GATE-RAMS-0160-5);
- the camera removal mechanism is in its operational state.

**Motion limits for safe operation** The motion limits are defined by:

- mechanical bumpers which prevent any overrun (C-SST-MEC-AAS-6);
- end limit safety switches to trigger the motion stop process at the drive level (C-SST-AUX-TCA-3);
- software-defined limits to prevent the reaching of the aforementioned hardware limits (C-SST-AUX-TCA-4 and -5);
- real-time software-defined limits (position of known strong sources such as the moon) to prevent any overexposure of the camera.

**Parking procedure** The parking procedure defines two points, the *parking point* itself and the *starting point*. The starting point is software-defined, whereas the parking point is hardware-defined with a safety limit-switch. As shown in Figure 3.1, the only motion allowed between these two points is along the elevation direction, either to or from the parking point. The parking procedure is as follows:

1. The telescope is moved to the starting point from its current position. The starting point is the entrance to the parking channel.
2. The telescope is moved along its elevation axis down to the parking point.
3. For long-term parking or maintenance purposes, a locking pin is engaged to prevent any telescope motion.

**Emergency parking procedure** In emergency cases where motion is allowed, the telescope is parked following the parking procedure.

**Parking to protect against sun-light** The shelter is closed while the telescope is *Off* or in the *Warm-up* mode, i.e. parked. Opening the shelter allows the telescope to switch to *Stand-by* mode.

**Software design** The software includes features designed to reduce the risk of human error (C-SST-GATE-RAMS-0200-2). These include:

- The software prevents the input of out-of-range values.

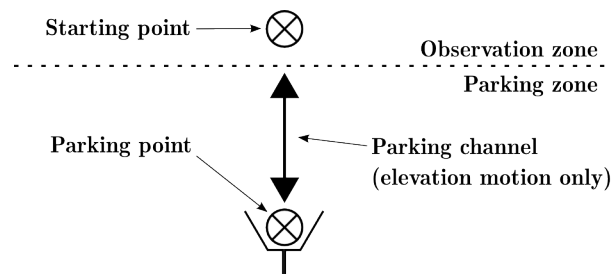


**Figure 3.1** – No azimuth movement is allowed in the parking channel. The observation zone is software limited (e.g. to an elevation of above 20°) during regular operation.

- Two control modes are foreseen, depending on the status of the user. The operator has access to a restricted range of commands (scientific operations) while the engineer has full control of the telescope (for maintenance and test purposes).
- The software has dialogue boxes which force the user to confirm critical actions.

**Design for lightning protection** Direct lightning strikes are rare and cause huge currents (between 25 and 200 kA). Preventing damage in this case is difficult and costly. Hence, the GCT lightning protection system is only designed to cope with indirect impacts. Protection must therefore be provided against the two main effects of indirect strikes, the change in ground potential and the magnetic field. To achieve this:

- A primary surge arrester is placed on the GCT local network power supply (in the power supply cabinet) with very short connections (typically  $\leq 50$  cm);
- A secondary surge arrester is placed in the fork cabinet, again with very short connections (this is required because of the distance between the power supply cabinet on the foundation and the fork cabinet).
- A strong equipotential bonding network is made throughout the telescope, with copper cable of area 35 mm<sup>2</sup> in the cable chains and classical flat tape lightning conductor for the external sections of the network.
- All cables are shielded with both ends grounded.
- Metal ducts are used to screen the cables against high frequencies with both ends grounded.

### Flood protection

- All electrical cabinets are at least 50 cm above ground level (A-RAMS-0230 — C-SST-FSS-GS-1 and C-SST-GATE-RAMS-0390-2).
- Waterproof cabling is used for all electrical connections less than 50 cm above ground level.

**Camera protection** Upon loss of communication with the camera control software for longer than 50 seconds, the camera backplane switches off the TARGET modules (including the sensors) and instructs the peripherals board to switch the peripherals to their safe state, including closing the camera lid.

## 3.1.3 Human Safety

Some human safety issues have been discussed in the instrument safety section above. Here, we list the specific systems implemented in the telescope structure and camera to ensure human safety.

During assembly and integration, safety equipment is used as dictated by the hazards associated with these operations (C-SST-GATE-RAMS-0190-4). Equipment provided includes helmets, gloves and laser protection glasses. The features implemented in the GCT design for mounting the M1 petals and the camera help protect the construction team against the risks of handling heavy apparatus, as well as preventing damage to the instrument.

Safety the risks are listed in the FMECA safety sheet and in Table 3.1.

**Table 3.1** – Main safety risks.

Function	Potential Failure Mode	RPN	Action
Protect personnel against motors and gears	Fingers can be caught by the movement of motors or gears or bearings	6	Prevent access to motors, gears or bearings while they are working, sensors are foreseen to inform of open access to motors or gears
Protect personnel against telescope systems	Human hazard in relation to moveable telescope elements	6	Display risks incurred and measures to be taken (helmets, gloves etc.) next to the telescope
Protect personnel against electronic systems of the telescope and camera	Electric shock hazard	4	circuit breakers.
Protect personnel against drive systems	Risk of human injury	4	provide interlocks and forbid access to electronics to untrained persons
Protect personnel against camera electronics	Risk of human injury	4	provide interlocks and forbid access to electronics to untrained persons; high voltage supplied on separate, isolated connectors
Control all movement of the telescope	Safety PLC failure	4	regular testing and inspection
Protect personnel against camera shutter	Fingers can be caught in shutter or persons struck	4	Alarm will sound 1 second before lid begins to open or close
Protect personnel and telescope systems against fire	Risk of fire in the shelter will damage the telescope elements	4	Norm NF Series P92 500 euroclass M2 for the shelter, idem for wires
Support the mass of the telescope	Risk of flooding	3	Protection of the telescope by the slab

Unless overall site security is guaranteed to a level which makes it superfluous, the GCT will be surrounded by a fence. Safety signs are placed on the this fence to warn people of the dangers of standing in the operating zone.

Safety procedures and signs are placed in the cabinet on the foundation where the maintenance tools are stored, and on the camera enclosure.

Safety is also managed through the Telescope Control System (TCS).

**Push-buttons for safe maintenance** Several push-buttons are placed on the foundation (C-SST-GATE-RAMS-0345-1 and -2):

- “Emergency Stop” buttons (mushroom-shaped red push-buttons) are used to cut the main power supply to the telescope; one is located near the door of the main power supply cabinet, on the foundation, and one is located near the doors of each of the two fork cabinets;
- “Motion Stop” buttons (standard red push-buttons) are used to trigger the motion stop process at the drive level to stop any telescope motion; there are three of them, located next to the Emergency Stop buttons.

#### Interlocks for safe maintenance

- An interlock “Telescope Zone” prevents any motion, or triggers the motion stop process, if the door of the fence surrounding the motion area of the telescope is opened (C-SST-GATE-RAMS-0190-5). If telescopes are not individually fenced off, replacing this interlock with a system based on motion sensors will be studied.
- A safety switch “Manual Operation Handle” prevents motor-driven motion of the telescope when the handle for manual telescope movement is not in its storage position (C-SST-GATE-RAMS-0160-5 and -0210-7).

- A key-operated switch prevents remote telescope control when the local control panel is being used for commissioning or maintenance purposes (C-SST-GATE-RAMS-0210-5).

## 3.2 Performance

In this section, the performance of the GCT telescope is assessed against the CTA requirements for the SST telescope [5] with reference to the Design Verification Document (DVD) for both the GCT telescope structure and mirrors [12] and the camera [13].

To design a telescope that fulfils the CTA requirements, a list of technical specifications, derived from these high level requirements, has been given to the engineers for the design. The DVD lists all these technical specifications and their relationship to the CTA requirements. It is thus possible use these to determine the implications of any change in the CTA requirements. It was ensured that the technical specifications completely describe the CTA requirements so that satisfying the technical specifications means fulfilling the CTA requirements. For the telescope structure and mirrors, a test plan is being developed which will describe the verification process that ensure that the design fulfils the technical specifications. A procedure is associated with each test and gives the equipment needed as well as the methodology of the test.

The first part of this section describes the opto-mechanical performance expected for the GCT telescope. This is detailed in four sections: mechanical performance with FEA results; optical performance expected from the optical design implemented in the GCT structure; system performance of the whole GCT telescope; and the control and command performance. Finally, the camera performance is described and an assessment of GCT performance SST with respect to the requirements is performed using Monte Carlo simulations and the results of lab tests on prototypes.

### 3.2.1 Mechanical Performance

The mechanical performance of the telescope has been studied using FE analysis with MD.Nastran (MSC Software). FE models of the telescope, briefly described in the annex E, were developed for this purpose. Performance analysis focused on normal modes of oscillation; mechanical behaviour in observing, transition and survival modes; thermal behaviour; and seismic behaviour. More details about the model and the FE analysis are given in the GCT FE analysis report [8] and in the CTA validation and FE analysis report [14].

#### Normal mode analysis

Normal mode analysis was performed for elevations of 0°, 20°, 60° and 90°, and in the parking position. The azimuth angle was not varied as it does not impact on the stiffness of the telescope. Table 3.2 summarizes the first ten normal modes. Computation of the first fifty modes was performed, covering about 85 % of the total effective mass. Effective mass fractions for the six degrees of freedom are reported in annex E for each tested configuration. Bending mode shapes of the telescope are shown when the telescope is at 20° elevation in Figure 3.2. The first five mode shapes are reported in annex E for each elevation and the parking position. As seen in Table 3.2, the first eigenfrequency is larger than 2.5 Hz, as is recommended by Toderó Peixoto and collaborators [15] to avoid wind-induced oscillations.

#### Structural analysis in observing mode

Structural analysis in observing mode focuses on the deformation of the optics in observing conditions (gravity loads and observing wind speed) for elevation angles between 20° and 90°. Displacements and rotations of the centres of gravity of the optical components, expressed in terms of decentering, piston and tilt and with respect to the calibration of the telescope at 90°, are compared to the allocation deduced from the error budget and are reported in Table 3.3. Detailed data are reported in annex E. Figures 3.3 and 3.4 show the deformed shape of the telescope for 20° elevation with and without a frontal wind load.

These data demonstrate that the telescope design largely fulfils the specifications regarding on-axis displacements in observing conditions.



**Table 3.2** – Summary of first ten normal modes for all elevation angles. Frequencies are given in Hz.

Mode	Description	0° stow	0°	20°	60°	90°
1	Rotation of the elevation system around azimuth axis	3.7	3.4	3.4	-	-
2	Bending of the telescope perpendicular to elevation axis	-	4.0	3.9	3.6	3.6
3	Bending of the telescope around elevation axis	8.7	4.9	4.7	4.5	4.4
4	Local mode of the M1	4.8	4.8	4.8	4.8	4.8
5	Local mode of the counterweight	5.4	5.4	5.4	5.4	5.4
6	Bending of the telescope perpendicular to elevation axis	7.5	7.9	7.8	7.8	7.8
7	Bending of the counterweight structure	7.9	8	7.9	7.8	7.9
8	Local mode of the M1	9.5	9.5	9.5	9.5	9.5
9	Bending of the telescope perpendicular to elevation axis	9.5	9.5	9.5	≥ 9.5	≥ 9.5
10	Local mode of the M1	9.5	9.5	9.5	9.5	9.5

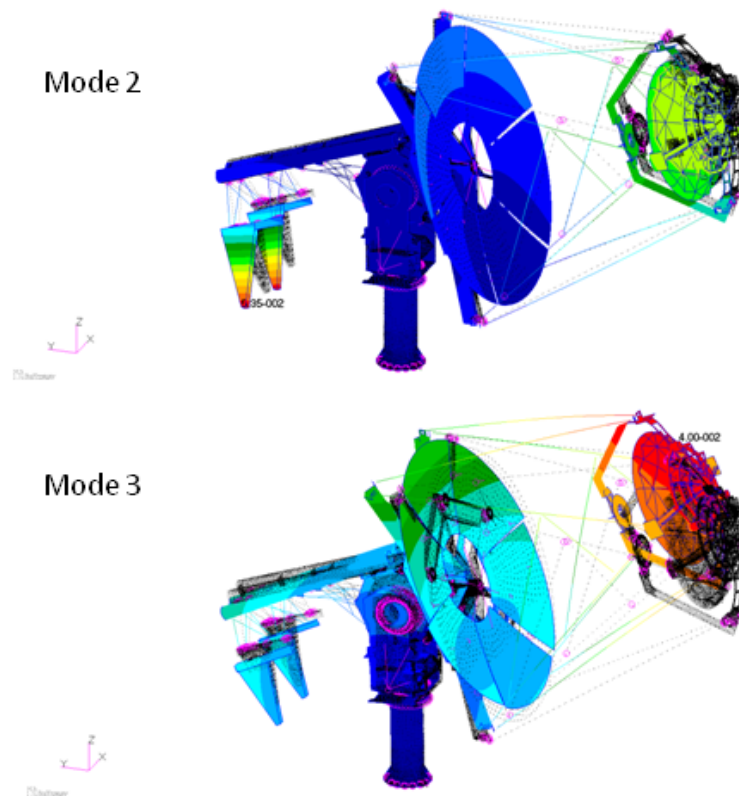


**Figure 3.2** – First bending modes of the telescope at 20° elevation. Mode 2 corresponds to bending of the telescope around an axis perpendicular to the elevation axis and occurs between 3.6 and 4 Hz, depending on the elevation angle. Mode 3 corresponds to bending of the telescope around an axis parallel to the elevation axis and occurs between 4.4 and 4.9 Hz, depending on the elevation axis.

### Thermal analysis

Plots of the temperature-induced  $z$ -displacements of the telescope are shown in Figure 3.5 for a 10° per hour thermal gradient. Deformations of the optical system  $a$  for a 17.5° degree per hour thermal gradient are compared to specifications defined by the thermal allocation in Table 3.4. These deformations are largely below the allowable values.

### Structural analysis in transition mode

**Table 3.3** – Maximal gravity- and wind-induced on-axis deformations of the optical components in observing conditions. Displacements are given in mm, while rotations are in arcsec.

	Dec M1M2	Dec M2Cam	Piston M1M2	Piston M2Cam	Tilt x M1M2	Tilt y M1M2	Tilt x M2Cam	Tilt y M2Cam
Spec (PtV)	8.5	8.5	7.75	7.75	900	900	900	900
Gravity	4.3	0.1	0.9	-0.7	26.5	0.6	-3,0	-17.9
Gravity + front wind	4.2	0.1	1.0	-0.7	26.0	≤ 1.0	-2,0	-14,0
Gravity + back wind	4.3	0.1	0.9	-0.7	29.0	13.8	-1,0	-48,0

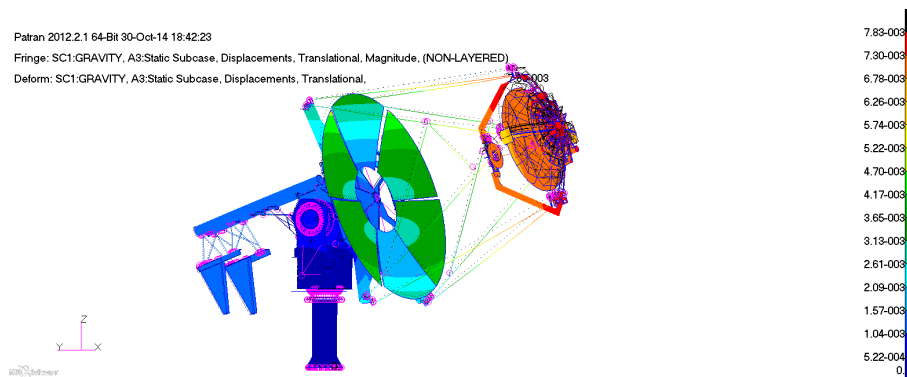


**Figure 3.3** – Plot of gravity-induced displacements for 20° elevation.

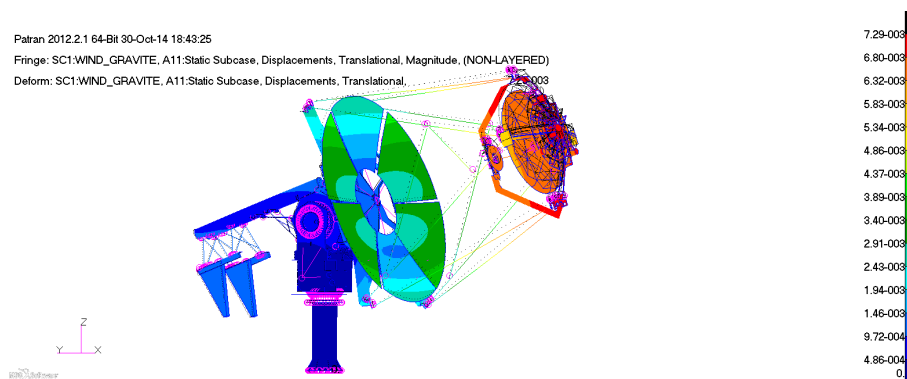


**Figure 3.4** – Plot of displacements for 20° elevation and frontal wind in observing conditions

Structural analysis in transition mode focuses on the reaction and bearing forces in transition conditions (moderate wind gusts) whatever the elevation angle and whatever the wind vector. The most critical conditions for the bearing forces occur for winds from the rear and side winds. These results are summarized in Tables 3.5 and 3.6. Bearing forces are larger in the elevation drives than in the azimuth drive.

### Structural analysis in survival mode

Structural analysis in survival mode focuses on the maximal stresses in the structure in survival conditions (high wind speed, ice and snow loads, and wind gusts) and reaction forces when the telescope is in its parking position. Maximal stresses are expressed in terms of utilisation factors  $U$ , as recommended in the CTA verification guidelines [16] and as defined in annex E. These utilisation factors must be smaller than 1.0 for a safe design. Stress analysis shows that the structure is not damaged. Utilisation factors are maximal in the Top Dish and in the mechanical structure of the Counterweight for gusts in survival conditions and are equal to 0.9, as shown in Figures 3.6 and 3.7, respectively.

Reaction forces as well as radial and tangential azimuth bearing forces are larger than in the transition state. They are summarised in Tables 3.7 and 3.8, respectively.

### Seismic analysis

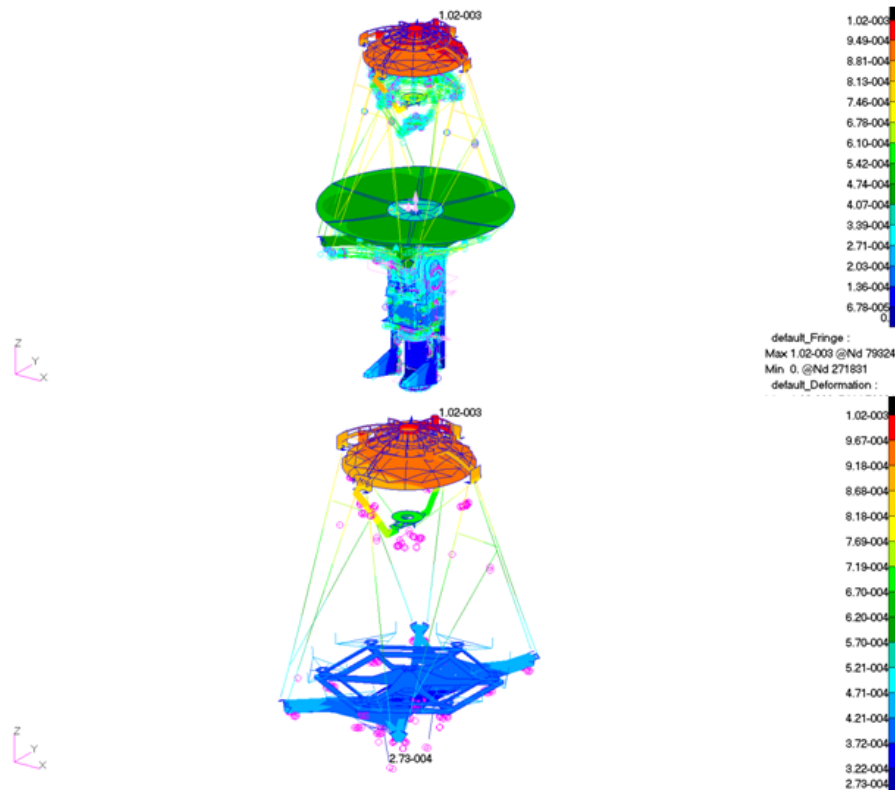


**Figure 3.5** – Magnitude of temperature-induced displacements (in m) in the telescope and in the OSS. Mirror M1 is not shown.

**Table 3.4** – Temperature-induced deformation of the optical system. Deformations and rotations are expressed in mm and in arcsec respectively.

	Dec M1M2	Dec M2Cam	Piston M1M2	Piston M2Cam	Tilt x M1M2	Tilt y M1M2	Tilt x M2Cam	Tilt y M2Cam
Spec (PtV)	1	1	1.1	1.1	47	47	47	47
Computed	0.02	0.1	0.9	-0.5	9.5	-5.4	-19.9	12.8

**Table 3.5** – Reaction forces  $F$  in kN expressed in the global Cartesian coordinate system for gusts in moderate wind conditions with respect to several wind vectors and for 0° elevation.

Wind vector	$F_x$	$F_y$	$F_z$
0° (front wind)	4.1	0	-78.5
45°	2.9	6.1	-78.5
90°	0	8.6	-78.5
135°	-2.9	6.1	-78.5
180° (back wind)	-4.1	0	-78.5

**Table 3.6** – Maximal bearing forces  $F$  in N and torques  $T$  in Nm for moderate wind gusts. Both are expressed in the local cylindrical coordinate system of the slew bearing.

Wind vector	$F_r$	$F_\theta$	$F_z$	$T_r$	$T_\theta$	$T_z$
Azimuth drive	-150/118	-83/132	-1,650/4,600	-284/283	-15/11	-1/2
Elevation drive	-605/589	-1,500/1,460	-561/376	-90/79	-2/5	-6/6

Peak acceleration responses at recovery points are reported in annex E. Figure 3.8 shows the deformed shape of the telescope for a 60° elevation angle and for several directions of the horizontal seismic acceleration. Details of the seismic analysis can be found in [14].

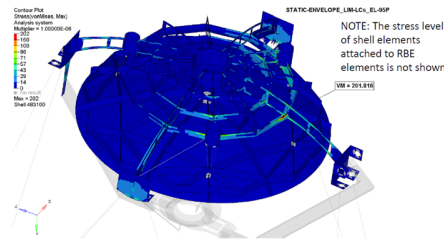


Figure 3.6 – Plot of Von Mises stresses in the Top Dish for gusts in survival conditions.

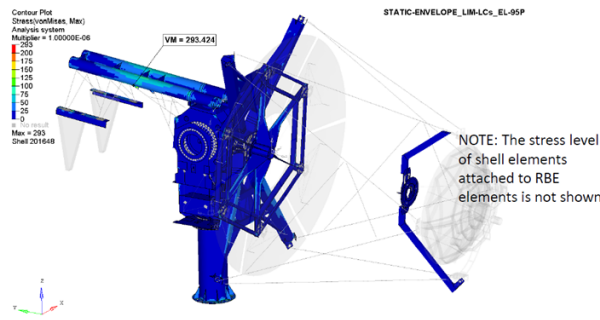


Figure 3.7 – Plot of Von Mises stresses in the Counterweight for gusts in survival conditions.

Table 3.7 – Reaction forces  $F$  in kN expressed in the global Cartesian coordinate system for high wind speeds including gusts and for several wind vectors.

Wind vector	Fx	Fy	Fz
0° (front wind)	23.7	0	-78.5
45°	16.7	35.3	-78.5
90°	0	49.9	-78.5
135°	-16.7	35.3	-78.5
180° (back wind)	-23.7	0	-78.5

Table 3.8 – Maximal bearing forces  $F$  in N and torques  $T$  in Nm in survival conditions. Both are expressed in the local cylindrical coordinate system of the slew bearing.

Wind vector	Fr	Fθ	Fz	Tr	Tθ	Tz
Azimuth drive	-420/387	-396/363	-512/3,600	-178/171	-12/5	-1/1
Elevation drive	-637/575	-908/910	-569/332	-70/70	-2/3	-3/3

Stress analysis points out the same two critical areas as for survival conditions. In these areas, stresses are larger than allowed. Solutions have been developed which increase the stiffness in these areas and which will be incorporated in the next GCT design. FEA verifies that these solutions provide the required stiffness.

**Conclusion**

The thermomechanical behaviour of the telescope has been studied using FEA. These analyses show that the current design of the telescope fulfils the requirements in terms of eigenfrequency and on-axis deformations of the optical system in observing modes with gravity loads, wind loads and thermal loads. Gusts in survival conditions are the most severe configuration for the telescope since stresses and reaction forces are maximal in these conditions. Bearing forces are larger in the elevation drives than in azimuth drives. Since slew bearings are sized to withstand maximal radial and axial forces of about 1,000 kN and maximal torques of about 250 kNm, they are compliant with the specification. Stress analysis reveals the existence of two critical zones where utilization factors are maximal. These are in the aluminium Top Dish and the steel structure of the counterweight. In survival conditions, the utilisation factors in these areas remain in the allowable range and no damage would occur. However, damage could occur in these regions during earthquakes. Solutions based on a local increase of rigidity (around

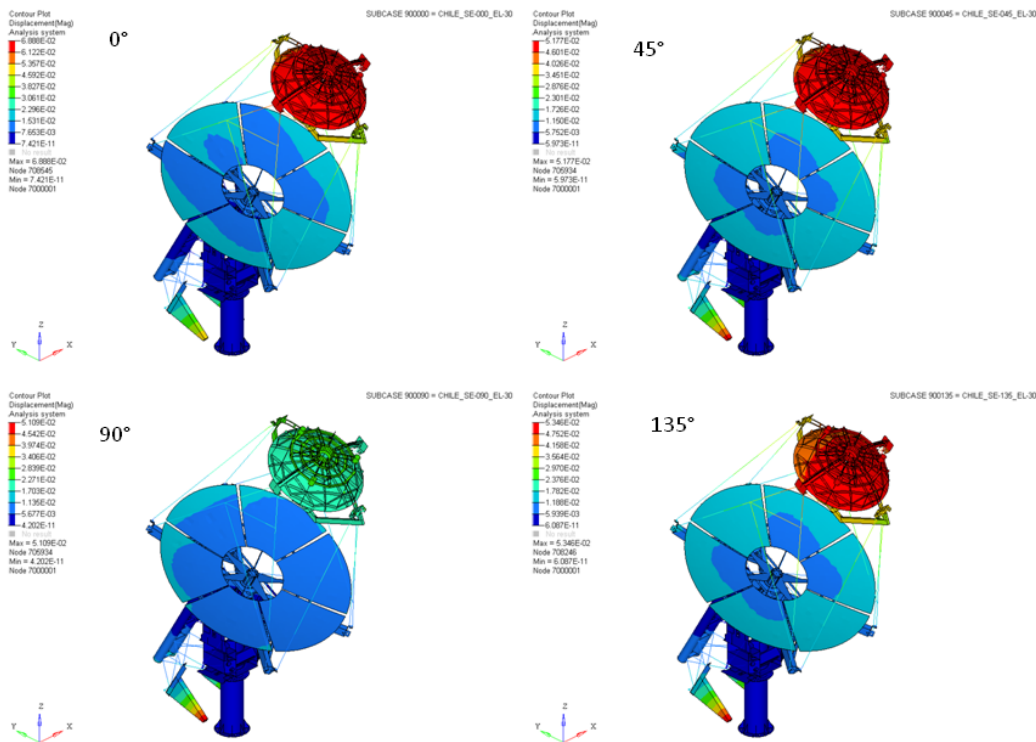


**Figure 3.8** – Plot of the deformed shape of the telescope for 60° elevation during an earthquake for several directions of the horizontal seismic acceleration.

the tubes of the counterweight, modification of the shape of the arms along the *x*-axis of the Top Dish or additional reinforcements tubes in the Top Dish) are proposed for the Pre-Production telescopes.

### 3.2.2 Optical Performance

The optical performance can be expressed in terms of the size of the PSF, here expressed as the radius of the circle which contains 80% of the light from a point source. When the GCT’s mirrors are perfect, and perfectly aligned, the PSF has a radius of 0.01° on-axis and 0.06° at a field angle of 4.5°. It is possible to optimise the optics to get either a better PSF on-axis, or off-axis, but the chosen compromise provides adequate performance across the entire FoV (B-SST-1140), while giving a relatively small PSF on-axis, which has some benefits for alignment, tracking and pointing studies.

The GCT is isochronous. The distribution of arrival times of photons from a point source on the focal plane has been shown using Zemax and ROBAST simulations to have an RMS of less than 1.5 ns, whatever the field angle (B-SST-0140).

#### Performance of the optical design

A Zemax calculation of the optical design was used to determine the how the PSF behaves as a function of the decentering, tilt, rotation and defocus of M1 and M2 as a whole and as a function of the same quantities for the mirror petals individually. This is illustrated for one case (tilt of M1) in Figure 3.9.

Calculation of the deterioration of the PSF for the combination of a large range of effects including the misalignment of the mirrors and their petals, thermal effects (expansion of the mirror, drift of their alignment) and the mechanical accuracy of the telescope (e.g. flexure with varying elevation) leads to the definition of an allowable error budget, as described further below.

The maximum degradation for decentering, tip, tilt and defocus is given in Table 3.9.

Monte Carlo calculations were used to evaluate the effects of random misalignments in all mirror positions. Figure 3.10 shows how the PSF worsens as a function of field angle for two allowed error

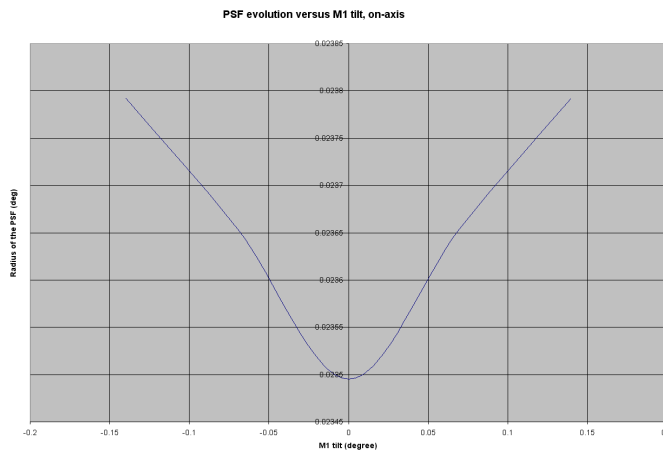


Figure 3.9 – PSF evolution versus the tilt of M1.

Table 3.9 – Enlargement of the PSF for various sources of misalignment. The axis for the decentering and tilt in column 2 is unimportant because the mirrors have cylindrical symmetry. For the third column, the axis that generates the worst case is considered.

	M1 or M2	M1 tiles
Decentering (5 mm)	10%	15%
Tilt (0.14°)	1%	5%
Defocus (5 mm)	30%	10%

envelopes (the full error budget and a fraction of the allowed error). It was also checked that the precise shape of the 6 M1 petals (trapezoidal or circular, the latter with two sizes) does not significantly affect the size of the PSF, as is shown in Figure 3.11.

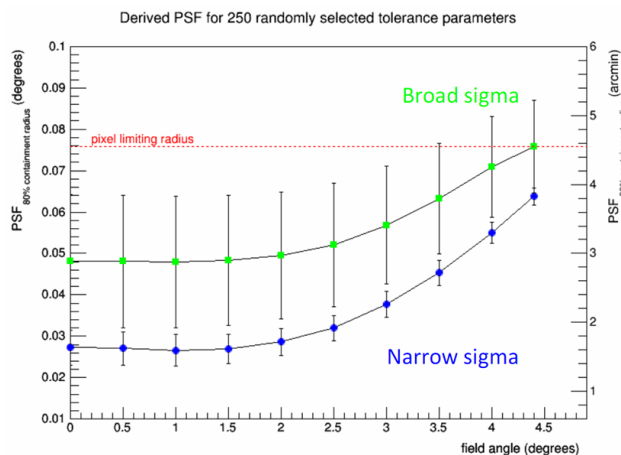


Figure 3.10 – Size of the PSF versus the field angle for two tolerancing options. The “broad sigma” case uses the full error budget allocation. The “narrow sigma” case uses 1/14 of the rotation and 1/3 of the decentering error allocation.

The shadowing caused by the GCT structure (mast, camera, etc.) has been calculated using ROBAST. Results are shown in Figure 3.12 which addresses the CTA requirements A-PERF-2020 and B-SST-0110.

Correct alignment of the optical elements is essential to the performance of the GCT. The alignment procedure during M1 construction uses a remote light source to illuminate the petals. Their tip and tilt is adjusted until the PSF viewed on a screen at the focal plane of the mirror matches the expectation for perfect alignment and is on the telescope’s axis. The expected accuracy is 40 arcseconds. This procedure and the achievable accuracy have been validated using a 1/10 scale optical model of the telescope. Following installation of the camera and the secondary, alignment of the secondary mirror

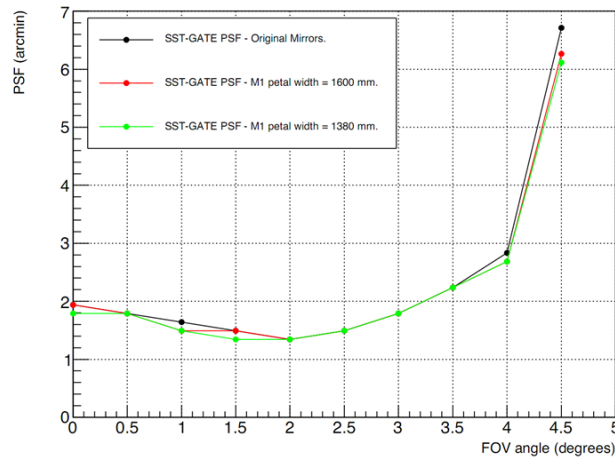


Figure 3.11 – Size of the PSF versus the field angle for different M1 petals.

can then be performed using an image projected onto the camera lid. Further alignment of all mirrors and mirror petals can be made using the actuators by analysing the PSF projected onto the camera lid and the effects on the PSF of moving individual mirrors and mirror petals. This procedure is described in [17].

The telescope also provides a positioning mechanism that allows movement (3 degrees of freedom) and rotation (2 degrees of freedom) of the camera in order to place it correctly with respect to the focal plane. The accuracies (0.1 mm and 0.01°) fulfill the relevant CTA requirements (B-SST-1110 and B-SST-1120). If this mechanism does not have sufficient stroke, it is possible to move the position of the focal plane of the telescope with respect to the camera using the mirror actuators.

Finally, the optical performance depends on the mirror quality. The CTA Mirror Test Facilities (MTF) group has measured the characteristics of the petals used in the optical model of the telescope and revealed that a roughness of 20 nm can be reached which allows a PSF smaller than the GCT pixel (0.15° to be achieved, with 2% light loss due to scattering. The CTA requirement is 0.25°) and less than 6% light loss due to scattering (B-SST-0130 and B-SST-1150).

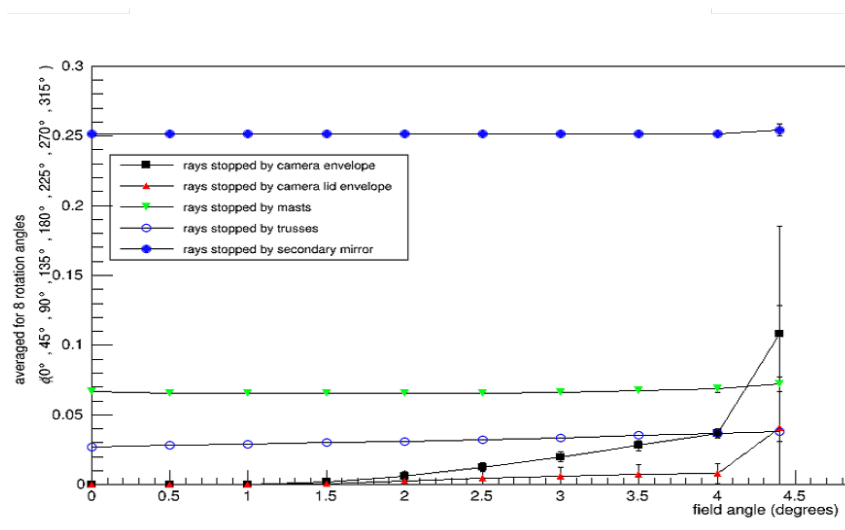


Figure 3.12 – Shadowing due to the different parts of the GCT telescope.

**Tracking accuracy**

A further performance requirement is the tracking accuracy of the telescope, which depends on the alignment of the optical elements, on its mechanical behaviour, and on the slew control performance. The alignment is discussed above. The mechanical behaviour of the telescope has been studied with FEA and tests of elements of the drive system. Using these results in a model of the telescope allows

the tracking accuracy to be evaluated. The expected tracking precision is 295 arc seconds, meeting the CTA requirement of  $0.1^\circ$  (A-PERF-2140).

The GCT specifications also address CTA requirements on the tracking speed. For example, the requirement that the telescope is able to point to any position on the sky above  $30^\circ$  in elevation within 60 seconds (B-SST-0220) leads to the specifications:

- C-SST-AUX-TCA-10: The control and command software must be capable of managing the Alt-Az movement fast enough to achieve the required movement speed.
- C-SST-FSS-GS-2: The power supply must be able to provide the power required to move the telescope at the required speed for all observing environmental conditions.
- C-SST-MEC-AAS-16: The azimuth drive system must be capable of moving at a speed of at least  $3^\circ/\text{s}$ .
- C-SST-MEC-AAS-17: The elevation drive system must be capable of moving at a speed of at least  $1^\circ/\text{s}$ .
- C-SST-MEC-AAS-38: The mechanical structure of the telescope must support the accelerations required for motion in the azimuthal direction.
- C-SST-MEC-AAS-39: The mechanical structure of the telescope must support the accelerations required for motion in the elevation direction.

The design of the telescope permits movement over the full azimuth range and over elevations from  $20^\circ$  to  $91^\circ$ , compliant with A-PERF-2110 and A-PERF-2120. The elements involved in the movement of the telescope have been designed to achieve a maximum mean speed of  $4^\circ/\text{s}$  (B-SST-0220) and to maintain tracking precision up to  $89.2^\circ$  in elevation (A-PERF-2130). The purchased drive components satisfy these requirements, as will be verified with tests on the prototype GCT in Meudon.

The telescope must also be able to move between states, e.g. from its parking position (Safe state) to the Observation state. This requires that it passes through the heating phase and the boot phase and then moves to the required position on the sky. A heating system will be installed to prevent condensation in the electronics cabinets. A thermal simulation of the cabinets with their electronics under various environmental conditions (winter/summer and wind/no wind) has demonstrated that the warm-up phase (the time required to get the electronics up to operating temperature) lasts no more than 30 minutes at minimum temperature ( $-20^\circ\text{C}$ ), compliant with A-PERF-2045. Tests on the GCT PLC show that the boot phase lasts less than 2 minutes, and the maximum duration of the movement to reach any direction on the sky is 1 minute (A-PERF-2040). Finally, before using the telescope in observing mode, the calibration of the camera has to be completed.

### Pointing monitor

The post-calibration pointing precision of the telescope is required to be better than 7 arc seconds (B-SST-0020). A performance budget has been allocated to the components contributing to pointing accuracy, including: calculation of coordinates (e.g. time, position in the sky); structure (bending, vibration); and the telescope mount (orientation, perpendicularity) with the goal of achieving an absolute pointing precision better than 6 arcminutes. Encoders have been purchased for the prototype which permit the measurement of the azimuth and elevation angles with an accuracy of 2 arcseconds to aid detailed study of the performance of the structure and its contributions to pointing precision. More information is provided in Section 3.2.6.

## 3.2.3 System Performance

In order to guide the design of the telescope, a performance budget was set up in the project. Unlike a classical error budget this gives the impact on the performance of a change in the error allocation. Building a performance budget requires a good understanding of the links between the different subsystems and how they contribute to global performance. A good description of subsystem function is necessary,



which helps guide the technical design as it is possible to experiment with different error allocations during the design phase. For CTA, the telescopes must have good tracking and pointing performance and good light-collection efficiency. These high-level features are used to derive the necessary characteristics of lower-level subsystems and hence their physical parameters. The figures 3.13 and 3.14 show the top-level of the GCT performance budget and the secondary mirror branch to illustrate this procedure.

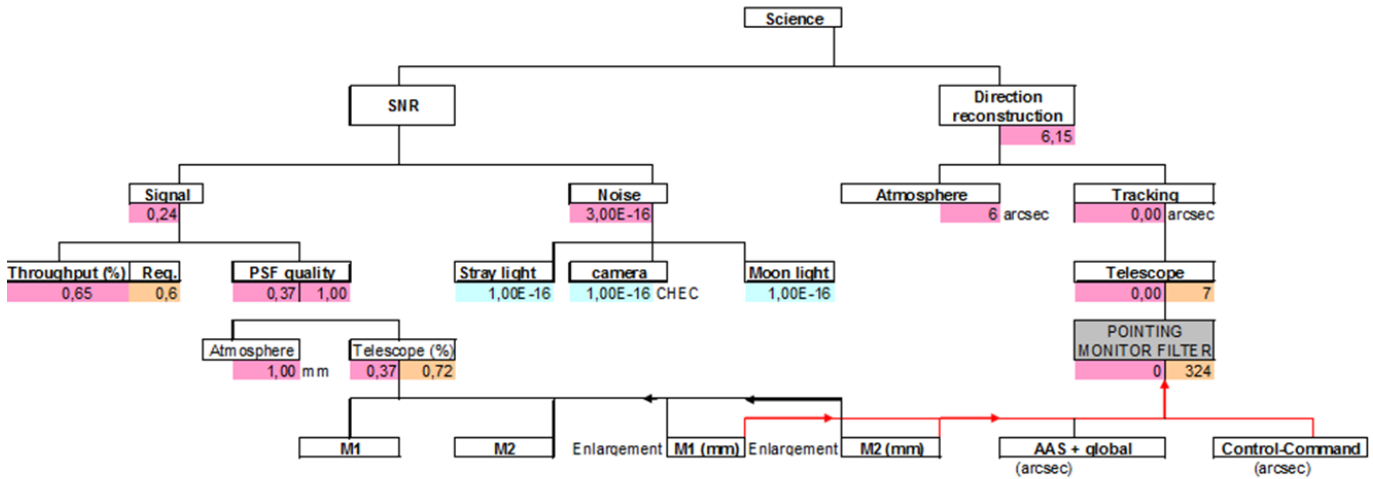


Figure 3.13 – Upper levels of the Performance Budget for GCT.

M2	
M2 tile enlargement (mm)	0.03
Relative loss in light due to tile	0.99
M2 tile (radial) (mm)	0.14
mounting	0.01
bending effects	0.1
thermal effects	0.10
M2 tile (radial perp.) (mm)	0.10
mounting	0.01
bending effects	0.1
thermal effects	0.1
M1 tile position (defocus) (mm)	0.71
alignment	0.5
mechanics	0.5
thermal effects	0.1
M2 tile rotation (radial) (deg)	0.02
mounting	0.01
bending effects	0.01
thermal effects	0.01
M2 tile rotation (radial perp.) (deg)	0.02
mounting	0.01
bending effects	0.01
thermal effects	0.01
M1 tile rotation (optical axis) (deg)	0.15
mounting	0.1
bending	0.05
thermal effects	0.1
NEGLIGIBLE	
M2 radius deviation	0
M2 shape (thermal asymmetric)	0
M2 shape (thermal homothetic)	0

Figure 3.14 – A specific branch of the GCT performance budget: allocations for the secondary mirror.

The performance budget was determined using extensive simulations of the telescope with Zemax to create a look-up table of PSF size (80% of encircled energy) versus the various optical (decentering, rotation, tiling, FoV, etc.) and mechanical (accuracy of the mount and of the alignment, wind effects, thermal effects etc.) parameters. Hence, when an allocation changes, the performance budget automatically calculates a new PSF and gives, to first order, the resulting telescope performance. The optical performance also takes into account atmospheric effects (throughput and uncertainty on refraction for instance), the mirror (error on the shape and on the alignment, thermal effects, reflectivity) for both the whole mirror and its tiles. The performance budget also estimates the pointing accuracy. It takes into account the misalignment of the mirrors (and their tiles), thermal effects, mechanical flexure, mechanical misalignment (between axes) and the pointing accuracy the software produces (time accuracy, vertical orientation of the tower, temporal error, etc.). Some parameters are common to both the optical and the pointing performance, such as the mirror alignment. The performance budget includes the accuracy of the alignment procedure in both cases.

The performance budget shows that the values given in the technical specifications given here allow the

GCT to fulfill the CTA requirements. The test plan will ensure that these values are indeed achieved by the system.

- C-SST-AUX-TCA-5: The astronomical calculations must provide an accuracy of better than 2 arc seconds.
- C-SST-AUX-TCA-9: The orientation of the telescope must be known with an accuracy of better than 2 arc seconds.
- C-SST-AUX-TCA-12: The temporal error must be lower than 0.2 second.
- C-SST-GATE-2: The RMS space-angle post-calibration pointing precision obtained by the SST-GATE telescope in favourable observation conditions must be  $< 7$  arc seconds.
- C-SST-MEC-AAS-24: The alt-azimuthal system gives the orientation of the azimuth and the elevation axes and their perpendicularity. They must be measured and implemented in the control loop software with an accuracy of 20 arc seconds and 10 arc seconds, respectively.
- C-SST-MEC-AAS-25: The angle between the mechanical and the optical axes of the telescope must be below 15 arc seconds.
- C-SST-MEC-AAS-34: The encoders must be chosen in order to achieve an RMS space-angle post-calibration pointing precision of  $< 7$  arcseconds.
- C-SST-MEC-AAS-43: The bending of the telescope structure must be known for all elevations with an accuracy of 60 arc seconds for input into the control loop software.
- C-SST-MEC-AAS-44: The tower orientation with respect to the local vertical impacts on the transformation of right ascension and declination coordinates into the Alt-Az system and must be known with an accuracy of 20 arc seconds for implementation in the control loop software.
- C-SST-MEC-AAS-45: During observing conditions, the amplitude of telescope structure vibrations must remain below 10 arc seconds.

The CTA requirements A-PERF-2060 have resulted in the following technical specifications:

- C-SST-OPT-PMS-3: The accuracy of the measurement of diffusion over the whole M1 mirror shall be better than 0.5%.
- C-SST-OPT-PMS-4: The accuracy of the measurement of reflectivity over the whole M1 mirror shall be better than 0.5%
- C-SST-OPT-SMS-2: The accuracy of the understanding of the shadowing of the M2 structure and detector shall be better than 0.3%.
- C-SST-OPT-SMS-3: The accuracy of the measurement of diffusion over the whole M2 mirror shall be better than 0.5%.
- C-SST-OPT-SMS-4: The accuracy of the measurement of reflectivity over the whole M2 mirror shall be better than 0.5%.

The test bench at the IRFU laboratory allows the measurement of the reflectivity of the GCT mirrors.

### 3.2.4 Control Command Performance

#### Tracking

The elevation range of the telescopes is  $25^\circ$  to  $89.2^\circ$ . The tracking motion profile used for the simulations is taken at the required maximum elevation for tracking, i.e. at  $89.2^\circ$  (C-SST-AUX-TCA-11), leading to an azimuth speed of  $0.3^\circ/\text{s}$  (C-SST-MEC-AAS-18).

## Slewing

The positions available for scientific observations range from 25° to 89.2° in elevation, for any azimuth direction (C-SST-GATE-AUX-TCA-6 and -7).

The slewing motion profile used is an *S-curve* with a finite value of the *jerk* – the derivative of the acceleration. This ensures a smooth start of the motion and does not excite the structure. As a consequence, the regulation loop does not need to handle overshoots and oscillations.

The S-curve shown in Figure 3.15 – with a maximum speed of 4.3°/s, a bus voltage of 162.5 V and a duration of 60 s (B-SST-0220) – allows a full stop of the axes of the telescope in less than 300 ms without requiring a brake resistor thanks to the low bus voltage and low telescope inertia. The stopping time would increase to 650 ms for a speed of 5°/s.

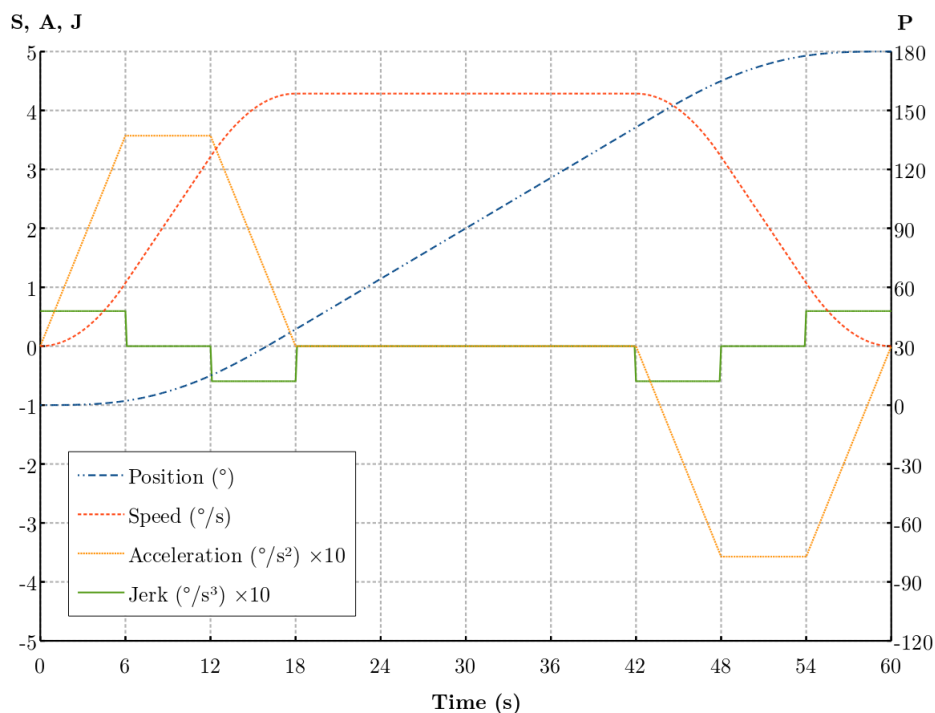


**Figure 3.15** – The positioning commands required to produce an S-curve ensuring soft starts and stops. An S-curve is characterised by the percentage of jerk time ( $\alpha$ ) and the percentage of time at full speed ( $\beta$ ); the figure shows an S-curve with  $\alpha = 10\%$  and  $\beta = 40\%$ .

## Power consumption

The energy consumption for a typical day is detailed in Table 3.10. While observing, it is assumed that the telescope shifts to a new source at every 20 minutes. The consumption in the *Off* mode comes from the regulation of the electronics cabinets and the Supervisor in idle mode.

**Table 3.10** – Estimate of the power consumption during a typical day (see text).

Activity	Mode	Hours	Temp	Wind	Energy (kWh)
Idle	Off	1200%	14°C	--	0.840
Calibration	Stand-by	200%	14°C	20 km/h	4.000
Observing	On-line	900%	13°C	20 km/h	23.267
Calibration	Stand-by	100%	14°C	20 km/h	2.000
<b>Total</b>					<b>30.107</b>

The peak power consumption is 3 kW. This is calculated for a wind gust of 150 km/h while slewing at full speed with the camera switched on; other parameters do not affect this value significantly.

## 3.2.5 Camera Performance

The overall plan for the validation of the camera design is given in an accompanying document [13]. Here, we compare both the CHEC-M and CHEC-S designs to requirements, with more detail given for the MAPM-based CHEC-M, where the characteristics are better determined at this point. We describe the relationship of key specifications to the requirements and briefly summarise simulation efforts performed as a first assessment of the suitability of the design to meet high level requirements, which cannot be verified with simple calculations. At the end of this section, we briefly describe how the prototyping efforts described in Section 2.3 will be used to complete the design validation process.

**Physical Dimensions** The compliance of specifications with performance requirements associated directly to physical dimensions can be analysed in a straight-forward way:

1. B-SST-1150 requires an angle of  $0.25^\circ$  for the flat-to-flat distance of a hexagonal pixel, corresponding to  $0.216^\circ$  for a square pixel with the same solid angle.

The effective plate-scale of the GCT is  $38.9 \text{ mm}/^\circ$  (see Section 2.1). A single  $6.0 \times 6.0 \text{ mm}^2$  pixel (C-SST-2M-CAM-10101) therefore subtends an angle of  $0.15^\circ$ .

2. B-SST-1130 requires that the focal plane be fully instrumented up to  $6.8^\circ$  (85% of  $8^\circ$ ) and have an average diameter  $>8^\circ$ . For the CHEC geometry, the average diameter is  $\approx 1.06$  times larger than the 'flat-to-flat' diameter across the camera. The flat-to-flat distance measured along the curved focal surface is 6 times the module width (51.4/52 mm) plus 5 times the average gap size. Given the platescale of  $38.9 \text{ mm}/^\circ$ , the resulting average FoV is  $9.15^\circ$  for CHEC-M and  $8.7^\circ$  for CHEC-S.

**Photo-detection efficiency** B-SST-1170 requires an average photon detection efficiency of the focal plane averaged over the reference spectrum given in the SST Requirements of 13%.

For CHEC-M this efficiency is a combination of the quantum and collection efficiencies of the MAPMs averaged over incidence angle, multiplied by the fractional active area. The weighted efficiency for a single MAPM pixel at normal incidence is 25% using datasheet curves. The camera dead space is 9%, the angular-weighted efficiency is lower by a factor of  $\approx 0.8$ , including MAPM collection efficiency the expected overall efficiency is 14.5%. For CHEC-S and future silicon-based cameras only sensors with significantly higher QE are considered, large incidence angle performance is improved and camera deadspace is reduced by a large factor: B-SST-1170 is therefore met in these systems by a comfortable margin.

**Signal and digitisation chain analysis** The CTA requirements on camera performance cover many aspects of opto-electronic performance that are best studied using detailed Monte Carlo simulations (prior to prototype evaluation), but can in part be analysed in a straight-forward way to establish the basic validity of the design. Considering firstly photosensor operation and the dynamic range of the system for CHEC-M:

1. The nominal operating gain of the H10966 is  $3.3 \times 10^5$ . CHEC will operate at a somewhat lower gain of  $10^5$ , sacrificing some of the (unnecessarily) fast pulse width and some single p.e. resolution, in exchange for improved lifetime in the presence of star and night sky background light, and the ability to observe in partial moonlight.
2. The range of required illuminations (A-ENV-1420) corresponds to a single photoelectron rate in each MAPM pixel of 12 to 60 MHz. The maximum total current drawn by each MAPM is therefore  $64 \times 1.5 \times 10^5 \times 1.602 \times 10^{-19} \times 6 \times 10^7 = 92 \mu\text{A}$ . The manufacturers quote  $100 \mu\text{A}$  as the maximum allowed current, but laboratory measurements suggest that performance and lifetime are stable up to  $\approx 160 \mu\text{A}$ . We therefore expect acceptable performance of the MAPMs over the full required operating illumination range.

3. A test exposure of a single MAPM to room lighting under HV (exceeding A-PERF-2260) indicates that no discernable permanent damage is caused for a 10 second exposure.
4. The excess noise factor (scaling factor on the Poisson photoelectron noise) of the MAPM at operating gain is  $\approx 1.15$ . The study described in [18] indicates that acceptable sensitivity can be reached with this value.
5. The output of the H10966 is linear to within 20% at 1000 p.e. – the maximum required charge from B-SST-1010. Calibration of this non-linearity to better than 50% (i.e. residual mis-calibration  $< 10\%$ ) will be required to meet the charge resolution requirement, this will be done with in-situ calibration flashers.
6. A single p.e. pulse from the MAPM, with typical amplitude of 0.8 mV, will be translated by the pre-amplifier to a pulse of typical peak voltage 2.4 mV and FWHM 5 to 9 ns (significantly slower than the MAPM output pulse to improve triggering efficiency). The maximum pre-amplifier output pulse height of 1.2 V is matched to the maximum input voltage of the TARGET module and corresponds to  $\sim 500$  photoelectrons.
7. Charge resolution above TARGET chip saturation is possible by fitting the saturated waveforms. This works well in simulations (see below) and will be tested in the laboratory (see below).
8. One ADC count in TARGET corresponds to approximately 0.3 mV or 0.13 p.e. Quantisation errors are therefore always much smaller than poisson fluctuations.
9. The electronic noise specification for the combined pre-amplifier/TARGET system is 1.1 mV (or 0.46 p.e.) RMS. Simulations indicate that this is the maximum allowable level before noticeable performance degradation begins.

For CHEC-S, dynamic range and noise considerations are very similar, but with the following additional considerations:

1. Optical cross-talk at operating gain must be low enough to ensure the excess noise factor is below 1.15.
2. Due to the different wavelength dependence of the SiPM response, night sky noise rates are higher than in the MAPM case, even if radiation at wavelengths  $> 550$  nm is blocked before the camera as planned. This increase should be compensated by the improvement in efficiency for signal photons.
3. Dark count rates at operating gain and temperature must be less than  $\sim 20\%$  of the dark sky NSB rate to ensure a negligible impact on performance.
4. In the case of CHEC-S, the shaping pre-amplifier must reduce rather than increase the pulse FWHM for optimal performance (5 to 9 ns as above).
5. With SiPM technology, the illumination levels of A-ENV-1420 are unproblematic for all available devices.

**Deadtime and readout window** The readout deadtime requirement of  $< 5\%$  (B-SST-1260) at the required readout rate of 300 Hz (B-SST-1280, or indeed the goal of 600 Hz, B-SST-1290) can easily be met. The back-end electronics are essentially deadtime free at these rates and the readout deadtime of TARGET is less than  $20 \mu\text{s}$  (i.e. 1.2% at 600 Hz) if 80 samples are read out, achieving the goal readout window of 80 ns (B-SST-1220) for **all** camera pixels (and hence meeting also B-SST-1250). Note that only the part of the ring buffer being read-out is dead, so the effective deadtime is much less than this. With 1 to 2 ns time-slices/sampling available at the analysis level, the fixed gate of 20 to 30 ns required in B-SST-1210 can be very easily met. The backplane will transmit information on all camera-level triggers, which can be compared to the TARGET data received to monitor deadtime (B-SST-1270).

**Simulations** The most robust means of analysing the performance of (and indeed optimising) our design prior to prototyping is through detailed Monte-Carlo simulations. The CORSIKA simulation package is used to produce lists of Cherenkov photons at ground-level which are then processed with a custom camera simulation/analysis package (*LTools*). We note that the reliability of CORSIKA has been demonstrated through numerous comparisons to data from currently operating Cherenkov Telescopes and that *LTools* has been cross-checked against the *sim\_telarray* package, which has been tested in detail on HESS data.

The primary performance criteria are the trigger threshold (B-SST-1230) and the charge resolution (B-SST-1010). Trigger probabilities and charge resolution curves have been generated for CHEC-M with camera properties corresponding to the current CHEC specifications. CHEC-S simulations are in progress.

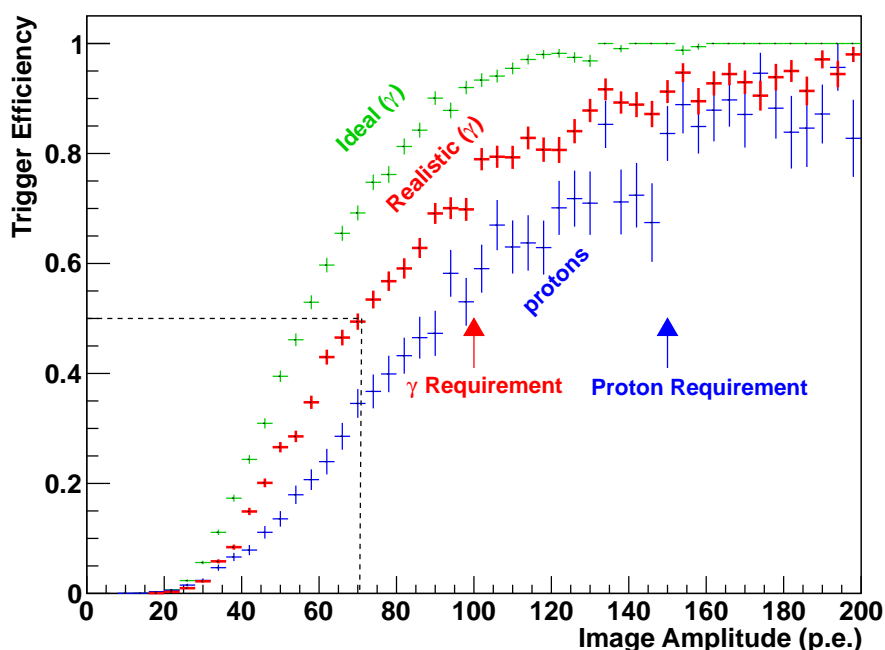


**Figure 3.16** – Simulated trigger efficiency for CHEC-M as a function of image amplitude. The requirements (B-SST-1230) for gamma-ray and proton images are indicated.

Figure 3.16 shows the simulated trigger performance, illustrating that for a realistic system simulation the goal of a 50% trigger efficiency for <80 photoelectron images given in B-SST-1240 can be met. Similarly, Figure 3.17 indicates that goal charge resolution can be met or exceeded at most charges, but that saturated pulse recovery is required to meet the requirement above 500 p.e.

Comprehensive simulations of the sub-system as a whole (and indeed the CTA system) have recently been performed, and are under analysis to establish compliance with the sub-system performance requirements A-PERF-1210 to A-PERF-1250.

**Compliance testing via prototyping** Several of the key specifications of the camera can (and must) be measured directly in a full-scale camera prototype, for example the level of electronic noise and the dynamic range. Such measurements will be performed for CHEC-M in the very near future and for CHEC-S after commissioning. For some performance requirements, e.g. charge resolution, laboratory measurements can be used to measure closely-related quantities, but simulations must still be used to link lab-measurable quantities to gamma-ray shower related requirements.

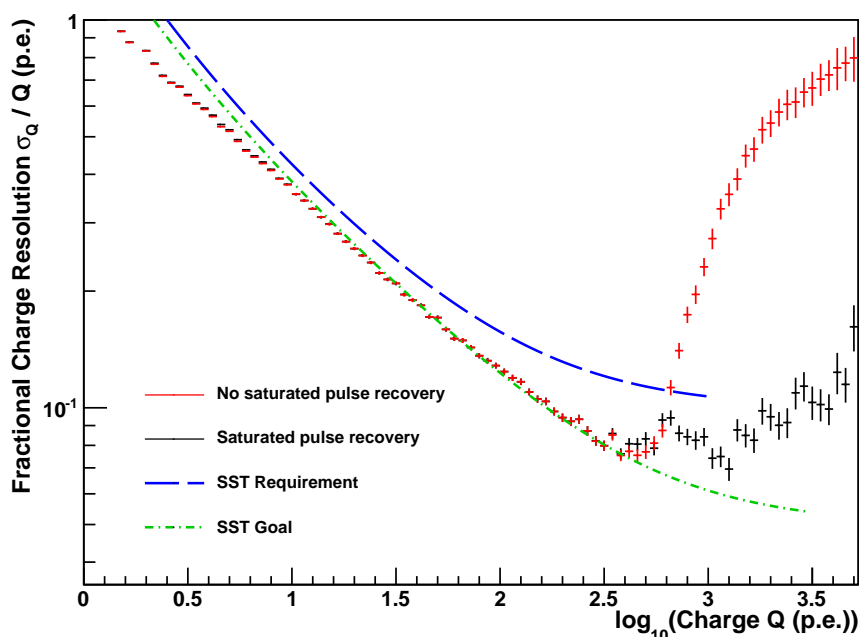


**Figure 3.17** – Simulated fractional charge resolution for CHEC-M as a function of Cherenkov signal charge in an individual pixel. Two simulation results are compared to the requirement B-SST-1010 and goal B-SST-1020.

**Calibration System** Compliance with performance requirements (and also the calibration requirement B-SST-1360) requires relative amplitude calibration of the camera pixels over the full amplitude range at a level of 5% RMS. The in-situ, continuous, calibration flasher system of the GCT camera is designed for this purpose, with the following specifications (to satisfy B-SST-1350). Four LED flasher units will be placed in the corners of the camera. To mimic the characteristics of Cherenkov light from showers in the energy range of the SST, a light pulse width of 3-4 ns (FWHM) at short (blue) wavelengths is required. Each unit must flash from 0.1 p.e., for absolute single-p.e. calibration measurements, up to 1000 p.e., to characterise the camera up to and at saturation. Independent ray-tracing analyses indicate that the LED flasher units should be oriented  $2^\circ$  away from the optical axis to cover the full focal plane.

The calibration system verification will include the measurement of output (optical) pulse shape and relative brightness for each LED on each flasher unit, before installation in the prototype. In addition, the flasher units on the prototype will be in constant use during laboratory and on-telescope tests, as a means of establishing reliability (in addition to the standard tests that will be applied to all PCBs).

### 3.2.6 Pointing System Performance

Simulations of a pointing calibration system based on measuring continuous starlight with the Cherenkov camera pixels have been performed and are briefly detailed here.

The GCT pointing system is based on measuring continuous starlight with the camera pixels, providing an immediate and precise measurement of the area of the sky that is imaged on the camera focal plane. Simulations were performed to determine the sensitivity of this pointing system. So far, these include realistic noise sources, NSB, gain variations of the photo-sensors, static image distortions and realistic star fields. A typical image is shown in Figure 3.18.

In the simulations, we achieve typically 5 arc-seconds (peak-to-peak) deviations in the pointing for a single star, with  $\sim 1$  arc-second residual drifts when averaging over all stars which are present with a signal-to-noise greater than  $\sim 3$  in a single image. As the simulations are made more realistic, the pointing accuracy is expected to decrease for the simple centroiding algorithm that has been employed up to now, so other more sophisticated fitting techniques are being developed. Several further verification

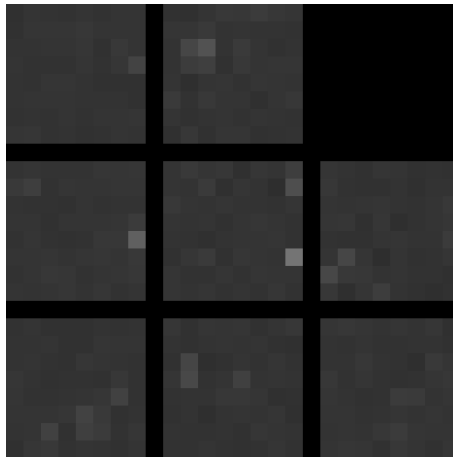


**Figure 3.18** – Typical simulated image for 1 quadrant of the CHEC camera. The gaps, as displayed in this image, are approximately to scale (correct width implemented in the simulations).

tests are planned, in simulations and on-sky as well as in the lab:

- More realistic simulations of the actual imaging of the stars through the telescope to the camera are being prepared in order to verify the on-line analysis software. These simulations include telescope vibrations and image distortions, noise sources that could decrease the sensitivity of the pointing system if not properly handled.
- The noise properties and sensitivity of the continuous light path of the Cherenkov camera is being tested in the lab, in order to provide accurate input to the simulations and estimate the on-sky sensitivity.
- A verification test is being prepared on the telescope prototype using a camera mounted in the central hole of the secondary mirror, looking at both the stellar images on a focal plane screen as well as calibration LEDs at the edge of the camera.

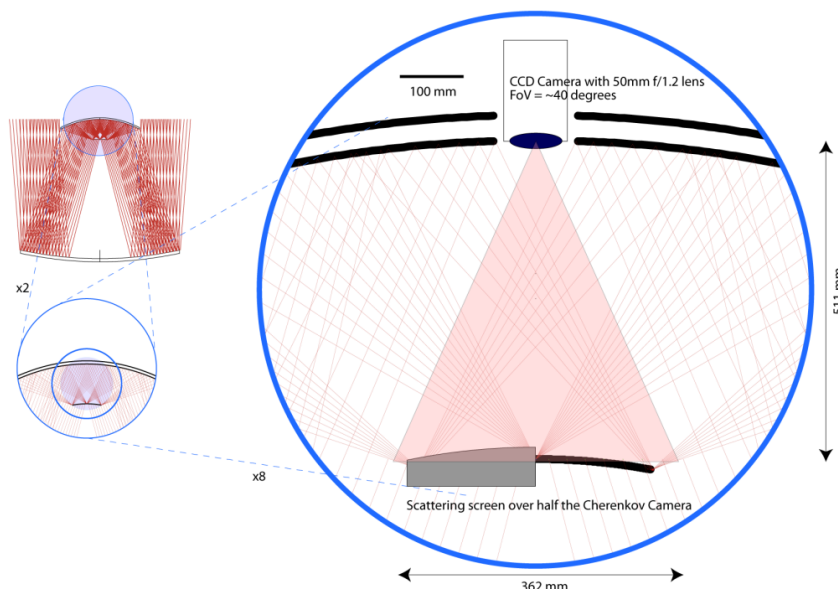


**Figure 3.19** – Schematic overview of the verification test installation of the pointing system on the GCT telescope prototype.

Figure 3.19 presents an overview of the verification test of the pointing system on the GCT telescope prototype. An interface exists on M2 which provides the possibility of directly measuring the stellar positions on the lid of the camera, for comparison with the pointing reconstructed from measuring continuous starlight with the camera's pixels.



### 3.3 Reliability

The reliability of the GCT determines the proportion of time it is available to make scientific observations, i.e. to point to the required position in the sky, track sources and take data using the camera. This is given by the performance of the telescope's subsystems, by maintenance requirements and also by the instrument's safety; damage causes delays while repairs are effected. The methodology for reliability calculations is based on CEI/EN 62061 and CEI/EN 61058.

For this study, we assume that GCT is a Markovian system i.e. that its evolution only depends on its current state and not on its history. This is true when the failure of one element does not depend on the state of other elements and when the probability of failure is well understood. To avoid "teething problems" (the probability of a component failing is high early in its life cycle and often poorly modelled) we have foreseen a delivery procedure that includes running all relevant components for 100 hours before installation.

#### 3.3.1 Reliability and FMECA

The DVD gives the specifications implemented in the GCT design which ensure compliance with the CTA requirements. Chapter 2.2.5 of this document describes in detail all the specifications implemented in the design and related to the reliability in the three main areas of performance, environment and RAMS. For each specification a verification method is described. We have developed and completed the FMECA using the telescope's failure tree. This has allowed us to focus on the major risks, to humans and the instrument, and find solutions to mitigate against to include in the design at an early stage. This study lengthened the duration of the design phase, but has reduced the level of risk in the project.

The mechanical structure of the telescope has a very low probability of failure (calculations have been made and described in internal technical report [19]). We therefore do not foresee holding spares to cover the effects of mechanical fatigue.

**Table 3.11** – Most critical elements of the GCT FMECA analysis.

ID n°	System	Risk	RPN	Action
ID 28	Anchor of the tower	Plastic deformation caused by extreme environment conditions	8	Margin in design
ID 33	Front end camera	Bad mechanical interfaces with an external Cherenkov camera	6	ICD
ID 34	Front end camera	Bad electronic interfaces with our CCD camera	8	ICD
ID 76	Telescope control and alignment system	Loss of scientific data	8	CHEC software

#### 3.3.2 Availability of the telescope

The availability of the telescope can be estimated from the the MTBF (Mean Time Between Failure) of its subcomponents and the time required to make repairs. Preliminary calculations based on the MTBF figures provided by manufacturers and estimates of the time required for repairs give an availability of 99%, provided the required spares are available on site. These estimates will be refined using the experience gained with the construction and operation of the telescope on the Meudon site and the results of tests of the camera.

The reliability of the telescope is enhanced by the use of the shelter. This allows maintenance operations to be carried out in weather that would otherwise prohibit work on the telescope (e.g. when wind-blown dust would otherwise prevent work). The shelter also increases the time between mirror recoatings.

Work is going on to try and quantify these benefits over the lifetime of the telescope.

### 3.3.3 Instrumentation for reliability

In accordance with the requirement A-RAMS-0400, sensors are installed on the GCT structure to monitor its behaviour. Further sensors are added for preventative maintenance purposes. These are designed to allow anticipation of serious failures, so maintenance and repair can be scheduled in the most efficient way, e.g. when operation is not possible for environmental reasons. These sensors are:

- A-RAMS-0400-1 Current sensors to monitor the performance of the motors.
- A-RAMS-0400-2 Strain gauges to monitor the mechanical structure of the telescope (proposed at least for the prototype in Meudon).
- A-RAMS-0400-3 Temperature sensors to monitor the environment and the optical and electronic elements of the telescope.
- Additional housekeeping sensors provide information on the environment and behaviour of the telescope (e.g. humidity, ambient light, wind speed...).
- Monitoring of many systems (electronics, drives...) is used to ensure telescope safety whatever the environmental conditions.

Further, to ensure that information is securely exchanged:

- The communication between the different components is permanent (specification A-RAMS-0420-1) and is ensured by an EtherCAT bus.
- The cables will be shielded against electromagnetic disturbance (A-RAMS-0450-2) and will be protected from environmental influences (fence, cable ducts where appropriate...).

All of the above sensors are easy to replace, except for the Heidenhain encoders that are embedded in the alt-az structure. The MTBF of these sensors is long (500 000 hours). To ensure a lifetime of 30 years for 35 telescopes, 8 spares will be purchased. This is more than is needed, as the probability of failure of the alt-az systems is very low (its MTBF, including the electronics and power supply, is estimated to be 25 years), but the additional spares are needed to cope with potential breakage during assembly and transportation. The assembly of the alt-az system is complex and time consuming, so it is currently proposed to mount 37 alt-azimuthal systems: 35 for the telescopes and 2 spares. This policy will reduce significantly the time taken for a repair. Further cost-benefit analysis of this and other aspects of the spares policy are underway.

It is anticipated that the GCT mirrors will have to be recoated after some period of operation. The M1 petal removal mechanism simplifies this operation and the GCT shelter will reduce the frequency with which it must be carried out.

Repainting of the structure will also be necessary. The paint chosen for the GCT should survive 10 years in a desert environment. Complete repainting requires removal of the mirrors and can be done in conjunction with recoating of some or all of the mirrors. Regular visual inspections will determine when repainting is necessary.

The telescope has also been designed to allow easy maintenance of its elements, e.g. mirrors, electronic components, sensors and alignment components. Given the required spares (see Section 4.5), these can all be replaced within a few hours, except for the Heidenhain encoders mentioned above. These elements also all have low weights, which means that no heavy lifting equipment is required. As an example, the M1 petals weigh 45 kg and the M1 mirror is able to turn on its axis so that the petals can be individually removed from ground-level and placed in storage/transport boxes. This saves time because there is no need to assemble scaffolding and reduces the risks to both humans and the mirrors. Thus,

changing all the M1 petals can be done within a day so that no observation time is lost. In addition to time and safety considerations, the simplicity of this procedure reduces the need for staff training, as important consideration for the operation of the telescopes over a 30 year period.

### 3.3.4 Camera Reliability

The FMECA for the GCT camera is ongoing and will evolve to include additional analysis on the timescale of the CHEC prototypes. The spreadsheet `GCT_FMECA_Cam.xlsx` shows the complete current set of failure modes and outlines their consequences. Here some of the primary considerations are summarised for CHEC-M.

The highest priority (critical) failure modes are identified as:

- The lid is open during rain/hail/high-winds. This can result in physical damage to all camera pixels and water ingress into the camera and therefore damage to electronics. To avoid the lid failing in the open position it must be extremely reliable. The lid will be controlled via a microprocessor, and on power-up will default to the closed position. Accelerated ageing tests to mimic the lifetime of the lid will be performed on the prototypes to assess the motors and hinges.
- The lid seal fails allowing water into the camera resulting in potential damage to camera pixels and electronics. The accelerated ageing tests to mimic the lifetime of the lid will also assess the seal.
- A cooling system failure resulting in potential damage to electronics. A monitoring/control loop and fail-safe power-down of the camera will be used to ensure no damage to the electronics occurs following a cooling failure. Hexid fluids will be used in the chiller system to prevent freezing, and the chiller is specified to operate down to the camera survival temperature if required.
- Loss of signal on all photosensors due to permanent damage to all photosensors resulting in the loss of all pixels from the data stream.

Some of the potential failure modes of CHEC-S are similar, but the SiPM-based camera is in general more robust than CHEC-M. This is partly due to the nature of the sensors themselves, but also to the CHEC-S design, which will incorporate a PMMA window in front of the sensors, reducing risks associated with lid malfunction.



## 4 Plans

### 4.1 Construction Plans

The GCT consortium aspires to build 35 complete SST-2M systems and provide these as an in-kind contribution to the CTAO. In the current prototyping phase of the project, one telescope and two camera prototypes are being built. These will be tested and then final design reviews performed to assess the prototype performance and make any design changes necessary to prepare for mass production or improve performance. Following these final design iterations, calls for tender will be prepared for the Pre-production phase to choose industrial partners for the manufacturing and assembly of the telescope and camera components. In the Pre-production phase (2016-2017), three complete GCTs will be assembled on the southern CTA site. The cameras required will be assembled and tested at three GCT institutes in Europe, allowing preparation of the facilities required to produce cameras at the rate needed for the production phase. The telescope components will be manufactured in industry in Europe. Assembly of telescope components will happen in Europe, and after shipment these will be put together on the CTA site and testing will commence. Telescope commissioning for science operation, with the cameras mounted, will conclude the Pre-production phase and, once all procedures have been assessed and validated based on the Pre-production phase experience, the final production of a further 32 GCTs will start. The production assembly procedure will be very similar to the Pre-production phase: the cameras will be fully assembled in Europe at three assembly sites, while the telescope components will be manufactured in industry in Europe and shipped for final assembly and camera mounting to the CTA southern site.

#### 4.1.1 Manufacture and Assembly

The manufacture and assembly process for the telescope mechanics and optics differs slightly between the prototype and Pre-production/Production phases. While the manufacturing process will not change drastically (with the possible exception of using moulding for some parts rather than machining and welding, which can help to decrease production cost and increase manufacturing speed), the assembly stage will differ. The assembly of the prototype is mainly carried out at the Observatoire de Paris and for the Pre-production and Production telescopes responsibility for integration will be transferred to a prime contractor. Some sub-systems will be pre-assembled before shipping and only the high level PBS systems will be put together on the CTA site.

#### Manufacture of Mechanical Assembly

The design of the mass production GCT telescope may differ slightly from the prototype; these modifications will be implemented following feedback from the companies manufacturing the prototype, the team assembling the telescope on site, and analysis of the prototype. Table 4.1 lists some potential design changes between the prototype and series construction telescopes.

#### **Mechanical production WBS 03 and 04.6G.03**

##### *Tower Production - WBS 6G.03.02*

The tower is machined. The steel tube is currently a COTS item. The tower structure may change to adapt the interface to the foundation on the CTA site. A cable support will be directly machined into the

**Table 4.1** – List summarising the manufacturing processes for the main PBS mechanical elements. Grade E36 steel corresponds to grade S355 for tubes and E235 for sheets.

PBS	Prototype manufacturing	Material	Change in assessment phase
Tower	Welding	E36	Interface flanges
AAS	Machining	Mainly E36 some in Inox	Simplification of some parts (drawings and / or manufacturing process)
MTS	Machining and Welding	E36	Manufacturing process (welding)
Dish M1	Machining and Welding	E36	Manufacturing process
Counterweight	Machining and Welding	E36 and Lead	Moulding process
M1	Machining, polishing, coating	Aluminium 5083 H111	Moulding process or glass mirror
M2	Machining, polishing, coating	Aluminium 5083 H111	Moulding process or glass mirror
Camera removal	Machining and Welding	E36	-
Support of actuators for M1	Machining / Welding	Aluminium grade 6	Moulding process
TCS	Purchase	Modules	-
Shelter	Purchase	Aluminium tubes and fabric	Installation to be confirmed

structure to ease cable routing on site. After manufacture, documentation (WBS 6G.03.01.02) must be completed by the company in order to certify the compliance of the tower with the specifications (number of holes, dimensions, non-conformity reports etc.).

#### *AAS Production - WBS 6G.03.02*

The AAS is manufactured as several sub systems (see WBS and description in section 2.1.2). It is composed of machined elements which are either welded and/or bolted together; some materials and manufacturing processes may change to ease mass production.

The fork is manufactured as an assembly of beams and plates that are welded together, and is delivered by the manufacturing company as a single piece. The bosshead consists of an assembly of lateral hexagonal plates with a central hole connected by beams and plates. This module is also welded and delivered by the manufacturing company in one piece.

The AAS is composed of 3 identical systems (one for azimuth two for elevation) that are assembled and aligned before shipping. The assembly of the AAS will be carried out by the prime contractor. The responsibility for the AAS assembly (manufactured elements and purchased items) is held by the prime contractor. The prime contractor will be the point of contact with the Observatoire de Paris. Before starting the assembly, the components must be commissioned and all the drive bearings characterised.

The assembly procedure is similar to the process developed in the lab of the Observatoire de Paris. The assembly of the motor shaft and drive system can proceed in parallel. The drive system is mounted with the fork and bosshead to form the main AAS. The motor shafts are assembled in industry but fixed to the main AAS on the CTA site.

The AAS is integrated and aligned by the company, on a mount named the “big foot”. This has the same interface as the tower, but is smaller, ensuring the top of the bosshead is at only 3.27 m above ground level for ease of working. The AAS assembly consists of the following steps:

1. Assemble the bearing system.
2. Assemble the motor shaft and test.
3. Mount the azimuth drive on big foot.
4. Mount the fork on the azimuth drive.

5. Fix the elevation drives to the bosshead.
6. Fix the elevation and bosshead assembly to the fork.
7. Align the AAS to ensure perpendicularity of the axis with the precision required.
8. Mount the motor shafts on the azimuth and elevation axis and test.

The AAS is shipped to the CTA site assembled and aligned. A specially designed crate is foreseen to avoid any damage during shipment.

Two trained technicians are needed for the assembly and test of the AAS. The assembly in takes 20 days and the alignment a further 5 days. Preparation for shipment requires 1 more day (remove and protect the motor shaft, organize the shipment).

#### *OSS Production - WBS 6G.03.03*

The OSS includes the MTS, the M1 dish and the counterweight.

The MTS is formed of the following parts:

- The MTS bottom dish composed of 5 different elements (see Figure 4.1); the rotation system is assembled by the company in Europe with the interface flange. Note that it is possible to ship the MTS bottom dish mounted, however the assembly of the dish takes only 2 days with 3 people and can be done on site.



**Figure 4.1** – The five elements composing the MTS bottom dish.

- The MTS tubes, with 2 double arms connected by reinforcing tubes and 4 single arms (see Figure 4.2); the arms are shipped separately in a crate.

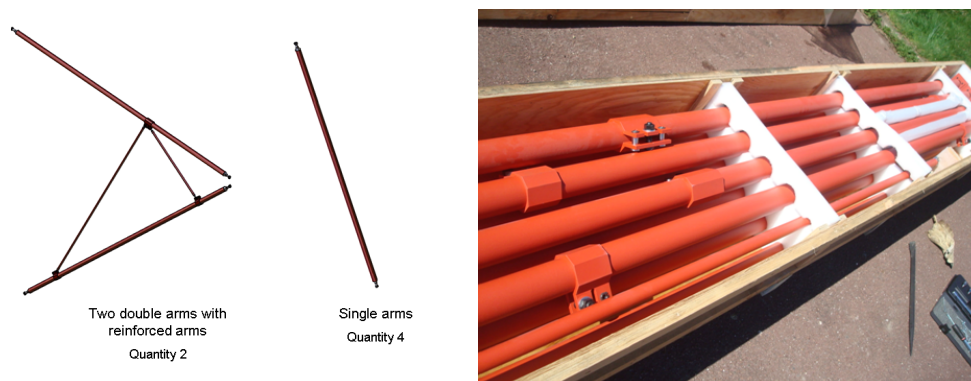


**Figure 4.2** – CAD view of the Serrurier tubes of the MTS (left); shown in their transport crate (right).

- The MTS top dish, which is a machined and welded item with one arm connecting the camera support system bolted to the dish (see Figure 4.3). The top dish is shipped in a crate.

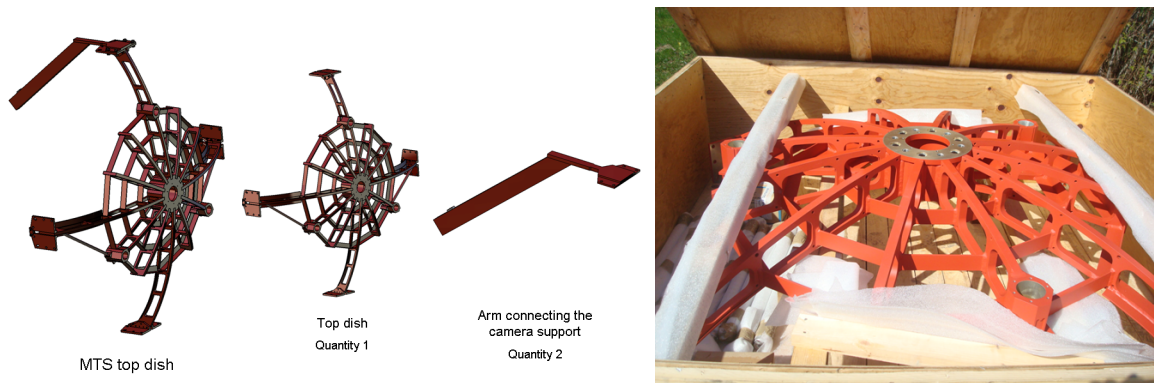


**Figure 4.3** – CAD view of the MTS top dish components (left); shown in their transport crate (right).

The M1 dish is composed of one central node, 6 main arms, 6 reinforcement plates and 6 plates to support the actuators (see Figure 4.4); it can be shipped as two halves.

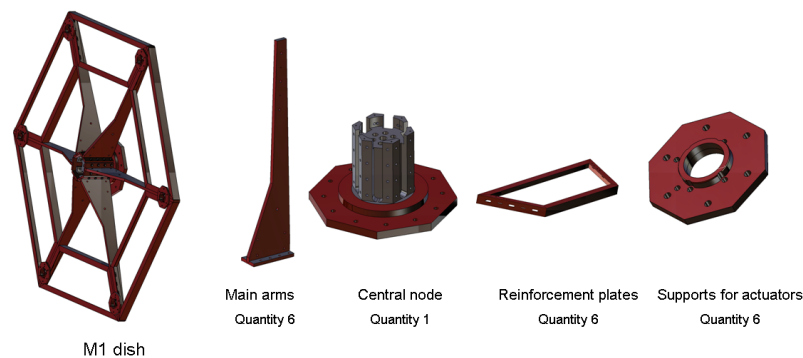


**Figure 4.4** – The elements forming the M1 dish.

The counterweight is composed of three sub-systems, a support structure and two masses. The main structure is machined in one piece. The mass and the moveable system are purchased and assembled in industry. The counterweight is shipped in one piece and delivered directly to the foundation on site.

The camera removal mechanism is composed of one arm, two reinforced tubes and a flange which interfaces to the camera (see Figure 4.5). The system is shipped as one piece and will be mounted on

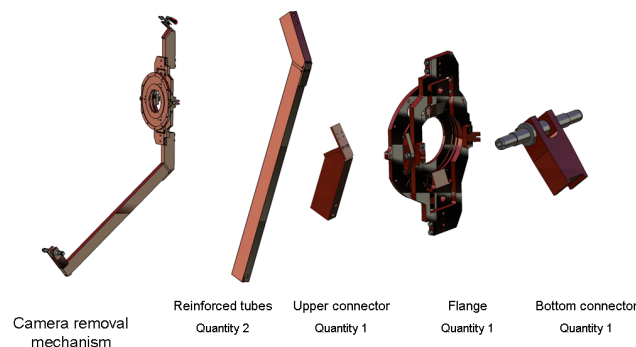


**Figure 4.5** – The camera removal mechanism elements.



the OSS in the integration hall.

The arms of the camera removal mechanism can be moulded for mass production. All these elements are manufactured in industry and reports certifying compliance with the specifications delivered for each module.

### *Mirrors*

The mirrors are the main elements of the telescope that may evolve between the prototyping and mass production phases. For the prototype, a manufacturing process has been developed using machining, polishing and coating of aluminium bulk samples. M1 has been produced as 6 petals and M2 has also been segmented to ease production. To prepare for mass production of M1 and M2, two options are being investigated.

1. Using the same process as for the prototype, but producing larger M1 petals, as described in section 2.1.3, and a monolithic M2.
2. Using glass technology to produce the M1 petals and/or M2.

At the end of the assessment phase, the best solution for the mirrors will be chosen. Both solutions are described here based on current knowledge.

#### 1. Metallic mirrors

The manufacture of metallic mirrors relies on three steps (machining, polishing and coating) performed by three different companies. The production phase M1 petals differ from the prototype M1 petals in that they are larger. The machining process may be improved and adapted to mass production by using moulding. This solution will be analysed during the assessment phase. Machine polishing will replace the manual polishing used for the prototype. The necessary equipment has been identified by the polishing company and will be purchased for mass production. Larger coating chambers will be used to allow the coating of the larger mirrors. The changes in the mirror manufacturing process will help to decrease the cost of the mirrors and improve their quality.

The prime contractor will have responsibility for mirror production.

M2, produced in the prototype phase as six petals, will be monolithic in the mass production phase. This monolithic production is technically feasible, and the cost of the larger bulk sample is compensated for by the simplified manufacturing procedure.

The changes in the M1 petal and the M2 manufacture will require a redesign of the rear supports of these mirrors, but similar structures will be used to those of the prototype mirrors.

#### 2. Glass mirrors

An alternative technology for the construction of the GCT mirrors using glass is being investigated with the company Glyndwr Innovations in the UK. First tests have now started. These involve the manufacture of a ceramic mould with a radius of curvature appropriate for M2 (about 2.1 m). BK7 glass of thickness 6 mm is then slumped onto this in an oven at high temperature. The mould contacts the reverse face of the mirror, allowing the reflecting surface to be polished before slumping to ensure the optical quality of the mirror. Current studies are dedicated to perfecting the slumping process and producing test mirrors for mechanical and optical testing. These will be coated with aluminium and quartz. If the tests prove this technique is suitable, both M1 and M2 could be produced in this way for the GCT pre-production and production telescopes. (These developments also have the potential to provide useful additional manufacturing capability for other CTA mirrors.)

The actuators will be purchased from industry. Three actuators are required to align each mirror unit. The same actuators are used for the M1 petals and the secondary mirror. A report certifying the compliance of the actuators with the specification must be produced by the manufacturer.

The actuators are the interface to the support structure of the mirrors. The M1 petals are shipped with their actuators, fixed to the triangular support structure. The secondary mirror is mounted on the MTS top dish via three actuators in the CTA integration hall.

### *Optical Tests*

Both M1 and M2 are produced in industry. Tests must be performed to validate their PSF and reflectivity. These can be performed either in industry or in a suitably equipped lab, e.g. the CEA IRFU or a CTA Mirror Test Facilities lab. The tests consist of:

- Verifying the roughness and shape of the mirror after the machining and the polishing.
- Measuring the PSF after coating.
- Measuring the reflectivity.

The M1 petals can be tested in one day; two further days are required to prepare the test. M2 can be tested in one and a half days.

After validation of the mirror quality, M1 and M2 are transferred to the prime contractor where the M1 petals are mounted on their triangular support structure with the actuators. This takes 2 days for two technicians. (Two people are required for mirror handling as the petals weigh 42 kg.) After assembly of the M1 petals and their supports, tests of the actuators are performed. These require three days with two technicians. The M1 petals are then shipped to the CTA site. Three mirrors are transported together in their shipping boxes. M2 is shipped alone. The M2 actuators are shipped separately in a protective case to prevent corrosion or other damage. M2 is mounted on the top dish that is shipped with the other GCT mechanical systems. The M2 actuators are attached on the CTA site in the integration hall; this task requires two people working for 1 day. M1 and M2 are shipped in 40 foot containers with appropriate protection: they are placed in a housing and box equipped with accelerometers to monitor shocks during the shipment.

### **Telescope Lab AIT WBS 03.6G.03.06**

In the Pre-production phase, the very first GCT structure will be completely assembled in the prime contractor's integration hall. The aim is to test the in-house assembly procedure and validate the design, particularly with regard to any changes that occur during the assessment phase.

After verification the telescope will be dismantled and sent to the CTA site.

### **Camera Assembly WBS 6G.03.05**

The mass production of the GCT cameras will begin with the upfront procurement of all components as single orders. Companies will be provided with manufacturing details where appropriate, and in some cases test rigs to verify camera components where this is efficient. One such example is the preamplifier boards, in which case it is more efficient to do test for and correct faults in the company than to ship items back and forth.

Once enough components are procured to produce 3 cameras, the sub-assembly production will begin at the GCT institutes. The mapping of this work with the institutes is shown in a RASCI matrix in Figure 4.10.

Each institute must be set-up to perform the production phase sub-assembly work prior to the production of the first camera, which may require specific test equipment. This preparation work is planned for in the WBS.

Upon receiving the components for a given sub-assembly, a participating institute must inspect, catalogue and store the items. Following this, any assembly of components and commissioning work is done. This will range from simply connecting cables, or building mechanical assemblies, to uploading and verifying firmware. Qualification work on some items will be needed to ensure functionality. A manageable sub-set of some sub-assemblies, such as the photodetector assemblies (consisting of the photodetector itself and a base PCB) (WBS 04.6G.05.02), will undergo performance testing. Documentation detailing the sub-assembly manufacturing process is required beforehand and must be followed as part of the quality assurance plan. Further documentation detailing the results of the sub-assembly production and

any testing will be filled in, following a template. The production of the sub-assemblies for 3 cameras is scheduled to take 8 weeks.

Following the sub-assembly production, items are shipped to each of 3 AIT sites (one per camera) in the UK, NL and Germany. There the items are catalogued upon receipt and inspected (WBS 04.6G.05.07.02). Approximately 1 week is allowed for the shipping and handling process. Assembly of the camera takes place following clear documentation in the following order according to WBS 04.6G.05.07.03:

- WBS 04.6G.05.07.03.01: Secure front-end buffers to TARGET modules with cables (with adhesive if appropriate).
- WBS 04.6G.05.07.03.02: Integrate all electronics with internal mechanics.

The fully integrated camera is time-consuming to access and electrically debug; thus once the electronics are integrated, basic electrical tests take place.

- WBS 04.6G.05.07.04.01: Install camera without external enclosure in bench-test facility.
- WBS 04.6G.05.07.04.02: Perform bench-top power-on tests with electronics out of enclosure.

At this point there is an opportunity to replace faulty parts. Then the assembly continues to produce the fully integrated camera:

- WBS 04.6G.05.07.03.03: Integrate lid assembly with enclosure.
- WBS 04.6G.05.07.03.04: Integrate internal mechanics and electronics with enclosure and thermal exchange unit.
- WBS 04.6G.05.07.03.05: Attach photosensors to focal plane.
- WBS 04.6G.05.07.03.06: Attach window to focal plane plate.

Once the full camera is available, commissioning and verification takes place:

- WBS 04.6G.05.07.04.03: Install full camera in test facility.
- WBS 04.6G.05.07.04.04: Perform full camera electronics and thermal tests
- WBS 04.6G.05.07.04.05: Perform full camera dark measurements
- WBS 04.6G.05.07.04.06: Replace any failed parts identified from tests with spares and verify

The above items all appear as WBS tasks (see Appendix B). At every stage of the production and assembly, components will be catalogued and the project progress and cost envelope will be followed by the GCT management (see the organigram in Section 4.2).

## Auxiliary Manufacture and Assembly

### **TCS cabinets and Power WBS 6G.06.01 and Network cabinets WBS 6G.06.02**

The auxiliary systems are largely purchased items that have to be integrated in the telescope structure. The most numerous are the items of the TCS which are integrated in the cabinets by the responsible GCT institute or by a company specialized in this assembly. The procurement and assembly process is as follows:

1. Purchase of the elements.

2. Integration in the cabinets.
3. Implementation of the software.
4. Validation of the behaviour either by tests at the responsible institute/company (for network and control command modules) or by certifying agencies such as APAVE (for electrical cabinets).

The cabinets are shipped in a dedicated housing to protect them from shocks and corrosion and are delivered to the integration hall to be mounted on the telescope structure; this step requires the installation of cables and cable supports.

Three technicians are required to assemble all the cabinets and the assembly of the TCS will take 9 days. The implementation of software takes one day and its test requires five days. A few hours are needed to prepare the shipment. The assembly of power and network cabinets takes two days each and tests require a further two days each. A few hours are needed to prepare their shipment.

### **Shelter WBS 6G.06.03**

The shelter is purchased from a company and shipped directly to the site in a dedicated container. Two shelters fit in a 20 foot container. The shelter is composed of four items: arms, fabric, cabinets and sensors. The cabinets are shipped, integrated and tested by the company with the necessary certifications.

## **Assembly of GCT on site**

The assembly on the southern site is foreseen in two steps:

- Delivery of the tower, counterweight and shelter to the foundation. The tower will be directly mounted on the foundation.
- Delivery of the OSS, AAS, mirrors and auxiliary systems to the integration hall. In the integration hall the team will:
  - commission the AAS and verify its alignment;
  - finalize the assembly of and commission the OSS;
  - install the mirrors in the optical support structure and align the optics.

Working in an integration hall has several advantages:

- If a problem has arisen during the shipment, repairs can be carried out using the tools in the hall. The verification of the AAS alignment can be performed using the optical instruments which are permanently fixed in the hall; the accuracy of their alignment is then guaranteed.
- The assembly of the OSS is made with simple equipment which does not require a technician with specific skills (use of a hoist rather than a crane).
- The alignment of the mirrors can be made without installing tools on the foundation.

If using an integration hall is not feasible, the assembly of the telescope will be done completely on the foundation. The planning of the shipping procedure will be altered to better match this scenario. The process of assembly will be similar to the above.

### **Telescope On-Site AIV WBS 6G.07.01**

The AAS, OSS, mirrors and cabinets are delivered to the integration hall for commissioning, final assembly and alignment. These steps can be carried out on the foundation if needed.

The commissioning of the AAS includes:

1. Verification of the AAS modules.
2. Alignment tests to verify that no damage has been caused by the shipment.
3. Verification of the greasing of the motor shafts, cabling and testing of the motors.

The AAS can then be transferred to the foundation and mounted on the tower.

The alignment of the AAS requires a precise laser tracker with the required sensitivity. Commissioning and greasing of the motor shaft and verification of the alignment takes 5 days for one person.

All mechanical parts of the OSS are delivered in crates. The assembly steps foreseen for the production phase are similar to the process developed on the Paris site for the prototype. Because the procedure is not complex and the size of the assembled MTS makes shipping as one piece awkward, the assembly of the MTS is done on the CTA site. The M1 rotation system is always assembled in industry (one person can assemble the system in half a day). The elements are delivered to the OSS area in the integration hall, near to the AAS commissioning area. (The AAS and OSS are assembled simultaneously). After checking that no damage has occurred during shipment, the OSS is assembled. This is done with the axis vertical, which simplifies the alignment of the mirrors (see below for the mirror assembly). The OSS is integrated on the “big foot” mount (as used for the AAS) which has the same interface as the bosshead to which the OSS will be fixed on the telescope.

The assembly sequence is:

1. Integration of the MTS bottom dish (assuming separate shipping because of the available container size):
  - (a) mount the lower flange on the big foot;
  - (b) assemble the two parts of the bottom dish with the upper flange;
  - (c) add the reinforced bars to the bottom dish;
  - (d) connect the ball pivots to each part.
2. Integration of Serrurier tubes:
  - (a) equip two of the lateral arms with their reinforcing tubes, repeat for the other two lateral arms;
  - (b) add the connectors to the two pairs of arms and the four single arms.
3. Mount the rotation system for the M1 dish.
4. Mount the M1 dish:
  - (a) attach the main arms to the central node;
  - (b) fasten the reinforcing plates between the arms;
  - (c) mount the supports for the actuators.
5. Mount the rotating system on the M1 dish.
6. Attach the M1 dish to the MTS bottom dish.
7. Fasten the Serrurier tubes to the MTS bottom dish.
8. Mount the MTS top dish on the Serrurier tubes.
9. Install the cabling inside the structure and some of the cabinets (see integration of auxiliary section below).
10. Integrate the optical elements necessary for the optical alignment.

Steps 1, 2, 3 and 4 can be realized in parallel in the integration hall. The equipment needed is:

- crane and slings;
- dynamometric torque wrench;
- the hoist in the integration hall.

During assembly, some tests are performed in order to check the distances between sub-systems and the coarse alignment of the mirrors, These require two persons and takes one day. The systems tested are:

- The MTS bottom dish: alignment of the dish with an inclinometer to ensure it is horizontal.
- The Serrurier arms: the test consists of measuring the the length of the Serrurier tubes from the bottom dish's connectors to the top dish's connectors, comparing these to the specification and adjusting their length if required. The tubes are manufactured to a tolerance of  $\pm 1$  mm.
- The MTS top dish: test of the alignment of the dish using the inclinometer, measurement of its height above the bottom dish.
- The rotation system interfacing the M1 dish and MTS bottom dish: the rotation of the dish is tested before adding the MTS arms.
- The bottom dish and MTS dish are aligned using laser targets places in their centres, this step ensures the coincidence of the mechanical and optical axes and is the first step in the mirror alignment procedure.

After these tests, the assembly and integration of mirrors and their optical alignment is possible. The manpower required for the commissioning of the OSS is two persons for two days. The assembly in the integration hall requires two persons for two days. The coarse alignment of the OSS needs two persons for one day.

The mirrors are delivered to the OSS area of the integration hall. It is first verified that the shipment did not damage the mirrors. Then:

1. The M1 petals are mounted on the M1 dish using the rotation system to ease access. The petals can be safely handled two people, a system of slings can be used as an aid if required.
2. The M1 petals are aligned using the optical elements placed inside the OSS and using the optical measurement equipment in the integration hall.
3. M2 is fixed on the MTS top dish: the mounting is done by putting M2 on the integration hall table with the rear surface pointing upwards. The MTS top dish is then positioned above this. Using the crane and the support rings at the back of the MTS top dish, the top dish is positioned on the mirror and fixed via the actuators.
4. The MTS top dish is then fixed to the Serrurier arms using the hoist in the integration hall.
5. M2 is aligned.

The equipment needed is:

- The hoist in the integration hall.
- Optical systems for the mirror alignment (source, targets, telemeter, computer to compare with Zemax theory...).
- Working platform at a maximum height of 5 m.

The optical alignment is simplified if light levels in the integration hall can be reduced.

In the integration hall, the commissioning of the six petals requires 1 day and the alignment can be done in 3 days by two people.

The commissioning of the secondary mirror can be done in one day by two people. Mounting the secondary on the MTS top dish requires two people for one day, including the test of the actuators. The alignment of M2 can be done by two people in one day.

The cabinets (telescope control and command and power and network cabinets) are shipped to the integration hall for commissioning. This requires five days. The verification of the power and network cabinets requires 2 days each (these tasks can be done in parallel) and one person is needed for each task. The cabinets are tested progressively during the assembly.

### **Telescope on site integration WBS 6G.07.01.03**

The tower, counterweight and shelter are delivered to the foundation and the tower is mounted on the foundation. The alignment of the tower must be adjusted using the stud anchors and verified using an inclinometer. Two people are required for the assembly and alignment. Both tasks can be done in one working day.

Once the AAS has been commissioned and the OSS equipped with M1 and M2, both systems are transferred to the foundation. The final assembly on the foundation is done with the GCT pointing vertically, in the following steps:

1. Integration of the AAS on the tower. This can be done in 50 minutes by 4 people using a crane.
2. Integrating the OSS on the bosshead. Four people can mount the structure in 90 minutes. (This job can also be done by two people, but takes twice as long.)
3. Fix the counterweight and balance the telescope. The counterweight can be mounted using a forklift truck and a cherry picker (Figure 4.7). The manpower required is three persons (one driving the forklift, one guiding the counterweight and one fastening the bolts). The mounting and verification can be done in 175 minutes (including 75 minutes for the fixing of the weights).
4. Cabling of the cabinets.
5. Rotation of the telescope to the horizontal.
6. Installation of the camera using the camera removal mechanism.

The two first steps require a specialised crane driver and two persons from the team to manage the assembly with two technicians. These steps take two days. The integration of the cabling is done by two technicians (this simplifies the threading of cables) in six days, including all checks. The integration of the camera can be done by three people, one from the camera team, one from the telescope team and one additional technician; the operation takes half a day.

The shelter is shipped to the foundation. It is assembled once the telescope is completely mounted to simplify access to the telescope. (If no assembly hall is available, this sequence may be redesigned.) The integration process is:

1. Fix the shelter to its 3 mounts on the foundation.
2. Install the arms.
3. Install the fabric.
4. Install the cabinet, motors and sensors.
5. Test the opening and closing of the shelter.



**Figure 4.6** – The assembly of the telescope - From top left to bottom right: AAS removed from the integration hall by a forklift, transfer to foundation and mounted on the tower; the bottom line shows the integration of the OSS on the bosshead of the AAS.



**Figure 4.7** – The mounting of the counterweight on the prototype.

Two people are needed for the assembly and test of the shelter. The operation takes 1.5 days for the assembly and at most half a day for the test.

Once the telescope is mounted and integrated, the test phase can be initiated in order to:

- Verify the optical alignment.
- Verify the TCS behaviour.
- Make the look-up tables (LUTs) describing the telescope's performance.
- Carry out first observations.



Once all the above have been successfully carried out, and all tests from the on-site test plan completed, the telescope can be used in the array and is handed over to the Observatory.

## 4.1.2 Procurement and Production

The objective of the GCT consortium is to construct 35 telescopes in two phases, 3 telescopes in the Pre-production phase and then a further 32 telescopes in the Production phase. The procurement and production for these two phases will start following the current Prototyping and assessment phases.

### **From the mechanical and optical prototype to the production design: the assessment phase**

Following the Prototyping phase is a phase of assessment in which the prototype design may be slightly modified using the results of the tests performed at the end of the Prototyping phase and in which the company chosen to be the prime contractor will be involved. Some potential changes are described above. After this assessment phase, the design of the GCT opto-mechanical structure will be complete and new mechanical drawings will be finalised to start the call for tender.

### **Procurement by call for tender**

The procurement of the GCT will be managed by a call for tender organised with bonds. The technical specifications detailed in the call for tender will rely on the results of the assessment phase and previous discussions with companies. The first bond is fixed and corresponds to the pre-production phase, i.e. the construction of three GCTs. Then the call will have conditional bonds, each of them for a batch of telescopes, in order to split the production according to the funding profile that the GCT institutes receive, which may be spread over a period of time.

The production is split, following the WBS, into mechanics, optics and auxiliary systems. Procurement will be managed in six main areas related to the main systems of the telescope:

- Procurement of the tower.
- Procurement of the AAS: the AAS is manufactured and assembled in industry, the motor shafts are mounted but are shipped separately.
- Procurement of mirrors M1 and M2: M1's petals are mounted on their support structure with their actuators and M2 is shipped separately.
- Procurement of the OSS and counterweight: these are shipped in separate crates and assembled on site.
- Procurement of the TCS: the cabinets are integrated in industry, the software is implemented in industry.
- Procurement of the shelter.

The prime contractor will have the responsibility of organising and overseeing the manufacture and shipment of the telescope components.

### *Procurement in Pre-production phase*

In the Pre-production phase, the procurement will be split into two parts. The first is focused on the production of the first telescope. Because some changes may have occurred in the design, the first GCT will be completely assembled in industry by the prime contractor to test all the interfaces and the mounting procedure. Once this is validated, the production of the two other telescopes will start, while the first is shipped to the CTA site to be assembled, commissioned and tested.

The production of the second and third telescopes does not involve the assembly of the telescope in the prime contractor's integration hall. Only the AAS system is assembled and aligned in house. All the other systems are assembled in the CTA integration hall.

### *Procurement in the Production phase*

Between pre-production and production, there will be about two months to organize the new purchasing

round (use of the second bond of the call for tender). This period can also be used to organize a meeting between the AIT teams on site and the manufacturers to verify that all processes are working well.

The production of the final 32 telescopes and spares will then start. The production, shipment and assembly on site are organised in batches. Eleven batches are required to construct all the GCTs, with one additional shipment for the spares.

#### **Procurement and shipment of the Tower**

The tower is manufactured in industry. The tower has to be transported to the prime contractor who will manage the shipment to the CTA site. The manufacturing of the first tower takes three weeks, and then a tower can be delivered every two weeks. The tower is shipped directly to the foundation for mounting.

#### **Procurement and shipment of the AAS**

The production of the AAS is managed by a lead contractor who assembles the complete AAS. During mass production, an AAS (structure and drives) can be delivered to the prime contractor every 2 weeks. The purchased items, mainly the slew bearings, worm gears and motors, are delivered in series every month. The procurements for these items can be done according to the following schedule:

- Slew bearing: delivery of 6 every month.
- Worm gear: delivery of 6 every month.
- Motors: delivery of 12 every 14 weeks.

In order to prepare them for mounting, the slew bearings have to be measured and two of the series paired for the elevation drives. The prime contractor may have to do additional characterisation of the bearings in order to identify the pairs. Almost one month is allowed for this; this is the delay between the delivery of the bearings and the delivery of the AAS structure before the start of assembly.

The assembly requires 20 days with one week to align the system. The alignment can be done in parallel with the assembly of a second AAS.

The first shipment is planned six months after the beginning of manufacturing. The shipments are organised regularly each three months as three AASs are manufactured, assembled and aligned. The container for these shipments is 20 feet long and customised as it requires rings in the roof and the floor to fix the AAS structure in place to ensure there is no damage during the transfer. To spread the stress, the AASs will be fixed to three corners of the container, and the fourth corner will be used for the counterweight. The centre of the container will be used to ship one secondary mirror and the cabinets.

The shipping and unloading take one month, so the container will be available for a new shipment every 3 months (one month margin allowed) which corresponds to the duration needed for the assembly of 3 AASs. On site, the commissioning of one AAS in the lab takes five days (commissioning, greasing, mounting the motor shaft and verification of the alignment), then it is mounted on the tower in one day by two persons, so in three months the three AASs can be verified in the lab and mounted on the towers that have already been installed on the foundations.

#### **Procurement and shipment of the OSS**

The construction of the OSS can be shared over several companies and consists mainly of machining and the purchase of connectors. Only the rotation system interfacing the M1 dish and the MTS bottom dish has to be assembled before shipping. The first of the OSS batches will require about 1 month to produce, but after this every three weeks an OSS can be delivered to the prime contractor. Given this, three completed OSSs can be shipped at the same time.

#### **Procurement and shipment of mirrors**

The procurement of the mirrors starts slightly before the Pre-production phase. This ensures the procurement schedule fits with the planning of the mechanical production. The manufacturing of mirrors requires four companies, one for machining, one for polishing, one for the coating and a further to carry out optical tests before shipping. The procurement of M1 takes 76 days. The planning depends on the manufacturing process and will be completely defined during the assessment phase.

### **Procurement and shipment of the Telescope Control System**

The TCS is the software and hardware required for the safe control and movement of the telescope. The main items that must be purchased are the cabinets, modules, sensors etc. The lead time for some of these purchases is a maximum of eight weeks, so the procurement of these items is not difficult. This procurement will be organised at the end of the Pre-construction phase, because it depends partly on GCT labs involved in the purchase and the assembly of the modules in the cabinets. The cabinets will be put together in industry. The implementation and test of the software will be managed by the GCT collaboration. The time required to assemble all TCS cabinets for one telescope is one week in industry. The foundation cabinet takes the longest, requiring about 3 days, whereas the cabinets in the structure require only one day. The company can test only basic functionality. The implementation of the software, which can be done by either one GCT lab or at the CTA integration hall, requires 1 day. Testing the cabinets requires one week. The cabinets for all three telescopes can be shipped at the same time as the opto-mechanical structure.

### **Procurement and shipment of shelter**

The shelter is composed of three different items that can be shipped separately and assembled on site. The procurement, the shipment, and the installation is managed by the prime contractor. The first shelter can be manufactured in 3 months; during mass production the shelter can be manufactured more quickly. The mounting of the shelter will be done after the complete installation of the GCT in order to simplify the mounting of the structure. Three shelters can be mounted every 3 months. To ease shipping, the installation of the shelter can be delayed in order to mount the shelters once half the telescopes are mounted. The mounting of the shelter takes 2 days.

### **Procurement of Camera Mechanics**

Camera mechanics can be procured from one of several companies and will be integrated at a GCT institution. All sets of mechanics will be procured upfront, to minimise cost. It is expected that the procurement of all mechanics will take no more than 6 months.

### **Procurement of Camera Photodetectors**

Photodetectors for the camera are the largest single cost, equating to approximately half the entire camera cost. They have a long lead time and require testing of samples and negotiations prior to placing an order. The testing of samples from different suppliers culminates in a milestone denoted 'Production phase photodetector choice made'. It is hoped that common photodetectors will be used with other CTA sub-systems, and that CTAO will negotiate a framework agreement with the suppliers(s). Such an agreement would allow funding from multiple agencies to be used to purchase the photodetectors at the same cost. Photodetectors for all cameras will be ordered upfront, including spares and possible upgrades for the pre-production cameras. It is expected that the delivery of all photodetectors will take no more than 6 months.

### **Procurement of Camera Electronics**

PCB manufacture will be done upfront for all cameras. The lead time for PCB manufacture is short, and it is expected that all PCBs can be produced within a few months. To avoid problems with import duty and tax, only manufactures in Europe will be used. Enough PCBs will be ordered for spare cameras, with an additional few percent of spare boards. Extra active parts, such as op-amps, will be procured at the few percent level to mitigate against obsolescence.

### **Procurement of Camera Auxiliary Systems**

All procurement is done by way of contracts negotiated with industrial partners. Chillers and PSUs from the pre-production phase will be utilised. All procurement is done upfront, but delivery may be in batches. Items will be delivered directly to the CTA site.

## **4.1.3 Logistics**

The logistics of shipments to the CTA site are coordinated with the CTAO. Container sizes and shipping requirements will be discussed and agreed between the CTAO and the GCT project prior to the pre-production phase. Shipping to the CTA site will take place in batches of 3 telescopes at once, and 3 cameras at once. Due to the small size and low mass of both the camera and the telescope, no

significant challenges are anticipated.

Internal logistics are also required between GCT institutes. In particular:

- The shipping of camera components from industrial partners to GCT sub-assembly institutes. For items with a reasonably short lead time, such as PCBs, it is expected that the components for all GCT cameras will be delivered in a single batch to the GCT institute in question. For items with longer lead times, such as the photodetectors, delivery will take place in several batches.
- The shipping of sub-assemblies between GCT institutes for AIT into cameras. Sub-assemblies will be produced in batches for 3 cameras. These 3 sets of items will then be sent to 3 AIT sites.
- If M1 petals are produced using glass technology, the production may be located in the UK. The petals will then have to be transferred to the relevant company to be mounted on the support structure and fixed to the actuators.

On-site logistics are required for the storage and qualification of assemblies, including a large assembly hall and a dark room with a calibration light source.

#### 4.1.4 Integration, Testing and Commissioning

Integration, testing and commissioning plans are outlined for the production phase. The starting point for this is assumed to be post-assembly as described in Section 4.1.1. For the camera, this is the point at which the camera is delivered to the CTA site. For the telescope mechanics, optics and auxiliary systems, this is the point at which items arrive on site and have been assembled into a telescope on the foundation.

Each system is commissioned in the integration hall or on the foundation (tower and counterweight). To minimise delays, cost, and schedule overruns on site, most critical testing is undertaken at the manufacturer's prior to shipment. Hence:

- For components that will be directly used on the telescope (cables, connectors etc.) no tests will be performed on site, but the company will provide a document that demonstrates their compliance with the relevant specifications and ISO norms. Some samples taken randomly will be kept for further investigation in case of failure.
- For assemblies or complex components, preliminary tests will be performed at the plant before shipment to the prime contractor. This includes the mirrors (inspection), the electronics (running tests) and the mechanical structure.

Once the telescope is mounted on site, tests will be performed to validate the compliance of the GCT with CTA requirements. These have the aim of verifying the two main scientific requirements: the optical and tracking performance of the telescope. The test plan will detail the tests to be done and the methods to be used and will address safety requirements first, then the science performance and finally the environmental requirements.

In each case, the sequence of tests performed is of increasing complexity and risk with the least complex and lower risk tests being performed first. This prevents unforeseen failures during high risk tests (such as the emergency stop) from delaying the overall test schedule.

The minimum level of acceptance is defined as the compliance of the telescope with CTA requirements, and the safety requirements defined by CTA, the host country and the country in which manufacture took place.

The test plan document includes a compliance matrix which details the kind of test (inspection, analysis, demonstration...) and where they must be undertaken. Specific documents will detail the tests to be done, the equipment needed and the skills required.

Once the telescope mechanics and optics have been assembled on the telescope foundation, the camera can be integrated. Upon arrival at the CTA site, the GCT camera will undergo basic tests in the central building before on-telescope deployment. Integration of the camera into the GCT system begins with the completion of stage-1 telescope commissioning, with a safe, controllable and aligned system in which to install the camera. The chiller and PSU are installed first, attached to the telescope structure and power and data connections made. Installation of the camera itself involves connection to the mounting point via three bolts and lifting from ground level into the focal plane using the camera removal system. Connection of the power and data cables and cooling pipes can then occur.

Following the complete telescope build and camera integration, the telescope will be tested for functionality and safety.

#### *Safety and Functional Tests*

The first tests with the telescope and camera are to ensure proper functionality and human and instrument safety. This is provided through both hardware and software mechanisms.

- Human safety: during the maintenance of the telescope, movement is prevented by sensors and/or by mechanical pins. These systems will be tested one by one, including the “mushroom” safety switches.
- User control: all user inputs will be verified in software to be within the authorised range. All user dialog boxes will be tested.
- Telescope design: the telescope has been designed with features to prevent injuries arising from the moveable elements of the telescope. These will be tested.
- Movement range: The allowed range of movement and all associated drive parameters change according to the telescope mode to reduce to the minimum the possible movement. A verification of the setup file according the telescope mode will be performed.
- Electrics: Visual inspection will be done when the cabinet is powered on and electrical safety will be verified (grounding, no electric discharge).
- Telescope software:
  - Any communication problems between ACTL and the telescope must not create unexpected movement or behaviour of the telescope. The capability of the software to maintain the telescope in a safe state despite bad data will be tested.
  - The software will provide and save all the information about the health of the telescope (housekeeping) and its displacement. The user will be informed of unexpected values.
  - The telescope modes have been designed so that any unexpected error or PLC failure places the telescope in a safe state. The same occurs if there is no communication with ACTL during one minute. These situations will be tested.
- Camera: All aspects of the camera (PSU and chiller control and operating states) will be exercised using a standard verified piece of software to stress the system in a pre-defined way. The CTA array control software will then be used to run through the camera state machine to verify state changes and ensure that no unexpected risk to human or instrument safety is likely when operating the camera.

#### *Performance Tests*

The performance of the telescope for CTA can be split into the following:

- Optical Performance:
  - The reflectivity of the mirrors will be individually measured with a test bench at the CEA/IRFU, by a commercial company or by the CTA MTF group.
  - The PSF size is measured on axis and at the edge of the FoV just before mounting the camera. This is done for different telescope elevations to determine the behaviour of the PSF with elevation.

- The field of view: several images of the sky will be taken using the camera to determine the real size of the FoV.
- Telescope Performance: The movement capabilities, which include fast displacements and the tracking mode, will be tested. For these tests, it is assumed that the LUTs are available.
  - The maximum speed will be tested by performing several pointings. Acquisition of images of the sky will give the accuracy of the movement.
  - The time taken to return to the parking position will be tested.
  - The emergency stop will be tested by simulating a power supply failure.
  - The tracking performance will be tested by following a star on the sky at different latitudes to encompass a large range of speeds.
- Camera Performance:
  - Pointing: Data taken with a slow-signal monitoring chain will be used to confirm/refine alignment. If necessary this will be verified with a CCD camera (to be installed if and when needed) by projecting images of stars onto the camera lid.
  - Read-out functionality: First data is taken with the lid closed until normal function is established. Cosmic ray observations (zenith pointing) will then be taken with continuous LED flasher events, to establish proper function of the camera.
  - Hardware performance: Once proper functionality is demonstrated, the expected performance (including trigger rate, image size and centroid distribution, recorded pulse widths and offsets) will be established.
- System Performance Tests: The performance of the telescope as part of the CTA array will be assessed. Functional tests will be made to verify that each telescope has been successfully integrated into the array.

#### *Environment*

A housekeeping database of the environmental conditions and telescope properties will be built up progressively with time to determine the behaviour of the telescope under different environmental conditions (wind, temperature etc).

#### *Additional mechanical tests*

Additional mechanical tests will be performed on a sub-set of telescopes during the Production phase. The purpose of these additional tests is to verify the dynamic behaviour of the GCT telescope structure and to determine the structural eigenfrequencies, eigenmodes, damping, dynamic amplification factors and dynamic stiffness. They also aim to verify that the assumptions made in the FEA are consistent with the real telescope structure. These tests have been described in section 2.3.7.

### 4.1.5 Decommissioning Outline

The breakdown of the telescope design into functional elements means that it can easily be dismantled. General steps are described below.

Firstly, the camera is removed; this is facilitated by the mechanism allowing access for maintenance. Once removed, the camera is transported to a workshop, either on-site or at a participating institute, to be dismantled and disposed of or displayed for outreach purposes.

Following the camera itself, the camera removal mechanism is dismantled; the connectors used allow easy dismantling.

The telescope is then positioned at zenith in order to dismount the counterweight.

The optical structure formed by the MTS and mirror dishes can then be dismantled using a crane. The MTS structure can then be dismantled. M1 and the M2 can be dismantled from their dishes; the interface used to mount the petals simplifies this procedure.

The AAS can be dismantled from the tower using a crane. It is preferable to keep the AAS system assembled.

The tower can then be dismantled if the foundation is made without additional cement around its base. If the same foundation system is used as for the Meudon GCT prototype, the studs will have to be cut to dismantle the tower. An easier solution for the foundation would consist of a reinforced concrete foundation with embedded studs onto which the tower is screwed. In this case the tower is dismantled by unscrewing the studs.

## 4.2 Management Structures

The GCT PBS, WBS, organisational structure and project schedule are described in this section.

The GCT consortium was formed from the GATE telescope team in France and the international CHEC camera team. The consortium's goal is to build 35 SST-2M telescopes as an in-kind contribution to CTA. The GCT currently consists of the following partners:

Adelaide University	Aix-Marseille Université / CPPM
Centre National de la Recherche Scientifique	Durham University
Max-Planck Institut für Kernphysik, Heidelberg	Nagoya University
Observatoire de Paris	Universität Erlangen-Nürnberg
University of Amsterdam	University of Leicester
University of Liverpool	University of Oxford

The GCT teams have agreed on a Declaration of Intent to formalise their collaboration. The initial organisation of the GCT is shown in Figure 4.8. The management of GCT activities takes place through two main groups. The Management Committee, led by the Spokesperson, is responsible for guiding and overseeing the project, including securing the required funds and manpower. The Technical Committee, led by the Project Manager, is responsible for the technical development of the instrument and, together with members of the Management Committee, who are typically formally responsible for grant money, manages the resources. Further details are given in Section 4.2.2.

### 4.2.1 Product Breakdown Structure

The PBS for GCT is shown down to the third level in Figure 4.9. Four of the five main branches address the instrument components, while the fifth is dedicated to the documentation required to produce, commission, verify and operate the telescopes.

The telescope Mechanical Assembly consists of the Telescope Base, the Optical Support Structure (OSS), the Alt-Azimuth System (AAS), the Camera Access system (the mechanical support and moveable arms that attach the camera to the secondary mirror) and the telescope Foundation (which will be specified by GCT, but provided by CTA as part of the infrastructure).

The Optical Assembly consists of the Primary Mirror Structure, the Secondary Mirror Structure and the Optical Alignment system required to align the telescope.

The Camera Assembly consists of the Camera Mechanics, the Photodetector Units (which are the photodetectors mounted onto electrical bases), the Camera Electronics, the Calibration System (including any items needed to locate the camera in the celestial coordinate system – i.e. pointing), the Camera Auxiliary System (PSU and Chiller), and the Camera Software. The extent and remit of this software depends on the project phase. For example, during prototyping, end-to-end software is needed, whereas in the Production phase, contributions to the global CTA software effort will be made. Software and firmware needed for low-level instrument control are included in the PBS at a level below that shown in Figure 4.9.

The Auxiliary System consists of the Slab Cabinets (mounted on the Foundation), the Telescope Cabi-

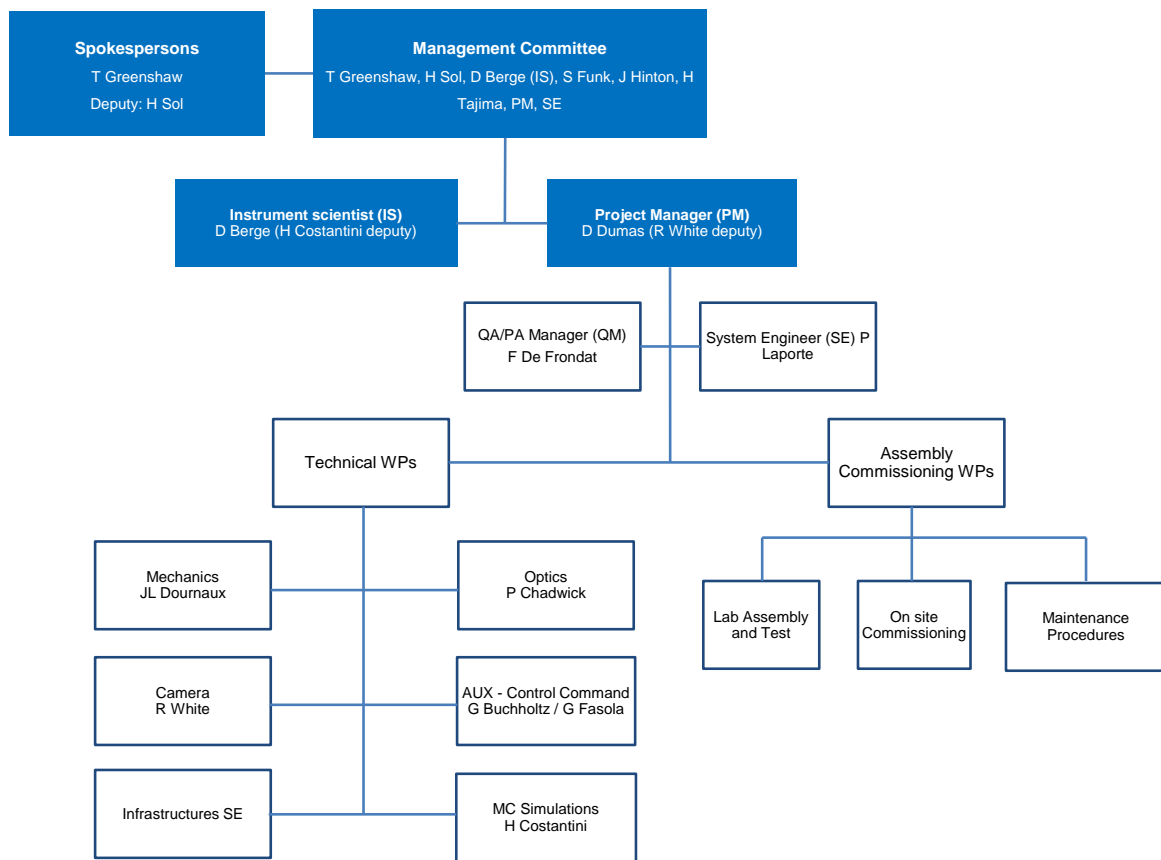


**Figure 4.8** – Top-level organization chart of the GCT consortium, including the names of people assigned to some of the organisational roles.



nets and the Shelter.

The full PBS can be found in Appendix A. The work involved in producing each PBS item is detailed in the Work Breakdown Structure (WBS), described in Section 4.2.3.

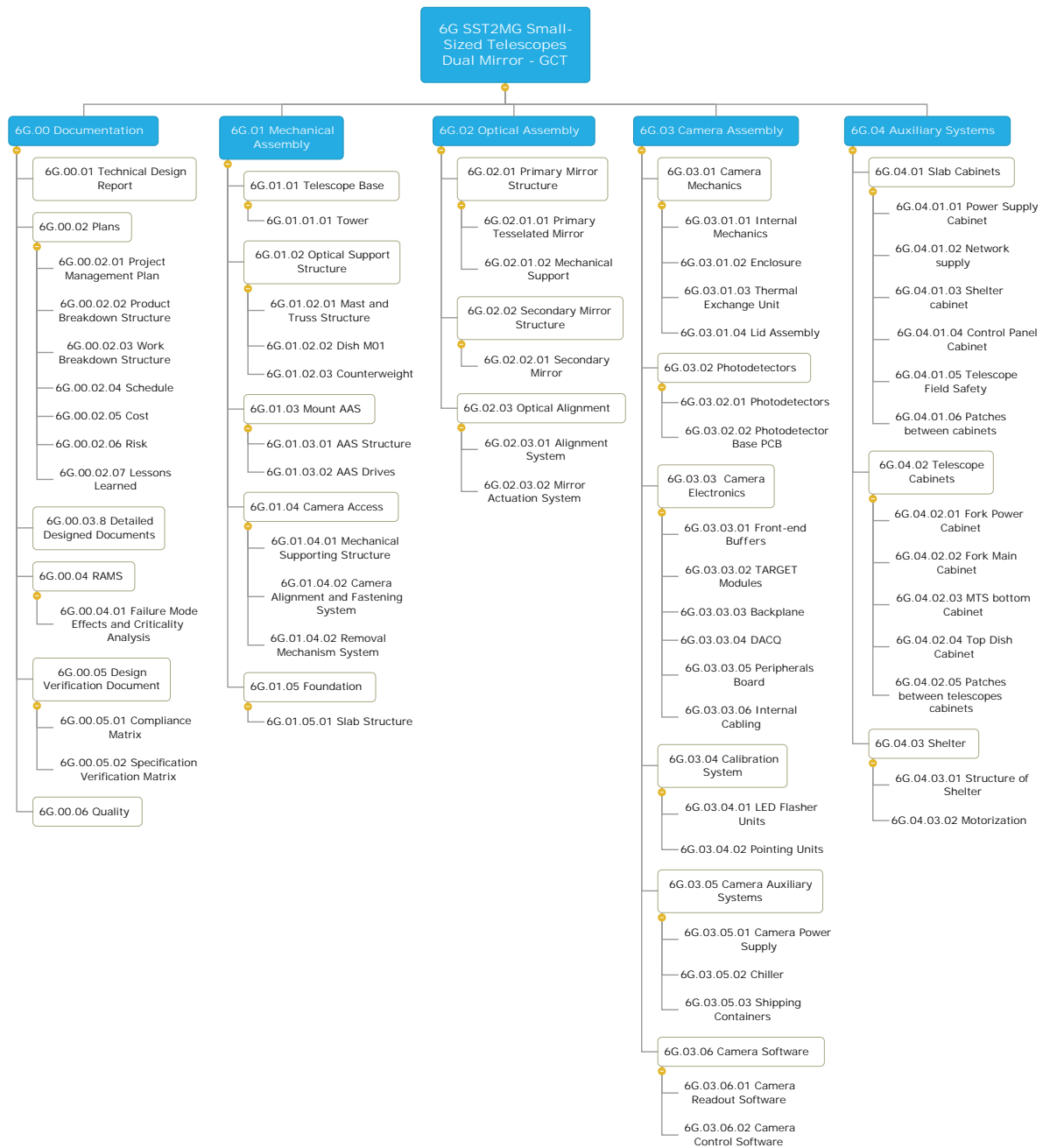


**Figure 4.9** – The GCT PBS is shown down to the third level here. The full PBS is presented in Appendix A. The full PBS spreadsheet is GCT\_PBS . x1 sm.



The GCT consortium will have a Management Committee formed of agreed representatives of each of the countries contributing significantly to the consortium. This Committee will elect, for a period of two years, the GCT Spokesperson, Deputy Spokesperson, and the Instrument Scientist. The Committee will furthermore appoint the Project Manager and Systems Engineer. These elected and appointed people will be ex officio members of the Management Committee (if not already members). The Management Committee will guide and oversee the construction of the GCTs. The Committee will strive to obtain consensus on all technical and organisational matters with respect to the design, construction and operation of the GCT array. The spokespersons are charged with organising the discussion and decision process. Where consensus cannot be reached, decisions will be taken by a simple majority vote. The work of the consortium will be organised in Work Packages (WPs). The scope of these will be decided by the Management Committee. Work Package coordinators will be appointed by the Committee in consultation with the institutes involved in the WP, for a period of two years.

The GCT organigram of Figure 4.8 shows the membership of the Management Committee and the Work Package coordinators as of the 29<sup>th</sup> October 2014. The membership of the consortium may change at any time, with the agreement of the Management Committee.

The GCT Spokesperson is responsible for the public presentation of the GCT project. The Deputy supports the Spokesperson in this role. The GCT Project Manager reports to the CTA Project Manager and is in regular attendance at the CTA Project Committee meetings, together with the Spokespersons. The Instrument Scientist is responsible for ensuring that the GCT design evolves in such a way as to maintain compliance with CTA requirements, working together with the GCT Systems Engineer and Project Manager through the V&V process.

A Technical Committee chaired by the Project Manager and consisting of the Instrument Scientist, Systems Engineer, Quality Manager and all WP coordinators is responsible for the technical deliverables of the project.

### 4.2.3 Work Breakdown Structure

The GCT WBS comprises three phases:

- Prototyping: Prototyping of the telescope and camera, culminating in the completed Pre-Production Phase design with detailed documentation and plans.
- Pre-Production: The production of 3 full GCT instruments, performance verification and installation on-site. Large amounts of preparatory work and documentation are included in this phase.
- Production: The production, verification, installation and commissioning of 32 GCT instruments.

Figure 4.11 shows the upper levels of the Prototyping (or Pre-Construction) Phase WBS. Work is currently focussed on prototype development and testing as described in Section 2.3.

Figure 4.12 shows the upper levels of the Production Phase WBS. Tasks are divided into eight main categories, covering all the work that must be done, from management through instrument production to on-site commissioning. The production of each instrument sub-assembly includes coordination tasks and travel. Upfront procurement is assumed (and specified at the lower levels) for the majority of items as single tasks.

Project management, systems engineering, quality assurance and coordination tasks are grouped together as a single Work Package and will be performed largely by the relevant individuals specified in Figure 4.8. Project management includes the management to be done by GCT members locally on grants, for example routine reporting to funding councils. This is necessary due to the distributed nature of the GCT consortium.

Monte Carlo simulations are included as a work package. The single GCT simulations carried out in this WP are all simulations that aim to understand and test the single telescope characteristics, such as the optics, the readout scheme, the charge reconstruction and trigger efficiency. Array simulations will

be performed to understand and optimise the performance of a partial and/or complete telescope array, testing different telescope layouts, analysis methods and observation modes. This work will be overseen by the Instrument Scientist and will happen in close cooperation with the Observatory.

The production of instrumentation takes place in four WPs: Mechanics, Optics, Camera and Auxiliary Systems. These WPs are responsible for the delivery of GCTs to the CTA site. Work done on the CTA site itself is contained in a final WP.

The Pre-Production phase WBS closely follows the Production phase WBS; at the level shown in Figure 4.12 they are identical. At lower levels, the Pre-Production phase WBS includes tasks for the re-design of the Production phase instrument (following Pre-Production experience), extended work on low-level firmware and software development, documentation and the preparation of training procedures.

The full WBS for all aspects and phases of GCT production is given in Appendix B.

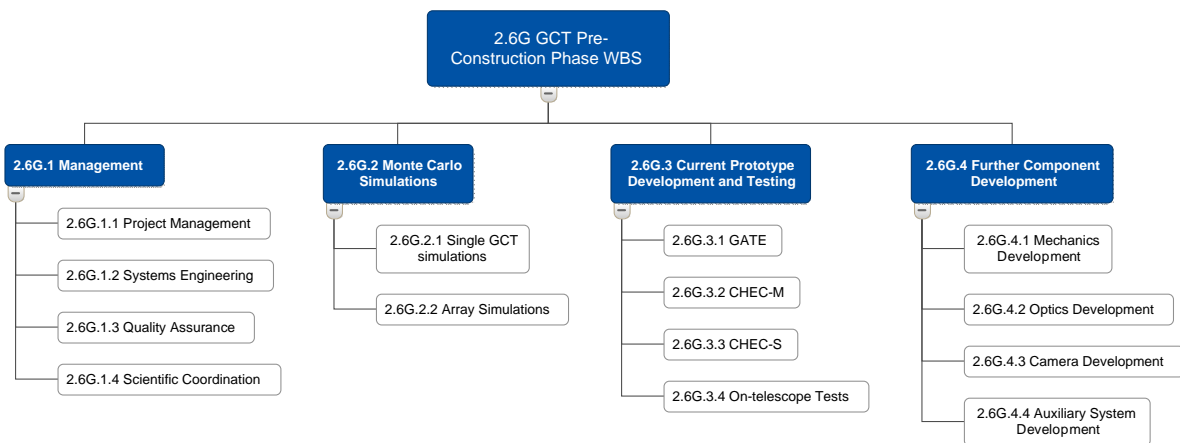


Figure 4.11 – The GCT Prototyping phase WBS, shown down to the third level. The full WBS can be found in Appendix B

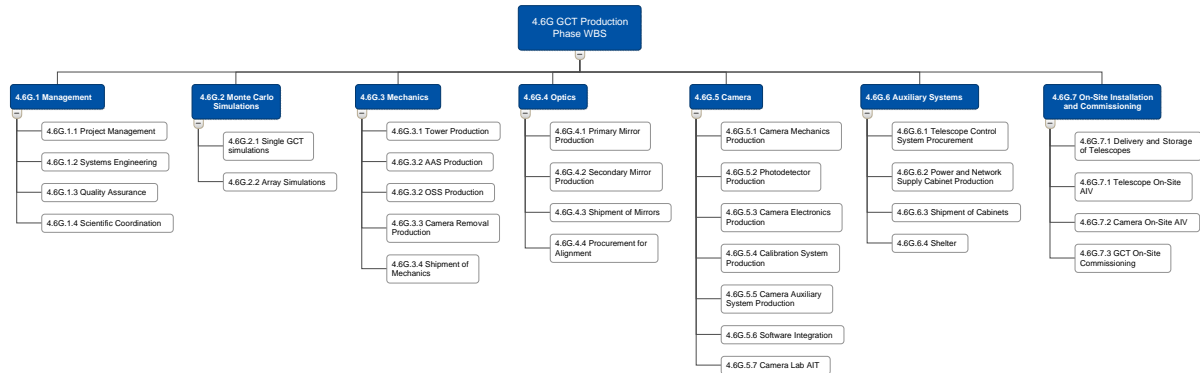


Figure 4.12 – The GCT Production phase WBS, shown down to the third level. The full WBS can be found in Appendix B

## 4.2.4 Schedule

After the completion of the GCT telescope and camera prototypes, a test phase will take place to validate the structure, the camera and the scientific performance of the telescope in order to prove compliance with CTA requirements. Following these tests, the mechanical structure may be slightly modified, either to improve the system performance or to simplify the production and assembly process. During this assessment phase, the manufacture of the pre-production primary and secondary mirrors will start.

Beyond CHEC-M and CHEC-S, further camera component prototyping is planned for items with a sub-optimal design and/or a design that does not meet the required performance. There will, for example,

probably be another iteration of the TARGET ASICs.

The Prototyping phase concludes with a design review and the finalising of the design of the GCTs for the Pre-Production phase.

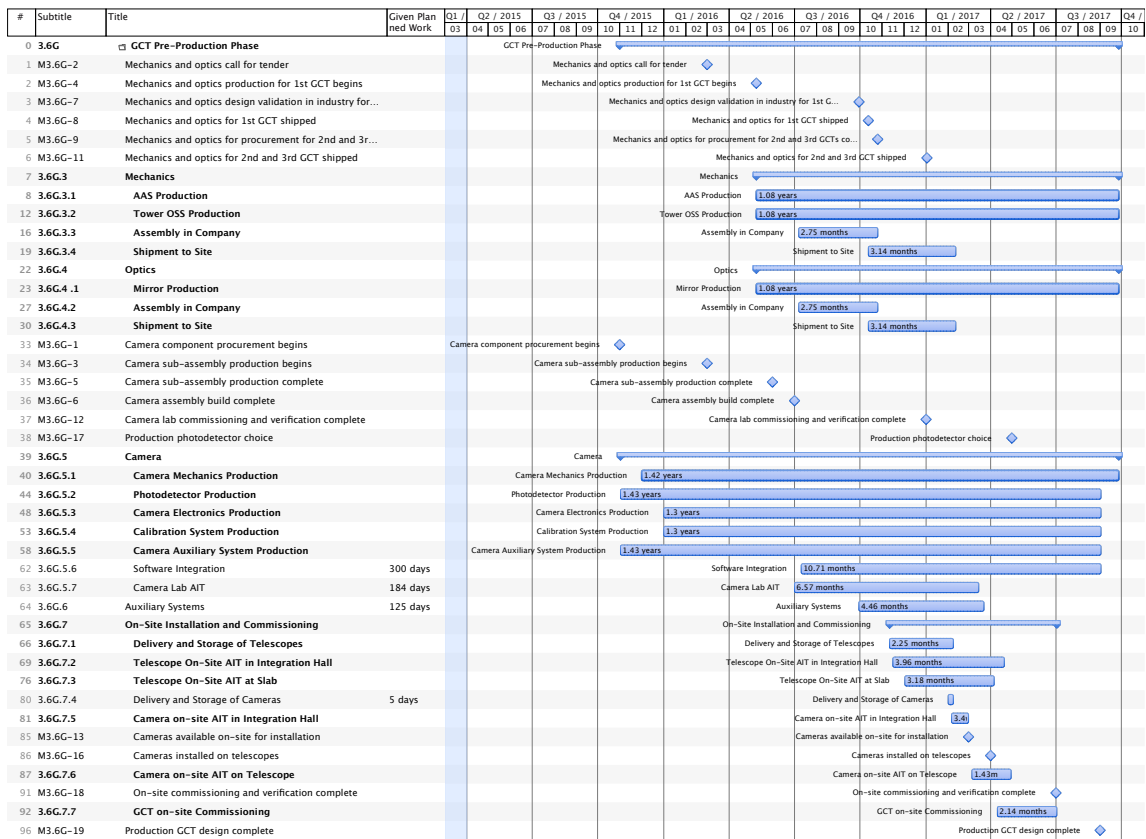


Figure 4.13 – The GCT Pre-Production schedule overview.

In the Pre-Production phase it is envisaged that 3 full GCTs will be built. The Pre-Production phase may overlap with the Prototyping phase and begins with the procurement of components with a long lead time that can be frozen prior to the full Pre-Production GCT design, such as photodetectors. Details of the Pre-Production phase schedule for the GCT camera are given in Figure 4.15 and for the telescope structures and mirrors in Figure 4.14. The on-site commissioning schedule is shown in Figure 4.13.

The first GCT structure and its mirrors will be completely assembled in industry by the project’s prime contractor, with the help of the Observatoire de Paris team to ensure transfer of the knowledge gained in the Prototyping phase. This first assembly (in Europe) will validate the new design and confirm the suitability of the manufacturing process. This first telescope will then be shipped to the CTA site to be assembled and commissioned. The second and third telescopes will be directly shipped to the CTA site without complete assembly in Europe; only the AAS is pre-assembled by the manufacturing company.

In the Pre-production phase, three GCT cameras will be produced in parallel to mimic the Production phase as closely as possible. Procurement, production, qualification and assembly of components into sub-assemblies will happen in the responsible institutes indicated in the matrix in Figure 4.10. For example, the University of Leicester will produce 3 sets of camera mechanics including the procurement of materials, the manufacture of the components and the assembly of these to form the camera enclosure. These institutes will deliver sub-assemblies to 3 AIT sites (in Leicester, Amsterdam and the MPIK). The AIT of the 3 cameras will take place in parallel and the cameras will be shipped (as integrated units requiring no further assembly) to the CTA site in separate boxes directly from these institutes.

On-site, the cameras will be unpacked, inspected and stored until basic functionality tests can be run in the on-site lab/workshop to verify that no damage has occurred during shipping, and then stored

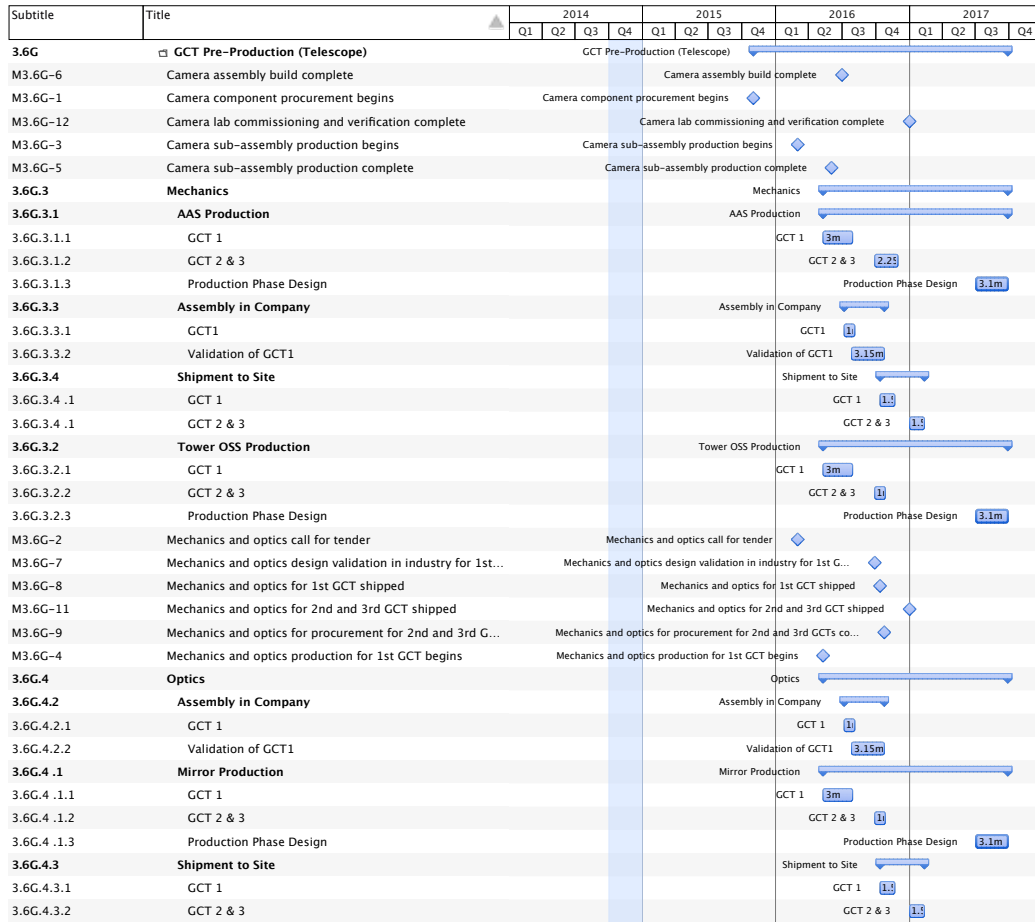


Figure 4.14 – The GCT Pre-Production schedule overview, with the telescope detailed.

again. Once the Pre-Production telescopes are ready to accept the cameras, they will be delivered to the telescope and installed. Commissioning and verification of the completed GCT instrument can then take place. It is envisaged that the on-site work will take place sequentially for each GCT.

During the Pre-Production phase, draft plans and procedures will be followed and revised in preparation for the Production phase. Work is included to revise the GCT design, and the Pre-Production phase concludes with the freezing of the final GCT design.

The Production phase schedule is shown in Figure 4.16, the institute responsibilities remain unchanged. Three cameras worth of sub-assemblies will be produced every 8 weeks and shipped to the 3 AIT sites. These sites will then assemble the complete cameras and verify them in an 8 week window.

For the telescope structures and optics, the prime contractor manages production and shipment to the CTA site. One shipment of three telescopes (and an additional three AASs) can be made every three months with four containers, plus one for the shelter that is managed by the company providing the shelter.

On-site, a similar procedure to that implemented for the Pre-Production phase will be followed (after an assessment of the Pre-Production phase). Some telescope components will be shipped directly to the foundation (tower, counterweight and shelter), while others will go to an integration hall (which is assumed to exist on site). Two areas are planned, one to assemble the Optical Support Structure and one to verify that the AAS alignment has not been damaged by the transport. The assembly of one OSS takes about three weeks (commissioning, assembly and alignment of mirrors). The commissioning of the AAS can be done in one week, with an additional week for installation and tests on the foundation. Thus a GCT telescope can be installed on site in one month, so the integration hall will be empty and the mounting phase can start again with the next shipment. Because commissioning the AAS is less

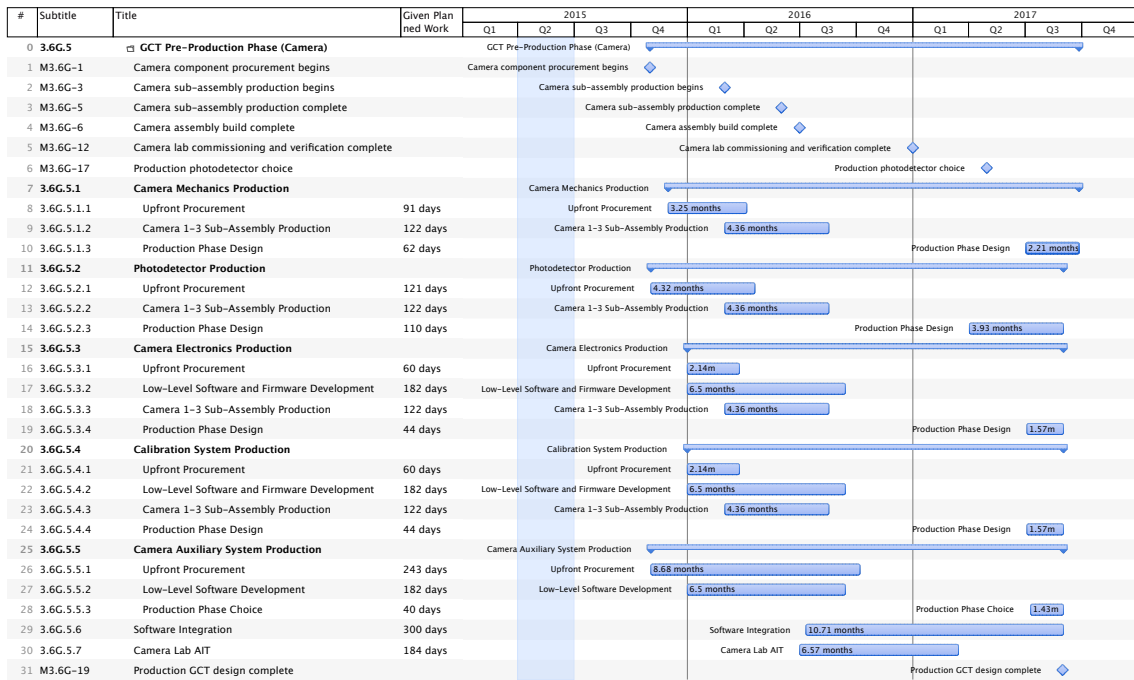


Figure 4.15 – The GCT Pre-Production schedule overview, with the camera detailed.

time-consuming, six can be commissioned and either installed on their towers once these are mounted on the foundations or stored. The cameras will begin arriving on-site later than the first telescopes, but will then arrive at the faster rate of three every eight weeks.

Commissioning of the GCTs with the installed cameras will proceed in parallel with construction. Up to six weeks per telescope for commissioning the first five telescopes is planned, reducing to three weeks for the remaining 30 GCTs. Time and resources for the replacement of faulty components at the AITs have been taken into account.

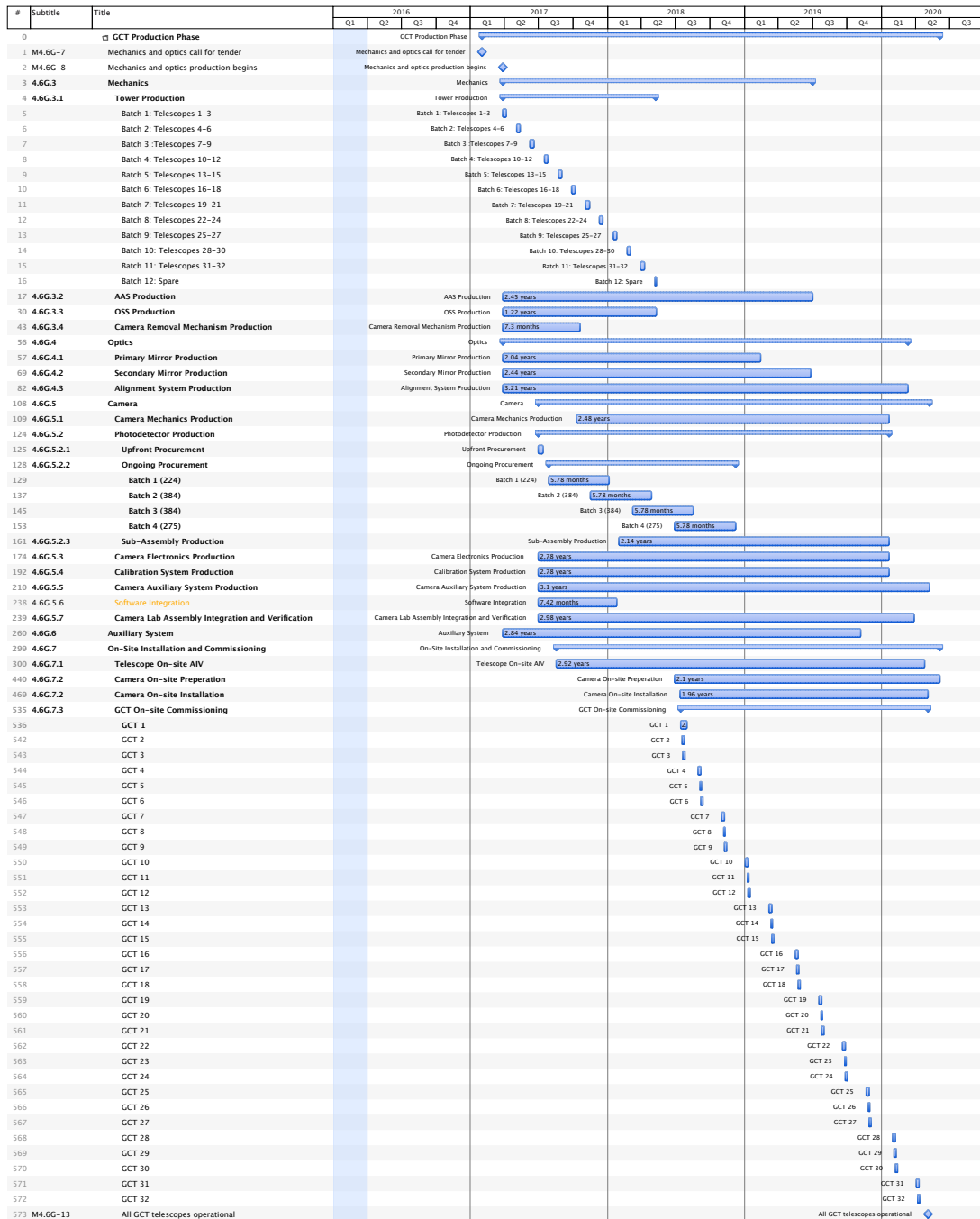


Figure 4.16 – The GCT Production schedule overview, with some items shown in more detail as examples.



### 4.3 Milestones

The milestones for the GCT Prototyping, Pre-Production and Production phases are shown in Figure 4.2. Milestones are numbered according to project phase. External CTA milestones are also included. Milestones in the Prototyping, Pre-Production and Production phases are indicated with an accuracy of one month.

Additional comments are made on some milestones in the following.

**Table 4.2** – The GCT project milestones. Red indicates telescope-specific milestones, blue indicates camera-specific milestones, and yellow indicates joint camera-telescope milestones.

Milestone	Description	Is a Deliverable?	Date			Status	On Critical Path?	Affected by external parties?
			Original	Target	Actual			
<b>External</b>								
MEx-1	Southern site decision		-	12/14		-		YES
MEx-2	Southern site ready to accept telescopes		03/16	03/16		-	YES	YES
MEx-3	Final TDR submission to PO for Critical Design Review		12/14	05/15	05/15	COMPLETE		YES
MEx-4	Critical Design Review		02/15	02/15		-		YES
MEx-5	Documentation submission to PO for Production Readiness Review		06/15	06/15		-		YES
MEx-6	Production Readiness Review		07/15	07/15		-	YES	YES
<b>Pre-Construction Phase</b>								
M2.6G-1	Preliminary GCT structure (SST-GATE) design frozen		02/13	02/13	02/13	COMPLETE		
M2.6G-2	Completion of GCT merger		07/14	10/14	10/14	COMPLETE		
M2.6G-3	CHEC-M built	YES	08/14	08/14	07/14	COMPLETE		
M2.6G-4	GCT structure design frozen		09/14	09/14	09/14	COMPLETE	YES	
M2.6G-5	CHEC-M lab evaluation complete		04/15	07/15		STARTED		
M2.6G-6	CHEC-S built	YES	05/15	01/16		STARTED		
M2.6G-7	Structure completed	YES	06/15	06/15		STARTED		
M2.6G-8	Assessment of structure started		08/14	08/14			YES	YES
M2.6G-9	Pre-production development of M1 started		06/15	06/15				
M2.6G-10	CHEC-M installed on telescope		06/15	06/15				
M2.6G-11	Pre-production development of M2 mirror started		09/15	09/15				
M2.6G-12	CHEC-S evaluation complete		10/15	10/15				
M2.6G-13	GCT + CHEC-M commissioning and testing complete		10/15	10/15				
M2.6G-14	Pre-production photodetector choice		11/15	11/15				YES
M2.6G-15	Camera component development complete		12/15	12/15				
M2.6G-16	Pre-production camera design complete		01/16	01/16				
M2.6G-17	Structure and optics development complete		01/16	01/16				
M2.6G-18	Pre-production structure and optics design complete		03/16	03/16				
<b>Pre-Production Phase</b>								
M3.6G-1	Camera component procurement begins		11/15	11/15				
M3.6G-2	Mechanics and optics call for tender		02/16	02/16				YES
M3.6G-3	Camera sub-assembly production begins		03/16	03/16				
M3.6G-4	Mechanics and optics production for 1st GCT begins		05/16	05/16				
M3.6G-5	Camera sub-assembly production complete		06/16	06/16				
M3.6G-6	Camera assembly build complete	YES	07/16	07/16				
M3.6G-7	Mechanics and optics design validation in industry for 1st GCT complete		07/16	07/16			YES	
M3.6G-8	Mechanics and optics for 1st GCT shipped	YES	08/16	08/16				
M3.6G-9	Mechanics and optics for procurement for 2nd and 3rd GCTs complete		07/16	07/16				
M3.6G-10	1st GCT built on site	YES	11/16	11/16				YES
M3.6G-11	Mechanics and optics for 2nd and 3rd GCT shipped	YES	12/16	12/16				
M3.6G-12	Camera lab commissioning and verification complete		01/17	01/17			YES	
M3.6G-13	Cameras available on-site for installation		03/17	03/17				
M3.6G-14	2nd GCT built on site	YES	01/17	01/17				YES
M3.6G-15	3rd GCT built on site	YES	02/17	02/17				YES
M3.6G-16	Cameras installed on telescopes		04/17	04/17				YES
M3.6G-17	Production photodetector choice		05/17	05/17				YES
M3.6G-18	On-site commissioning and verification complete		07/17	07/17			YES	YES
M3.6G-19	Production GCT design complete		09/17	09/17			YES	
<b>Production Phase</b>								
M4.6G-1	Camera component procurement begins		05/17	05/17				
M4.6G-2	Camera sub-assembly production begins		11/17	11/17				
M4.6G-3	Camera m of 35 sub-assembly production complete		M4.6G-2 + 8wks per batch of 3	M4.6G-2 + 8wks per batch of 3				YES
M4.6G-4	Camera m of 35 commissioning complete		M4.6G-3 + 8wks per batch of 3	M4.6G-3 + 8wks per batch of 3				YES
M4.6G-5	Camera m of 35 available on-site for installation	YES	M4.6G-4 + 2wks per batch of 3	M4.6G-4 + 2wks per batch of 3				
M4.6G-6	Camera m of 35 installed on telescope		M4.6G-5 + 2wks per camera	M4.6G-5 + 2wks per camera			YES	YES
M4.6G-7	Mechanics and optics call for tender		02/17	02/17				
M4.6G-8	Mechanics and optics production begins		04/17	04/17				
M4.6G-9	First shipment - batch 1 (3 telescopes)		09/17	09/17			YES	
M4.6G-10	Mechanics and optics for GCT x 3 (batch n of 12) shipped		M4.6G-19 + 8wks per batch of 3	M4.6G-19 + 8wks per batch of 3				
M4.6G-11	GCT m of 35 structure built on site	YES	M4.6G-20 + 6wks per GCT	M4.6G-20 + 6wks per GCT			YES	YES
M4.6G-12	GCT m of 35 commissioned and verified	YES	M4.6G-6 + 3wks per GCT	M4.6G-6 + 3wks per GCT				YES
M4.6G-13	All GCT telescopes operational	YES	07/20	07/20			YES	YES

**M2.6G-1 Preliminary GCT structure (SST-GATE) design frozen:** This milestone represents the first complete structure design.

**M2.6G-2 Completion of GCT merger:** The text of the Declaration of Intent for the GCT group has been agreed by the Management Committee and this document circulated for signing by the participants.

**M2.6G-3 CHEC-M built:** The MAPM version of the GCT camera is now being tested in the laboratory in Leicester.

**M2.6G-4 GCT structure design frozen:** Some changes to the mast and truss structure were necessitated by an increase in the load due to M2. These have been incorporated and assessed using FEA.

**M2.6G-7 Structure completed:** The structure is assembled on the Meudon site on the existing foundation and tower. The shelter also in place.

**M2.6G-8 Assessment of structure started:** Much of the instrumentation for these studies has already been purchased, e.g. a laser tracking system to allow precise measurement of the deflections of the structure.

**M2.6G-12 CHEC-S evaluation complete:** Completion of this milestone will ensure that there is data on the performance of cameras based on MAPMs (milestone M2.6G5) and SiPMs and will help inform the choice of sensor for the Pre-production and Production cameras.

**M2.6G-14 Pre-production photodetector choice:** In addition to the testing of CHEC-M and CHEC-S, developments in sensors will be followed and new sensors investigated until this point. Delaying the choice of photosensor to this date allows the use of the best possible sensors. This is of particular importance for SiPMs, where performance is improving rapidly.

**M2.6G-18 Pre-production structure and optical design complete:** At this point, the final design of the complete Pre-production telescope is available, incorporating the information from studies of the prototypes and feedback from industrial partners concerning mass production considerations.

**M3.6G-8 Mechanics and optics for first GCT shipped:** Achieving this milestone relies on the successful completion of negotiations in relation to the southern site and the provision of the necessary infrastructure (roads, foundations, power, data access, water, accommodation, workshop and storage space, etc.).

**M3.6G-12 Pre-production structure and optical design complete:** Cameras will be assembled and tested in three laboratories (in Germany, Holland and the UK) ensuring that the expertise required for large scale production is developed in sufficient locations for later mass production.

**M3.6G-17 Production photodetector choice:** Again, delaying the choice of photosensor to this point will ensure that the best possible sensors are used for the production telescopes. The GCT groups are working with other SiPM users in CTA to ensure that common SiPM specifications are developed and communicated to manufacturers, ensuring that we reap the benefits of mass production.

**M3.6G-19 Production GCT design complete:** The final design of the complete Production telescope will benefit from the lessons learned during the construction, assembly, shipping, commissioning and operation of the Pre-production telescopes.

**M4.6G-1 Camera component procurement begins:** This milestone indicates the start of up-front component procurement for the camera. It is not marked as on the critical path. Even though some components have a long lead time, if procurement slips it is likely that there will still be enough components delivered in time for the production of the first 3 sets of camera sub-assemblies. As many components will be procured across GCT institutes, this milestone will be triggered by the order of the longest lead time component, the photodetectors, and therefore Nagoya University plays a large part in its completion. The GCT Project Manager has overall responsibility for the procurement process. This milestone requires that negotiations and contracts have been completed, and that the Production phase photodetector choice has been made (M3.6G-17). Problems may occur if negotiations with suppliers become delayed or complicated.

**M4.6G-2 Camera sub-assembly production begins:** Once the upfront component procurement in industry for the camera is complete, the sub-assembly production in GCT institutes may begin. This milestone represents the end of the up-front processes and the start of the set of repetitive tasks needed to produce batches of cameras. This milestone is not on the critical path, as work may begin before procurement of all components is complete. This milestone will be marked as completed once camera sub-assembly starts in any GCT institute.

**M4.6G-3 Camera m of 35 sub-assembly production complete:** This milestone requires that all components and sub-assemblies for a camera have been procured, catalogued, commissioned (for example by uploading firmware) and qualified (for example by passing basic electrical tests). It involves all GCT institutes responsible for the production of camera sub-assemblies (see the RASCI matrix in Figure 4.10 for more details). This milestone repeats 3 times every 8 weeks, for each of 12 batches of 3 cameras, until the full 35 are produced.

**M4.6G-4 Camera m of 35 commissioning complete:** This milestone indicates that a camera has been fully assembled, integrated, passed quality-control tests and been lab-calibrated.

**M4.6G-5 Camera m of 35 available on-site for installation:** This milestone indicates that a camera has been delivered to site, unpacked, and made ready in the workshop for installation onto a telescope structure.

**M4.6G-6 Camera m of 35 installed on telescope:** This milestone indicates that a GCT has been built on-site and the camera plus auxiliary systems integrated.

**M4.6G-7 Mechanics and optics call for tender:** The second bond of the call for tender for the production phase is applied.

**M4.6G-8 Mechanics production begins:** The production of the 32 telescopes is started, organisation in batches is planned.

**M4.6G-9 First shipment - batch 1 (3 telescopes):** Following the production planning, the first batch is shipped, then the shipment of other batches is scheduled.

**M4.6G-10 Mechanics and optics for GCT x 3 (batch n of 12) shipped:** The production is continuous, the shipment of each batch is organised once the production of all systems for 3 telescopes is complete, the shipment is organised on a cycle of about 3 months or 55 days.

**M4.6G-11 GCT m of 35 structure built on site:** GCTs are built progressively once they are delivered on site, three GCTs are assembled during a rotation of container deliveries. The delivery is periodic (about 55 days) and 45 days are required to mount a GCT on site.

**M4.6G-13 All GCT telescopes operational:** This milestone indicates the completion of the hardware contribution to the project. It indicates that the full GCT sub-system is available for normal scientific observations. This depends on the previous milestones, but may also depend on the other CTA telescopes and the availability of the final array control and data acquisition chain. It requires a large number of telescopes to be operated simultaneously. However, this will be a gradual process during commissioning, so no large problems are foreseen.

## 4.4 Construction Costs

The capital costs and estimated manpower requirements for the production of GCT telescopes and cameras during the Pre-Production and Production phases are summarised in Table 4.3. Here, the effective capital cost is defined as the per-GCT capital cost to provide CTA with 35 telescopes and cameras in the Production phase, including spare assemblies, components and parts, and assuming the use of Pre-Production telescopes and cameras.

**Table 4.3** – Capital costs and estimated manpower requirements for the production of GCT telescopes and cameras during the Pre-Production and Production phases.

SST-2M GCT Costs		Pre-Production Phase				Production Phase					
WBS Code	Item	Effective Capital Cost Per GCT			Total Capital for 3 GCTs	Total Required Manpower (FTE Years)	Effective Capital Cost Per GCT			Total Capital for 35 GCTs	Total Required Manpower (FTE Years)
		Min	Best Estimate	Max			Min	Best Estimate	Max		
<b>x.6G</b>	<b>GCT</b>										
x.6G.1	Management										
x.6G.1	Project Man. (Overall Management)				2.0						3.0
x.6G.1	Project Man. (MC Coordination)	0.1 k€	0.7 k€	0.9 k€	2.2 k€	1.0	0.2 k€	0.2 k€	0.4 k€	8.4 k€	1.0
x.6G.1	Project Man. (Mechanics Coordination)	1.2 k€	1.2 k€	1.4 k€	3.6 k€	0.8	0.3 k€	0.4 k€	0.6 k€	13.2 k€	2.8
x.6G.1	Project Man. (Optics Coordination)	3.2 k€	3.2 k€	3.7 k€	9.6 k€	0.8	0.4 k€	0.4 k€	0.7 k€	15.4 k€	2.4
x.6G.1	Project Man. (Camera Coordination)	3.3 k€	4.7 k€	6.3 k€	14.0 k€	4.4	0.9 k€	1.2 k€	1.6 k€	42.0 k€	3.2
x.6G.1	Project Man. (Aux Coordination)	0.6 k€	0.6 k€	0.7 k€	1.8 k€	0.8	0.2 k€	0.2 k€	0.3 k€	6.6 k€	1.0
x.6G.1	Project Man. (On-site Coordination)	19.8 k€	20.5 k€	23.9 k€	61.5 k€	1.0	2.5 k€	2.6 k€	3.0 k€	90.2 k€	2.0
x.6G.1	Systems Engineering					1.0					3.0
x.6G.1	Quality Assurance					1.0					1.0
x.6G.1	Scientific Coordination					1.0					3.0
x.6G.2	Monte Carlo Simulations	2.0 k€	2.0 k€	2.3 k€	6.0 k€	2.6	0.2 k€	0.2 k€	0.3 k€	7.0 k€	2.0
x.6G.3	Mechanics	185.5 k€	218.5 k€	252.9 k€	655.6 k€		142.7 k€	167.6 k€	192.9 k€	5,864.8 k€	
x.6G.4	Optics	221.9 k€	260.7 k€	289.9 k€	782.0 k€	0.0	166.4 k€	206.4 k€	236.9 k€	7,222.9 k€	0.1
x.6G.5	Camera	266.9 k€	292.3 k€	353.1 k€	876.9 k€	22.1	130.8 k€	145.4 k€	184.0 k€	5,087.7 k€	23.4
x.6G.6	Auxiliary	37.5 k€	85.9 k€	99.9 k€	257.8 k€		30.3 k€	73.0 k€	83.9 k€	2,555.7 k€	
x.6G.7	On-site Assembly Integration and Verification	7.1 k€	7.1 k€	7.1 k€	21.4 k€	6.8					13.3
	<b>Total</b>	<b>749 k€</b>	<b>898 k€</b>	<b>1,042 k€</b>	<b>2,693 k€</b>	<b>45</b>	<b>749.2 k€</b>	<b>897.5 k€</b>	<b>1,042.2 k€</b>	<b>2,692.5 k€</b>	<b>61</b>

### 4.4.1 Pre-Production Phase

The Pre-Production costs are further expanded on in Table 4.4. In this phase, 3 full telescope and camera systems are envisaged. The total capital cost, including all required travel and shipping, is ~877 k€. The largest assembly cost in this phase is the camera at ~292 k€. This cost is in turn dominated by the photodetectors and the ASICs used in the TARGET modules (which are subject to a large one-off setup charge). The Pre-Production phase includes significant manpower for the finalisation

of the hardware designs, firmware and low-level (device) software as well as project management and commissioning of the instruments on site.

**Table 4.4** – Capital costs and estimated manpower requirements broken down for the production of GCT telescopes and cameras during the Pre-Production phase.

SST-2M GCT Pre-Production Phase Costs		Capital Cost Per GCT				Required Manpower For 3 GCTs								
		k€				FTE Years								
WBS Code	Item	Hardware	Travel	Shipping	Total	Helper	Administration	Technician	Electronic Eng.	Mechanical Eng.	Computer	Scientist	Specialist	Total
<b>3.6G</b>	<b>GCT</b>													
<b>3.6G.1</b>	<b>Management</b>													
3.6G.1.1	Project Man. (Overall Management)				0.7 k€							2.00	0.00	2.0
3.6G.1.1	Project Man. (MC Coordination)		0.7 k€		0.7 k€				1.00					1.0
3.6G.1.1	Project Man. (Mechanics Coordination)		1.2 k€		1.2 k€	0.00			0.78				0.00	0.8
3.6G.1.1	Project Man. (Optics Coordination)		3.2 k€		3.2 k€	0.01			0.76				0.00	0.8
3.6G.1.1	Project Man. (Camera Coordination)		4.7 k€		4.7 k€						4.40		0.00	4.4
3.6G.1.1	Project Man. (Aux Coordination)		0.6 k€		0.6 k€	0.00		0.84					0.00	0.8
3.6G.1.1	Project Man. (On-site Coordination)		20.5 k€		20.5 k€	0.00			0.78		0.25		0.00	1.0
3.6G.1.2	Systems Engineering												1.00	1.0
3.6G.1.3	Quality Assurance													1.0
3.6G.1.4	Scientific Coordination											1.00		1.0
<b>3.6G.2</b>	<b>Monte Carlo Simulations</b>		2.0 k€		2.0 k€								2.60	2.6
<b>3.6G.3</b>	<b>Mechanics</b>													
3.6G.3.1	Tower Production	5.6 k€			5.6 k€									
3.6G.3.2	AAS Production	129.7 k€			129.7 k€									
3.6G.3.3	OSS Production	68.6 k€			68.6 k€									
3.6G.3.4	Camera removal Production	10.8 k€			10.8 k€									
3.6G.3.5	Telescope Lab AIT	3.8 k€			3.8 k€									
<b>3.6G.4</b>	<b>Optics</b>													
3.6G.4.1	Primary Mirror production	144.4 k€			144.4 k€	0.01		0.01						0.0
3.6G.4.2	Secondary Mirror production	71.7 k€			71.7 k€	0.00		0.00						0.0
3.6G.4.3	Shipment of mirrors in container 1	3.7 k€			3.7 k€									
3.6G.4.4	Procurement for alignment	41.0 k€			41.0 k€									
<b>3.6G.5</b>	<b>Camera</b>													
3.6G.5.1	Camera Mechanics Production	16.6 k€	0.40 k€	0.13 k€	17.1 k€	0.14	0.03	0.51		0.62		0.07		1.4
3.6G.5.2	Photodetector Production	83.5 k€	0.10 k€	0.17 k€	83.8 k€	0.20	0.05	0.15	0.46	0.06		0.90		1.8
3.6G.5.3	Camera Electronics Production													
	Front-end Buffers	16.4 k€	0.10 k€	0.03 k€	16.6 k€	0.27	0.00	0.07	0.30			0.25		0.9
	TARGET Modules	106.8 k€	0.40 k€	0.05 k€	107.3 k€	0.22	0.01	0.38	0.84			0.27		1.7
	Backplane	12.3 k€	0.33 k€	0.02 k€	12.7 k€	0.28	0.01	0.25	1.47			1.30		3.3
	DACQ	7.3 k€		0.02 k€	7.3 k€	0.30	0.01	0.09	1.46			0.31		2.2
	Peripherals Board	2.4 k€		0.02 k€	2.4 k€	0.17	0.01	0.19	0.72			0.64		1.7
	Internal Cabling	0.8 k€		0.06 k€	0.8 k€			0.01	0.07	0.09				0.2
3.6G.5.4	Calibration System Production	1.5 k€		0.04 k€	1.6 k€	0.15	0.01	0.18	0.62	0.00		0.77		1.7
3.6G.5.5	Camera Auxiliary System Production	10.2 k€		0.60 k€	10.8 k€	0.05	0.01	0.15				0.55		0.8
3.6G.5.6	Software Integration											0.80		0.8
3.6G.5.7	Camera Lab Assembly Integration and Verification	30.0 k€		2.0 k€	32.0 k€	2.38	0.04	0.62		0.07		2.52		5.6
<b>3.6G.6</b>	<b>Auxiliary</b>													
3.6G.6.1	TCS Cabinets production	33.5 k€			33.5 k€									
3.6G.6.2	Power and Network Cabinets production	9.4 k€			9.4 k€									
3.6G.6.3	Shelter	43.0 k€			43.0 k€									
<b>3.6G.7</b>	<b>On-site Assembly Integration and Verification</b>													
3.6G.7.1	Telescope On-site AIV	7.1 k€			7.1 k€	0.40		0.60					0.02	1.0
3.6G.7.2	Camera On-site AIV					0.20	0.01	0.21						0.4
3.6G.7.3	GCT On-site Commissioning					2.52		0.73				2.06		5.3
	<b>Total</b>	<b>860 k€</b>	<b>34 k€</b>	<b>3 k€</b>	<b>898 k€</b>	<b>7.3</b>	<b>0.2</b>	<b>5.1</b>	<b>9.3</b>	<b>1.8</b>	<b>4.7</b>	<b>16.0</b>	<b>1.0</b>	<b>45</b>

### 4.4.2 Production Phase

The Production-phase costs are shown in Table 4.5.

As indicated in Figure 4.17, the Production phase capital cost is dominated by the telescope structure and optics, followed by the camera. Figure 4.18 shows the capital costs of individual WBS tasks arranged by increasing fraction of the total hardware cost. The production of both mirrors, the telescope drives, the photodetectors and the shelter together make up > 50% of the entire hardware cost.

Whilst the cost of the shelter is relatively well known, there is a large uncertainty in the cost of the other components. For example, the Production phase capital cost of the photodetectors, which accounts for ~30% of the total camera cost, is based on a quote for currently available technology in Japanese Yen and is therefore subject to both exchange rate fluctuations and changes in the cost as SiPM technology develops.

**Table 4.5 – Capital costs and estimated manpower requirements broken down for the production of GCT telescopes and cameras during the Production phase.**

SST-2M GCT Production Phase Costs		Capital Cost Per GCT				Required Manpower For 35 GCTs								
		k€				FTE Years								
WBS Code	Item	Production	Travel	Shipping	Total	Helper	Administration	Technician	Electronic Eng.	Mechanical Eng.	Computer	Scientist	Specialist	Total
<b>4.6G</b>	<b>GCT (Production of 32 telescopes + spares and 35 cameras + spare parts)</b>													
<b>4.6G.1</b>	<b>Management</b>													
4.6G.1.1	Project Man. (Overall Management)											3.00	0.00	3.0
4.6G.1.1	Project Man. (MC Coordination)		0.2 k€		0.2 k€				1.00				0.00	1.0
4.6G.1.1	Project Man. (Mechanics Coordination)		0.4 k€		0.4 k€	0.02			2.75				0.00	2.8
4.6G.1.1	Project Man. (Optics Coordination)		0.4 k€		0.4 k€	0.02			2.34				0.00	2.4
4.6G.1.1	Project Man. (Camera Coordination)		1.2 k€		1.2 k€					3.15			0.00	3.2
4.6G.1.1	Project Man. (Aux Coordination)		0.2 k€		0.2 k€	0.02		0.94					0.00	1.0
4.6G.1.1	Project Man. (On-site Coordination)		2.6 k€		2.6 k€	0.00			1.39	0.60			0.00	2.0
4.6G.1.2	Systems Engineering												3.00	3.0
4.6G.1.3	Quality Assurance								1.00					1.0
4.6G.1.4	Scientific Coordination											3.00		3.0
<b>4.6G.2</b>	<b>Monte Carlo Simulations</b>		0.2 k€		0.2 k€							2.00		2.0
<b>4.6G.3</b>	<b>Mechanics</b>													
4.6G.3.1	Tower Production	4.9 k€			4.9 k€									
4.6G.3.2	AAS Production	90.8 k€			90.8 k€									
4.6G.3.3	OSS Production	65.9 k€			65.9 k€									
4.6G.3.4	Camera removal Production	4.4 k€			4.4 k€									
4.6G.3.5	Shipment of mechanics	1.6 k€			1.6 k€									
<b>4.6G.4</b>	<b>Optics</b>													
4.6G.4.1	Primary Mirror production	113.9 k€			113.9 k€	0.06		0.06						0.1
4.6G.4.2	Secondary Mirror production	63.5 k€			63.5 k€	0.01		0.01						0.0
4.6G.4.3	Shipment of mirrors in container 1	0.8 k€			0.8 k€									
4.6G.4.4	Procurement for alignment	28.2 k€			28.2 k€									
<b>4.6G.5</b>	<b>Camera</b>													
4.6G.5.1	Camera Mechanics Production	13.1 k€	0.03 k€	0.13 k€	13.2 k€	0.66	0.06	1.51		0.18		0.04		2.5
4.6G.5.2	Photodetector Production	50.5 k€	0.01 k€	0.04 k€	50.6 k€	0.67	0.07	0.74	0.17			0.46		2.1
4.6G.5.3	Camera Electronics Production													
	Front-end Buffers	12.2 k€	0.01 k€	0.03 k€	12.2 k€	0.67	0.01	0.26	0.01			0.31		1.3
	TARGET Modules	40.5 k€	0.03 k€	0.05 k€	40.6 k€	1.03	0.02	1.50	0.09			0.72		3.4
	Backplane	7.7 k€	0.03 k€	0.02 k€	7.8 k€	0.54	0.02	0.35	0.06			0.40		1.4
	DACQ	5.1 k€		0.02 k€	5.1 k€	0.30	0.02	0.33	0.04			0.22		0.9
	Peripherals Board	1.6 k€		0.02 k€	1.7 k€	0.91	0.06	0.33	0.19			0.77		2.3
	Internal Cabling	0.5 k€		0.06 k€	0.6 k€			0.01	0.06					0.1
4.6G.5.4	Calibration System Production	1.2 k€		0.04 k€	1.3 k€	0.33	0.03	0.56	0.22	0.00		0.55		1.7
4.6G.5.5	Camera Auxiliary System Production	8.9 k€		0.62 k€	9.5 k€	0.31	0.04	0.62				0.33		1.3
4.6G.5.6	Software Integration											0.38		0.4
4.6G.5.7	Camera Lab Assembly Integration and Verification	0.9 k€		2.0 k€	2.9 k€	2.56	0.21	1.86		0.04		1.51		6.2
<b>4.6G.6</b>	<b>Auxiliary</b>													
4.6G.6.1	TCS Cabinets production	30.1 k€			30.1 k€									
4.6G.6.2	Power and Network Cabinets production	8.0 k€			8.0 k€									
4.6G.6.3	Shelter	35.0 k€			35.0 k€									
<b>4.6G.7</b>	<b>On-site Assembly Integration and Verification</b>													
4.6G.7.1	Telescope On-site AIV					4.30		6.48					0.20	11.0
4.6G.7.2	Camera On-site AIV					0.63	0.02	0.61						1.3
4.6G.7.3	GCT On-site Commissioning					0.11		0.65				0.27		1.0
	<b>Total</b>	<b>589 k€</b>	<b>5 k€</b>	<b>3 k€</b>	<b>598 k€</b>	<b>13.2</b>	<b>0.6</b>	<b>16.9</b>	<b>8.3</b>	<b>1.2</b>	<b>3.8</b>	<b>14.0</b>	<b>3.2</b>	<b>61</b>

Figure 4.19 shows the manpower cost associated with the Production phase. In this case, the dominant factors are the on-site telescope AIV (11 FTE years), the coordination of the mechanics production (9.4 FTE years), and the lab AIV for the camera (6.2 FTE years).

In the Production phase, 32 full telescope structures with mirrors will be produced, verified and installed on site with the existing 3 Pre-Production telescopes. Two spare sets of mechanical and optical components will be procured. A total of 35 full cameras will be produced in the Production phase, with the 3 Pre-Production cameras acting as spares. Additionally, spare components and parts will be provided during the Production phase, roughly following a policy of 2% spare populated PCBs, 2% spare unpopulated PCBs and 2% spare components/parts (including sensors and fans). Spare ASICs will be procured at the higher level of 20% to allow for failures and sub-standard performance at the time of assembly. It may be necessary to upgrade the 3 Pre-production cameras to act as like-for-like spares for the Production phase cameras. As the nature of such an upgrade is not yet known, the associated capital cost and manpower can not be precisely included in the cost estimates. However, the most likely scenario would be an upgrade to the photodetectors. As such, the procurement (and mounting to base PCBs) of 10% spare photodetectors is included in the Production phase cost estimate. The best estimate hardware

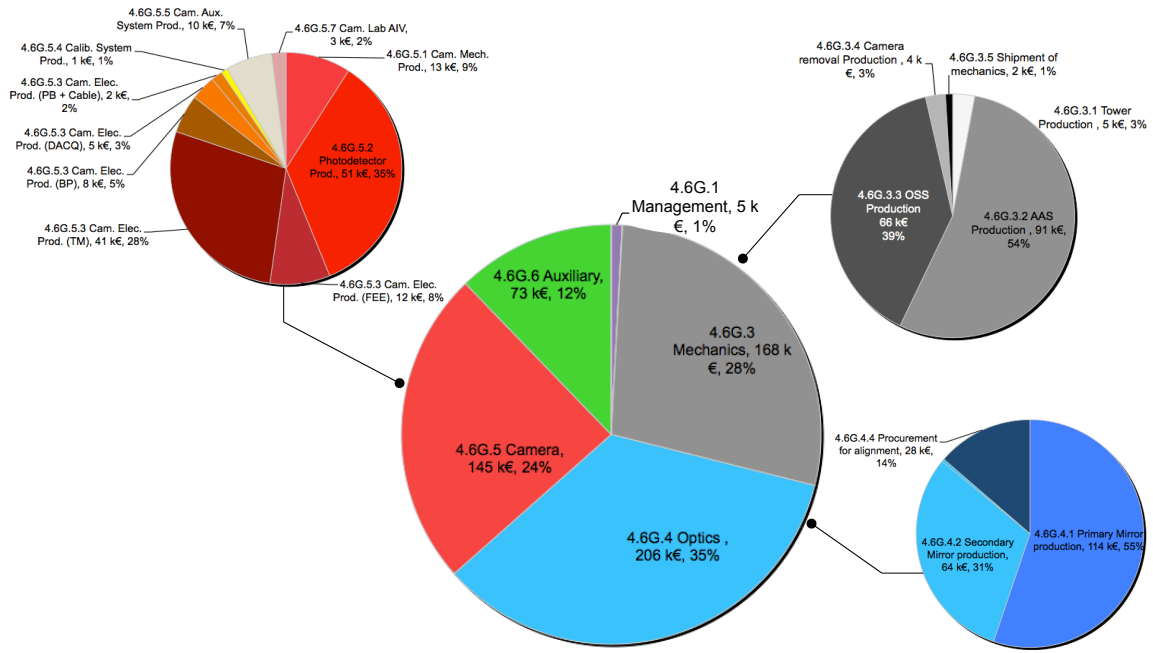


Figure 4.17 – Capital costs during the Production phase.

cost of the camera is reduced by 6.9 k€ if no spare components/parts are included.

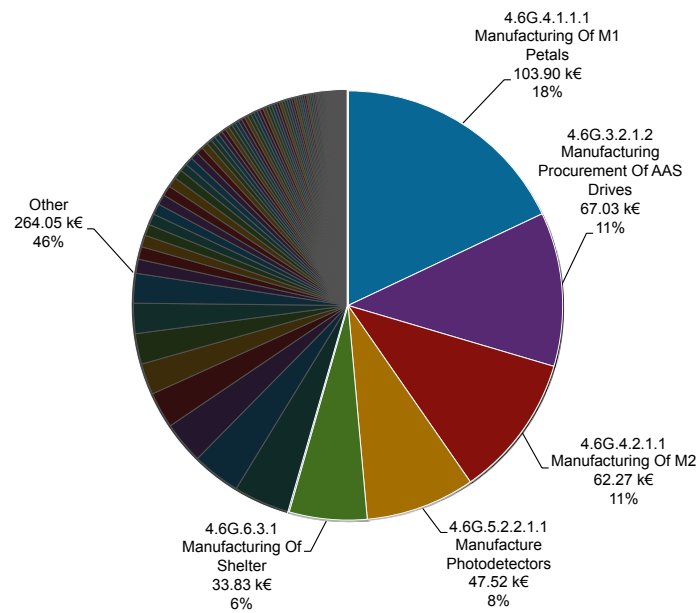


Figure 4.18 – Capital costs of individual WBS tasks in the Production phase indicating the cost drivers.

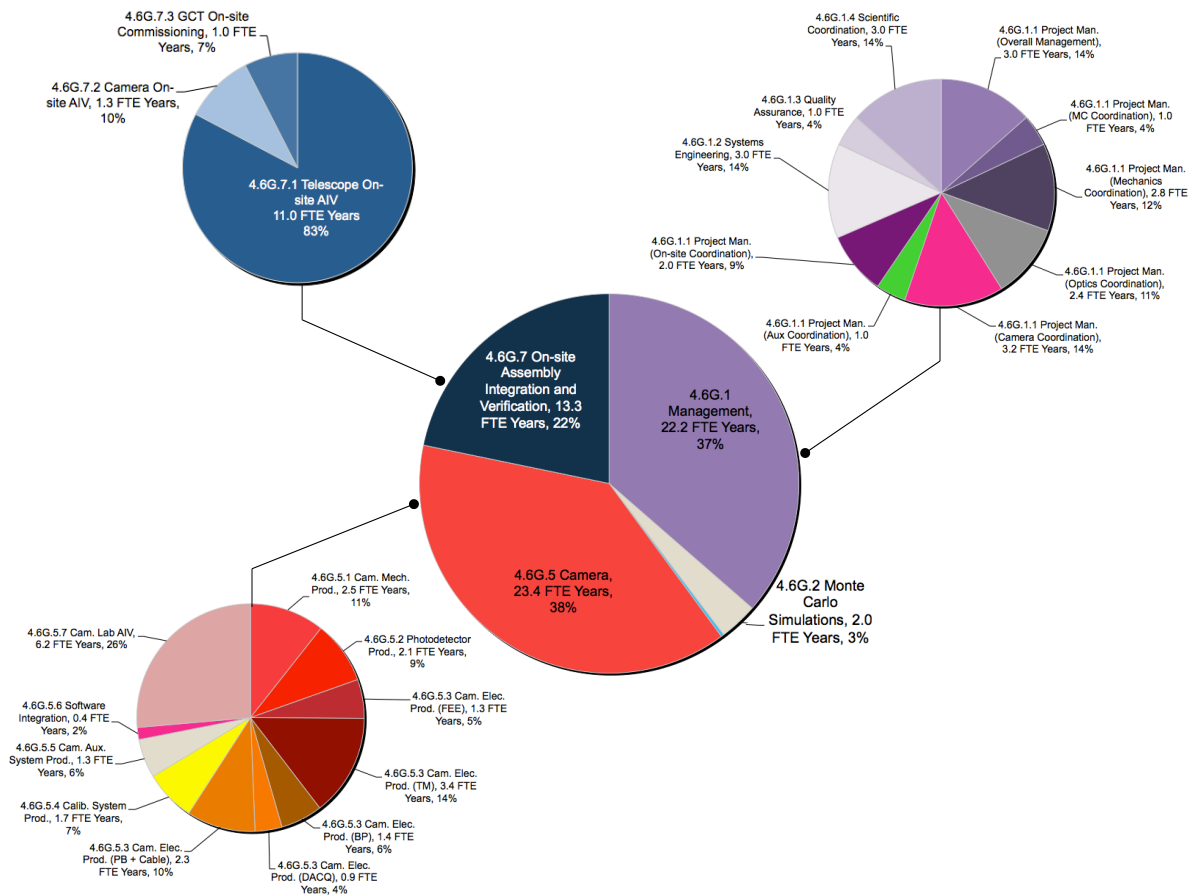


Figure 4.19 – Manpower costs during the Production phase.



## 4.5 Maintenance & Operation Plans

### 4.5.1 Overview

The CTA requirements are designed to produce telescopes capable of performing in a harsh environment with the minimum possible maintenance over the assumed 30 year lifetime of the Observatory. With these goals in mind, we focussed on the following topics during the design phase:

- Identify and assess risks to the project, instrument and personnel as early as possible (through FMECA and safety analyses – CEI/EN 61058 and CEI/EN 62061).
- Apply corrective actions as early as possible during the design phase.
- Simplify the assembly and maintenance as far as possible and minimise the amount of specialist equipment needed.
- Use reliable COTS provided by experienced companies (e.g. ETEL, Beckhoff).

In this section we explain how we estimated the availability of the GCT telescope and the number of spares needed to ensure a life-time of at least 30 years. For more details, refer to the document “JGCT maintenance and reliability of the GCT telescope”.

The maintenance of the telescope was considered during the design phase, the goal being to ensure it requires only a few hours per month. There are five main maintenance tasks:

1. Visual inspection to verify that no unexpected problems have occurred since the last inspection (signs of rust, of leakage, status of the mirrors, condensation on the electronics cabinets etc.).
2. Test of safety systems.
3. Regular maintenance jobs (greasing, cleaning...).
4. On-demand maintenance following the detection of problems (in particular imminent failures) by the telescope monitoring systems.
5. Exceptional maintenance, i.e. repair following an unexpected failure.

The maintenance breakdown file details the tasks to be performed, their duration and the equipment needed to carry them out.

Several methods exist for defining a spares policy, depending on the availability of new components, the risk that components become obsolete, the volume available for storage and the associated cost. An attempt was made to optimise these constraints in the spares policy we developed. The following components were considered:

1. Parts for which exchange is scheduled (e.g. due to wear).
2. Parts that will be exchanged when they fail.
3. Spares for systems with a long life-time but which:
  - (a) could be damaged accidentally;
  - (b) cannot be easily purchased or can only be purchased following a long delay;
  - (c) are very expensive.

## 4.5.2 Estimate of the number of spares

For the components that have a life-time longer than 30 years (e.g. the mechanical structure) and a low probability of failure, the number of spares is fixed to two for a set of 35 telescopes to mitigate against unexpected (and poorly-modelled) events (e.g. damage during assembly or mounting).

For other parts, the number of spares needed is estimated as the number of failures that give a cumulative probability of 99% over a duration of 5 years, assuming 35 telescopes. The resulting list is given in the *IGCT maintenance and reliability of the GCT telescope* and never exceeds 8 spares.

## 4.5.3 Housekeeping data analysis

Regular inspections are carried out. These will check, for example, that animals or dust are not blocking ventilation holes. Parallel to this inspection, the recorded telescope monitoring data are analysed at the end of each observation night (as a minimum). Parameters such as power consumption can indicate potential drive failures. Monitoring the camera fans allows potential failures to be identified and the camera exchanged before high temperatures cause the camera to be switched off and observing time to be lost.

If a system is not running efficiently, needs repairing, or needs to undergo regular maintenance, it is removed, replaced with a spare, and repaired in the integration hall. The modular design of the telescope facilitates this procedure. For instance, the removal of a motor shaft takes 20 minutes, and its replacement 30 minutes.

## 4.5.4 Line Replaceable Units

After a period of 5 years, estimates of the number of spares will be more reliable and purchases organised accordingly. Our suppliers will indicate when a component becomes obsolete so we have a chance to renew our stock of these items.

## 4.5.5 Use of Shelter

The reliability and availability of the telescope will be influenced by the use of the shelter. For example, this allows maintenance during the rain or high winds. Our estimate is that it saves about 13 person hours per telescope per year and decreases by about a factor of 2 to 3 the cost of mirror recoating. A similar factor is expected with regard to telescope repainting costs. Considered over a life-time of 30 years, this compensates for the cost of the shelter while simultaneously simplifying maintenance.

# 4.6 Assumptions, Dependencies and Caveats

In this section the assumptions, dependencies and caveats for the GCT project are outlined.

## 4.6.1 Assumptions

The following assumptions are made with regards to the GCT project:

- GCT-A01: The responsibility of the GCT consortium is to install and commission the specified number of telescopes on the CTA southern site. Once the performance of these has been verified, they will be given to the CTAO as an in-kind contribution, together with documentation such as a user's manual and maintenance plan. The CTAO will then take over operation of the telescopes.

- GCT-A02: GCTs will only be required on the southern CTA site.
- GCT-A03: Following performance verification, maintenance of the GCT sub-system will be taken over by the CTAO.
- GCT-A04: Installation of the GCTs will be carried out by GCT and CTAO staff. Technicians working at the CTAO will be trained by GCT personnel and provided with appropriate documentation by the GCT group.
- GCT-A05: The CTAO will help to coordinate the shipping and storage of GCT components to allow the smooth installation and commissioning of all telescopes.

The following assumptions are made with regards to the direct interface of GCT with the CTAO infrastructure:

- GCT-A06: A lightning protection system will be specified as part of the CTA infrastructure in collaboration with the GCT consortium. The GCT consortium will design and provide a lightning protection system on the telescope following this specification. The GCT consortium assumes that all installation and earthing components on the foundation will be provided by CTAO.
- GCT-A07: The power and network interface of the GCT telescope with the array is situated at the general supply cabinet on a concrete slab in close proximity to the telescope.
- GCT-A08: The telescope foundation is provided as part of the CTAO infrastructure.
- GCT-A09: The telescope foundation will be designed in collaboration with the GCT consortium.
- GCT-A10: A 230/400 V – 50 Hz three-phase power supply for 10 kW is provided as part of the CTA infrastructure.
- GCT-A11: Local weather monitoring will be provided by the CTAO.

The following assumptions are made with regards the to the available on-site infrastructure::

- GCT-A12: Roads large enough for trucks to directly access the telescope foundations will be available.
- GCT-A13: An suitably-sized assembly hall will be available.
- GCT-A14: Adequate storage facilities for telescopes and cameras will be available and easily accessible during commissioning.
- GCT-A15: A large crane will be available on-site for the installation (and maintenance) of the telescopes.
- GCT-A16: A small camera removal tool/crane capable of lifting 50 kg will be made available following specification from the GCT consortium.
- GCT-A17: A mechanical workshop equipped to repair components will be available in accordance with the GCT RAMS analysis.
- GCT-A18: A facility for the commissioning and debugging of cameras will be available, including a dark room large enough to contain a single GCT camera and a light source in accordance with the GCT RAMS analysis.
- GCT-A19: Transport will be provided on-site to reach the telescopes.
- GCT-A20: A platform/slab will be provided to mount equipment for the alignment of the telescope.
- GCT-A21: An air compressor will be available to clean the mirrors regularly to maintain the maximum reflectivity between re-coatings.

The following assumptions are made with regards to data acquisition, control and timing:

- GCT-A22: Network infrastructure is provided to the telescope with a data capacity of at least 10 Gbps and a separate 1 Gbps link for timing.
- GCT-A23: A Network Time Protocol server (Stratum 1) is provided to avoid the need for each telescope to have its own GPS.
- GCT-A24: A timing board is provided for installation in the camera providing the required absolute timing accuracy.
- GCT-A25: The timing board will require a 1 Gbps link to the base of the telescope to be provided by the GCT consortium.
- GCT-A26: A central PC farm for data acquisition, trigger logic and control will be provided.
- GCT-A27: A software-based array trigger using hard time-stamps will be accommodated.

## 4.6.2 Dependencies

The GCT project is dependent upon:

- GCT-D01: The CTA southern site decision being made at least 1 year prior to fixing the telescope design, as the environmental conditions will influence the telescope design.
- GCT-D02: Availability of funding sufficient to construct and deploy 35 complete GCTs over the period 2016-2020.
- GCT-D03: Successful completion of the CDR process by CTA as a whole and the GCT in particular.
- GCT-D04: Development of adequate control and data processing software in collaboration with the DATA and ACTL teams.
- GCT-D05: Timely development of the GCT foundation with the CTAO (this may influence the tower structure and any additional FEA must be done before production phase).
- GCT-D06: Timely and predictable lead times from suppliers, in particular the photodetector manufacturer.
- GCT-D07: Accurate cost estimates from suppliers for the Production phase during Pre-Production to ensure funding is adequate.

## 4.6.3 Caveats

The following caveats apply to the GCT project:

- GCT-C01 If the CTA southern site choice is delayed, the GCT design may not be able to be finalised at the anticipated time and the project schedule may slip.
- GCT-C02 If the CTA requirements change, additional design simulations and lab tests may have to be performed, delaying the final telescope and camera design and resulting in a possible slip of the project schedule.
- GCT-C03 If the funding profile is not coordinated between funding agencies such that funding arrives in a foreseeable and timely manner, then the project schedule may need to be changed. This may result in increased costs.
- GCT-C04 If exchange rates change by a larger amount than expected, the cost of the envisaged number of telescopes may rise.

- GCT-C05 If CTAO, working with the GCT and other interested groups, does not put framework agreements in place with (the) photodetector manufacturer(s) then SiPM costs are likely to be inflated.
- GCT-C06 If the CTAO decides not to fund the telescope foundation and/or the telescope shelter then additional funding will need to be requested by the GCT project.
- GCT-C07 If the CTA southern site is not ready to receive telescopes at the anticipated point in either the Pre-Production or Production phase, then complications including delays and additional costs may be incurred as some items will ship direct from industrial partners.
- GCT-C08 If aspects of the CTAO maintenance policy are unclear, then the GCT maintenance plan may be inadequate (e.g. regarding the provision of a mirror coating facility on site).

## 4.7 Risks

This section summarises the 20 highest project risks and explains the mitigation methods adopted. To clarify the correspondence between this section and the full risk register spreadsheet (*GCT\_RiskRegister.xls*), the risk ID is given. The risks for which the recommended action has already been implemented in the GCT project are shown in italics.

**ID 57 Exchange rate variability (RPN = 36)** The recommended action can be split into two items:

- Use of the money by placing the majority of orders in the same currency as that in which funding is awarded to reduce the loss in currency exchanges.
- Time, by trying to keep a window of several months for orders of large foreign components (e.g. SiPMs) and by favouring a small delay over cost overrun.

**ID 56 Ageing and wear inadequately predicted (RPN = 36)** The first step has been to choose companies in which we can have confidence to produce or to provide the elements. The second step will consist of testing the prototype and the elements manufactured or purchased during the pre-production phase including, when possible, long-term testing. The V&V procedures will be re-written to take this into account.

**ID 38 Delivery of Production Phase items to site incur unforeseen delays (RPN = 32)** The action is to include a margin between the scheduled date of the delivery and the scheduled date for the integration. Storage facilities on-site are foreseen to minimise the impact of delivery times that may exceed the margin. Finally, the use of a dedicated (CTA allocated) shipping company can minimise the probability of import/export delays.

**ID 39 Maintenance plan inadequate (RPN = 27)** The action to minimise this risk was started several month ago by carefully choosing the providers of the crucial elements such as safety-critical items or those involved in the movement of the telescope. These well-known companies (Beckhoff, ETEL...) have long experience in their field and provide components with a very long life-time. Moreover, the reliability estimate takes this risk into account in the estimation of the number of spares required as well as in the number and duration of the maintenance tasks.

**ID 40 V&V procedure fails to detect broken/sub-standard components (RPN = 24)** Once the pre-production telescope is ready, a series of functional tests will be performed to verify the global performance of the telescope with respect to the CTA requirements. These tests will involve all the major components and will inform us about possible V&V failures.

**ID 41 Lack of envisaged Production funding across one or more GCT partners (RPN = 24)** The first step is obviously to coordinate funding applications across GCT partner institutes. This has already started. The second step is to use the Pre-Production experience to produce accurate cost estimates.

**ID 42 Costs underestimated prior to Production funding applications (RPN = 24)** The experience of the Pre-Production phase will provide important input to these costings and experience in dealing with the companies involved. We will work as far as possible with industrial partners involved in the Pre-Production phase for the production phase.

- ID 43 *Manpower underestimated prior to Production Phase (RPN = 24)*** Again, the prototype and the Pre-Production phase will allow us to better estimate the manpower needs for the production phase.
- ID 44 *Loss of critical persons during the Pre-Construction or Pre-Production Phase (RPN = 24)***  
The recommended action to prevent the loss of essential personnel is to name them in funding applications to secure their positions. If they wish to leave the project, the recruitment of replacement(s) will start as early as possible, allowing for some overlap. Another action is to fully utilise the existing and experienced manpower within GCT institutes and CTA as much as possible. Finally, we will ensure sharing of expertise by having at least 2 people contribute to all parts of the GCT. Note that this risk applies to high-level skilled roles such as firmware development. Tasks that can be well documented will be to allow personell to be more easily replaced.
- ID 45 *Loss of critical individuals during the Production Phase (RPN = 24)*** The same recommended procedure as for ID 44 can be used to reduce this risk.
- ID 46 *Time lost due to ill health (RPN = 24)*** A provision has been included in the schedule based on an estimate of the time likely to be lost due to illness. Monitoring of actual time lost during Pre-Production Phase will permit a better estimate to be made.
- ID 47 *Gold-plating inflates scope – i.e. the project team members add their own product features that are not in the requirements or change requests (RPN = 24)*** The recommended action is to ensure that the GCT DVD is accurate and up-to-date so it serves as a reference point for the GCT specifications.
- ID 48 *Activities are missing from scope/WBS (RPN = 24)*** This risk will be minimised using the experience gained in the Prototyping phase and a more accurate WBS will be built for the Pre-Production and Production phases.
- ID 35 *Delays to Pre-Production Phase commissioning on-site (RPN = 16)*** To reduce this risk, the GCT team will monitor delays in the telescope mounting. The spares policy ensures spares are available to help cope with unexpected events (damage, loss. . . ) during assembly. Commissioning procedures will be tested on-site before the first telescope arrives.
- ID 36 *Requirements provided by CTA are incomplete/inadequate (RPN = 16)*** CTA requirements cover scientific, safety and environmental considerations. The modular GCT telescope design simplifies design changes prompted by changes in any of these requirements.
- ID 37 *Environment inadequately predicted (RPN = 16)*** This has already occurred with regard to altitude and maximum wind speed. We successfully changed the design of the telescope in reaction to the changing understanding of the environment and we are aware that these requirements can change again as the site is not yet chosen. The modular telescope design will aid reaction to any further changes.
- ID 38 *Change requests result in a design that is in conflict with requirements (RPN = 16)*** This is mitigated via the DVD. To reduce this risk, an up-to-date DVD will be maintained.
- ID 39 *GCT Project team misunderstands CTA requirements (RPN = 16)*** See action for ID 35.
- ID 40 *Force Majeure (act of God) impacts project (RPN = 16)*** Such events are by definition unexpected. To reduce this risk, the GCT planning has margins of error.
- ID 7 *Technical inputs required for tender or production are inadequate (RPN = 12)*** Action (already started) consists in engaging companies early in the design phase to better understand the needs for the production phase.

## 5 Lessons Incorporated

The GCT prototype is built upon experience gained in previous and on-going high-energy astrophysics and particle physics experiments, such as HESS, VERITAS, AUGER, ANTARES, H1, and ATLAS, as well as experience designing on-going optical instruments such as the X-shooter spectrograph at the European Southern Observatory, space-based missions such as the Gaia satellite and a variety of industrial projects. This large variety of experiences allows GCT to take advantage of a wide spectrum of scientific and mechanical expertise, from FEA analysis of mechanical structures to front-end electronics read-out for ground-based gamma-ray telescopes. In this section the lessons learnt from previous projects and GCT's on-going prototyping activities are summarised. The summary is broken in 3 main sections, reflecting the structure of GCT's PBS: the Mechanical Assembly (PBS item G6.1), the Optical Assembly (PBS item G6.2) and the Camera Assembly (PBS item G6.3).

### 5.1 Mechanical Assembly Lessons Learnt

Lesson	Source of lesson	How lesson was incorporated
A long camera-mounting process reduces observing time and increases likelihood of telescope damage.	HESS-II	The camera is mounted in a simple cradle, supported by two arms. One arm is hinged, while the other is detachable. This allows the cradle to be rotated, affording quick and easy mounting/dismounting of the camera. Furthermore, when rotated, the camera is accessible on the ground, decreasing the potential risk of damage to the telescope structure.
The original tower design had material dimensions that were company specific.	Observatoire de Paris	The tower diameter has been enlarged in order to use COTS.
On-site construction of the telescope structure requires that the assembly process be simplified.	Observatoire de Paris	Allowances for on-site construction are best designed for during the prototype stage. As such, GCT has a counterweight to progressively balance the telescope structure as more components are added.
To reduce cost and maintenance time, similar azimuth and elevation drives should be considered.	Observatoire de Paris	The drive design is similar for azimuth and elevation; the only exception is one screw. The mechanical systems are similar, except that the elevation drive has additional mechanical parts to protect it from dust and rain.
FEA simulation during the prototype stage allows us to confirm that GCT conforms to CTA specifications.	Observatoire de Paris	The original structure design has been changed to a Serrurier configuration, with 4 pairs of arms supporting the secondary mirror.

After FEA, an additional design optimisation phase allows us to maximise structure rigidity whilst minimising structure weight and optical shadowing.	Observatoire de Paris	Design optimisation was conducted with the Nastran optimization tool.
The camera mounting interface should allow for fine adjustment.	Observatoire de Paris	The GCT's camera is attached to the structure via a mounting plate attached to the back of the camera, opposite to the camera's focal plane. This mounting plate can be camera-specific.

## 5.2 Optical Assembly Lessons Learnt

Lesson	Source of lesson	How lesson was incorporated
Three actuators in a triangular configuration allows each mirror facet to be aligned in all three axes.	HESS	The interface between the GCT's M1 dish and the individual M1 mirror facets consists of a triangular configurations of actuators, with similar specifications to that of HESS.
Minimising the exposure of the structure to the elements decreases the aging of the telescope's drive, mirror and camera elements, ultimately reducing maintenance time and costs.	HESS, VERITAS, Observatoire de Paris	A (military) solution in the form of a clam-shell shelter has been chosen. The shelter can survive 200 km/h wind and protect the telescope from rain, ice and snow.
The colour of the telescope must be optimised to reduce reflection of ambient light, whilst minimising heat absorption during the day.	HESS	Based on the analysis made for HESS, the same colour (RAL 3016) has been chosen for the GCT prototype and production designs.
Considering the optical quality needed for the SST mirrors, the traditional glass mirror solution may represent a non-optimal solution for GCT with unnecessary weight and cost implications.	LAM, Marseille	A new method has been developed whereby aluminium panels are mechanically deformed and then polished to satisfy CTA's optical smoothness specification. The panels are then coated in a similar process to IRFU's MST mirrors.
Collaboration with others within CTA, to reduce mirror costs, is desirable.	IRFU	GCT's mirrors are currently coated by the same company that coated IRFU's MST mirrors.
Glass-based mirrors cannot necessarily be used for mirrors with small radii of curvature.	Observatoire de Paris	GCT's M2 has been developed using a similar process to the petals of M1, that is, using aluminium bulk sample machined polished and coated. The main consequence is that the mass of the secondary mirror M2 is larger than originally designed for, thus necessitating a change in the structure design.

## 5.3 Camera Lessons Learnt

Lesson	Source of lesson	How lesson was incorporated
--------	------------------	-----------------------------



Dust ingress into the camera is difficult to avoid with an air-cooled system.	HESS, VERITAS, MAGIC	The GCT camera uses a sealed system with liquid cooling, to avoid ingress of dust and water.
Analog transmission over coaxial cables is subject to signal loss. Furthermore, coaxial cable connections are a major point of failure.	VERITAS	Front-end electronics to digitise the analog signals are placed in the focal plane, directly behind the photosensors, avoiding any need for analog signal transmission over large distances.
Analog transmission over fibres is subject to signal fluctuation, reducing reliability.	MAGIC	As above: front-end electronics placed in the focal plane, directly behind the photosensors.
Electrical noise pickup within the camera electronics can degrade the performance of the camera.	GCT prototyping	Preamplifiers are placed directly behind photo sensors and directly before the trigger and readout (TARGET) module.
PMTs can be damaged by accidental exposure to bright light when HV is on.	HESS	Ambient light sensor installed as a safety cut-out.
High temperatures can increase camera component failure rates.	HESS, VERITAS, MAGIC	A thermal cut-off switch is incorporated into the GCT camera design.
Coaxial cables with ground-shields connected at both ends can cause ground loops that are difficult to detect.	VERITAS	We have defined in the ICD that the transmission side of any ground-shielded coaxial cable is left unconnected.
Triggering and sampling on a single ASIC chip is difficult	CHEC-M camera prototype	The latest design of front-end electronics has the trigger/sampling functionality split onto two chips.
A reconfigurable trigger system is desirable.	GCT camera prototyping	Camera triggering is allocated to 4 FPGAs on the TARGET module.
A modular design allows for easier reconfiguring during prototyping.	GCT camera prototyping	Camera DACQ and peripherals controlled by boards separate from the camera back plane.
Camera desiccator mounting plate prone to warping during welding, rendering the hole thread useless	Mechanical prototyping	Purchase new hole tap for prototype. For long term solution, increase the size of the mounting plate.
Recesses on the sides of the camera front plate allowed the pooling of water during environmental tests resulting in water seeping through camera lid seals.	Environmental testing	Redesigned the camera front plate to minimise the potential for water to pool.
The camera body's metal plates can warp during machining.	Mechanical prototyping	For CHEC-M, the warping was within tolerance. However, for CHEC-S, aluminium tool plate was used and the material was machined equally from both sides.
The camera paint finish does not fully adhere to the metal surface.	Mechanical prototyping	A full hard anodising for the aluminium structure is the best solution.
Heat exchanger copper inlet and outlet pipes not properly aligned with the associated hole in the camera body to allow for compression seals.	Mechanical prototyping	For CHEC-M, the pipe locations were measured and the holes were drilled in the camera body to suit. For CHEC-S, the pipes will be soldered to hold them in the correct position.

Glue bonding used to fix glass diffusers of the calibration flashers failed temperature cycling tests.	Environmental testing	A new glass-metal light-cured adhesive was sourced, tested and found to pass the temperature cycling tests.
Insertion and extraction of photosensors at the focal plane was found to be very fiddly and time consuming.	Mechanical Prototyping	A tool has been designed and built to extract photon sensors quickly and safely from the focal plane interface.
Placement of micro ICs on the LED flasher board was time-consuming, with a high fail rate.	Flasher unit prototyping	While a short-term solution was found for the CHEC-M/S prototypes, the long term solution is to use industry to place the micro IC components during production.
Placement of LEDs on flasher unit by industry had a unsatisfactory high failure rate.	Flasher unit prototyping	Spacers were included in the final LED mounting design. This removed the risk of LED placement damaging the soldering and thus creating short-circuits.
Moving parts within a calibration unit, such as an array of neutral density filters, are prone to breaking.	HESS	A simple gate circuit with select LEDs was chosen as the basis for the flasher calibration units, with the brightness varied via resistors controlling current variations.
Insufficient capacity in the original camera controller / DACQ board solution to cope with all the peripheral systems need in the camera slow control and monitoring.	Camera Peripherals prototyping	A peripherals board was designed that would be a serial between the many and various peripherals and the DACQ board.
Commercial solutions, such as off-the-shelf encoders for lid positioning, do not always works as advertised.	CHEC lid prototyping	Reading of the position encoders was achieved with the PSoC design of the CHEC peripherals board. However, for the long term solution, an alternative motor supplier was found, but without an absolute position encoder capability.
The operational limits of commercial solutions, such as gearboxes for small electric motors, are not always accurate.	Environmental testing	Do not operate commercial components close to the advertised operational limits until thoroughly tested in the lab. Eg., for the GCT's camera lid, a larger motor is currently used so as to reduce the requirements from the selected gearbox.
The self capacitance of an LED ultimately limits the speed with which it can provide a light flash. Commercial forces mean that many modern UV LEDs are designed for constant illumination and so do not have the quick response of older LED designs.	VERITAS, HESS, GCT prototyping	LEDs from a wide variety of manufacturers were tested for the fast pulse circuits. Experience from previous versions of the calibration flasher circuit were input into the LED selection. Good contact is maintained with the manufacturer of the chosen LED. A backup solution, more technically demanding and expensive to implement, is available if LEDs suitable for the the favoured simple gated circuit become unavailable.

Initial design of focal plane plate resulted in a sub-optimal alignment of the flasher units.	GCT prototyping	The flasher mounting for the CHEC-M and CHEC-S prototypes was modified.
Silicon seals for environmental protection do not bond easily to surfaces, especially those with a small radius of curvature.	GCT prototyping	Lid design was modified to mount the silicon seal in a mould that is constructed of a material that allows a firmer bond (in this case plastic onto carbon fibre).
Interfaces are common points of failure/unforeseen cost	Many	Minimised the number of internal interfaces, as well as producing ICDs for each of them.



## A Full Product Breakdown Structure

Figures A.1-A.5 show the full GCT PBS.

PBS Code	Item	Acronym
6G	SST2MG Small-Sized Telescopes Dual Mirror - GCT	SST2MG
6G.00	Documentation	SST2MG-DOC
6G.00.01	Technical Design Report	SST2MG-DOC-TDR
6G.00.02	Plans	SST2MG-DOC-PLANS
6G.00.02.01	Project Management Plan	SST2MG-DOC-PLANS-PMP
6G.00.02.02	Product Breakdown Structure	SST2MG-DOC-PLANS-PBS
6G.00.02.03	Work Breakdown Structure	SST2MG-DOC-PLANS-WBS
6G.00.02.04	Schedule	SST2MG-DOC-PLANS-SCHED
6G.00.02.05	Cost	SST2MG-DOC-PLANS-COST
6G.00.02.06	Risk	SST2MG-DOC-PLANS-RISK
6G.00.02	Lessons Learned	SST2MG-DOC-PLANS-LL
6G.00.03	Detailed Designed Documents	SST2MG-DOC-DDD
6G.00.04	RAMS	SST2MG-DOC-RAMS
6G.00.04.01	Failure Mode Effects and Criticality Analysis	SST2MG-DOC-RAMS-FMECA
6G.00.05	Design Verification Document	SST2MG-DOC-DVD
6G.00.05.01	Compliance Matrix	SST2MG-DOC-DVD-COMPL
6G.00.05.02	Specification Verification Matrix	SST2MG-DOC-DVD-SVM
6G.00.06	Quality	SST2MG-DOC-Q
6G.01	Mechanical Assembly	SST2MG-MECH
6G.01.01	Telescope Base	SST2MG-MECH-TB
6G.01.01.01	Tower	SST2MG-MECH-TB-TW
6G.01.01.01.01	Mechanical Structure of Tower	
6G.01.01.01.02	Mechanical Fixing of the Tower	
6G.01.01.02.01	Fastening to the slab	
6G.01.01.02.02	Interface Tower to AAS	
6G.01.02	Optical Support Structure	SST2MG-MECH-OSS
6G.01.02.01	Mast and Truss Structure	SST2MG-MECH-OSS-MTS
6G.01.02.01.01	MTS Bottom Dish	
6G.01.02.01.01.01	Mechanical Structure	
6G.01.02.01.01.02	Fastening System	
6G.01.02.01.01.03	Fixing System to Bosshead	
6G.01.02.01.02	Serrurier Tubes	
6G.01.02.01.02.01	Truss Simple Tubes	
6G.01.02.01.02.02	Truss Double Tubes	
6G.01.02.01.02.03	Fastening System To Top Dish	
6G.01.02.01.02.04	Fastening System To Bottom Dish	
6G.01.02.01.02.05	Tubes Connectors - Bottom Dish Side	
6G.01.02.01.02.06	Tubes Connectors - MTS Top Dish Side	
6G.01.02.01.03	MTS Top Dish	
6G.01.02.01.03.01	Structure	
6G.01.02.01.03.02	Fastening System	
6G.01.02.01.03.03	Interface Top Dish / MTS Tubes	
6G.01.02.01.03.04	Support Cabinet	
6G.01.02.02	Dish M1	SST2MG-MECH-OSS-DM
6G.01.02.02.01	Mechanical Structure of Dish	
6G.01.02.02.01.01	Hexagonal Structure	
6G.01.02.02.01.02	Fastening System	
6G.01.02.02.01.03	Locking System Interface to MTS Bottom Dish	
6G.01.02.02.02	Rotative System	
6G.01.02.02.02.01	Mechanical support	
6G.01.02.02.02.02	Fastening system	
6G.01.02.02.02.03	Interface to dish M1	
6G.01.02.02.02.04	Interface to MTS bottom dish	
6G.01.02.03	Counterweight	SST2MG-MECH-OSS-CTW
6G.01.02.03.01	Mechanical Structure	
6G.01.02.03.01.01	Support Structure	
6G.01.02.03.01.02	Fastening System to AAS	
6G.01.02.03.02	Fixed Mass CW	
6G.01.02.03.02.01	Y fixed mass	
6G.01.02.03.02.02	Fastening system of the y mass	
6G.01.02.03.02.03	Movement mechanism	
6G.01.02.03.03	Moveable Mass CW	
6G.01.02.03.03.1	Mass Structure	
6G.01.02.03.04	Interface CW to bosshead	
6G.01.02.03.04.01	Reinforced CW to AAS	
6G.01.02.03.04.02	Reinforced CW to BD	
6G.01.03	Mount AAS	SST2MG-MECH-AAS
6G.01.03.01	AAS Structure	SST2MG-MECH-AAS-ST
6G.01.03.01.01	Fork	
6G.01.03.01.01.01	Structure	
6G.01.03.01.01.02	Mechanical Fixing of the Fork on Azimuth	
6G.01.03.01.02	Bosshead	
6G.01.03.01.02.01	Structure	
6G.01.03.01.02.02	Mechanical Fixing of the Bosshead to the Elevati	
6G.01.03.02	AAS Drives	SST2MG-MECH-AAS-DR
6G.01.03.02.01	Azimuth System	
6G.01.03.02.01.01	Drive System	
6G.01.03.02.01.02	Motor Shaft	
6G.01.03.02.02	Elevation 1	
6G.01.03.02.02.01	Drive System	
6G.01.03.02.02.02	Motor Shaft	
6G.01.03.02.03	Elevation 2	
6G.01.03.02.03.01	Drive System	

Figure A.1 – Page 1(/5) of the GCT PBS.

PBS Code	Item	Acronym
6G.01.04.02	Camera Alignment and Fastening System	SST2MG-MECH-CA-CAF
6G.01.04.02.01	Fastening of Scientific Camera	
6G.01.04.02.01.01	Flange to Connect Camera	
6G.01.04.02.01.02	CHEC-M / CHEC-S Adaptor	
6G.01.04.02.01.03	Fixing System of Camera	
6G.01.04.02.02	Tip Tilt Defocus Sub-Assembly	
6G.01.04.02.02.01	Structure	
6G.01.04.02.02.02	Actuators for tip tilt	
6G.01.04.02.03	Translation Sub-Assembly	
6G.01.04.02.03.01	Structure	
6G.01.04.02.03.02	Actuator for translation	
6G.01.04.02	Removal Mechanism System	SST2MG-MECH-CA-RMS
6G.01.04.02.01	Rotation axis	
6G.01.04.02.01.01	Structure	
6G.01.04.02.01.02	Fastening of rotation axis	
6G.01.04.02.01.03	Cable system	
6G.01.04.02.01.04	Removal mechanism elements	
6G.01.04.02.01.05	Fastening of cable system	
6G.01.04.02.02	Safety system	
6G.01.04.02.02.01	Safety elements	
6G.01.04.02.02.02	Fastening of locking system	
6G.01.05	Foundation	SST2MG-MECH-FOU
6G.01.05.01	Slab Structure	SST2MG-MECH-FOU-SS
6G.01.05.01.01	Concrete Slab	
6G.01.05.01.02	Maintainability Path	
6G.01.05.01.03	General Supply Trench	
6G.01.05.01.04	Foundation for Shelter	
6G.02	Optical Assembly	SST2MG-OPT
6G.02.01	Primary Mirror Structure	SST2MG-OPT-PMS
6G.02.01.01	Primary Tesselated Mirror	SST2MG-OPT-PMS-PM
6G.02.01.01.01	Mirror Unit	
6G.02.01.02	Mechanical Support	SST2MG-OPT-PMS-MS
6G.02.01.02.01	Triangular Structure	
6G.02.01.02.02	Fixing System	
6G.02.01.02.02.01	Fixing to M1 Dish	
6G.02.01.02.02.02	Fixing to Actuators	
6G.02.02	Secondary Mirror Structure	SST2MG-OPT-SMS
6G.02.02.01	Secondary Mirror	SST2MG-OPT-SMS-SM
6G.02.02.01.01	Mirror M2	
.02.02.01.01.01	M2 segments	
.02.02.01.01.02	Assembly to form monolithic	
6G.02.02.01.02	Interface Mirror Actuators	
6G.02.02.01.02.01	Mechanical System	
6G.02.02.01.02.02	Fixing to Actuators	
6G.02.03	Optical Alignment	SST2MG-OPT-OA
6G.02.03.01	Alignment System	SST2MG-OPT-OA-AS
6G.02.03.01.01	Alignment Modules	
6G.02.03.01.01.01	Optical Systems	
6G.02.03.01.01.02	Mechanical Systems	
6G.02.03.01.02	Focal Plane Instrumentation	
6G.02.03.01.02.01	CCD	
6G.02.03.01.02.02	Mechanical Fastening System	
6G.02.03.02	Mirror Actuation System	SST2MG-OPT-OA-MAS
6G.02.03.02.01	Actuators Modules	
6G.02.03.02.01.01	Actuators	
6G.02.03.02.01.02	Datum Switches	
6G.02.03.02.01.03	End Switches	
6G.02.03.02.01.04	Local Driver Electronics Unit	
6G.02.03.02.01.05	Stroke Sensors	
6G.02.03.02.02	Fastening System	
6G.02.03.02.02.01	Fixing system	

Figure A.2 – Page 2(/5) of the GCT PBS.

PBS Code	Item	Acronym
6G.03	Camera Assembly	SST2MG-CAM
6G.03.01	Camera Mechanics	SST2MG-CAM-MECH
6G.03.01.01	Internal Mechanics	SST2MG-CAM-MECH-INT
6G.03.01.01.01	Rack	
6G.03.01.01.02	Fixings for Internal Mechanics	
6G.03.01.02	Enclosure	SST2MG-CAM-MECH-ENC
6G.03.01.02.01	Entrance Window	
6G.03.01.02.02	Focal Plane Plate	
6G.03.01.02.03	Backplate	
6G.03.01.02.04	Case	
6G.03.01.02.04.01	Case Components	
6G.03.01.02.04.02	Case Fixtures, Fittings, Seals	
6G.03.01.02.04.03	Desiccators	
6G.03.01.03	Thermal Exchange Unit	SST2MG-CAM-MECH-TEU
6G.03.01.03.01	Heatsinks	
6G.03.01.03.02	Copper Piping	
6G.03.01.03.03	Base	
6G.03.01.03.04	Fan Support	
6G.03.01.03.05	Adhesive, Inlet Seals, Insulation, Connectors and Fixin	
6G.03.01.04	Lid Assembly	SST2MG-CAM-MECH-LID
6G.03.01.04.01	Lid	
6G.03.01.04.02	Lid Brackets	
6G.03.01.04.03	Lid Locking System	
6G.03.01.04.04	Lid Seal, Fixtures and Fittings	
6G.03.02	Photodetectors	SST2MG-CAM-PD
6G.03.02.01	Photodetectors	SST2MG-CAM-PD-PD
6G.03.02.02	Photodetector Base PCB	SST2MG-CAM-PD-BASE
6G.03.03	Camera Electronics	SST2MG-CAM-ELEC
6G.03.03.01	Front-end Buffers	SST2MG-CAM-ELEC-BUF
6G.03.03.01.01	Front-end Buffer PCB(s)	
6G.03.03.01.02	Front-end Buffer to TARGET Module Cables	
6G.03.03.02	TARGET Modules	SST2MG-CAM-ELEC-TM
6G.03.03.02.01	Mechanics	
6G.03.03.02.02	ASICs	
6G.03.03.02.03	Power and Monitoring PCB	
6G.03.03.02.04	ASIC and Readout PCB	
6G.03.03.02.05	TARGET Module FW	
6G.03.03.02.06	TARGET Module Low-Level SW	
6G.03.03.03	Backplane	SST2MG-CAM-ELEC-BP
6G.03.03.03.01	Backplane Mother Board	
6G.03.03.03.02	Backplane Power Daughter Board	
6G.03.03.03.03	Backplane Supporting Items	
6G.03.03.03.04	Backplane FW	
6G.03.03.03.05	Backplane Low-Level SW	
6G.03.03.04	DACQ	SST2MG-CAM-ELEC-DAC
6G.03.03.04.01	DACQ PCB	
6G.03.03.04.02	DACQ Supporting Items	
6G.03.03.04.03	DACQ Firmware	
6G.03.03.04.04	DACQ Low-Level SW	
6G.03.03.05	Peripherals Board	SST2MG-CAM-ELEC-PB
6G.03.03.05.01	Peripherals Board PCB	
6G.03.03.05.02	Peripherals	
6G.03.03.05.02.01	Lid Control	
6G.03.03.05.02.02	Fans	
6G.03.03.05.02.03	Temperature and Humidity Sensors	
6G.03.03.05.02.04	Ambient Light Sensor	
6G.03.03.05.03	Peripherals Cables	
6G.03.03.05.03.01	Peripherals Board to backplane cables	
6G.03.03.05.03.02	Motor cables	
6G.03.03.05.03.03	Fan cables	
6G.03.03.05.03.04	Temperature and humidity sensor cables	
6G.03.03.05.03.5	Ambient Light Sensor cables	
6G.03.03.05.04	Peripherals Board FW	
6G.03.03.05.05	Peripherals Board Low-Level SW	
6G.03.03.06	Internal Cabling	SST2MG-CAM-ELEC-CAB
6G.03.03.06.01	Internal Power Distribution	
6G.03.03.06.01.01	Power cable with case bulk-head connector	
6G.03.03.06.01.02	Power Distribution Busbar	
6G.03.03.06.01.03	Thermostat-power Cutout Circuit	
6G.03.03.06.02	Internal Fibre Distribution	
6G.03.04	Calibration System	SST2MG-CAM-CAL
6G.03.04.01	LED Flasher Units	SST2MG-CAM-CAL-FLSH
6G.03.04.01.01	LED Flasher Unit LED PCBs	
6G.03.04.01.02	LED Flasher Unit Mechanics & Diffuser	
6G.03.04.01.03	LED Flasher Unit Support Items	
6G.03.04.01.04	LED Flasher Unit FW	
6G.03.04.01.05	LED Flasher Unit Low-Level SW	
6G.03.04.02	Pointing Units	SST2MG-CAM-CAL-PNT
6G.03.04.02.01	Pointing Unit Electrical Components	
6G.03.04.02.02	Pointing Unit Optical / Mechanical Components	
6G.03.05	Camera Auxiliary Systems	SST2MG-CAM-AUX
6G.03.05.01	Camera Power Supply	SST2MG-CAM-AUX-PSU
6G.03.05.01.01	Power Supply Unit	
6G.03.05.01.02	Power Supply Supporting Items	
6G.03.05.01.02.01	Power Supply AC Power Cable (Internal to Top D	
6G.03.05.01.02.02	Power Supply DC Power Cable to Camera (via C	
6G.03.05.01.02.3	Power Supply Communication Cable (Internal to T	
6G.03.05.01.03	Power Supply Low-Level SW	
6G.03.05.02	Chiller	SST2MG-CAM-AUX-CHIL
6G.03.05.02.01	Chiller Unit	
6G.03.05.02.02	Chiller Pipework	
6G.03.05.02.03	Chiller Supporting Items	
6G.03.05.02.04	Chiller Low-Level SW	
6G.03.05.03	Shipping Containers	SST2MG-CAM-AUX-SHIP
6G.03.05.03.01	Transport Case	
6G.03.06	Camera Software	SST2MG-CAM-SW
6G.03.06.01	Camera Readout Software	SST2MG-CAM-SW-CS
6G.03.06.02	Camera Control Software	SST2MG-CAM-SW-CC

Figure A.3 – Page 3(5) of the GCT PBS.



PBS Code	Item	Acronym
6G.04	Auxiliary Systems	SST2MG-AUX
6G.04.01	Slab Cabinets	SST2MG-AUX-SC
6G.04.01.01	Power Cabinet	SST2MG-AUX-SC-PSC
6G.04.01.01.01	Cabinet	
6G.04.01.01.01.01	Cabinet enclosure	
6G.04.01.01.01.02	Power supply elements	
6G.04.01.01.01.03	Safety system	
6G.04.01.01.01.04	Power supply elements	
6G.04.01.01.02	Patches in power cabinet	
6G.04.01.01.02.01	Alimentation	
6G.04.01.01.03	Fastening system	
6G.04.01.01.03.01	Bracket Supporting Cabinet	
6G.04.01.01.03.02	Fixing System	
6G.04.01.02	Network supply	SST2MG-AUX-SC-NS
6G.04.01.02.01	Cabinet	
6G.04.01.02.01.01	Cabinet enclosure	
6G.04.01.02.01.02	Network elements	
6G.04.01.02.02	Cables	
6G.04.01.02.02.01	Optical Fibers	
6G.04.01.02.02.02	Copper Cables	
6G.04.01.03	Shelter cabinet	SST2MG-AUX-SC-SCS
6G.04.01.03.01	Electrical Cabinet	
6G.04.01.03.02	Safety System	
6G.04.01.03.02.01	Left end switch closed	
6G.04.01.03.02.02	Left end switch open	
6G.04.01.03.02.03	Right end switch closed	
6G.04.01.03.02.04	Right end switch open	
6G.04.01.03.03	Relays	
6G.04.01.03.03.01	Safety relays	
6G.04.01.04	Control Panel Cabinet	SST2MG-AUX-SC-CPC
6G.04.01.04.01	Cabinet	
6G.04.01.04.01.01	Cabinet enclosure	
6G.04.01.04.01.02	Power supply elements	
6G.04.01.04.01.03	Monitoring elements	
6G.04.01.04.01.04	Safety System	
6G.04.01.04.01.05	Housekeeping	
6G.04.01.04.02	Patches in control panel cabinet	
6G.04.01.04.02.01	Housekeeping	
6G.04.01.04.02.02	Alimentation	
6G.04.01.04.02.03	Network	
6G.04.01.04.03	Fastening system	
6G.04.01.04.03.01	Mechanics	
6G.04.01.04.03.02	Fastening system	
6G.04.01.05	Telescope Field Safety	SST2MG-AUX-SC-TFS
6G.04.01.05.01	Safety Barrier	
6G.04.01.05.01.01	Interlock	
6G.04.01.05.01.02	Safety tools	
6G.04.01.05.02	Parking Sensor	
6G.04.01.05.02	End switches	
6G.04.01.06	Patches between cabinets	SST2MG-AUX-SC-PC
6G.04.01.06.01	Slab cabinet to fork cabinet	
6G.04.01.06.01.01	Alimentation plug and cables	
6G.04.01.06.01.02	Network plug and cables	
6G.04.01.06.02	External word to slab cabinet	
6G.04.01.06.02.01	Alimentation plug and cables	
6G.04.01.06.02.02	Network plug and cables	

Figure A.4 – Page 4(5) of the GCT PBS.

PBS Code	Item	Acronym
6G.04.02	Telescope Cabinets	SST2MG-AUX-TC
6G.04.02.01	Fork Power Cabinet	SST2MG-AUX-TC-FPC
6G.04.02.01.01	Chiller Cabinet	
6G.04.02.01.01.01	Mechanical support	
6G.04.02.01.02	Electrical cables	
6G.04.02.01.03	Fastening system	
6G.04.02.01.03.01	Mechanical support	
6G.04.02.01.03.02	Anti-vibration system	
6G.04.02.02	Fork Main cabinet	SST2MG-AUX-TC-FMC
6G.04.02.02.01	Cabinet	
6G.04.02.02.01.01	Cabinet enclosure	
6G.04.02.02.01.02	Power supply elements	
6G.04.02.02.01.03	Monitoring elements	
6G.04.02.02.01.04	Housekeeping	
6G.04.02.02.01.05	Safety system	
6G.04.02.02.02	Patches in Fork main cabinet	
6G.04.02.02.02.01	Motors housekeeping	
6G.04.02.02.02.02	Alimentation	
6G.04.02.02.02.03	Network	
6G.04.02.02.03	Fastening system	
6G.04.02.02.03.01	Mechanical support	
6G.04.02.02.03.02	Fastening system	
6G.04.02.03	MTS bottom Cabinet	SST2MG-AUX-TC-MBC
6G.04.02.03.01	Cabinet	
6G.04.02.03.01.01	Cabinet enclosure	
6G.04.02.03.01.02	Power supply elements	
6G.04.02.03.01.03	Monitoring elements	
6G.04.02.03.01.04	Housekeeping	
6G.04.02.03.01.05	Safety system	
6G.04.02.03.02	Patches in MTS cabinet	
6G.04.02.03.02.01	Housekeeping	
6G.04.02.03.02.02	Alimentation	
6G.04.02.03.02.03	Network	
6G.04.02.03.03	Fastening system	
6G.04.02.03.03.01	Mechanical support	
6G.04.02.03.03.02	Fastening system	
6G.04.02.04	Top Dish Cabinet	SST2MG-AUX-TC-TDC
6G.04.02.04.01	Cabinet	
6G.04.02.04.01.01	Cabinet enclosure	
6G.04.02.04.01.02	Power supply elements	
6G.04.02.04.01.03	Monitoring elements	
6G.04.02.04.01.04	Housekeeping	
6G.04.02.04.01.05	Safety system	
6G.04.02.04.01.06	Camera interface	
6G.04.02.04.02	Patches in Top cabinet	
6G.04.02.04.02.01	Housekeeping	
6G.04.02.04.02.02	Alimentation	
6G.04.02.04.02.03	Network	
6G.04.02.04.03	Fastening system	
6G.04.02.04.03.01	Mechanical support	
6G.04.02.04.03.02	Fastening system	
6G.04.02.05	Patches between telescope cabinets	SST2MG-AUX-TC-PTC
6G.04.02.05.01	Fork cabinet to Bottom cabinet	
6G.04.02.05.01.01	Alimentation plug and cables	
6G.04.02.05.01.02	Network plug and cables	
6G.04.02.05.02	Bottom cabinet to top cabinet	
6G.04.02.05.02.01	Alimentation plug and cables	
6G.04.02.05.02.01	Network plug and cables	
6G.04.03	Shelter	SST2MG-AUX-SHL
6G.04.03.01	Structure of Shelter	SST2MG-AUX-SHL-SS
6G.04.03.01.01	Fabric	
6G.04.03.01.02	Armatures	
6G.04.03.01.03	Mechanical Link between Shelter and Foundation	
6G.04.03.02	Motorization	SST2MG-AUX-SHL-SMZ
6G.04.03.02.01	Motors	
6G.04.03.02.02	Hardware	
6G.04.03.02.03	Sensors	
6G.04.03.02.03.01	End Switches	

Figure A.5 – Page 5/(5) of the GCT PBS.

## **B Full Work Breakdown Structure**

The full WBS can be found electronically in: GCT-WBS\_v3p10.xls.



## C Cost Estimates

Full cost details are included electronically as spreadsheet: GCT-WBS\_v3p10.xls.



## D Risk Register

The full risk register is included electronically as spreadsheet `GCT_RiskRegister.xls`, and given in Figures D.1–D.3.

Risk Category	Risk Description	Project Impact	Severity			Detection method	Accept / Review	Recommended Action / Mitigation	Contingency Plan (what do if the risk does)			
			Internal / External	Severity	Probability of occurrence					Criticality		
Industrial Relations	Complications in the timescale for generating tender requests	Delays to the start of procurement in the Pre-Production and Production Phases.	Internal	4	4	1	4	Communication between suppliers and GCT Project Manager.	Accept	Organisation of tender processes for Production Phase to start at the earliest stage.	Additional FTE with the desired skills integrated in the call for tender.	
	Delay in the contract negotiation process with suppliers	Delays to the start of procurement in the Pre-Production and Production Phases.	Internal	3	6	1	6	Communication between suppliers and GCT Project Manager.	Reduce	Start discussions early with suppliers to streamline the process at the start of the Production Phase.	Accept additional delay, but begin discussions with alternative suppliers as soon as appropriate.	
	Insufficient interest in tender process from industrial partners	Delays to the start of procurement in the Pre-Production and Production Phases.	External	4	4	2	8	Communication between suppliers and GCT Project Manager.	Reduce	Approach suppliers early on for discussions before producing tender requests.	Approach specific suppliers and re-write tender requests.	
	Potentially different prices and time-scales for different GCT partners when purchasing the same item, complicating the procurement process and increasing costs.		External	3	1	3	2	6	Communication between CTA Project Manager and GCT Project Manager.	Beyond Project Control		Negotiate contracts with suppliers within the GCT project.
	Failure for CTA to put framework agreements in place where appropriate		External	3	1	3	2	6	Communication between CTA Project Manager and GCT Project Manager.	Beyond Project Control		Negotiate contracts with suppliers within the GCT project.
	Delay in production and/or qualification of components in industry	Delays to the start of procurement in the Pre-Production and Production Phases.	External	3	3	9	1	9	Communication between suppliers and GCT Project Manager. Internal project deadlines missed.	Reduce	Engage companies early on to obtain a close working relationship. Include penalty clause in contracts for late delivery of large orders.	Accept delay, reschedule appropriately.
	Technical inputs required for tender or production are delayed	Delays to the start of procurement in the Pre-Production and Production Phases, potential to create incorrect cost and delivery time estimates from industry.	Internal	3	2	6	1	6	Internal project deadlines missed.	Reduce	Engage companies early on to acquire knowledge of the details required for production.	Accept delay, reschedule appropriately.
	Technical inputs required for tender or production are inadequate	Sub-standard component production that does not meet V&V, requiring re-production resulting in increased schedule and cost impact.	Internal	3	2	6	2	8	Feedback from industry.	Reduce	Engage companies early on to acquire knowledge of the details required for production.	Revise inputs and accept delay, reschedule appropriately.
	Inaccurate time estimates from manufacturers	Delays to the start of production in the Pre-Production and Production Phases.	External	3	2	6	2	8	Post Pre-Production Phase procurement evaluation.	Reduce	Engage companies early on, and place preliminary orders in the Pre-Construction and Pre-Production Phases to ensure accurate time estimates are provided.	Accept delay, reschedule appropriately. Cancel and re-place order with alternative company if more efficient, include penalties in contracts for late delivery.
	Inaccurate cost estimates from manufacturers	Potential cost over-run, or insufficient funds to produce envisaged number of telescopes (reduced scope).	External	3	1	3	3	9	Post Pre-Production Phase procurement evaluation.	Reduce	Engage companies early on, and place preliminary orders in the Pre-Construction and Pre-Production Phases to ensure accurate cost estimates are provided.	Accept cost overrun, re-negotiate or find alternative supplier if this has a smaller impact on the project outcome. Request additional funding if needed, or reduce project scope.
	Failure to negotiate a reasonable price for contracts	Potential cost over-run, or insufficient funds to produce envisaged number of telescopes (reduced scope).	Internal	3	1	3	1	3	Communication between suppliers and GCT Project Manager.	Accept	Engage companies early on, and place preliminary orders in the Pre-Construction and Pre-Production Phases to ensure accurate and reliable cost estimates are provided.	Find alternative supplier or request additional funding.
	Unacceptable contract terms	Delays to the start of production in the Pre-Production and Production Phases.	Internal	2	2	4	1	4	Communication between suppliers and GCT Project Manager.	Accept	Engage companies early on to obtain a close working relationship.	Locate alternative supplier, or involve legal / administrative teams at institutes.
	Conflict with vendor leads to project issues	Delays to the start of production in the Pre-Production and Production Phases.	Internal	3	2	6	1	6	Communication between suppliers and GCT Project Manager. Internal project deadlines missed.	Reduce	Engage companies early on to obtain a close working relationship.	Locate alternative supplier, or involve legal / administrative teams at institutes.
	Unforeseen technical production issues	Potential delays, additional costs and sub-standard components.	External	3	1	3	3	9	Internal project deadlines missed.	Reduce	Minimise changes between Pre-Production and Production manufacturing runs and try to use the same industrial partners.	Accept delays and reschedule. Find alternative suppliers and request additional funding if necessary.
	Delays in payment to the company	Delays to the start of production in the Pre-Production and Production Phases, potentially additional cost implications.	Internal	2	1	2	1	2	Communication between suppliers, involved institutes and GCT Project Manager.	Accept	Engage institute purchasing departments at time of contract negotiations. Implement a 'goods management' system to ensure that the Project Manager is aware when contracts have been fulfilled.	Direct manpower to resolve payment between institutes purchasing departments and suppliers.
	Technical	Company bankruptcy / closure	Industrial partners fail to deliver and others must be found, creating delays and possibly resulting in insufficient funds to produce envisaged number of GCT telescopes (reduced scope).	External	4	1	4	3	12	Communication between suppliers and GCT Project Manager.	Beyond Project Control	
Production of sub-standard components that fail V&V		Re-production elsewhere resulting in increased schedule and cost impact	External	4	2	8	1	8	V&V	Reduce	Minimise changes between Pre-Production and Production manufacturing runs and try to use the same industrial partners. Provide accurate and detailed requirements and include quality clauses in contracts. If appropriate provide industrial partners with specific test rigs for components.	Locate alternative supplier, or involve legal / administrative teams at institutes. Request additional funding if necessary.
Pre-Construction Phase component development takes longer than planned to meet requirements		Pre-Production design schedule	Internal	4	3	12	1	12	Monitoring of schedule and technical progress by Project Manager.	Reduce	Minimise additional component development and request component development funding beyond current budgetary cap.	Accept delays to Pre-Production Phase, or de-scope Pre-Production Phase.
Pre-Production Phase component technical problems		Delay to Production design, de-scope of Pre-Production phase, increased cost to Pre-Production phase	Internal	4	2	8	1	8	Communication between work-package coordinators and team members.	Reduce	Spend adequate time in Pre-Construction Phase on component development and documentation.	Further component development, accept delays and reschedule.
Pre-Production Phase AIT technical problems		Delay to Production design, de-scope of Pre-Production phase, increased cost to Pre-Production phase	Internal	3	2	6	1	6	Communication between work-package coordinators and team members.	Reduce	Document prototyping AIT in Pre-Construction Phase to minimise uncertainties in Pre-Production Phase.	Accept delays, adapt AIT plans for future use in Production Phase and reschedule.
Pre-Production Phase Assemblies fail to pass V&V		Delay to Production design, de-scope of Pre-Production phase, increased cost to Pre-Production phase	Internal	4	2	8	1	8	V&V	Reduce	Spend adequate time in Pre-Construction Phase on component development.	Further component development, accept delays and reschedule.
Final CTA array layout delayed		Delays to / sub-optimal Production design	External	2	3	6	1	6	Communication between GCT Project Manager and CTA PO.	Beyond Project Control		Accept possible sub-optimal GCT design.
Complications in production and/or qualification of Production Phase components in house		Production Phase schedule	Internal	3	2	6	1	6	Communication between work-package coordinators and team members.	Reduce	Spend adequate time in Pre-Construction and Pre-Production Phases on documentation of component production and qualification. Implement Quality Assurance procedures with institutes responsible for production and qualification.	Accept delays and re-schedule, attempt to redistribute work to other institutes.
Production Phase components become redundant post final design		Re-design required during Production resulting in delays to Production Phase schedule, possibly insufficient funds to produce envisaged number of telescopes (reduced scope).	External	3	1	3	3	9	Noticed during Production Phase procurement and reported to the Project Manager.	Reduce	Confirm component life-cycles and availability prior to design finalisation. Procure spares upfront in Production Phase.	Re-design of affected sub-assemblies.
Production Phase components become prohibitively expensive post final design		Re-design required during Production resulting in delays to Production Phase schedule, possibly insufficient funds to produce envisaged number of telescopes (reduced scope).	External	4	2	8	1	8	Noticed during Production Phase procurement and reported to the Project Manager.	Reduce	Obtain component quotes for Production Phase as early as possible, including spares, and where appropriate agree contracts with vendors to guarantee price.	Re-design system to use alternative components, or source current components from alternative vendor.
Production Phase components fail to pass V&V post final design		Re-design required during Production resulting in delays to Production Phase schedule, possibly insufficient funds to produce envisaged number of telescopes (reduced scope).	Internal	4	2	8	1	8	V&V	Reduce	Spend adequate time in Pre-Construction Phase on component development and documentation.	Further component development, accept delays and reschedule.
Complication in preparation of Production Phase AIT facilities		Production Phase schedule	Internal	2	2	4	1	4	Communication between work-package coordinators and team members.	Accept	Spend adequate time in Pre-Production Phase on AIT site development and documentation.	Accept delays, but assign additional resources if possible to minimise delays.
Loss of GCT camera AIT site in Production Phase		Production Phase schedule	Internal	2	2	4	2	8	Communication between work-package coordinators and team members.	Reduce	Several AIT sites should be made available in the Production Phase to minimise the temporary / permanent loss of any one site.	Re-distribute resources and work-load to other existing AIT sites.
Delivery of Production Phase components to AIT sites not scheduled promptly		Production Phase schedule	Internal	2	2	4	1	4	Communication between GCT Project Manager and CTA PO.	Accept	Allocate time and resource to produce a shipping schedule in conjunction with the CTA PO.	Accept delays, reschedule, document.
Delivery of Production Phase components to AIT sites incur unforeseen delays		Production Phase schedule	External	1	2	2	2	4	Monitoring of shipping progress by GCT Project Manager, or other delegated individual.	Accept	Include a working margin between delivery and integration times and storage facilities on site to minimise the impact. Work with a dedicated (CTA allocated) shipping company to minimise the probability of import / export delays.	Accept delays, reschedule.
Production Phase components damaged during handling to AIT sites		Production Phase schedule and cost	External	3	2	6	1	6	Inspection at AIT site.	Reduce	Implement Quality Assurance procedures. Work with reputable shipping companies.	Use spares, request further funding / pursue insurance for replacement / repair.
Production Phase components damaged during handling and assembly at AIT sites	Production Phase schedule and cost	Internal	3	1	3	1	3	Inspection prior to commissioning at AIT site.	Accept	Introduce Quality Assurance procedures and handling methods including training. Provide adequate spares.	Use spares, request further funding for if needed for additional procurement.	
Production Phase Assemblies fail to pass V&V	Could result in a re-build or re-design during Production resulting in delays to Production Phase schedule, possibly insufficient funds to produce envisaged number of telescopes (reduced scope).	Internal	4	1	4	1	4	V&V	Accept	Spend adequate time in Pre-Production Phase on Assembly qualification and documentation.	Further component development, accept delays and reschedule.	

Figure D.1 – GCT risk register, page 1.





Risk ID	Risk Category	Risk Description	Cause	Impact	Likelihood	Severity	Risk Score	Mitigation Strategy	Residual Risk Score	Mitigation Status	Comments			
												External	Internal	Financial
67	Site Availability	CTA southern site selection delay	Delay to final GCT design, delay to Pre-Production telescope deployment	External	2	6	1	6	GCT presence on CTA Project Committee meetings	Beyond Project Control	-	Proceed with design suitable for worst-case environmental conditions.		
		Delay to CTA southern site availability (i.e. INFRA) at Pre-Production	Delay to Pre-Production GCT onsite commissioning and V&V	External	2	6	1	6	GCT presence on CTA Project Committee meetings	Beyond Project Control	-	Accept delays to Pre-Production Phase, or shorten / de-scope Pre-Production Phase on-site testing.		
		Delay to CTA southern site availability (i.e. INFRA) at Production - boundaries and lower	Delay to final GCT Production	External	3	6	1	6	GCT presence on CTA Project Committee meetings	Beyond Project Control	-	Accept delays to on-site commissioning.		
		Delay to CTA southern site availability (i.e. INFRA) at Production - network communications	Delay to final GCT Production	External	2	4	1	4	GCT presence on CTA Project Committee meetings	Beyond Project Control	-	Continue with mechanical installation and await networking.		
68	Executive Support	GCT Management Committee fail to support project or become disengaged	Poor / unfriendly decisions resulting in non-optimal design, lack of funding, inappropriate manpower acquisition.	Internal	4	1	4	2	Regular communication between GCT Management Committee and Project Manager	Reduce	Written commitments from all institutes with agreed FTE contributions for senior staff prior to Production. Regular changes to representation on the Management Committee.	Replace Management Committee members.		
		Conflict between GCT grant Pis, or other stakeholders that disrupts project	Delays to design complete and / or production.	Internal	3	2	6	1	6	Regular communication between GCT Management Committee and Project Manager	Reduce	Develop a clear management procedure to deal with issue resolution.	GCT Project Manager spends time resolving issues.	
		Movement of senior project members disrupts project	Loss of critical knowledge and delays.	Internal	3	3	9	1	6	Regular communication between GCT Management Committee and Project Manager	Beyond Project Control	-	Redistribute tasks to other GCT institutes and / or incur delays whilst project members relocate.	
69	Project Management	Failure to follow methodology	Inefficiency resulting in cost overruns, delays and possibly conflict between project members.	Internal	2	2	4	1	4	Communication between GCT Project Manager and WP Coordinators.	Accept	Appoint experienced Project Manager, who reports to the GCT Management Committee regularly. Produce Project Management plan and distribute to WP Coordinators.	Review methodology, move forward in a pragmatic way minimise delays.	
		Timescale of the GCT Production Phase exceed that planned by CTA	May not be able to take part in previous organization of CTA site, INFRA and AIT integration within the consortium.	Internal	4	3	12	1	6	Communication between Project Manager and CTA Project Manager	Reduce	Preparation of Production Phase plans should incorporate CTA (external) milestones.	CTA full operations delayed.	
		Problems associated with the distributed nature of the GCT sub-consortium across several countries (e.g. large overhead generates additional coordination effort).	Risk of redundancy and/or missing element (e.g. documents/AIT both in labs and onsite non-optimal and incurs delays.	Internal	3	1	3	2	6	Communication between GCT Management Committee and GCT Project Manager	Reduce	Appoint experienced Project Manager, who reports to the GCT Management Committee regularly. Require that members request support for local grant management.	Request additional funding and / or manpower for management and coordination.	
		Lack of management or control	Inability to predict cost / schedule changes, disorganisation between project parties and CTA, likely resulting in delays and even complete failure to provide the end product.	Internal	4	2	8	1	8	Communication between GCT Management Committee and GCT Project Manager	Reduce	Appoint experienced Project Manager, who reports to the GCT Management Committee regularly.	Revise management plan and consider manpower changes.	
		Errors in key project management processes	Costs underestimated, tasks lined incorrectly resulting in delays, manpower under or over estimate.	Internal	3	2	6	1	6	Communication between GCT Project Manager and CTA Project Manager	Reduce	Appoint experienced Project Manager, who reports to the GCT Management Committee regularly.	Revise management plan and consider manpower changes.	
		Low individual / team motivation	Potential for lack of communication, failure to meet deadlines, poor quality work, disruption to other parts of the project.	Internal	2	2	4	1	4	Communication between work-package coordinators and team members.	Accept	Engage team members in wider CTA context. Request travel funding to allow team members to fully engage with the project and CTA. Avoid over-loading staff. Allow team members to have some 'ownership' of work, rather than 'following orders'.	Provide team-members with Project context and engage them with CTA. Provide individuals with 'ownership' where appropriate.	
		Lack of commitment from individuals responsible for the delivery of components	Failure to meet deadlines, potential to create substantial delays and de-rail the project.	Internal	3	2	6	1	6	Communication between work-package coordinators and team members.	Reduce	Ensure the responsibility matrix is clear and that responsible / accountable individuals are adequately supported to work on the project. Ensure some redundancy in knowledge by having at least 2 individuals contribute / understand a given piece of critical work.	Recruit / appoint replacement manpower, or outsource to industry or other CTA institutes.	
		Technical problems with the Project Management tools	Results in lack of control.	Internal	2	4	8	1	8	Regular use of tools.	Reduce	Make an early choice of tools and stick with them. Choose well documented tools with support options.	Utilise IT support at GCT member institutes.	
		Failure to integrate efficiently with CTA PO and WPs	Could result in a non-compliant design that requires later changes. Failure to take advantage of existing solutions, resulting in extra work, delays and increased cost.	External	2	2	4	1	4	GCT presence on CTA Project Committee meetings.	Accept	Request travel funding to allow team members to fully engage with the project and CTA. Regular presence at PC meetings.	GCT Project Manager, or others to spend time directly at CTA PO.	
		Conflict over proposed changes	Delays and non-optimal final design.	Internal	3	2	6	1	6	Regular communication between all project members.	Reduce	Well defined change management system, regular communication between technical members of the project.	Create an 'issue' and follow a well-defined issue management process to resolve.	
		Lack of a change management system	Potential for interface failure in the final design.	Internal	3	2	6	1	6	Project management	Reduce	Include the production of a change management system as WBS activities. Liaise with CTA PO on the production of the change management system.	Accept delays and reallocate manpower to create a change-management system.	
		Change requests are of low quality (e.g. ambiguous)	Potential for interface failure in the final design.	Internal	3	3	9	1	9	Communication between the individual making the request and the team member(s) implementing it.	Reduce	Well defined change management system making the request and the regular communication between technical members of the project.	Communication between individual making the request and the technical project team. Possible changes to the change management system.	
		Change requests result in a design that is in conflict with requirements	Potential for a product that fails the V&V process.	Internal	4	2	8	2	10	V&V	Reduce	Review DVD as part of change management process.	Make changes to the design and reassess.	
		63	Scope	Conflict over technical issues	Delays and non-optimal final design.	Internal	3	4	12	1	6	Communication between Project Manager, work-package coordinators and team members.	Reduce	Regular communication between technical members of the project.
64	GCT Project team misunderstand CTA requirements	Potential for a product that passes the internal V&V process, but fails CTA testing and is not expected by CTA. Potential for an over-engineered (gold-plated) product.		Internal	4	2	8	2	10	CTA reviews of GCT design.	Reduce	Ensure GCT DVD is accurate and up to date as a reference point for the GCT specifications and how they address the CTA requirements.	Adapt specifications to re-address requirements. Possible re-design.	
65	Communication overhead under resourced - communication meetings and calls) requires more manpower than anticipated	Results in a lack of communication, or key personnel spending more time than anticipated on communication, resulting in delays in key work.		Internal	2	3	6	1	6	Slower than expected progress and/or lack of communication becomes apparent.	Reduce	Produce communications plan as part of the project management plan and review prior to Production Phase funding applications.	Redirect resources, refine communication plan.	
66	Lack of communication	Potential for delays, and non-optimal design.		Internal	3	3	9	1	6	GCT Management Committee inspection.	Reduce	Produce communications plan as part of the project management plan.	Redirect resources towards communication, refine communication plan.	
67	Impacted individuals are not kept informed about decisions / changes	Design features have to be incorporated later than optimal, increasing cost and design cost. Possibility that interfaces fail.		Internal	4	3	12	1	6	Lack of communication becomes apparent.	Reduce	Clear RASCI matrix, regular communication between technical members of the project. Well defined ICD and change-control process.	Accept delays, adapt communication plan to prevent future incidents.	
68	Gold plating inflates scope - i.e. the project team add their own product features that aren't in requirements or change requests.	Over-engineered product that increased cost, longer development time and possibly longer production time.		Internal	4	2	8	3	13	V&V, internal design reviews.	Reduce	Ensure GCT DVD is accurate and up to date as a reference point for the GCT specifications and how they address the CTA requirements.	Simplify product before Production Phase if there is a significant cost benefit, otherwise accept over-specified product.	
69	Activities are missing from scope / WBS	Schedule, cost and manpower will all be underestimated resulting in delays and increased costs during the Production Phase, and a possibly incomplete product.		Internal	3	4	12	2	14	Communication between Project Manager, work-package coordinators and team members.	Reduce	Further iterations of the WBS as Production Phase approaches.	Add missing WBS activities and re-schedule / divert resources.	
70	Requirements provided by CTA are incomplete / inadequate	Possibly insufficient (or gold-plated) specifications and/or V&V procedure resulting in a non-optimal product. Tightening specifications at a late stage will increase costs and increase the final design time. Gold-plating results in an over-engineered product at increased cost.		External	3	2	6	3	12	Communication between Project Manager, work-package coordinators and team members and feedback to CTA PO.	Beyond Project Control	-	Re-design once requirements are accurate.	
71	CTA Acceptance	CTA has an inaccurate expectation of what the GCT Project will deliver		Clarification and agreement may impact the GCT schedule, cost and the nature of what is delivered (scope).	External	4	1	4	2	6	CTA reviews of GCT design.	Reduce	Ensure GCT DVD is accurate and up to date as a reference point for the GCT specifications.	Adoption of GCT design to incorporate CTA requests and / or adoption of CTA infrastructure / specifications to accurate GCT.
72		CTA rejects the proposed GCT design		Re-design required, resulting in delays to the start of the Production Phase, changes to the project scope may be required.	External	4	2	8	1	6	CTA reviews of GCT design and V&V results.	Reduce	Complete further (planned) component development work in Pre-Construction Phase to produce Assemblies that pass V&V.	Re-design and delays.
73		CTA rejects the finished, built, GCT product		Re-design and re-build / re-fit required resulting in significant delays, increased costs and severe danger that the project is not completed / the CTA completion date is affected.	External	4	3	12	1	6	CTA reviews of GCT design and V&V results.	Reduce	Complete further (planned) component development work in Pre-Construction Phase to produce Assemblies that pass V&V.	Request additional funding for re-design and build.
74	External	Legal & regulatory change in one or more GCT partner countries or institutes impacts project		Possible loss of funding prior-to or during Production Phase resulting in insufficient funds to produce envisaged number of GCT telescopes (reduced scope).	External	4	1	4	3	12	Communication between GCT and CTA Resource Board.	Reduce	GCT partners to engage funding councils (and governments if appropriate) in the project.	Request additional funding, or redistribute resources to minimise delays and / or disruption.
75		Force Majeure (act of nature) impacts project		Potential for impact on schedule, cost and scope.	External	4	1	4	4	16	None possible	Beyond Project Control	-	Accept delays, apply for additional funding if feasible.

Figure D.3 – GCT risk register, page 3.

## E Finite Element Analysis

### Description of the FE model

The table E.1 describes the assumptions of the FE model for the definition of mass and stiffness of the components of the telescope. Table E.2 describes the way the mechanical interfaces are modelled in the FE model.

Component	FE type	Stiffness	Mass
<b>Telescope Base &gt; Tower</b>			
Mechanical structure of tower	Shell	From model	From model
Mechanical fixing of the tower on slab	Beam	From model	From model
<b>Optical Support Structure &gt; MTS &gt; MTS bottom dish &gt; Mechanical structure</b>			
Bottom flange	Shell	From model	From model
Solid interface component	Solid	From model	From model
Base	Shell	From model	From model
Arm 1	Shell	From model	From model
Arm 2	Shell	From model	From model
Arm 3	Shell	From model	From model
Lateral reinforcement	Shell	From model	From model
Bottom dish fixing structure	Shell	From model	From model
Upper flange	Shell	From model	From model
<b>Optical Support Structure &gt; MTS &gt; MTS bottom dish &gt; Rotative system</b>			
Flange to fix on MTS	Shell	From model	From model
Rotative system axis	Beam	From model	From model
Flange to fix on dish M1	Shell	From model	From model
<b>Optical Support Structure &gt; MTS &gt; Serrurier tubes &gt; Truss tubes</b>			
Main tubes	Beam	From model	From model
Secondary tubes	Beam	From model	From model
Kneecaps (truss tubes connectors)	RBE2	Rigid & kneecaps	without
<b>Optical Support Structure &gt; MTS &gt; MTS top dish</b>			
Structure	Shell & beams	From model	From model
<b>Optical Support Structure &gt; Dish M1 &gt; Mechanical structure of dish</b>			
Hexagonal structure	Shell & solid	From model	From model
<b>Optical Support Structure &gt; Counterweight</b>			
Mechanical structure > Support Structure	Shell & beams	From model	From model
Moveable mass CM > Lead mass	Lumped mass	without	User defined
Fixed mass CW > mass	Solid	From model	From model
<b>Mount AAS &gt; AAS Structure</b>			
Fork > Structure	Shell	From model	From model
Bosshhead > Structure	Shell & solid	From model	From model
<b>Mount AAS &gt; AAS drives &gt; Azimuth and Elevation 1 &amp; 2 systems &gt; Drive system</b>			
Fix Support of bearing	Shell	From model	From model
Moveable support of bearing	Shell	From model	From model
Inner & outer raceways of the slew	Beam	From model	From model
Bearing of the slew bearing	CBUSH	User defined	without
<b>Camera access &gt; Mechanical supporting structure</b>			
Arms > Tubes	Shell & beams	From model	From model
Fastening > Flange to connect cam to arms	Shell	From model	From model
Fastening > CHEC-M CHC-S adapt. Flange	Shell	From model	From model
Fastening > Tip tilt def > Plate for tip tilt	Shell	From model	From model
Fastening > Tip tilt def > Actuators	RBE2	Rigid	without
Fastening > Transl. Sub Ass. > Actuators	RBE2	Rigid	without
<b>Optical assembly &gt; Primary Mirror Structure</b>			
Primary Tesselated Mirror > Mirror unit	Shell	From eqv model	From eqv model
Primary Tesselated Mirror > CoG	Lumped mass	without	without
Triangular structure	Shell	From model	From model
<b>Optical assembly &gt; Secondary Mirror Structure</b>			
Secondary Mirror	Shell	From model	From model
CoG of the secondary mirror	Lumped mass	without	without
<b>Optical assembly &gt; Alignment module &gt; Actuation system</b>			
Actuators	RBE2	Rigid	without
<b>Camera</b>			
Camera mechanics	Lumped mass	without	User defined
<b>Auxiliary System &gt; Telescope Cabinets</b>			
Fork Power Supply cabinet	Lumped mass	without	User defined
Fork Main cabinet	Lumped mass	without	User defined
MTS Cabinet	Lumped mass	without	User defined
Top Dish Cabinet	Lumped mass	without	User defined

Component	Linked to	Via (FE)	Via (Physical)
<b>Telescope Base &gt; Tower</b>			
Mechanical fixing of the tower on slab	Foundation > Slab Structure > Concrete Slab	Rigid link	Contact
	Mechanical structure of tower	Rigid link	Contact
<b>Mount AAS &gt; AAS drives &gt; Azimuth system &gt; Drive system</b>			
Fix Support of bearing	Mechanical structure of tower	Model continuity	Finite stiffness bolts
	Outer raceway of the Slew bearing	Model continuity	Finite stiffness bolts
Outer raceway of the Slew bearing (fixed part)	Inner raceway of the Slew bearing (rotating part)	Finite stiffness links	Bearing
Inner raceway of the Slew bearing (rotating part)	Flange of the moveable support of bearing	Rigid link	Finite stiffness bolts
Flange of the moveable support of bearing	Main struct. of the moveable support of bearing	Model continuity	Finite stiffness bolts
<b>Mount AAS &gt; AAS Structure &gt; Fork</b>			
Structure	Main struct. of the moveable support of Az. bearing	Rigid link	Finite stiffness bolts
	Main struct. of fix support of bearing (elevation)	Model continuity	Finite stiffness bolts
	Aux system > Telescope cab > Fork Power Supply Cab	Rigid link	Finite stiffness bolts
	Aux system > Telescope cab > Fork Main Cabinet	Rigid link	Finite stiffness bolts
<b>Mount AAS &gt; AAS drives &gt; Elevation 1 &amp; 2 &gt; Drive system</b>			
Main struct. of fix support of bearing	Flange of fix support of bearing	Model continuity	Finite stiffness bolts
Flange of fix support of bearing	Inner raceway of the slew bearing (fixed part)	Rigid link	Finite stiffness bolts
Inner raceway of the slew bearing (fixed part)	Outer raceway of the slew bearing (mov. part)	Finite stiffness links	Bearing
Outer raceway of the slew bearing (mov. part)	Moveable support of bearing	Rigid link	Finite stiffness bolts
Moveable support of bearing	Bosshead		
<b>Mount AAS &gt; AAS drives &gt; AAS structure &gt; Bosshead</b>			
Structure	OSS > MTS > MTS Btm Dish > Mech. struct. > Btm	Model continuity	Finite stiffness bolts
	OSS > MTS > MTS Btm Dish > Mech. struct. > Int. Tubes	Rigid link	Finite stiffness bolts
	OSS > Counterweight > Mech. Struct > Support struct.	Model continuity	Annular link
	OSS > Counterweight > Mech. Struct > Support struct.	Rigid kneecap	Kneecap
<b>Optical Support Structure &gt; MTS &gt; MTS bottom dish &gt; Mechanical structure</b>			
Bottom flange	Rotative system > Flange to fix on MTS	Model continuity	Finite stiffness bolts
	Solid interface component	Rigid link	Finite stiffness bolts
	Lateral reinforcement	Rigid link	Finite stiffness bolts
Solid interface component	Base	Rigid link	Finite stiffness bolts
	Upper flange	Rigid link	Finite stiffness bolts
Arm 1	Base	Model continuity	Welded
	Arm 2	Model continuity	Welded
	Lateral reinforcement	Model continuity	Welded ?
Arm 2	Truss tubes > Bottom dish fixing structure	Model continuity	Finite stiffness bolts
	Arm 3	Model continuity	Welded
	Interface tubes with bosshead	Rigid link	Finite stiffness bolts
Auxiliary system > Telescope cab > MTS Cabinet	Rigid link	Finite stiffness bolts	
<b>Optical Support Structure &gt; MTS &gt; MTS bottom dish &gt; Rotative system</b>			
Flange to fix on MTS	Rotative system axis	Rigid link	Finite stiffness bolts
Rotative system axis	Flange to fix on dish M1	Rigid link	Finite stiffness bolts
<b>Optical Support Structure &gt; MTS &gt; Serrurier tubes &gt; Truss tubes</b>			
Main tubes	Bottom dish fixing structure	Rigid link	Kneecap
	MTS top dish	Rigid kneecap	Kneecap
	Secondary tubes	Rigid link	Kneecap
<b>Optical Support Structure &gt; MTS &gt; MTS top dish</b>			
Structure	Camera access > Mech. Supp. struct. > Arms > Tubes	Rigid kneecap	Kneecap
	Optical assembly > SMS > Secondary Mirror > M2	Rigid link	Actuators
	Aux system > Telescope cab > Top Dish Cabinet	Rigid link	Finite stiffness bolts
<b>Optical Support Structure &gt; Dish M1 &gt; Mechanical structure of dish</b>			
Hexagonal structure	MTS Btm Dish > Mech struct. > Upper flange	Rigid link	Finite stiffness bolts
	Rotative system > Flange to fix on dish M1	Model continuity	Finite stiffness bolts
	Fixing system for triangular support	Rigid link	Finite stiffness bolts
<b>Optical assembly &gt; PMS &gt; Mechanical support</b>			
Triangular structure	Opt assembly > PMS > Primary tess mirror > Mirror unit	Rigid link	Actuators
	Fixing system for triangular support	Rigid link	Finite stiffness bolts
<b>Optical Support Structure &gt; Counterweight &gt; Mechanical structure</b>			
Support Structure	Fixed mass	Rigid link	Finite stiffness bolts
	Moveable mass	Rigid link	Finite stiffness bolts
<b>Camera access &gt; Mechanical supporting structure &gt; Fastening of scientific camera</b>			
Flange to connect camera to the arms	Camera access > Mech. Supp. struct. > Arms > Tubes	Rigid link	Finite stiffness bolts
	Tip-tilt defocus sub assembly > Plate for tip-tilt	Rigid link	Actuators (washers, screw)
Tip-tilt defocus sub assembly > Plate for tip-tilt	CHEC-M CHEC-S adaptation flange	Rigid link	Actuators (washers, screw)

Figure E.2 – Modelling of mechanical interfaces

### Normal mode analysis

The first five mode shapes for 20 degrees and 90 degrees elevation are plotted in figures E.3 and E.4 respectively. Effective mass fractions for the first ten modes are detailed in figures E.5 to E.9 in parking position and for 0, 20, 60, 90 degrees elevation.

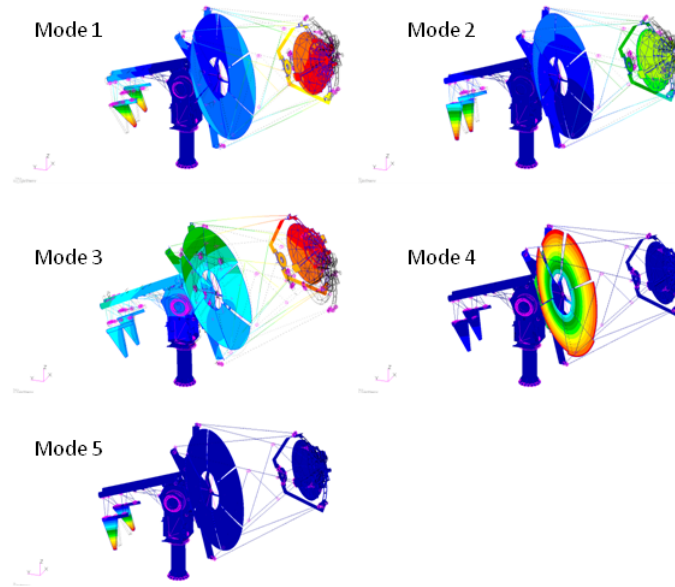


**Figure E.3** – First five mode shapes for 20 degrees elevation. Non-deformed shape is plotted in black dot lines.

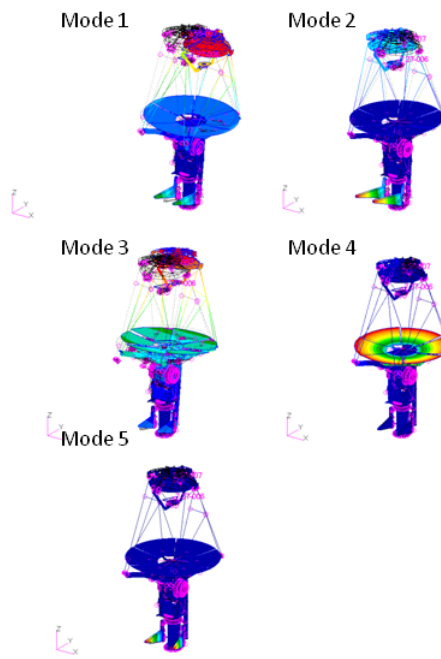


**Figure E.4** – First five mode shapes for 90 degrees elevation. Non-deformed shape is plotted in black dot lines.

Mode	f (Hz)	Description	Tx	Ty	Tz	Rx	Ry	Rz
1	3.7	Rotation of the elevation system around azimuth axis	12.2%	0%	0%	0%	10.5%	22.5%
2	4.8	Local mode of the M1	< 1%	0%	0%	0%	8.5%	< 1%
3	5.4	Local mode of the CTW	0%	< 1%	0%	0%	0%	0%
4	7.5	Bending of the telescope perp. to the elevation axis	<b>55.5%</b>	0%	0%	0%	<b>68.2%</b>	16.9%
5	7.9	Bending of the CTW structure	0%	1.1%	4.6%	3.2%	0%	< 1%
6	8.7	Bending of the telescope around elevation axis	0%	<b>58.0%</b>	0.7%	<b>67.3%</b>	0%	0%
7	9.5	Local mode of the M1	0%	0%	0%	0%	0%	0%
8	9.5	Bending of the telescope perp. to the elevation axis	3.1%	< 1%	0%	0%	6.6%	9.2%
9	9.5	Local mode of the M1	0%	0%	0%	0%	0%	0%
10	9.5	Local mode of the M1	0%	0%	0%	0%	0%	0%
<b>Total</b>			<b>71.7%</b>	<b>59.3%</b>	<b>5.3%</b>	<b>70.5%</b>	<b>93.8%</b>	<b>49.2%</b>

Figure E.5 – Effective mass frations in parking position.

Mode	f (Hz)	Description	Tx	Ty	Tz	Rx	Ry	Rz
1	3.4	Rotation of the elevation system around azimuth axis	0%	0%	0%	0%	< 1%	<b>83.5%</b>
2	4.0	Bending of the telescope perp. to the elevation axis	29.4%	0%	0%	0%	31.1%	7.7%
3	4.0	Local mode of the M1	< 1%	< 1%	0%	< 1%	5.0%	< 1%
4	4.0	Bending of the telescope around elevation axis	0%	18.6%	3.1%	<b>78.1%</b>	0%	0%
5	5.4	Local mode of the CTW	0%	0%	0%	0%	0%	0%
6	7.9	Bending of the telescope perp. to the elevation axis	34.5%	2.7%	< 1%	< 1%	44.8%	< 1%
7	8.0	Bending of the CTW structure	6.3%	14.5%	5.1%	3.8%	8.0%	< 1%
8	9.5	Local mode of the M1	0%	0%	0%	0%	0%	0%
9	9.5	Bending of the telescope perp. to the elevation axis	2.5%	< 1%	0%	0%	5.4%	3.5%
10	9.5	Local mode of the M1	0%	0%	0%	0%	0%	0%
<b>Total (at 10th mode)</b>			<b>72.8%</b>	<b>35.9%</b>	<b>9.1%</b>	<b>82.9%</b>	<b>94.6%</b>	<b>95.2%</b>
<b>Total (at 50th mode)</b>			<b>83.1%</b>	<b>84.1%</b>	<b>26.7%</b>	<b>98.9%</b>	<b>98.8%</b>	<b>98.9%</b>

Figure E.6 – Effective mass frations for 0° elevation.

Mode	f (Hz)	Description	Tx	Ty	Tz	Rx	Ry	Rz
1	3.4	Rotation of the elevation system around azimuth axis	1.1%	0%	0%	0%	10.7%	<b>84.0%</b>
2	3.9	Bending of the telescope perp. to the elevation axis	30.0%	0%	0%	0%	31.4%	4.0%
3	4.7	Bending of the telescope around elevation axis	0%	23.9%	2.9%	<b>82.2%</b>	0%	0%
4	4.8	Local mode of the M1	< 1%	0%	0%	0%	4.3%	1.1%
5	5.4	Local mode of the CTW	0%	0%	0%	0%	0%	0%
6	7.8	Bending of the telescope perp. to the elevation axis	26.8%	6.7%	< 1%	1.5%	30.4%	0%
7	7.9	Bending of the CTW structure	11.9%	14.7%	1.2%	3.2%	13.4%	0%
8	9.5	Local mode of the M1	0%	0%	0%	0%	0%	0%
9	9.5	Bending of the telescope perp. to the elevation axis	0%	0%	0%	0%	0%	0%
10	9.5	Local mode of the M1	0%	0%	0%	0%	0%	0%
<b>Total</b>			<b>69.9%</b>	<b>45.3%</b>	<b>4.6%</b>	<b>86.8%</b>	<b>90.2%</b>	<b>89.1%</b>

Figure E.7 – Effective mass frations for 20° elevation.

Mode	f (Hz)	Description	Tx	Ty	Tz	Rx	Ry	Rz
1	3.6	Bending of the telescope perp. to the elevation axis	7.6%	0%	0%	0%	46.8%	<b>50.9%</b>
2	3.9	Bending of the CTW structure	26.2%	0%	0%	0%	17.6%	0.9%
3	4.5	Bending of the telescope around elevation axis	0%	32.1%	1.0%	<b>86.9%</b>	0%	0%
4	4.8	Local mode of the M1	< 1%	0%	0%	0%	1.5%	16.0%
5	5.4	Local mode of the CTW	0%	0%	0%	0%	0%	0%
6	7.8	Bending of the telescope perp. to the elevation axis	31.6%	1.1%	< 1%	< 1%	25.4%	0%
7	7.8	Bending of the CTW structure	1.6%	19.2%	< 1%	3.4%	1.4%	0%
8	9.5	Local mode of the M1	0%	0%	0%	0%	0%	0%
9	9.5	Local mode of the M1	0%	0%	0%	0%	0%	0%
10	9.5	Local mode of the M1	0%	0%	0%	0%	0%	0%
<b>Total</b>			<b>67.1%</b>	<b>52.4%</b>	<b>1.7%</b>	<b>90.5%</b>	<b>92.7%</b>	<b>67.8%</b>

Figure E.8 – Effective mass frations for 60° elevation.

Mode	f (Hz)	Description	Tx	Ty	Tz	Rx	Ry	Rz
1	3.6	Bending of the telescope perp. to the elevation axis	11.3%	0%	0%	0%	<b>58.0%</b>	0.6%
2	3.9	Bending of the CTW structure	23.7%	0%	0%	0%	12.9%	4.9%
3	4.4	Bending of the telescope around elevation axis	0%	34.0%	0%	<b>87.7%</b>	0%	0%
4	4.8	Local mode of the M1	0%	0%	0%	0%	0%	39.7%
5	5.4	Local mode of the CTW	0%	0%	0%	0%	0%	0%
6	7.8	Bending of the telescope perp. to the elevation axis	30.4%	0%	0%	0%	22.7%	0%
7	7.9	Bending of the CTW structure	0%	14.4%	5.3%	2.5%	0%	0%
8	9.5	Local mode of the M1	0%	0%	0%	0%	0%	0%
9	9.5	Local mode of the M1	0%	0%	0%	0%	0%	0%
10	9.5	Local mode of the M1	0%	0%	0%	0%	0%	0%
<b>Total</b>			<b>69.9%</b>	<b>45.3%</b>	<b>4.6%</b>	<b>86.8%</b>	<b>90.2%</b>	<b>89.1%</b>

Figure E.9 – Effective mass fractions for 90° elevation.



### Static analysis in observing mode

Displacements of the optical components between 20 and 90 degrees are detailed below.

Gravity loads

Elevation (deg)	Dec M1M2 (mm)	Dec M2Cam (mm)	Tilt M1M2 (arcsec)	Tilt M2Cam (arcsec)	Piston M1M2 (mm)	Piston M2Cam (mm)
Spec (PtV)	8,5	8,5	900	900	7,75	7,75
20	4,3	0,1	26,5	-2,6	1	-1
40	3,5	0,1	28,5	-8,8	1	< 1
60	2,3	0,1	21,9	-9,7	< 1	< 1
90	0	0	0	0	0	0

Gravity and wind loads (low wind speed)

Elevation 0°

Wind vector (°)	Dec M1M2 (mm)	Dec M2Cam (mm)	Piston M1M2 (mm)	Piston M2Cam (mm)	Tilt x M1M2 (arcsec)	Tilt y M1M2 (arcsec)	Tilt x M2Cam (arcsec)	Tilt y M2Cam (arcsec)
0	4,4	0,1	1,4	-1,0	16	0,6	12	-7
45	4,5	0,1	1,4	-1,0	16	-5,6	12	-73
90	4,5	0,1	1,4	-0,9	16	-8,1	12	-114
135	4,5	0,1	1,4	-0,9	18	-5,6	12	-106
180	4,6	0,1	1,4	-0,9	18	0,8	10	-52
Max	4,6	0,1	1,4	1,0	18	8	12	114
Spec (PtV)	8,5	8,5	7,75	7,75	900	900	900	900

Elevation 20°

Wind vector (°)	Dec M1M2 (mm)	Dec M2Cam (mm)	Piston M1M2 (mm)	Piston M2Cam (mm)	Tilt x M1M2 (arcsec)	Tilt y M1M2 (arcsec)	Tilt x M2Cam (arcsec)	Tilt y M2Cam (arcsec)
0	4,2	0,1	1,0	-0,7	26	0,6	-3	-14
45	4,2	0,1	0,9	-0,7	26	-0,4	-3	-26
90	4,3	0,1	0,9	-0,7	26	-0,8	-3	-33
135	4,3	0,1	0,9	-0,7	26	-0,4	-1	-31
180	4,3	0,1	0,9	-0,7	29	13,8	-1	-48
Max	4,3	0,1	1,0	0,7	29	14	3	48
Spec (PtV)	8,5	8,5	7,75	7,75	900	900	900	900

Elevation 60°

Wind vector (°)	Dec M1M2 (mm)	Dec M2Cam (mm)	Piston M1M2 (mm)	Piston M2Cam (mm)	Tilt x M1M2 (arcsec)	Tilt y M1M2 (arcsec)	Tilt x M2Cam (arcsec)	Tilt y M2Cam (arcsec)
0	2,2	0,1	0,2	-0,3	21	0,3	-14	0
45	2,3	0,0	0,2	-0,3	22	1,2	2	-12
90	2,3	0,1	0,2	-0,2	22	-1,1	-10	-17
135	2,4	0,1	0,2	-0,2	23	-0,7	-7	-14
180	2,4	0,1	0,2	-0,2	24	0,3	-7	-4
Max	2,4	0,1	0,2	0,3	24	1	14	17
Spec (PtV)	8,5	8,5	7,75	7,75	900	900	900	900

Elevation 90°

Wind vector (°)	Dec M1M2 (mm)	Dec M2Cam (mm)	Piston M1M2 (mm)	Piston M2Cam (mm)	Tilt x M1M2 (arcsec)	Tilt y M1M2 (arcsec)	Tilt x M2Cam (arcsec)	Tilt y M2Cam (arcsec)
0	<0,1	<0,1	<0,1	<0,1	< 1	< 1	< 1	< 1
45	<0,1	<0,1	<0,1	<0,1	< 1	< 1	< 1	< 1
90	<0,1	<0,1	<0,1	<0,1	< 1	< 1	< 1	< 1
135	<0,1	<0,1	<0,1	<0,1	< 1	< 1	< 1	< 1
180	<0,1	<0,1	<0,1	<0,1	< 1	< 1	< 1	< 1
Max	0,0	0,0	0,0	0,0	0	0	0	0
Spec (PtV)	8,5	8,5	7,75	7,75	900	900	900	900

### Seismic analysis

Recovery points and corresponding peak acceleration responses are detailed below.

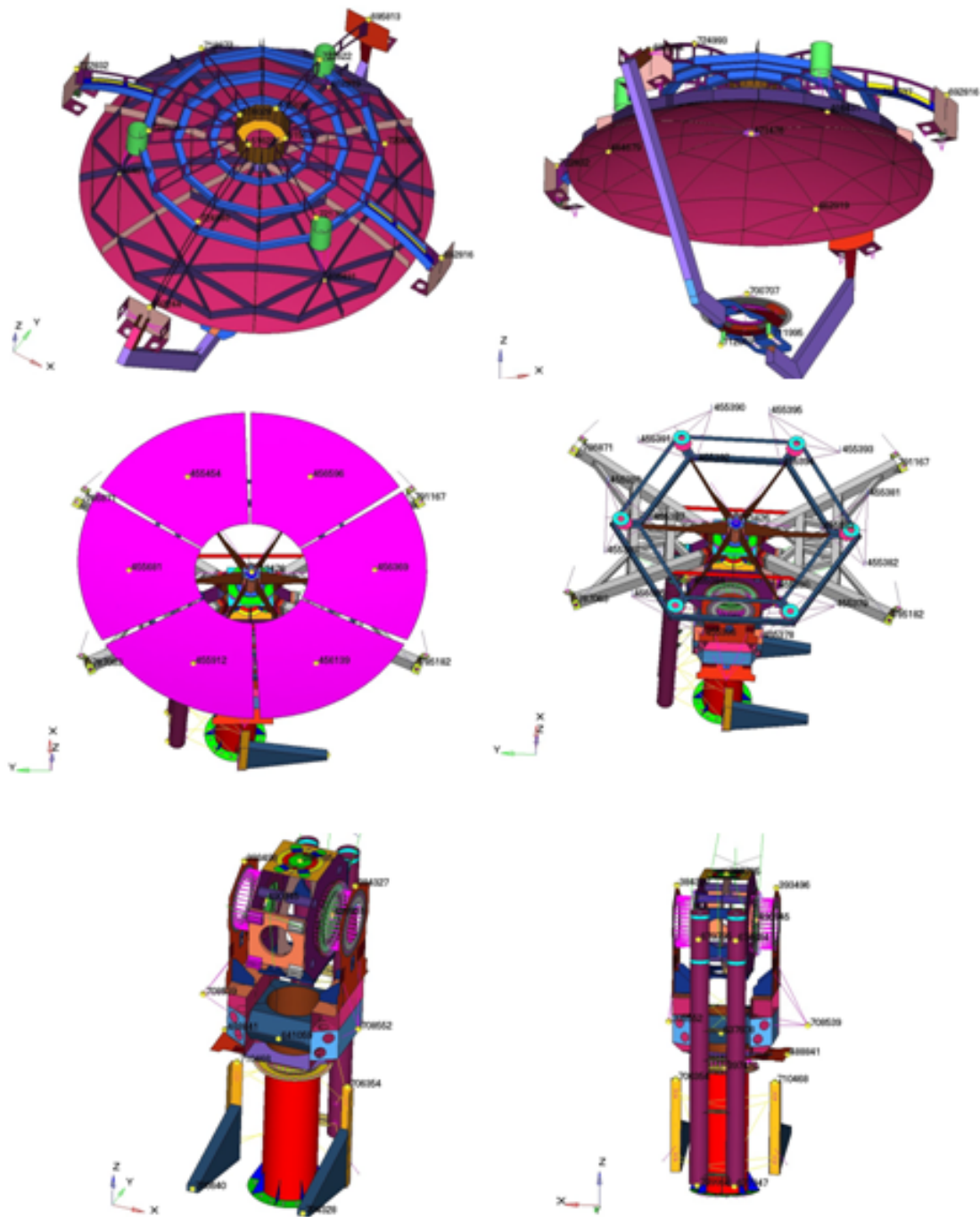


Figure E.10 – Recovery points used for the seismic analysis (from [14]).

PEAK ACCELERATION RESPONSES: Mirror Coord Output			
COMPONENT	ID	MAX ACC [g]	LOADCASE
MIRROR 1D - actuator 2	455378	3.36	SEISMIC: ELEV = 00° Operat - AZIMUTH = 135°
MIRROR 1D - actuator 3	455379	3.72	SEISMIC: ELEV = 00° Operat - AZIMUTH = 045°
MIRROR 1D - actuator 1	455380	2.98	SEISMIC: ELEV = 00° Operat - AZIMUTH = 000°
MIRROR 1E - actuator 3	455381	3.63	SEISMIC: ELEV = 00° Operat - AZIMUTH = 000°
MIRROR 1E - actuator 2	455382	3.77	SEISMIC: ELEV = 00° Operat - AZIMUTH = 000°
MIRROR 1E - actuator 1	455383	3.51	SEISMIC: ELEV = 00° Operat - AZIMUTH = 000°
MIRROR 1C - actuator 1	455384	3.05	SEISMIC: ELEV = 00° Operat - AZIMUTH = 000°
MIRROR 1C - actuator 2	455385	3.32	SEISMIC: ELEV = 95° Parked - AZIMUTH = 090°
MIRROR 1C - actuator 3	455386	4.25	SEISMIC: ELEV = 00° Operat - AZIMUTH = 090°
MIRROR 1B - actuator 1	455387	3.52	SEISMIC: ELEV = 00° Operat - AZIMUTH = 000°
MIRROR 1B - actuator 2	455388	3.75	SEISMIC: ELEV = 00° Operat - AZIMUTH = 000°
MIRROR 1B - actuator 3	455389	3.63	SEISMIC: ELEV = 00° Operat - AZIMUTH = 000°
MIRROR 1A - actuator 2	455390	3.78	SEISMIC: ELEV = 00° Operat - AZIMUTH = 135°
MIRROR 1A - actuator 3	455391	3.30	SEISMIC: ELEV = 00° Operat - AZIMUTH = 045°
MIRROR 1A - actuator 1	455392	2.99	SEISMIC: ELEV = 00° Operat - AZIMUTH = 000°
MIRROR 1F - actuator 2	455393	3.54	SEISMIC: ELEV = 00° Operat - AZIMUTH = 000°
MIRROR 1F - actuator 1	455394	2.97	SEISMIC: ELEV = 00° Operat - AZIMUTH = 000°
MIRROR 1F - actuator 3	455395	3.35	SEISMIC: ELEV = 00° Operat - AZIMUTH = 090°
MIRROR 1A	455454	2.68	SEISMIC: ELEV = 00° Operat - AZIMUTH = 000°
MIRROR 1B	455681	3.41	SEISMIC: ELEV = 00° Operat - AZIMUTH = 000°
MIRROR 1C	455912	2.69	SEISMIC: ELEV = 00° Operat - AZIMUTH = 000°
MIRROR 1D	456139	2.75	SEISMIC: ELEV = 95° Parked - AZIMUTH = 000°
MIRROR 1E	456369	3.42	SEISMIC: ELEV = 00° Operat - AZIMUTH = 000°
MIRROR 1F	456596	2.71	SEISMIC: ELEV = 95° Parked - AZIMUTH = 135°
MIRROR 2 - POS A	462919	3.63	SEISMIC: ELEV = 00° Operat - AZIMUTH = 000°
MIRROR 2 - POS B	464679	3.92	SEISMIC: ELEV = 30° Operat - AZIMUTH = 000°
MIRROR 2 - POS C	466431	3.88	SEISMIC: ELEV = 30° Operat - AZIMUTH = 000°
MIRROR 2 - CENTRE	471476	3.73	SEISMIC: ELEV = 00° Operat - AZIMUTH = 000°
CAMERA	700707	4.15	SEISMIC: ELEV = 60° Operat - AZIMUTH = 000°
MIRROR 1 - CENTRE	713426	3.45	SEISMIC: ELEV = 00° Operat - AZIMUTH = 000°

Figure E.11 – Peak acceleration responses of the optical components expressed in the local cylindrical coordinate system of the OSS (from [14]).

PEAK ACCELERATION RESPONSES: Global Coord Output			
COMPONENT	ID	MAX ACC [g]	LOADCASE
see pictures	384327	1.20	SEISMIC: ELEV = 95° Parked - AZIMUTH = 090°
see pictures	386785	1.07	SEISMIC: ELEV = 95° Parked - AZIMUTH = 090°
see pictures	387515	1.05	SEISMIC: ELEV = 95° Parked - AZIMUTH = 090°
see pictures	393496	1.14	SEISMIC: ELEV = 95° Parked - AZIMUTH = 090°
TOWER TOP	397410	0.29	SEISMIC: ELEV = 95° Parked - AZIMUTH = 090°
see pictures	488841	0.40	SEISMIC: ELEV = 60° Operat - AZIMUTH = 000°
see pictures	489931	1.03	SEISMIC: ELEV = 95° Parked - AZIMUTH = 090°
see pictures	490945	1.00	SEISMIC: ELEV = 95° Parked - AZIMUTH = 090°
see pictures	515632	3.84	SEISMIC: ELEV = 60° Operat - AZIMUTH = 000°
see pictures	515830	3.81	SEISMIC: ELEV = 60° Operat - AZIMUTH = 000°
see pictures	516028	3.84	SEISMIC: ELEV = 60° Operat - AZIMUTH = 000°
see pictures	516226	3.88	SEISMIC: ELEV = 60° Operat - AZIMUTH = 000°
see pictures	637608	0.53	SEISMIC: ELEV = 95° Parked - AZIMUTH = 090°
see pictures	641059	0.53	SEISMIC: ELEV = 95° Parked - AZIMUTH = 090°
CW SUPPORT (TOP -X)	674684	1.37	SEISMIC: ELEV = 95° Parked - AZIMUTH = 090°
CW SUPPORT (BOTTOM -X)	677347	1.69	SEISMIC: ELEV = 60° Operat - AZIMUTH = 090°
CW SUPPORT (TOP +X)	677975	1.39	SEISMIC: ELEV = 95° Parked - AZIMUTH = 090°
see pictures	692244	3.10	SEISMIC: ELEV = 60° Operat - AZIMUTH = 000°
see pictures	692816	3.82	SEISMIC: ELEV = 00° Operat - AZIMUTH = 000°
see pictures	695813	3.21	SEISMIC: ELEV = 90° Operat - AZIMUTH = 000°
COUNTERWEIGHT +X nodeA	704328	6.01	SEISMIC: ELEV = 90° Operat - AZIMUTH = 090°
COUNTERWEIGHT +X nodeB	706354	1.91	SEISMIC: ELEV = 95° Parked - AZIMUTH = 090°
COUNTERWEIGHT -X nodeA	706640	5.82	SEISMIC: ELEV = 30° Operat - AZIMUTH = 090°
CHILLER (CONM2)	708539	0.67	SEISMIC: ELEV = 95° Parked - AZIMUTH = 135°
AAS ELECTRONIC CABINET (CONM2)	708552	0.57	SEISMIC: ELEV = 95° Parked - AZIMUTH = 090°
CW SUPPORT (BOTTOM +X)	709958	1.68	SEISMIC: ELEV = 60° Operat - AZIMUTH = 090°
COUNTERWEIGHT -X nodeB	710468	1.79	SEISMIC: ELEV = 95° Parked - AZIMUTH = 090°
see pictures	711995	3.81	SEISMIC: ELEV = 60° Operat - AZIMUTH = 000°
see pictures	712063	3.83	SEISMIC: ELEV = 60° Operat - AZIMUTH = 000°
see pictures	715611	1.16	SEISMIC: ELEV = 95° Parked - AZIMUTH = 090°
see pictures	718872	3.75	SEISMIC: ELEV = 00° Operat - AZIMUTH = 000°
see pictures	720637	3.76	SEISMIC: ELEV = 00° Operat - AZIMUTH = 000°
see pictures	721766	3.91	SEISMIC: ELEV = 60° Operat - AZIMUTH = 000°
see pictures	722194	3.92	SEISMIC: ELEV = 60° Operat - AZIMUTH = 000°
see pictures	722622	3.76	SEISMIC: ELEV = 00° Operat - AZIMUTH = 000°
see pictures	722832	3.78	SEISMIC: ELEV = 00° Operat - AZIMUTH = 000°
see pictures	724993	3.98	SEISMIC: ELEV = 60° Operat - AZIMUTH = 000°
see pictures	785182	1.51	SEISMIC: ELEV = 30° Operat - AZIMUTH = 000°
see pictures	786871	2.17	SEISMIC: ELEV = 95° Parked - AZIMUTH = 000°
see pictures	787063	2.16	SEISMIC: ELEV = 95° Parked - AZIMUTH = 000°
see pictures	791167	1.62	SEISMIC: ELEV = 90° Operat - AZIMUTH = 090°

Figure E.12 – Peak acceleration responses of the mechanical structure expressed in the global Cartesian coordinate system (from [14]).



## F Author List

<b>Editor</b>	<b>Institute</b>
Delphine Dumas	Observatoire de Paris
Richard White	MPIK Heidelberg
Jean-Philippe Amans	Observatoire de Paris
Jean-Laurent Dournaux	Observatoire de Paris
Gilles Fasola	Observatoire de Paris
Tim Greenshaw	University of Liverpool
Jean-Michel Huet	Observatoire de Paris
Philippe Laporte	Observatoire de Paris
Helene Sol	Observatoire de Paris
David Berge	University of Amsterdam
Anthony Brown	University of Durham
Paula Chadwick	University of Durham
Heide Costantini	Aix-Marseille Université

**Table F.1** – Editors of the GCT TDR document



# References

- [1] Vassiliev V., Fegan S. & Brousseau P. (2007). *Wide field aplanatic two-mirror telescopes for ground-based  $\gamma$ -ray astronomy*. *Astroparticle Physics*, **28**, 10
- [2] Schwarzschild K. (1905). *Untersuchungen zur geometrischen optik ii*. *Astronomische Mitteilungen der Koeniglichen Sternwarte zu Goettingen*, **Vol. 10**, 1
- [3] Couder A. (1926). *Compt. Rend. Acad. Sci.*, **138**, 1276
- [4] The CTA Consortium (2015). *SST-2M ASTRI Technical Design Report*. Document ID: SST-TDR/140530
- [5] Hinton, J. et al. (2013). *SST Requirements*. Document ID: MAN-PO/120808
- [6] Bechtol K., Funk S., Okumura A. et al. (2012). *TARGET: A multi-channel digitizer chip for very-high-energy gamma-ray telescopes*. *Astroparticle Physics*, **36**, 156
- [7] The CTA Consortium (2015). *Array Control & Data Acquisition Technical Design Report*. Document ID: ACTL-TDR/140415
- [8] Dournaux J.L. (2014). *Finite-element analysis of the GCT telescope, Issue 2*. Document ID: SST-2M-PM/130402
- [9] Amral et al. (1989). *Description of a scattering apparatus: application to the problems of characterization of opaque surfaces*. *App.Opt.*, **28**, 2723
- [10] Marioge, J.-P. *Surfaces Optiques : modélisation des défauts et contrôle*. pp. 12–16. *Techniques de l'ingénieur*
- [11] Lang, T. and Antelo, E. (2000). *CORDIC-based computation of arccos and  $\sqrt{1-t^2}$* . *Journal of VLSI signal processing*, **25**, 19
- [12] Dumas, D. et al. (2013). *SST-2M-GATE Preliminary Design Verification Document*. Document ID: SST-2M-PM/130402
- [13] White, R. et al. (2013). *CHEC (SST-2M) Preliminary Design Verification Document*. Document ID: SST-2M-CAM/130925
- [14] Eder, J. (2014). *GCT Structure Analysis*. Document ID: MAN-PO/141212
- [15] Todero Peixoto C.J. et al. (2012). *Research plans for the next five years CTA*. Internal document CTA
- [16] Eder, J. (2013). *Structural Verification Guidelines, Issue 2*. Document ID: MAN-PO/130410
- [17] Schmoll, J. (2011). *A study of the optics of a 4m dual-mirror SST*. Internal Note, CTA-MC-Note-6
- [18] Ohm, S. and Hinton, J. (2012). *Impact of measurement errors on charge resolution and system performance*. Internal Note, SCI-MC/121113
- [19] Laporte, P. (2014). *Analysis of reliability for SST-GATE telescope*. Internal Technical Document, 503-SYS-GEPI-TN-20141128









# Glossary

AAS	Alt-Azimuthal Structure
CHEC	Compact High Energy Camera
CHEC-M	MAPM version of CHEC
CHEC-S	SiPM version of CHEC
CTA	Cherenkov Telescope Array
CTAO	Cherenkov Telescope Array Observatory
DACQ	Data Acquisition
DC	Direct Current
FE	Finite Element
FoV	Field of View
FPGA	Field Programmable Gate Array
FWHM	Full Width Half Maximum
GCT	Gamma-ray Cherenkov Telescope
H.E.S.S.	High Energy Stereoscopic System
HSDDL	High Speed Deterministic Time Data Link
HV	High Voltage
I/O	Input / Output
IC	Integrated Circuit
LED	Light Emitting Diode
LVDS	Low Voltage Differential Signal
MAPM	Multi-anode Photomultiplier
MC	Monte-Carlo
MTS	Mass Truss System
NSB	Night Sky Background
OSS	Optical Support Structure
p.e.	Photoelectron(s)
PBS	Product Breakdown Structure
PCB	Printed Circuit Board
PSoC	Programmable System on Chip
RMS	Root Mean Square

---

SC	Schwarzschild-Couder
SFP	Small Form-factor Pluggable
SiPM	Silicon Photomultiplier
SLAC	Stanford Linear Accelerator Center
SPI	Serial Peripheral Interface
SST	Small Sized Telescope
SST-2M	Dual-mirror SST
SST-GATE	SST GAMMA-ray Telescope Elements
TARGET	TeV Array Readout with GSa/s sampling and Event Trigger
TBC	To be confirmed
TBD	To be determined
TCS	Telescope Control System
TDR	Technical Design Report
UCTS	Unified Clock distribution and trigger Time Stamping board
UPS	Uninterruptible power supply
WBS	Work Breakdown Structure